SAGO STARCH: BEHAVIOUR AND MANUFACTURE OF EXPANDED IRON-FORTIFIED EXTRUDATES

by

SHANTI FITRIANI

(BSc., MSc.)

Thesis submitted to the University of Nottingham

for the degree of Doctor of Philosophy

Division of Food Sciences
School of Biosciences
University of Nottingham
Sutton Bonington Campus
Loughborough, LE12 5RD
United Kingdom

September 2016

Acknowledgements

First and above all, I praise God the Almighty, for providing me with this opportunity and granting me the capability to proceed successfully.

I am very grateful to my first supervisor, Dr. Bettina Wolf for her excellent supervision, encouragement and valuable guidance. I want to express my deep thanks to my second supervisor, Professor Sandra Hill for her support during the whole period of my study, and especially her patience and guidance during the writing process.

I would like to give special thanks to Val Street and Steven Johnson, Emily Fong, Dr. Bill MacNaughtan, Dr. Guy Channel, Khatija, Newton Carolyn, all academics and staff at the Division of Food Sciences and friends in Sutton Bonington Campus for their essential assistance, guidance, hospitality and friendship. My appreciation also to Christine Grainger-Boultby from the School of Pharmacy for her kind assistance with the SEM images.

I would particularly like to acknowledge the Ministry of Research, Technology and Higher Education of the Republic of Indonesia and the University of Riau (UR) for providing me with the scholarship and opportunity which make it possible for me to pursue my study in the UK. I would also like to express my sincere gratitude to my best colleague, Dr. Yusmarini at UR who continuously gives her endless encouragement.

I greatly appreciate to all my friends in Indonesian Community for the spiritual supports, joyful gatherings and assistance and friendship for me and my husband during the study.

I warmly thank and appreciate my parents and my mother and father-in-law for their love, material and spiritual support in all aspects of my life. I also would like to thank my brother, sisters, and brothers and sisters-in-law, for providing support in numerous ways. And finally, I would like to express my sincerest gratitude to my lovely husband, Dr. Irwan Taslapratama, for his constant support, love and spiritual guidance as a tremendous source of motivation and inspiration for me. Without all of this, I could not have finished this work. I can just say thanks for everything and may God give you all the best.

Abstract

Sago starch is extracted from the trunk of sago palm (*Metroxylon spp.*), which is found throughout South East Asia. In Indonesia sago is considered an underutilised crop and moreover Iron Deficiency Anaemia (IDA) is prevalent among particularly women and children. Creation of a ready to eat product from sago, which was fortified with iron, would address issues of food security both in terms of nutrition and as a non-imported carbohydrate source. With this aim studies for the manufacture of a thermomechanical directly expanded snack product using a commercial source of sago starch were conducted.

Composition and properties of sago starch were analysed and compared with rice and cassava. Sago starch differed in several aspects from the two other starches widely processed in Asia. Sago starch had large granules, had the highest amylose levels and gelatinisation temperature (76 °C). X-ray diffraction suggested an A-type packing for all samples, including the sago where literature suggest a C-type ordering.

Conversion of the starches (30% moisture) and their flow were studied in a capillary rheometer. A stable extruded product was achieved, but it did not expand. Capillary rheometer data showed pseudoplastic behaviour of the moistened sago starch. With increasing temperature viscosity decreased and no impact of the presence of iron (ferrous sulphate heptahydrate 800 ppm) on the flow behaviour was found, but the inclusion of iron made the extrudates brown in colour. The losses of crystallinity were measured on the extrudates from the rheometer. Levels of order loss were predicted from the state diagram and by comparison with the DSC enthalpy changes for uncooked sago at higher moisture contents. When processed at 70 °C the samples showed more amorphous material than anticipated. When processed at 100 °C still 30% of the order remained. This indicated that shear and moisture levels are critical in the processing of the starch.

Thermomechanical extrusion was carried out on a twin screw pilot scale machine (Thermo Fisher, Prism). The screw and die configuration and feed rate for the sago starch (8 kg/h) were fixed. The impact of variable processing parameters of water feed rate (16.5 to 25% wwb), screw speed (200, 300 and 400 rpm) and die temperature (120, 140 and 160 °C) on the physical and physicochemical properties of extruded sago starch were investigated. At the lower water feed rates expansion occurred as the product left the extruder to form a stable extrudate with multiple air cells, which gave a crispy texture. The specific mechanical energies needed to create the expanded product were high at 400-500Whr/kg. The properties of the extrudates were more affected by water feed rate than by alterations in screw speed or die temperature.

In order to reduce discolorations, iron-fortified sago starch extrudates were made using iron and ascorbic acid (1:6 ratio). The presence of additives at low water feed rate had no detrimental impact on the extrudates. The recommended extrusion parameters for the manufacture of an extruded sago starch product would be: feed rate of 8 kg/h, screw speed of 300 rpm, die temperature at 140 °C, and water feed rate at 4 mL/min (equivalent to 16.5% wwb), and it is possible that machine settings that produce even higher SME values may allow a more expanded product. From this work it appears that an iron fortified directly expanded sago product could be manufactured. Its nutritional properties and commercial applicability would need to be ascertained.

List of Symbols and Abbreviations

a^*	redness (positive value), greenness (negative value)
AA	ascorbic acid addition
ALL	iron and ascorbic acid addition
ANOVA	Analysis of Variance
b^*	yellowness (positive value), blueness (negative value)
cm	centimetre(s)
Con A	Conconavalin A
cP	centipoise
CuKα	Copper K-alpha
D	capillary diameter
D(4,3)	mean diameter on a volume basis
D10	cut-off point as the diameter where 10% of the distribution lies below this values
D50	cut-off point as the diameter where 50% of the distribution lies below this values
D90	cut-off point as the diameter where 90% of the distribution lies below this values
DMSO	dimethyl sulphoxide
DSC	Differential Scanning Calorimetry
dwb	dry weight basis
g/g	gram gel per gram dry starch
GI	Glycaemic Index
GOPOD	glucose oxidase reductase
GRiSP	Global Rice Science Partnership
h	hour(s)
IDA	Iron Deficiency Anaemia
K	consistency
L	capillary length
L^*	lightness
mbar	millibar
n	flow behaviour index
n	sample size
NaFeEDTA	ferric sodium ethylenediaminetetraacetate
NIL	without addition of iron or ascorbic acid
Q	volumetric flow rate
rpm	revolutions per minute
RVA	Rapid Visco Analyser
SD	standard deviation
SEM	Scanning Electron Microscopy
SF	iron-fortified processed sample
SME	Specific Mechanical Energy
SS	processed sample without iron
T	temperature
T_e	endset temperature
T_f	final temperature
Tg	glass transition temperature
Tm	melting temperature
T_o	onset temperature
T_p	peak temperature
T_s	start temperature
v/v	volume to volume
w/w	weight to weight
WAI	Water Absorption Index
WHO	World Health Organization

WSI	Water Solubility Index
wwb	wet weight basis
x	loss of enthalpy
XRD	X-ray diffraction
y_w	mass fraction of water
η	apparent viscosity
$\dot{\gamma}$	shear rate
$\dot{\gamma}_{app}$	apparent shear rate
$\dot{\gamma}_w$	wall shear rate
τ_w	wall shear stress
$\times g$	gravitation
ΔH	gelatinisation enthalpy of processed sample
ΔH_0	gelatinisation enthalpy of native raw starch
ΔP	pressure drop over the capillary
°C	degrees Celcius
°F	degrees Fahrenheit

Table of Contents

CHAPTER 1
Introduction

In Indonesia sago is an underutilised crop. The research reported in this thesis was to establish if sago starch could be used to make an acceptable snack food and whether this product could be fortified with iron. This product, if it had acceptable eating quality, could combat against nutritional iron deficiency in Indonesian children via the provision of an iron fortified healthy snack product. It would also enhance the use and acceptance level of sago starch within the food manufacturing industry. A manufactured sago product that appeals to children and also promotes their health will encourage parents to buy the product. The children will then get used to sago as a manufactured food ingredient and the next generation may be more positive towards this carbohydrate source.

Indonesia has large forests (1.25 million ha) of wild sago palms, and this makes Indonesia one of the leading world producers of sago starch. About 96% of the sago palm is located in Papua, the largest and easternmost province of Indonesia. The total world area occupied by sago palm is estimated at 2.25 million ha of wild stands and 0.2 million ha of semi-cultivated stands (Flach, 1997). A single palm can produce more than 200 kg of starch (Malviya et al., 2010) and the productivity is about 25 tonnes/hectare/year; four times that of paddy rice (Flach, 1997).

Despite the high productivity of sago palm and therefore the high availability of sago starch, it is not a common staple food in Indonesia

except in a small part of the east of the country. Rice is the carbohydrate choice for most people in Indonesia. Based on data from the Global Rice Science Partnership (GRiSP, 2013), rice consumption per capita for Indonesians in 2009 was 127.40 kg/year. The dependency on rice raises concerns over food security, since currently Indonesia has to import millions of tonnes of rice. There is a need to reduce the dependency on rice through food diversification using local sources, such as cassava and sago. Indonesia is a major world producer of cassava. It is consumed directly as food and a large amount is used locally, but it is also exported to the European Community as feed, and smaller amounts are processed to flour, tapioca, and other products (Djazuli and Bradbury, 1999).

Sago has been a more major source of food for the indigenous population of Eastern Indonesia, particularly in Papua Island, but its use has recently decreased. This may be due to a psychological barrier with sago being considered as food for the poor and primitive people (Purwani et al., 2006). When the Indonesia Government put in place a program to increase rice production between 1968 to 1988 there was a cultural implication that rice was a first-class staple food and other foodstuffs such as maize, yam, cassava and sago were inferior (Sinjal, 2008). Even when compared with non-rice food sources of carbohydrates such as cassava, sweet potato, potato and maize, in Indonesia the national average consumption is lowest for sago, only about 0.41 kg/capita/year being eaten (IPB, 2010). Despite sago starch being used in various traditional food products, as well as in industrial applications (Sim, 1986; Flach, 1997; Abd-Aziz, 2002; Karim et al., 2008b), its consumption in Indonesia is very low.

Fortification of foods is often regarded as the most cost-effective and long-term approach to reducing the prevalence of nutrient deficiencies, such as iron deficiency (Hurrell, 1997). Iron deficiency anaemia (IDA) is one of the high prevalent nutrient deficiencies in the developing world and, to a lesser extent, in developed countries. Pregnant women and women of reproductive age as well as young children are especially at risk of IDA (WHO, 2002). In fact, the prevalence of IDA in Indonesia is wide spread. Basic Health Research (known as *Riset Kesehatan Dasar*) in 2007 showed that 60% of IDA occurred in women in child bearing age, and 59% occurred in pregnant women (Sudargo et al., 2013). Iron fortification of appropriate food items combined with iron supplements in specific population groups has proven to be efficient to tackle this massive problem (Hurrell, 1997).

Today one of the most successful technologies used to make snack foods is thermomechanical extrusion. Extrusion cooking advantages over conventional cooking/processing techniques include energy efficiency, lack of process effluents and versatility with respect to ingredient selection. In addition, it also has the ability to develop a range of products with distinct textural advantages including expansion, crispiness and overall mouthfeel. An expanded crisp or crunchy snack can appeal to children. Many carbohydrate sources have been studied, but less is known about sago starch extrusion. Many researchers have reported the effects of extrusion process variables on the characteristics of produced snacks. There is also extensive literature on mixtures with nutrition benefit being extruded, for example, corn extrudates fortified with yam (Chiu et al., 2013), fortified extruded rice products (Ayoub et al., 2013), fortification of corn starch-based extrudates with common bean flours (Anton et al., 2009) and effect

of guar gum content on starchy extruded products (Parada et al., 2011), just to name a few.

There are some examples of research on sago starch extrusion. Govindasamy et al. (1996) used twin screw extruder to pre-treat sago starch for subsequent saccharification, focusing on employment of this technology as an integral part of a commercial processing operation. In that and a subsequent paper (Govindasamy et al., 1997c) they reported on the influence of extruding sago starch at high feed moisture contents, similar to those of the starch after centrifugation. These studies are a continuation of work previously reported (Govindasamy et al., 1997d) on extrusion of sago starch in a Brabender single-screw extruder where they found that feed moisture content and enzyme concentration were found to be the most significant variables affecting most of the measured physicochemical properties of the extrudates. Another study using single screw extruder by Govindasamy et al. (1995) explored the feasibility of utilising a single-screw extruder for the simultaneous gelatinisation and liquefaction of sago starch using a thermostable a-amylase for subsequent saccharification to optimise saccharification conditions for conversion of sago starch to glucose syrups. Their next study (Govindasamy et al., 1997b) used twin-screw extruder as a bioreactor for the thermomechanical gelatinisation and liquefaction of sago starch using a lower enzyme/substrate (grams of enzyme/grams of starch) ratio than the single screw system. However, the process conditions have to be optimised for sufficient gelatinisation and liquefaction with minimum enzyme inactivation (Govindasamy et al., 1997a).

Furthermore, Ansharullah (1997) studied the characterisation of sago starch and investigated its modification through extrusion, as well as its

possible uses in a food application. The results of the study indicated that within the experimental conditions on twin-screw extrusion, the extrusion had modified the structure and the pasting properties of the sago starch. The products obtained might be used directly in a food system, and might be suitable to be used as a pre-gelatinised starch. Extrusion of sago starch in combination with other materials has been reported. Alias and Karim (2006) studied the effect of substitution of 20% rice and 20% sago on the physicochemical and microstructure properties of extruded snack product made from corn grits using a direct expanded single screw extruder. Substitution with sago also produced a better quality extruded snack in terms of expansion ratio, bulk density, cutting-force and colour as compared to 100% corn extruded snack but not as good as extruded snack made by 80% corn + 20% rice.

It therefore seems possible that a directly expanded product could be made from sago, but there is little fundamental understanding of the processing conditions needed to produce an acceptable directly expanded sago snack by thermomechanical extrusion. It is important that a sago snack food should also have some nutritional benefits, for example iron-fortification.

Most publications on extruding in the presence of iron are found for rice. In industrialised countries, rice is often enriched with iron to restore the iron content found in the un-milled grains (Hunnell et al., 1985). A promising extrusion technology has been reported for making iron-fortified rice grains by Kapanidis and Lee (1996). However, the processed extruded rice grains had lower overall acceptability than natural Jasmine rice, possibly due to a metallic aftertaste. Later, Ayoub et al. (2013) reported the results of the production of fortified extruded rice with sensory

properties that compare well against natural rice. This was made possible through extrusion with low shear and high thermal input in a preconditioning stage.

There is a need to promote sago as a food material and it may be possible to create an expanded snack food that could be fortified with iron. A much greater understanding of the behaviour of sago starch was required to underpin the development of any novel extruded snack product. The work presented in this thesis provides some of this knowledge.

Some background information is provided in Chapter 2 and more in-depth literature reviews on the different elements of this research are integrated into Chapters 4 to 7. Chapter 3 details the materials and methods that were common for the different elements of this research. Specific materials and methods relevant to the individual chapters are described in the relevant place. Chapter 4 details the physicochemical properties of sago starch compared to rice and cassava starches and includes a literature review on the properties of sago starch, as well as rice and cassava starches. Chapter 5 is dedicated to reporting the experimental work and the results of using high temperature and high pressure capillary rheometry as a tool to predict the extrusion behaviour of sago starch including when fortified with iron. This chapter includes a section on the principles of capillary rheometry. Chapter 6 is about extrusion processing of sago starch and includes a literature review on extrusion processing of starchy materials. Chapter 7 is in the manufacture of an iron-fortified extruded snack bar, including a literature review on fortifying foods with iron.

The overall aim of this PhD research was to generate the fundamental understanding of extrusion processing of sago starch with a goal to produce an iron-fortified snack as a healthy snack for young children. The specific objectives were: (1) to characterize the physicochemical properties of sago starch in comparison with rice starch and cassava starch; (2) to measure the flow properties of sago starch melts using a capillary rheometer and thereby establish if its starch could successfully be used in a thermomechanical extruder; (3) to investigate the processing parameters of water feed rate, screw speed and die temperature on the physical and physicochemical properties of an extruded sago starch snack product; and (4) to establish if the incorporation of additives associated with fortification altered the properties of an extruded product.

CHAPTER 2
Background Information

Within this chapter information on three areas is given to provide terminology and background knowledge. More details and reviews of the literature on the specific topics are provided in the relevant chapters of this thesis.

2.1 Introduction to Sago

The primary focus of the work described in this thesis was to use sago starch, which could be a major commodity but is currently less well known than cereal or root/tuber starches.

2.1.1 Sago palm

The sago palm is a species of the genus *Metroxylon* belonging to the Palmae family (Figure 2.1). It is distributed throughout Southeast Asia and many islands in the Western Pacific. It is one of the few tropical crops that can tolerate wet growing conditions, including peat swamps. Sago palm can be advantageous in such swamps (Abd-Aziz, 2002), for example preventing floods and droughts, and maintaining a source of clean ground water. Other commercial crops require the draining of peat swamps. The most important product of sago palm is sago starch. It is extracted from the trunk of the palm. Besides their starch, durable leaves that can be used as thatch is the primary use of the sago palm. As the leaves are strong, they can also be woven into bags, baskets, cages, or rope (Abd-

Aziz, 2002). Table 2.1 shows present uses of the sago palm and its residues.

Figure 2.1 Sago palm cluster (trunking and suckering palms) (Karim et al., 2008b).

Table 2.1 Utilisation of sago palm (Abd-Aziz, 2002).

Sago palm part	Usage/utilisation
Refined sago starch	An ingredient of noodles, vermicelli, biscuits, and many other foods. Used industrially in products such as mono-sodium glutamate, glucose, fructose syrups, etc.
Sago leaves	Used for waterproof thatched roofs
Sago fibre	Provides bulk for rumen fermentation
Sago pitch	Used as an animal feedstuff and in the livestock industry
Sago fronds	Used in the pulp and paper industries

The scale of operation is the only differentiation between traditional and commercial methods of sago palm extraction. Following selection and felling of palms, the bark-like layer is stripped from the trunk and cut into sections or floated as a whole to a central processing facility. In order to

pulverise the pith and loosen starch particles within the fibres, it is reduced to battens and rasped either manually or mechanically. After that, the fibres are separated from the starch by manual kneading, trampling by foot or by a spray of water. The starch-laden water runs into a settling container, where the starch is precipitated and the water overflows. The starch is then removed and dried (Kamal et al., 2007).

2.1.2 Sago starch utilisation

The common traditional food in Papua that is made from sago starch is *papeda* (Figure 2.2a). This is a main dish and is made from wet sago starch which is mixed with hot water to become a glue-like mass and this is eaten with some fish, vegetables or hot soup. *Sagu ega* is sago paste wrapped with sago leaves (Purwani et al., 2006). Furthermore, moist sago starch is used to produce sago pearls (Figure 2.2b). The moist starch cake is pressed through a perforated sheet of iron or coarse screen. The small particles of wet starch are then rolled and heated. The pearls are subsequently dried, sorted, and sold (Singhal et al., 2008).

a)  b) 

Figure 2.2 Example of food made from sago starch; a) *papeda*, and b) sago pearls.

Other uses of sago starch for food are categorised as a snack, where the method of preparation could be baking, boiling, and/or frying. *Lempeng* is

a moulded form made from baked sago starch in Sarawak, Malaysia. It is usually made entirely of starch, but they may occasionally contain other foods as well, such as ground peanuts or other pulses. Besides that, many kinds of cookies are made from sago starch mixed with water and baked, these are *tabaloi* (Sarawak), *bagea* (Moluccas) (Flach, 1997) and *kue bangkit* (Riau Island). Some of these cookies were made by people at home during festive periods, but recently they can be bought from the shops. There is another unique snack made from sago, eggs, oil and sugar called *sagu rendang*. It is crispy, of sweet savoury taste, small in shape and brown in colour just like pepper. Table 2.2 shows the utilisation of sago flour in some small-scale industries in Sarawak, Malaysia.

Table 2.2 Uses of sago flour in small industries in Sarawak, Malaysia (Sim, 1986).

Type of industry	Remarks on the use of sago flour
Noodles	25% incorporation may cause slight changes in colour. Less fresh looking.
Chilli and tomato sauce	20% to 30% sago flour in the sauce is acceptable but reported to be less viscous.
Biscuits	Moisture <5% of the flour is necessary.
Chips	Product is acceptable.
Kwayteoh (flat noodles)	20% sago flour will make *kwayteoh* harder and darker and no difference in taste is noted.
Bread	25% sago flour is incorporated and no difference in taste, texture or colour is noted.
Buns	20% sago flour is acceptable.

In the Peninsular Malaysian states of Kelantan, Terengganu and some parts of Pahang, fish is processed into snacks called *keropok* (dried fish crackers) with more than 100 small-scale processors being engaged in the

business. The crackers are made by mixing minced fish meat with sago flour, tapioca flour, salt and monosodium glutamate. The mixture is then moulded into cylinders, steamed, cooled, sliced and sun-dried. Before consumption the slices are fried in hot oil, after that the *keropok* expands into a porous low-density product. Crispness is the most important parameter governing the quality of *keropok* (Siaw et al., 1985). The quality of expanded foods is judged from their crispness, which in turn is determined by their expanded volume (Chinnaswamy and Hanna, 1988b).

One prospective use of sago in the food industry is in noodles, a popular product for Indonesian people. Currently, most noodles are made from imported wheat flour. Sago noodles are obviously different from other regular noodles made from wheat flour since they are made from gluten-free starch. Heat-moisture treatment is a promising technique for improving the quality of sago noodle and is performed by exposing the starch to high temperatures (110 °C, 16 h) at 25% moisture content (Purwani et al., 2006).

2.1.3 Future use of sago starch

It is clear that sago, especially in the form of starch, can be used as human food. Although most traditional foods are mostly high moisture, there are examples of sago starch being used to form expanded crispy foods. The processing of the starch from its native state to one that supports bubble wall structure is imperative to form the expanded structures. An understanding of the native starch and its transformation would allow an informed decision on how it should be processed.

2.2 Starch

Starch is the major storage carbohydrate of many plants and is mainly composed of biopolymers formed from anhydroglucose units. Starch can be widely found in cereal grain seeds (e.g. corn, wheat, rice and sorghum), tubers (e.g. potato), roots (e.g. cassava, sweet potato and arrowroot), legume seeds (e.g. peas, beans and lentils), fruits (e.g. green bananas, unripe apples and green tomatoes), trunks (e.g. sago palm) and leaves (e.g. tobacco). The manufacturing techniques to obtain the starch are often a combination of grinding of the starch-rich crop followed by wet separation techniques. Due to their higher density, the starch granules will sediment in water. Native starch is a white powder, with bland taste and flavour and is insoluble in cold water (Chen, 2003).

2.2.1 Starch composition

In general, amylose and amylopectin are the two major macromolecule fractions occurring as the storage carbohydrate in starches. Amylose comprises in between 15 and 25% of the starch dry weight for most starches (Liu, 2005). The ratio of amylose and amylopectin in starch varies from one starch to another, but a typical value for "normal" starch is 25% amylose and 75% amylopectin. There are different starches depending on botanical source and major differences even within the same species. There can be an increase in amylopectin content (waxy varieties) or an increase in amylose content (high amylose or amylostarches) (Eliasson and Gudmundsson, 2006). Waxy maize starch is commonly used and modification through genetics have resulted high-amylopectin potato, wheat and rice starches (Visser et al., 1997; Jane et al., 1999; Svegmark et al., 2002). High amylose starches are also grown commercially. The

amylose and amylopectin ratios may be relevant for processing as the two starch components have different properties and are thus not suited for the same applications (Zobel, 1988).

In addition to the starch molecules, the starch granules also contain other components that are present in low amounts (minor components), such as proteins, lipids, phosphate, inorganic substances and non-starch polysaccharides (Liu, 2005; Eliasson and Gudmundsson, 2006). Based on their location, these components can be classified into three groups, namely particulate material, surface components and internal components (Galliard and Bowler, 1987). The amount of these components varies among different sources of starch and on how the starch granules are isolated. Even though they are only present in small amounts, these components play important roles in the physicochemical properties of starch.

Protein content within starches varies depending on the botanical sources. In general, cereal starches have higher protein content than tuber and root starches. The presence of protein can cause unwanted colour in processed starch and starch hydrolysis products via reaction between amino acid groups and reducing sugars (Mailard reaction). Moreover, proteins may also affect surface charge and the rate of hydration (Cui, 2005).

Cereal starches contain higher levels of lipids compared with tuber and legume starches. During heating these lipids can occupy the core of helices of amylose. The lipid may therefore prevent amylose from contributing to the thickening power of gelatinised starch by forming complexes with amylose within the starch paste (Swinkels, 1985). Surface

lipids affect the diffusion of water into starch granules. As a consequence, lipids may alter starch properties by reducing water binding capacity, swelling and solubilisation of starches. In addition, surface lipids may also create undesirable flavours by oxidation of unsaturated lipid.

2.2.2 Amylose

In amylose, long chains of glucose units are joined together by α-1,4 linkages (Figure 2.3). Amylose forms structures that are mostly straight chains which can form a helix in aqueous environments. The interior of the helix contains hydrogen atoms that allow amylose to form a complex with free fatty acids, alcohols, lipids, or iodine. These amylose complexes are essentially insoluble in water. Amylose is easily leached out from swollen granules when the molecular order within the granule is lost (Liu, 2005).

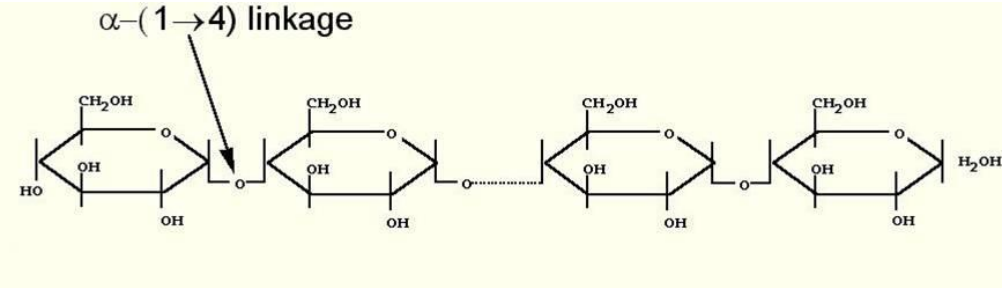

Figure 2.3 An indication of the structure of an amylose molecule.

The proportion of amylose in starch can be determined using several methods. Blue values (absorbance at 680 nm for starch-iodine complex using amylose and amylopectin standards), potentiometric and amperometric titration all are a measure of the amylose-iodine affinity. A typical method is based on the formation of the amylose-iodine complex. The amylose levels by these methods may be influenced by certain factors, such as the starch source, the sample preparation, the molecular

structure of the starch, the long linear chains of amylopectin and monoacyl lipids present in starch (Liu, 2005).

2.2.3 Amylopectin

Amylopectin is a highly branched polysaccharide which consists of α-D-glucopyranose residues linked mainly by several (1→4)-linkages and many non-random (1→6)-linkages to give a highly branched structure (Figure 2.4). According to their chain length and branching points, amylopectin can be categorized into three types, namely A, B, and C chains (Figure 2.5). The A chains are the shortest and carry no branch chains. The B chains are branched by A chains or other B chains (B1, B2, B3) while the C chain carries B chains and contains the sole reducing terminal residue (Liu, 2005). Another feature of amylopectin may be the presence of phosphate monoesters, such as occurs in potato starch, that are covalently linked to the C3 or C6 position of the glucose monomers (Thomas and Atwell, 1997).

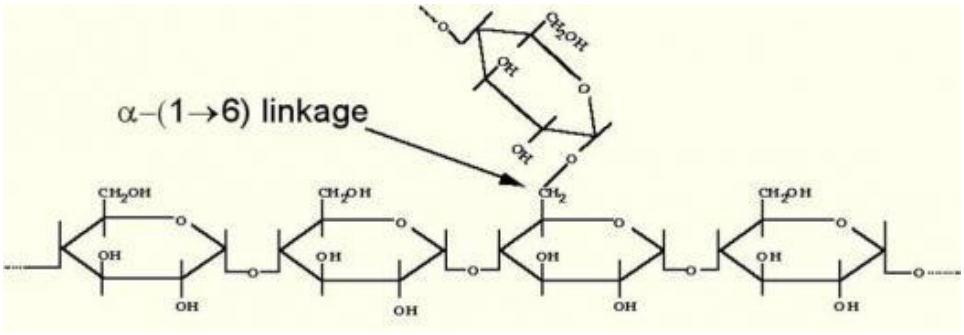

Figure 2.4 An indication of the structure of an amylopectin molecule.

Figure 2.5 shows a schematic of the possible organization of the various chains occurring in amylopectin.

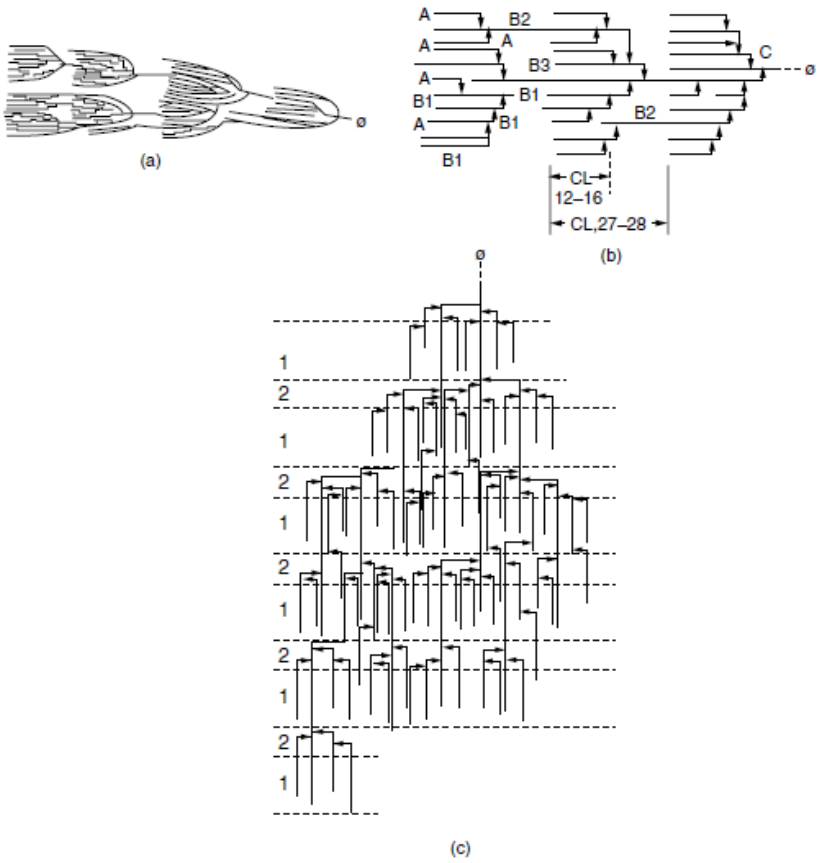

Figure 2.5 Schematic models of amylopectin molecule: In models ø is the reducing end. (A), (B) (B1, B2 and B3), and (C) chains are defined in the text. CL represents chain length. Crystalline and amorphous granular regions are represented by area (1) and (2), respectively. Adapted fom (a) French (1972), (b) Hizukuri (1986), (c) Robin et al. (1974) as quoted in Liu (2005).

The type of structures formed by the A chains of amylopectin to create the crystallinity can be detected by X-ray diffraction (XRD). Starches are composed of two types of polymorph structure, A and B. These polymorphs differ in the packing of double helices into the crystallites; A-type being denser than B-type. Native maize starch and cereal starches have the A-type structure. On the other hand, tuber such as potato and amylose-rich starches are characterised by having B type polymorphs in their crystalline structure, called B-type. The C form is found in certain root, tuber and legume starches which are characterised by having both A and B polymorphs within their crystallites (Zobel et al., 1988; Buléon et

al., 1998). Figure 2.6 shows the standard XRD patterns seen for A- and B-type XRD pattern. For semi-crystalline polymers like starch, methods of crystallinity measurements by X-ray diffraction are usually employed with the background estimated by drawing a smooth curve from tail to tail following the general scope of the continuous background scattering (Frost et al., 2009).

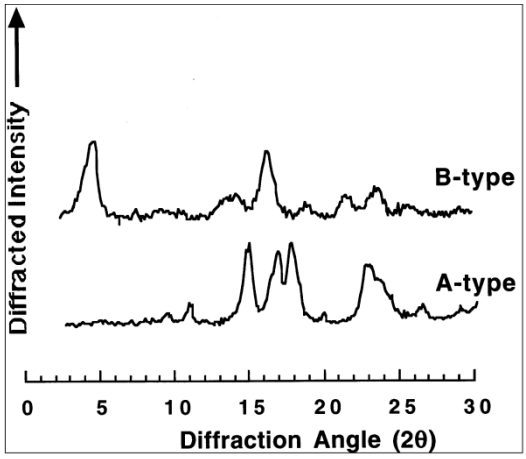

Figure 2.6 Typical X-ray diffraction of native maize starch and native potato starch indicated A and B-type pattern, respectively (adapted from Buléon et al. (1998)).

2.2.4 Morphology of starch granules

Starch is laid down in the plant in the form of granules, which may differ in size, shape, or the position of hilum (the original growing point of the granule). The granules of root and tuber starches generally are voluminous, oval in shape with an eccentric hilum (Pomeranz, 1991; Hoover, 2001). Cereal starches may have polygonal or round shaped granules (Swinkels, 1985). Usually, the size of starch granules is expressed as a range or as the average length of the longest axis. The range of granule size is 2-100 μm (Cui, 2005). Table 2.3 shows characteristics of selected starch granules. Generally, cereal starches have

smaller granules than root starches (Swinkels, 1985). Meanwhile sago starch granules are oval in shape, have a broad size range between 10 and 50 μm in diameter with an average granule diameter of 32 μm (Wang et al., 1995; Ahmad et al., 1999). The granules are generally bigger than those of rice or cassava. The granule surface is generally smooth, but some pitting on some sago starch granules has been observed (Sim et al., 1991).

Table 2.3 Characteristics of some starch granules (Swinkels, 1985).

Starch	Type	Size (μm)	Shape
Tapioca	Root	4-35	Oval, truncated
Rice	Cereal	3-8	Polygonal, angular
Wheat	Cereal	1-45	Round, lenticular
Maize	Cereal	2-30	Round, polygonal
Potato	Tuber	5-100	Oval, spherical

The particle size of starch is one of the most important characteristics of starch granules, which may influence other physicochemical properties such as swelling power, paste clarity, and water-binding capacity (Singh et al., 2003). The size of the starch granule may be important in determining the suitability of the starch for certain food applications.

2.2.5 Swelling behaviour of starch

A starch granule swells when heated in presence of sufficient water. The hydrogen bonds stabilizing the structure of the double helices with the amylopectin in the crystallites are broken and replaced by hydrogen bonds of water (Tester and Karkalas, 1996). As water enters the granule the

overall size of the starch granule increases. Starch swelling is a property of amylopectin, whereas amylose may restrict. It has been suggested that the rigidity of a starch granule might be proportional to its amylose content and inversely proportional to the degree of granular swelling (Lii et al., 1996).

The ability of a granule to take up water and swell may be quantified by its swelling power, which is the weight of swollen starch (Leach, 1967). This property may be very important for certain starch applications like those in the food industry where the quality of starch-based products is strongly related to the capacity of starch granules to retain water and swell. A direct consequence of starch swelling is the increase of its solubility, paste clarity and viscosity (Nemţanu and Braşoveanu, 2010). Several factors, including the ratio of amylose to amylopectin, molecular mass of each fraction, degree of branching, conformation, length of outer branches in amylopectin and also on the presence of non-carbohydrate components such as proteins and lipids, influence the swelling power of the starch granule on the molecular level. Certain starches, for example, maize, rice, and sorghum show restricted swelling compared to the waxy types due to the presence of stronger and a greater number of intermolecular bonds (Leach, 1967).

2.2.6 Gelatinisation and pasting behaviour of starch

The uptake of water by native starch granule below a certain temperature is a reversible process due to the starch's stable semi-crystalline structure. When a suspension of starch granules, in excess of water, is heated above a certain temperature, the starch granule will lose its birefringence and crystallinity and this is concurrent with a major swelling of the granules.

This change is irreversible and is known as "gelatinisation" (Evans and Haisman, 1982). Pasting is the state that follows gelatinisation of starch. During this pasting process, heating continues and more granules become swollen accompanied by an increase in viscosity. There is also an increase in leaching of amylose and amylopectin from granules. When most of the granules have undergone this process, the peak viscosity is reached (Thomas and Atwell, 1997) and further heating and shearing causes a decline in the paste viscosity.

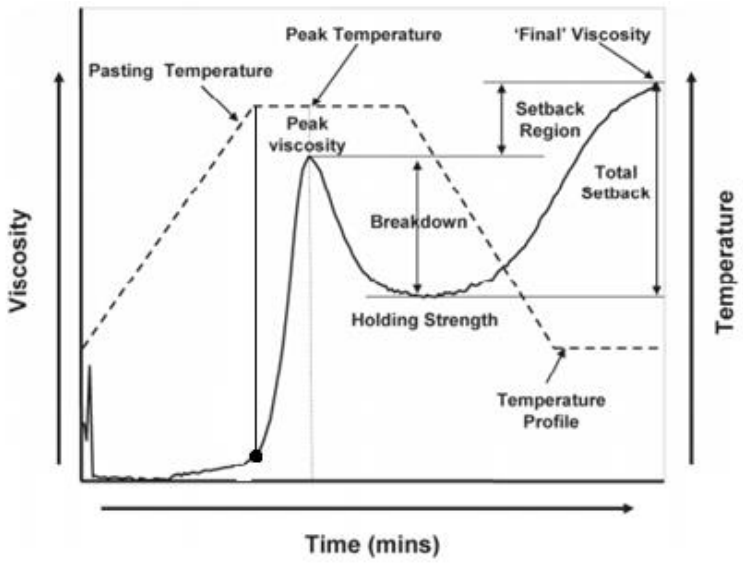

Figure 2.7 Typical Rapid Visco Analyser pasting curve identifying commonly measured characteristic (Saunders et al., 2011).

Pasting viscosity can be recorded using Brabander Viscoamylograph, Rapid Visco Analyzer (RVA) or others viscometers which record continuously the viscosity of pastes as a function of heating, holding and cooling temperatures. Figure 2.7 shows a typical viscosity profile for starch as it is heated and sheared in excess water at concentration of about 9 to 15% starch. The pasting temperature can be defined as the temperature at which the viscosity of the stirred starch suspension begins to rise (as marked on Figure 2.7) (Swinkels, 1985). This temperature indicates when

the granules are swollen enough to impact upon one another and hence markedly influence the viscosity.

Many factors such as amylose leaching, starch crystallinity, amylose and amylopectin chain lengths and friction between swollen granules impact on the pasting properties. This property of starches is very important for starch characterization and their applications. There is also evidence that the pasting properties relate to the molecular size of the starch polysaccharides (Mitchell et al., 1997).

Starch order loss and hence its ability to swell is often measured by a differential scanning calorimeter. A DSC can measure the heat released or absorbed by a material during phase transitions or reactions. Therefore the gelatinisation temperature and energy absorbed by the starch–water systems during hydrothermal treatment of starch can be determined precisely by a production of well-defined plot (thermogram) (Wang and Copeland, 2013).

A typical DSC thermogram for starch is shown in Figure 2.8. The transition temperatures are: the onset temperature (T_o), the intersection point of tangents to the thermogram at the start temperature and the down slope of heat flow; the peak temperature (T_p), the temperature of maximum heat flow; the endset temperature (T_e), which is the intersection point of tangents to the trace at the up slope after T_p and an estimate of the baseline. The heat input/enthalpy change (ΔH) is defined as the area under the line drawn from the start temperature (T_s) to the final temperature (T_f).

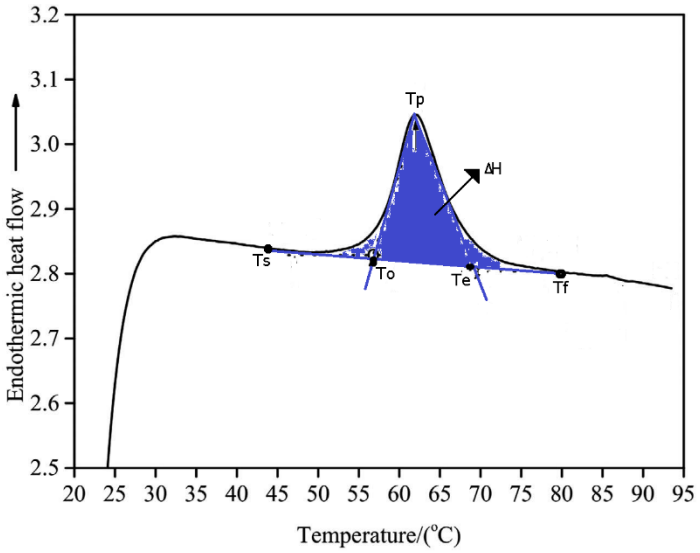

Figure 2.8 A typical DSC thermogram of a starch-water system with a heating rate of 10 °C/min. The letter shown represented the temperature as start (T_s), onset (T_o), peak (T_p), endset (T_e) and final (T_f). Blue area indicated enthalpy change (ΔH). Adapted from Wang et al. (2016) with slight modification.

Furthermore, starch gelatinisation has been investigated extensively by DSC in combination with other techniques. One of the techniques is X-ray diffraction (XRD) (see section 2.2.3 and Figure 2.6).

2.2.7 Relevance of plasticiser level on starch loss of order

Starch undergoes a number of irreversible changes when heated in the presence of water. When sufficient water is present, this phenomenon is referred to as gelatinisation. The gelatinisation involves: 1) hydration of the starch, followed by swelling of the granule; 2) the loss of crystallinity of the granule, as can be observed by the loss of birefringence and the x-ray diffraction pattern; and 3) loss of amylose from the swollen granule. These processes usually take place simultaneously, or nearly so (Donovan, 1979). As the native starch, granules are typically of low moisture content.

The first event is moisture entering the amorphous regions of the starch grains and mobilising the material. The temperature at which the amorphous material becomes less rigid (rubbery) is known as the glass transition temperature (Tg). The Tg and the melting temperature (Tm) of the crystalline fraction of raw dry starch are higher than their decomposition temperature (Nashed et al., 2003). Figure 2.9 shows the effect of water content on Tg of starch in wheat flour.

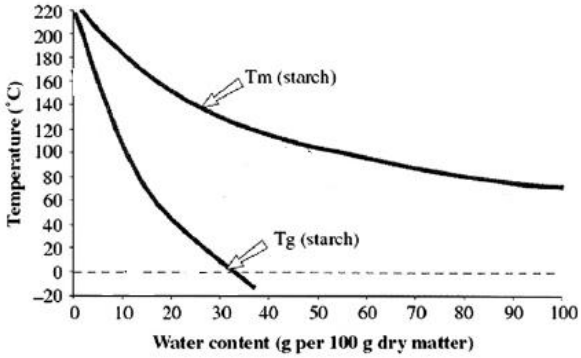

Figure 2.9 Schematic representation of the temperature-water content state diagram for the starch in wheat flour. Tg is the glass transition temperature, Tm is the melting point (Petitot et al., 2009).

A plasticiser, which is a low molecular weight material, can lower the Tg and Tm values of macromolecules. For foods, water often acts to allow mobility of the structuring materials. For starches, the level of water can play a very important role in the gelatinisation temperature as demonstrated by the gelatinisation enthalpies for potato starch at different water levels (Figure 2.10).

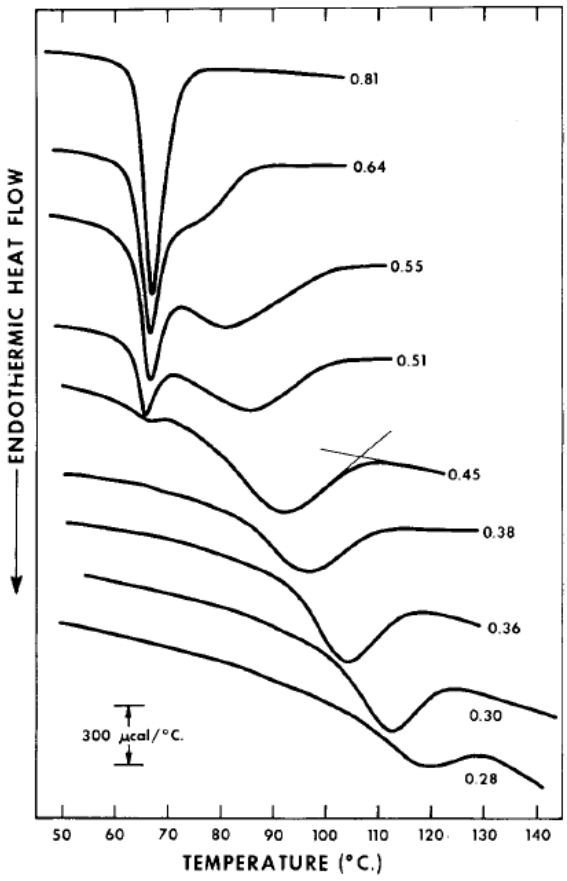

Figure 2.10 DSC thermograms of potato starch obtained at a heating rate of 10°C/min, labelled with volume fraction of water present. Weight of starch (dry basis), from top to bottom: 1.59, 2.05, 3.19, 2.33, 2.62, 2.05, 2.78, 3.99 and 3.30 mg. The intersection of the straight lines drawn in the 0.45 fraction thermogram shows the method of extrapolation to determine Tm. Molar ratios of water to starch for these experiments, from top to bottom, are 24.8, 10.1, 6.97, 6.12, 4.83, 3.64, 3.27, 2.50 and 2.25 (Donovan, 1979).

Another factor relevant to the moisture content of the starches when heated is the movement of the amylopectin and especially the amylose from the constraints of the granule into the continuous aqueous phase. If moisture levels are low, even though the crystal of amylopectin can melt and the amylose chain mobilised, there is insufficient water for granule swelling and bulk movement of the starch macromolecules. In the presence of excess water, the observed phase transition is that of the

disordering of individual starch chains that are being separated ("stripped") from ordered regions of the granules by the swelling action of water. This process is commonly termed "gelatinisation" (Donovan, 1979). When only low levels of water are present, the transition is the "melting" of crystallites in the starch granule; the transition temperature being determined by the amount of water present. In this transition, on the crystallite scale, both the starch chains and the crystallite become disordered.

The term starch conversion may be used as a generic term for the changes in starch and would encompass this type of change. The gelatinisation terminology then can be used for the specific cases where the starches are heated in "excess water" (at least two times the weight of water to starch).

2.2.8 Concept of starch conversion

Starch conversion is defined as a continuum, ranging from the intact crystalline starch granule to monomeric glucose (Mitchell et al., 1997). The behaviour of starch in an excess water environment at different levels of conversion is shown schematically in Figure 2.11. The diagram also suggest the importance of heat, mechanical energy input and the chemical and enzymatic environment as factors that determine the degree of conversion.

Different degrees of starch conversion can be found in different food products. Observation of birefringence and X-ray methods can monitor order or the first levels of starch conversion with the loss of crystallinity. However, these methods cannot determine the degree of starch

conversion between samples. Products that contain starches with no crystalline order as observed by DSC an X-ray methods can have very different behaviour. An example is a comparison between breakfast cereals processed by conventional pressure cooking and extruded cereals. Typically the degree of conversion of extruded cereals is greater than the breakfast cereal because of the greater mechanical energy input, even though the extruded cereals have been subjected to processing at high temperatures for much shorter times than their conventional counterparts (Guy, 1986; Colonna et al., 1989).

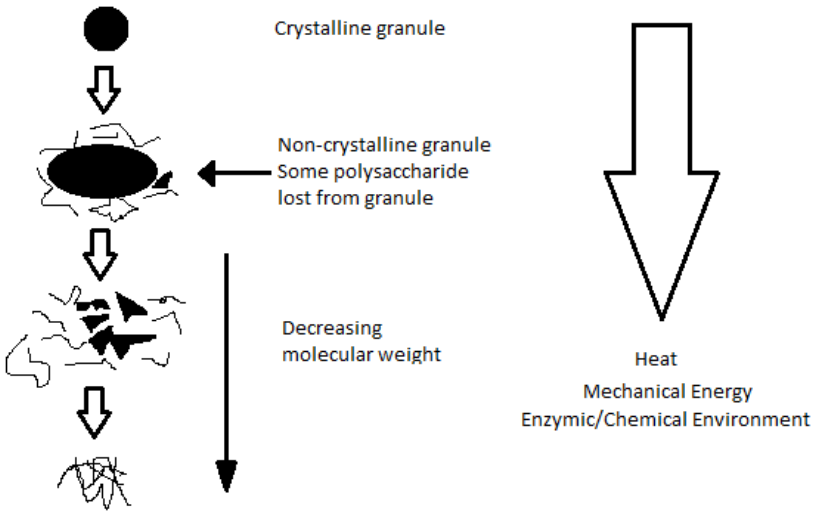

Figure 2.11 The behaviour of starch with increasing levels of conversion in excess water (Mitchell et al., 1997).

The difference in starch conversion can be determined by range of methods. Three that may be helpful are: 1) the water solubility index, which is a measure of the amount of polysaccharide found outside the granule; 2) the water absorption index, which is the volume occupied by the swollen granular phase; and 3) the molecular weight difference, as

monitored by measurements of the intrinsic viscosity of the solubilised starch (Diosady et al., 1985).

The typical conditions in thermomechanical extrusion have low moistures, temperatures that exceed 100 °C and high shear. In these conditions the breakage of starch structures are likely to be dominated by the mechanical forces to which the pre-heated and plasticised starches are subjected. The concept of the starch conversion and the formation of an amorphous mass that can act as bubble walls in an expansion process needs to be applied to understand a directly expanded snack product. The thermomechanical extrusion and direct expansion will be further explained in Chapter 6.

2.2.9 Starch as a food

Starch is a plant polysaccharide which is important for humans. It is the macro-constituent of many foods and the main carbohydrate in the diet that provides energy. Most starch consumed by humans has experienced some form of processing or cooking with water. The rate at which the energy from starches can be assimilated when eaten depends on how they have been processed. Term like "glycaemic index" (GI) gives an indication on how rapidly the carbohydrate can be broken down to low molecular weight (sugar) that then can be absorbed by the human body. Crystalline starches, either due to being native or that the amylose and amylopectin has recrystallized (retrogradation) are normally less readily absorbed than amorphous material. Starches that have been extruded and then directly expanded typically are rapidly digested. This can be considered a positive or negative attribute. For the target consumer of the product to be developed in this work, easily digested starch will be a positive factor in

terms of getting energy for their activity and needs in growing and developing.

In addition to nutritive content, the "liking" of a product is very important for its acceptance. Snack foods with an expanded format result in texture that make them appetising and crisp (Brennan et al., 2013). Thermomechanical extrusion cooking, which is enormously versatile in the production of snacks, would seem a useful processing methods for the creation of a snack based on sago starch which is easily digestible and crisp.

2.3 Extrusion Processing

2.3.1 Introduction to extruder and extrusion cooking

Extrusion cooking is an important processing technique in the food industry and has been used since the mid-1930 for the production of breakfast cereals, ready to eat snack foods, and other textured foods. High temperature, high pressure and short time duration are typical conditions for a hot/cooking extrusion processes (Harper, 1981). Food extrusion is a process in which food ingredients are forced to flow, under one or several conditions of mixing, heating and shear, through a die that forms and/or puff-dries the ingredients. Food extruders can be visualised as devices that can transform a variety of raw ingredients into intermediate and finished products. The cooking temperature can be as high as 180–190 °C (355–375 °F) during extrusion, but residence time is usually only 20–40 s (Riaz, 2001).

During extrusion cooking, the raw materials may undergo many chemical and structural transformations, and in the case of starch, for example, loss of original crystalline order, polymer degradation and complex formation between amylose and lipids can occur (Ilo and Berghofer, 1999). Chemical reactions such as degradation of vitamins and pigments may also impact on food quality. Extrusion processing characteristics such as extruder type, screw configuration, feed moisture and temperature profile in the barrel sections, screw speed and feed rate can influence the variety of qualities of the extruded product (Ding et al., 2005). Extrusion cooking is considered as versatile, having a high productivity with low operating

costs, being energy efficient with shorter cooking times than traditional cooking methods (Brennan et al., 2011).

2.3.2 General design features of an extruder

There are several possible designs and types of food extruder, operating over a wide range of conditions. A typical extruder is structured with a motor, feeder, barrel, screw, die and control panel (Harper, 1981). A schematic of a cross-section through a typical food extruder can be seen in Figure 2.12. Shear energy is produced in the barrel section with the help of the screws' rotating action. The pressure inside the barrel rises with the effect of shear energy and high temperature of extrusion. This causes food material to undergo chemical and rheological changes.

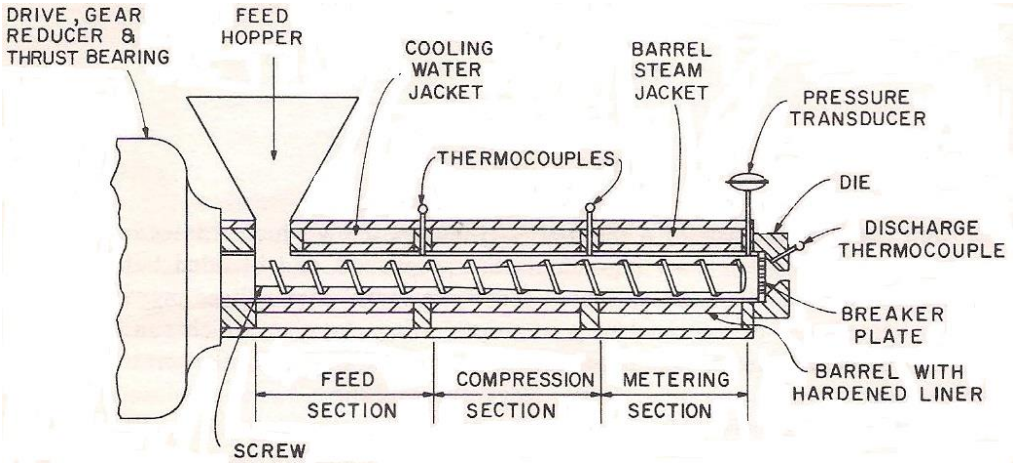

Figure 2.12 Cross section of a typical food extruder (Harper, 1981).

Many biopolymers will melt within the extruder barrel. Starch will lose its granule structure and crystallinity to form a homogenous amorphous melt under the correct extrusion conditions. This viscous mass undergoes significant shear forces as it is forced along the barrel to the die. Water cannot turn to steam within the extruder barrel and has a major influence

on the viscosity of the molten starch mass. At the die the pressure is atmospheric and the emerging hot melt will rapidly dehydrate as the water turns to steam. Puffed and porous directly expanded products are a consequence of evaporation of water and concomitant expansion of the extrudate when the food material leaves the barrel through a die and experiences a rapid pressure drop. The die also presents the final shape of extrudate. The resistance the food material encounters at the exit depends on the diameter of the hole in the die; where the smaller the size, the higher the resistance which increases the inside pressure and also causes more backflow of the food material (Moscicki and van Zuilichem, 2011).

2.3.3 Screw elements

Depending on the function an extruder can be designed in several different ways, but the extruder is often categorised by the number and type of screw design used. This is shown in Figure 2.13.

Twin-screw extruders consist of two screws in its barrel of equal length, whereas if the extruder has only one screw it is a single-screw extruder. The screws contain flights and these move and compress the material being extruded. The terminology used to define the screws and flights is given in Figure 2.13 and Figure 2.14. A single-screw extruder usually has a one piece screw with a variable depth, but constant pitch, or a modular screw with a constant channel and variable pitch. The mixing function of a single-screw can be limited because of the laminar flow conditions that can be induced, but this can be improved by the addition of mixing screw elements in the design of the total screw components (Harper, 1989; Riaz and Rokey, 2012).

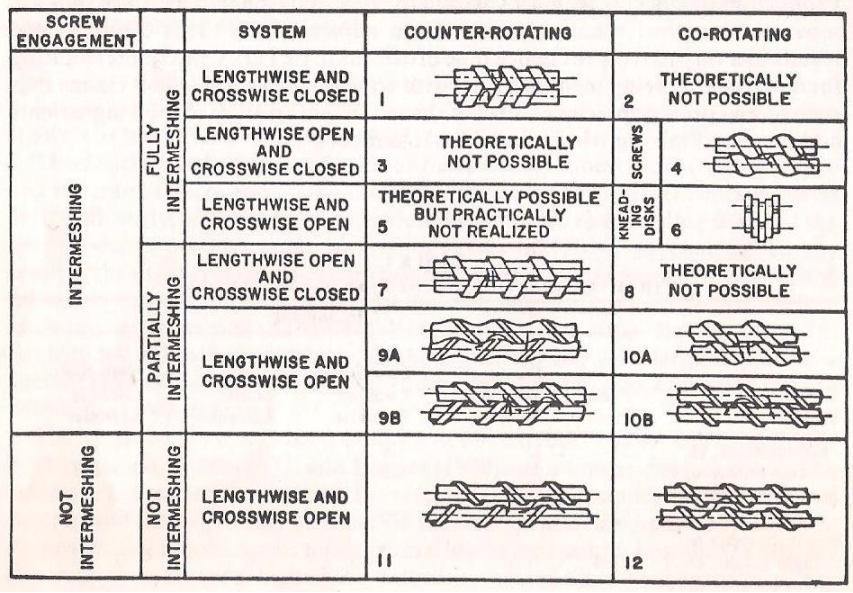

Figure 2.13 Various screw configurations used in twin-screw extruders screw designs (Ziminski and Eise (1980) as quoted in Harper (1989)).

Based on the configuration and rotation of the screws, twin-screw extruders are grouped as intermeshing or non-intermeshing, and co-rotating or counter-rotating. An intermeshing twin-screw extruder is the type where the screws penetrate each other; otherwise, it is non-intermeshing. Meanwhile, the direction of the screws' rotation determines the classification of co-rotating and counter-rotating, being in the same or opposite direction, respectively (Giles et al., 2005; Riaz and Rokey, 2012). The counter-rotating screws tend to get blocked by solids and have poor mixing abilities. Today most food extruders are of the co-rotating design. The equipment used for the work described in this thesis was a twin-screw co-rotating and fully intermeshing extruder.

All extruders consist of a screw(s) which conveys the premixed ingredients through the barrel. Regardless of whether the machine is single- or twin-screw type, several principles apply. Screws generally are suspended only from the drive end of the barrel and rest on the product at the exit (die)

end. As a result, the greatest stress and wear on the screw and barrel occur at the exit, and these parts need refurbishing or replacement first. Except for very small or old extruders, both the screw and barrel are segmented (Riaz, 2001).

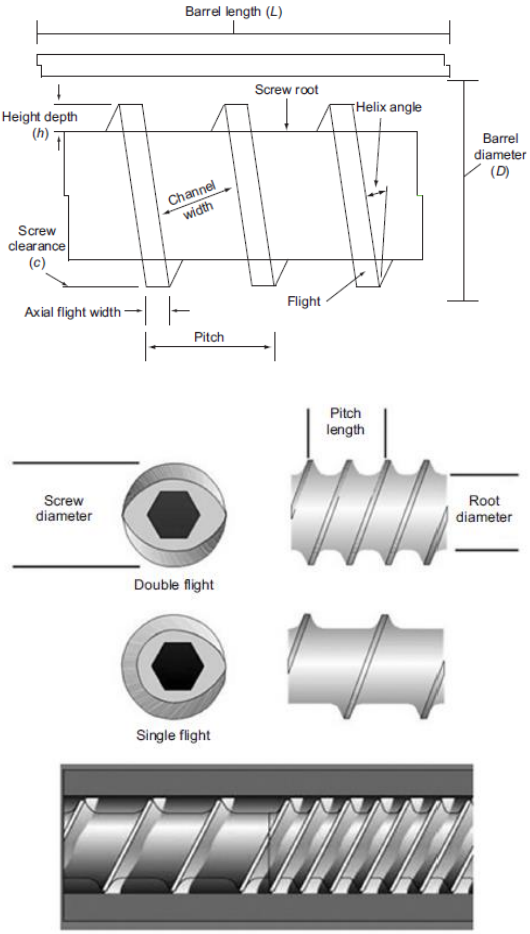

Figure 2.14 Screw terminology and the elements (Riaz and Rokey, 2012).

Screws can be made in one piece, but most are constructed of a central spline onto which different screw elements are attached. The screw is usually a cylindrical or conical shape, around which the flight is wound (Riaz and Rokey, 2012), see Figure 2.14. Many different screw configurations can be achieved by choice of the pitch, channel width and screw root, in addition there can be cut-outs in the flights where the

product can pass through. Assembly of the different elements can also be varied. The choice of screw and flight design is based on the following functions along the barrel: feeding, compression, and metering.

2.3.4 Twin-screw extruder

In the mid-1970's the use of twin-screw extruders for the combined process of cooking and forming of food products was introduced and developed. This development was partly as an answer to the restrictions of single-screw extruder equipment in terms of its inability to handle the ingredients at higher moisture levels, poor mixing and inadequate thermal control and partly because the twin–screw extruders tend to give better results on scale up from the laboratory extruder types to use for product development (Moscicki and van Zuilichem, 2011). However, the drawback of twin-screw extruders is their complex design and high cost (Riaz and Rokey, 2012).

A typical twin-screw extruder design is shown in Figure 2.12. In intermeshing co-rotating twin-screw extruders, the screws partially overlap each other in a figure '8' barrel track, resulting in positive pumping, efficient mixing and self-wiping action. These extruders are like a positive displacement pump, forcing material between the barrel and the screws to move product towards the die by the rotation of the screws (Riaz, 2001).

Twin-screw extruders were originally developed for processing plastics. They have been used for products that could not be made with single-screw machines like sticky caramels and candies. Currently, twin-screw extruders are being utilised for many different foods and feed items; even

those that are very viscous, oily, sticky or wet. Additionally, twin-screw extruders can handle recipe ingredients with wide ranging particle sizes with the direct fed into the extruder. A preconditioner can be used to pre-hydrate and heat the ingredients but this showed not be necessary for a starchy direct expansion snack (Riaz, 2001).

2.3.5 Extrusion cooking

Extrusion cooking involves three key steps. First is feeding and mixing, the raw material is fed into a hopper and then into the barrel. The second stage is kneading, where the mixture is forced to flow through the passage between a rotating screw(s) and a stationary barrel. The third step is metering, this section is just before the die where the material typically undergoes high shear. This is where the well-mixed ingredients are compacted and fill the screws and are pressurised against the end of the barrel before exiting through a small die (Riaz and Rokey, 2012).

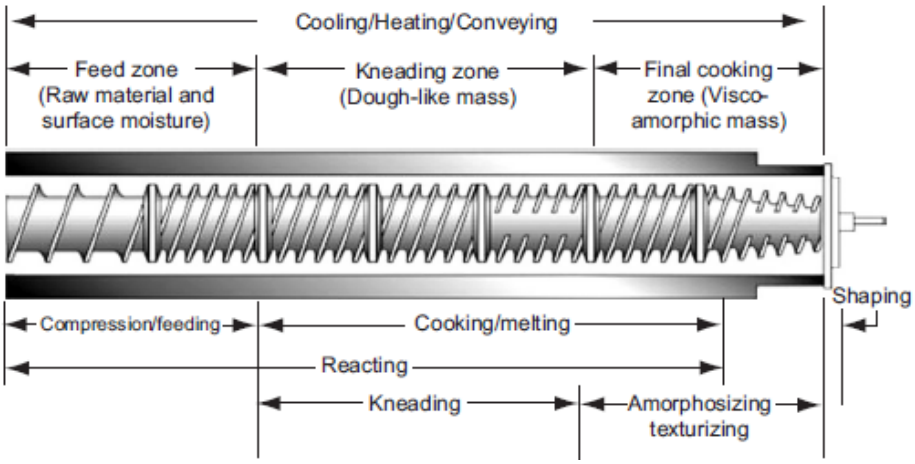

Figure 2.15 Processing zones in an extruder (Riaz and Rokey, 2012)

The three steps correspond to the three general processing zones in the barrel in a single- and twin-screw extruders (see Figure 2.15). The

combination of all three steps determines the physical attributes of the final product (Akdogan, 1999). Extrusion parameters and product properties are significantly dependant on the extrusion variables, composition and particle size distribution of the feed material (Ryu et al., 1993).

The preconditioned or dry material enters the feeding zone which has deep channels to receive the feed. The materials are then conveyed to the kneading zone. Water may be injected at this point to help develop a dough and improve heat transfer in the extruder barrel. The density of materials increases because of water and steam addition when the material is conveyed into the kneading zone. The screw pitch and the flight angle decreases to facilitate mixing and a higher degree of barrel fill. This zone applies compression, mild shear and thermal energy to the feedstock. At this point, the extrudate, if it is starch-based, begins to lose some of its granular integrity. The feed material should be a viscoamorphic mass at or above 100 °C by the end of this zone (Faubion et al., 1982). The mechanism of shear begins to play a dominant role because the barrel should be fully filled in this zone. Steam injection, which increases thermal energy and the moisture content of the extrudate, can be injected in the early part of this zone. The material begins to form an increasingly cohesive flowing dough mass as it moves through the kneading zone. This condition typically reaches its maximum compaction and exhibits a rubbery texture similar to a very warm dough. The material then enters the extruder final cooking zone at this stage. The typical screw flights in this zone are shallow and with a short pitch. In this zone, the material is compressed and pumped in the form of a plasticized mass to the die. Due to the extruder screw configuration, temperature and pressure typically increase very rapidly in this zone. Another variable,

shear, is highest in this zone, and product temperature reaches its maximum and is held for less than 5 s before the product is forced through the die (Harper, 1981). Moisture vaporisation results in the expansion of the product as it exits through the die into a region of lower pressure. The extrudates can then be cut into desired lengths by the knife attachment (Riaz and Rokey, 2012).

2.4 Conclusion

2.4.1 Summary

Starch shows change from a viscoelastic mass that can flow into a solid mass as the water is lost and the product cools. On solidification the bubbles cannot expand, but the walls will retain their shape once the steam is no longer providing a positive pressure. The size of the bubbles, the thickness of the bubble walls and the viscosity will provide the textural eating quality. Twin-screw extrusion should provide the thermal and mechanical shear that is required to break down the native structure of a starch to form an amorphous melt. This melt can then be expanded by the steam generation on exiting the die.

2.4.2 Aims

A range of starches have been used in thermomechanical extrusion to provide the necessary characteristics of the successful snack products. The objective now is to ascertain if these can be achieved with sago starch.

CHAPTER 3
Materials and Methods

This chapter outlines all of the materials utilised in this research and analytical methods applied throughout. Processing and analytical methods that only apply to: 1) characterisation of the physicochemical properties of sago, rice and cassava starches (Chapter 4); 2) evaluation of sago starch by capillary rheometry (Chapter 5); or 3) in the research concerned with extrusion processing (Chapters 6 and 7) are described in the relevant chapters.

3.1 Materials

3.1.1 Starches

Three types of starches were used in this research: sago, rice and cassava. Sago starch was donated by PT Riau Sago Lestari (Indonesia). Rice starch was purchased from Sigma-Aldrich (Gillingham, UK) and cassava starch was supplied by Ingredion (Manchester, UK). The starches were used as received.

3.1.2 Main additives

Extrudates were fortified with iron as ferrous sulphate heptahydrate ($Fe_2SO_4.7H_2O$) and ascorbic acid was used to adjust the colour. The iron additive and ascorbic acid were purchased from Fischer Scientific, UK and

Sigma-Aldrich, UK, respectively. Both additives met the analytical specification of the Food Chemical Codex. They were used as received.

3.1.3 Chemical reagents and kits

Chemical reagents including dimethyl sulphoxide (DMSO), ethanol, sodium azide (all analytical grade), acetic acid glacial and sodium hydroxide (both certified ACS) were from Fischer Scientific, Loughborough, UK. Sodium acetate, sodium chloride (both analytical grade), calcium chloride dihydrate ($CaCl_2.2H_2O$), magnesium chloride hexahydrate ($MgCl_2.6H_2O$), manganese(II) chloride tetrahydrate $MnCl_2.4H_2O$ (all puriss p.a. grade) and glycerol for microscopy observation and pasting properties of ground extrudates (certified ACS) were from Sigma-Aldrich, Gillingham, UK. The Megazyme kits for amylose/amylopectin assay were acquired from Megazyme International Ireland, Bray, Ireland. The kits contained: freeze dried Con A, amyloglucosidase plus fungal α-amylase, glucose oxidase reductase (GOPOD) reagent buffer, GOPOD reagent enzymes, and a starch reference sample (with specified content of amylose) (all kits are analytical purity grade).

3.1.4 Solutions used for Megazyme assay kits for determining amylose content of the starch

3.1.4.1 95% (v/v) ethanol in water solution

Deionised water (5 mL) was added to 95 mL of analytical grade ethanol (99%) in order to make up 95% (v/v) ethanol in water solution. The solution was stored at 4 °C.

3.1.4.2 Concentrated Conconavalin A (Con A) solvent (600 mM in acetate, pH 6.4)

Anhydrous sodium acetate (49.2 g) was added to 175.5 g of sodium chloride, 0.5 g of $CaCl_2.2H_2O$, 0.7 g of $MgCl_2.6H_2O$ and 0.7 g of $MnCl_2.4H_2O$ in 900 mL of deionised water. The pH was adjusted to 6.4 by dropwise addition of glacial acetic acid then the volume was adjusted to 1 L with deionised water. The solvent was stored at 4 °C for up to 2 weeks.

3.1.4.3 Con A solvent (working concentration)

Concentrated Con A solvent (30 mL) as prepared above was diluted to 100 mL with deionised water. This solution at working concentration was used on the day of preparation and not stored for future use.

3.1.4.4 Sodium Acetate buffer (100 mM, pH 4.5)

To make the buffer, 5.9 mL of glacial acetic acid (1.05 g/mL) was added to 900 mL of deionised water. The pH was adjusted to 4.5 by the addition of 1 M (4 g/100 mL) sodium hydroxide solution (approximately 30 mL is required). To preserve the solution, 0.2 g of sodium azide was added and the volume was adjusted to 1 L. This buffer solution was stored at 4 °C and was stable for up to 2 years.

3.2 Processing Methods

The detail of processing methods especially for capillary rheometer and extrusion cooking are described in the methods section in each relevant chapter (Chapter 5, 6 and 7).

3.3 Analytical Methods

The analytical methods given below were used in several of the results chapters (Chapter 4, 5, 6 and 7).

3.3.1 Moisture content

Moisture content for materials and extrudates were determined by standard oven drying, adapted from Bradley (2003). Weighed samples (1 - 2 g) were put into pre-weighed aluminium foil cups and dried for approximately 24 h to constant weight in a drying oven (Memmert, Schwabah, Germany) set at 105 °C. Upon removal from the drying oven, samples were re-weighed on a Sartorius MC 1 Analytic AC 120 S analytical balance (Sartorius, Epsom, UK). The moisture content of samples was then calculated based on wet weight basis.

3.3.2 Amylose content

The method used on this assessment was based on the Megazyme commercial kit procedure (K-AMYL 07/11) (Megazyme International Ireland, Bray, Ireland) and adapted from Gibson et al. (1997). The general steps in the assay will first be described followed by the exact required action. Samples were first treated in dimethyl sulphoxide (DMSO) to solubilise the starch. Lipids were removed by precipitating the sample in ethanol and recovering the precipitated starch. The precipitated sample was re-solubilised in DMSO followed by addition of the concentrated Con A solvent. The amylopectin could then be specifically precipitated by conconavalin A (Con A) and removed via centrifugation. An aliquot of the supernatant containing amylose was enzymically hydrolysed into glucose, which was analysed using the glucose oxidase/peroxidase reagent

(GOPOD). A separate aliquot of the total starch sample in the salt/acetate solution was hydrolysed into glucose and measured spectrophotometrically. The amount of amylose in the sample was estimated as the ratio of the GOPOD absorbance of the supernatant from the Con A precipitated sample (containing only amylose) to the absorbance of the total starch solution (containing both amylose and amylopectin) (Megazyme International Ireland, Bray, Ireland). At least two standard reference starch samples of known total amylose content were run during each experimental procedure.

3.3.2.1 Starch pre-treatment and preparation

About 20-25 mg of sample (to the nearest 0.1 mg) was weighed into a 14 mL glass test tube (15 mm x 100 mm). 2 mL of DMSO was added to the tube, which was being continuously stirred on a vortex mixer (Heidolph REAX top, Heidolph, Schwabach, Germany) at medium speed to high speed. The tubes were then heated in a boiling water bath (Mickle Laboratory Engineering Co., Surrey, UK) with regular intermittent stirring to ensure no gelatinous lumps of starch remained. If any signs of non-dissolved gel occurred, the samples were mixed and heated again. Once it was certain the sample did not contain gel lumps, the test tubes were placed into a boiling water bath and heated for 15 min with further intermittent high-speed stirring on a vortex mixer. After heating and mixing, the tubes were stored at room temperature for approximately 5 min before 4 mL of 95% (v/v) ethanol (prepared according to section 3.1.4.1) was added with continuous vortex mixing. A further 6 mL of ethanol was added and the tubes were capped with parafilm and inverted to mix in order for a precipitate to form. The tube was allowed to stand for 15 min at room temperature. The tubes were then centrifuged at 2,000 x*g* for 5 min on a JOUAN CR3i multifunction centrifuge (Thermo Fisher

Scientific, Hamphshire, UK). The supernatant was discarded and tubes were drained on a tissue paper for 10 min. The tubes were gently rotated to ensure all the ethanol had drained. The pellet was used in the subsequent amylose and starch determinations. With gentle Vortex mixing, 2 mL of DMSO was added to the starch pellet and the tubes were capped with parafilm. The tubes were then placed in a boiling water bath for 15 min and mixed occasionally with intermittent vortex mixing to ensure that there are no gelatinous lumps. The tubes were then removed from the boiling water bath, and 4 mL of Con A solvent (prepared according to section 3.1.4.3) was immediately added and mixed thoroughly. The contents of the sample tube were then quantitatively transferred (by repeated washing with Con A solvent) to a 25 mL volumetric flask. The sample solution was made up to the volume with Con A solvent (this is solution A). This solution A was analysed within 2 h and not left for an extended period as the amylose would tend to retrograde.

3.3.2.2 Con A Precipitation of Amylopectin and Determination of Amylose

A 1 mL of solution A was transferred to a 2 mL microfuge tube (Sarstedt, Nümbrecht, Germany) then 0.5 mL of Con A solution (hydrated as described in the Megazyme kit instruction) was added, capped and gently mixed by repeated inversion. Frothing of the sample was avoided. The tube was allowed to stand for a 1 h at room temperature. The tube was then centrifuged using a HERAEUS Fresco 21 bench-top centrifuge (Thermo Fisher Scientific, Haphshire, UK) at 14,000 x*g* for 10 min at 25 °C. After removal from the centrifuge, 1 mL of the supernatant was transferred to a 15 mL centrifuge tube (Sarstedt, Nümbrecht, Germany).

3 mL of 100 mM sodium acetate buffer, pH 4.5 (prepared as described in section 3.1.4.4), was added to the centrifuge tube and the tube was lightly capped. The tube was then heated in a boiling water bath for 5 min to denature the Con A. The tube was then placed in a water bath (DMU26 water bath, Fisher Scientific UK, Loughborough, UK) at 40 °C and allowed to equilibrate for 5 min. Amyloglucosidase/α-amylase enzyme mixture (0.1 mL) (hydrated as described in the Megazyme kit instruction) was added to the tube and incubated at 40 °C for 30 min in a water bath. The tube was then centrifuged at 2,000 x*g* for 5 min. GOPOD Reagent (hydrated as described in Megazyme kit) was added (4 mL) to 1 mL aliquots of the supernatant and the tube was incubated at 40 °C for 20 min. The reagent blank and the D-glucose controls were incubated concurrently as well as the total starch samples (as prepared according to the procedure below). The reagent blank was prepared by adding 1 mL of 100 mM sodium acetate buffer to 4.0 mL of GOPOD reagent and incubated at 40 °C for 20 min. Duplicate D-Glucose Controls were prepared by comprising 0.1 mL of D-glucose standard solution (1 mg/mL), 0.9 mL of sodium acetate buffer and 4 mL of GOPOD reagent. This value was not used in the calculation; however, this was performed to ensure that there were no problems with this part of the assay (Megazyme International, Bray, Ireland). The absorbance of each sample and the D-glucose controls were read at 510 nm against the reagent blank using a CARY 50 Probe UV-Visible Spectrophotometer (Varian, Palo Alto, USA).

3.3.2.3 Determination of total starch

In 14 mL glass test tubes, 0.5 mL of solution A (prepared in section 3.3.2.1) was mixed with 4 mL of 100 mM sodium acetate buffer, pH 4.5. The amyloglucosidase/α-amylase solution was added to the tube (0.1 mL) and the mixture was incubated at 40 °C for 10 min. 1 mL aliquots of this

solution was transferred (in duplicate) to 14 mL glass test tubes, and 4 mL of GOPOD reagent was added and the tube mixed well. The tubes were then incubated at 40 °C for 20 min concurrently with the samples and standards from the amylose assay as described above.

3.3.2.4 Calculation of the amylose-amylopectin ratio

$$\text{Amylose, \% (w/w)} = \frac{\text{Absorbance (Con A supernatant)}}{\text{Absorbance (total starch aliquot)}} \times \frac{6.15}{9.2} \times \frac{100}{1}$$

$$= \frac{\text{Absorbance (Con A supernatant)}}{\text{Absorbance (total starch aliquot)}} \times 66.8 \qquad (3.1)$$

Where 6.15 and 9.2 are dilution factors for the Con A and total starch extracts respectively (Amylose/amylopectin assay procedure, K-AMYL 07/11).

3.3.3 Protein, total fat and phosphorus content

The quantification of the protein, total fat, total carbohydrates, phosphorus and ash content of the starches was outsourced to an external laboratory (Eurofins Food Testing UK Limited, Wolverhampton, UK). Protein was determined using a Nitrogen analyser, total fat by acid hydrolysis, ash by muffle furnace, total carbohydrate by calculation and the method of Inductively Coupled Plasma-Optical Emission Spectrometer (ICP-OES) was applied to quantify phosphorus.

3.3.4 Particle size analysis

The particle size distributions of the dry starch samples were acquired with a laser diffraction particle size analyser (LS 13 320, Meritics, Beckman Coulter Inc., High Wycombe, UK) fitted with dry module (Beckman Tornado Dry Powder System, Meritics, UK). About 3 - 4 g of sample was

placed to the tube kit to run the analysis. The measuring regime used for each sample was as follows: rinsing, measuring offset, rinsing, measuring sample (3 times at 1 min each) followed by another rinse. The instrument was "rinsed" repetitively with garnet abrasive (G35, nominal 35 μm Garnet Particles, Beckman Coulter) between samples. Three replicates were taken for each sample and data obtained was used to plot particle size distributions based on volume density with the differential volume (%) on the y-axis versus particle diameter (μm) on the x-axis. The volume distributions were analysed for D10, D50, D90 and D[4,3], respectively. D10, D50, and D90 are the 10%, 50%, and 90% cut-off point as the diameter where 10%, 50% and 90% of the distribution lies below these values respectively. D[4,3] is the mean diameter on a volume basis. Span that indicated the width of granule size distribution was also calculated, see Equation (3.2) (Horiba Instruments, 2012).

$$\text{Span} = \frac{\text{D90} - \text{D10}}{\text{D50}} \tag{3.2}$$

3.3.5 Granule morphology and Birefringence

Morphology of the starch granules and birefringence of ground extrudates were observed using a light microscope employing brightfield illumination and polarized light (Leitz-Diaplan, Ernst Leitz Wetzlar GMBH, Germany) fitted with a PixeLINK PL-A662 digital camera (Pixelink, Ottawa, Canada). Samples were prepared by placing a small amount of starch powder (about 0.1 g) onto a flat microscope glass slide using a fine spatula. This was followed by addition of one drop of deionised water for dry starch (and with glycerol for ground extrudates) using a disposable Pasteur pipette and the sample was dispersed evenly using a fine spatula. The sample was then gently covered with an 18 mm × 18 mm glass cover slip

and viewed immediately under the microscope. Birefringence of the sample was observed using an attached circular polarising filter. Images were taken using 40× magnification based on the size of the starch granules.

3.3.6 Swelling power

The swelling power of starches was obtained using the mass balance method modified from Leach et al. (1959) and Crosbie (1991). To determine swelling power, dry starch samples (0.3 g ± 0.001 g) were loaded into centrifuge tubes and 30 mL of deionised water was added into each tube using a rapid dispensing pipette (Eppendorf Multipipette® Xstream). The cap was fitted and the contents of the tube were mixed immediately to avoid lump formation within the sample. The tube was then placed in a constant temperature water bath (DMU26 water bath, Fisher Scientific UK, Loughborough, UK) at 95 ± 2 °C and mixed by gently inversing twice at intervals of 20 s for the first 3 min when the sample was gelatinised as indicated by clear appearance. Then mixing took place at 30 s intervals for 2 min, then every 1 min for 5 min, and every 5 min up to a total time of 30 min. Once removed from the water bath, the tubes were immediately placed on ice until they had cooled to room temperature. The sample tubes were then put into a 25 °C water bath for 5 min before being centrifuged at 1,000 x*g* for 20 min (JOUAN CR3i multifunction centrifuge, Thermo Fisher Scientific, Hamphshire, UK). The supernatant was removed into pre-weighed aluminium foil cups using a disposable plastic Pasteur pipette and the weights of the swollen granules were recorded. Three replicates were carried out for all starches. The supernatant was weighed before being dried in an oven (Memmert, Schwabah, Germany) at 105 °C overnight. The swelling power was calculated as the ratio of the weight of

the wet swollen granules to the dry weight of the starch sample after correcting for the weight of soluble dry matter from the supernatant using Equation (3.3) and is expressed as grams of swollen sample per gram of dry weight of sample (dry basis).

$$\text{Swelling power (g/g)} = \frac{\text{Weight of swollen sample}}{\text{Weight of dry (original) sample} - \text{Weight of dried supernatant}} \quad (3.3)$$

3.3.7 Pasting properties

Pasting profiles were acquired for suspensions of native starches and for suspensions of ground extrudates using the Rapid Visco Analyser (Model RVA Super 4, Newport Scientific Pvt Ltd, Warriewood, Australia). Standards aluminium canisters with the recommended corresponding plastic paddles were used. All samples were measured using profiles written and configured using the preloaded software for the RVA unit, Thermocline for Windows version 2.4 (Newport Scientific Pvt. Ltd., Warriewood, Australia). Numerical results including parameters such as peak or cold peak, final and setback viscosities and pasting temperatures were obtained using the software.

3.3.7.1 'Standard 1' profile

Native starches were weighed into RVA aluminium samples canisters and dispersed in deionised water at 12.5% w/w dry weight basis and 28 g total sample weight. Stirred viscosity was then measured using the default 'standard 1' profile; starting temperature of 50 °C for 1 min followed by gradual heating to 95 °C over 4 min, holding at this temperature for 2 min, cooled down to 50 °C over 4 min, and finally held at 50 °C for 2 min.

The stirrer was set to rotate at 960 rpm for the first 10 s and then at 160 rpm throughout the remainder of the 13 min test. The intervals between readings were 4 s. The experiment was repeated three times, and results are shown as means (centipoise) ± SDs.

3.3.7.2 'Extrusion with ethanol' profile

The ground extrudates were prepared as in the standard 1 profile, but 1 mL of ethanol was added before addition of water. After adding ethanol to the canister, the sample was pre-mixed by hand using the paddle to avoid any lumps before adding the water. The 'extrusion with ethanol profile' had an initial stirring rate at 960 rpm for 10 s followed by constant stirring rate at 160 rpm for 20 min. For the first 2 min, the sample was held at 25 °C followed by gradual heating to 95 °C over 5 min. The sample was then held at 95 °C for 3 min and then gradually cooled down to 25 °C over 7 min. Finally, the sample was held at 25 °C for 3 min. The total test duration was 20 min with 4 s intervals between readings. The experiment was repeated three times, and results are shown as means (centipoise) ± SDs.

3.3.8 Thermal properties

The thermal properties of native and processed starch samples were determined in excess of water using a differential scanning calorimeter (DSC). The DSC quantifiably measures the temperatures and transitions that occur during the heating of a sample, when it is cooled or held isothermally (Gabbott, 2008). The measurements were made using a DSC-823e (Mettler-Toledo, Columbus, OH, USA) which was coupled with a sample robot (TS0801RO Mettler Toledo, Columbus, OH, USA). Heat flow and temperature were calibrated using pure indium.

The starch samples were mixed with water at a starch:water ratio of approximately 1:3 directly into the pre-weighed stainless steel sample pans. These were then hermetically sealed and reweighed. All sealed samples were equilibrated at room temperature for at least 12 h to allow sample hydration, before being heated at 10 °C/min from 20 to 100 °C in order to observe the presence of any residual enthalpy gelatinisation peaks. Temperature profiles and enthalpy of samples (expressed as J/g of dry sample) were determined using the instrument's software (Mettler Toledo STARe default DB analysis programme software version 9.0). For Chapter 4, the measured onset (T_o), peak (T_p) and endset (T_e) temperatures were associated with starch gelatinisation and retrogradation (reheated of gelatinised starch after being stored at 4 °C for seven days). Meanwhile, the degree or percentage (loss) of transformation of starch (x) that described in Chapter 5, was determined by using the decrease of the DSC endotherm area, a measure of the mass of unconverted starch, and expressed by:

$$x = \frac{\Delta H_0 - \Delta H}{\Delta H_0} \times 100\% \qquad (3.4)$$

Where ΔH_0 is the gelatinisation enthalpy of native raw starch (J/g) and ΔH is the gelatinisation enthalpy of the processed sample (J/g).

3.3.9 Colour properties

The colour of the sago extrudates was measured using a benchtop spectrophotometer (ColorQuest XE, HunterLab, Virginia, USA). The colour of a sample was denoted by the three dimensions; L^*, a^* and b^* and were recorded using Universal HunterLab's software. The L^* value gives a measure of the lightness of the product from zero for black to 100 for perfect white. The values a^* and b^* have no scale and can assume

positive and negative values. A positive *a** value is a measure for redness, a negative *a** value indicates greenness. Yellowness and blueness is quantified by a positive and a negative *b** value, respectively. A light and white calibration plate was used to standardize the equipment prior to colour measurements. Extrudate samples were cut longitudinally, and the colour was measured in three places of each sample. Measurements were taken on 10 randomly selected pieces of extrudates and the results are reported as mean ± standard deviation.

3.3.10 Expansion ratio

The expansion ratio of the extrudates was determined as the ratio between the diameter of the extrudates and the diameter of the die exit (Gujska and Khan, 1990). A digital Vernier calliper was used to measure the diameter of the extrudates and expansion ratio was calculated as:

$$\text{Expansion ratio} = \frac{\text{diameter of the extrudate}}{\text{diameter of the die nozzle}} \tag{3.5}$$

Measurements were taken on 10 randomly selected pieces of extrudates and the results are reported as mean ± standard deviation.

3.3.11 Bulk density

Density (ρ) in g/cm^3 was determined according to the method of Alvarez-Martinez et al. (1988) by measuring the diameter (d) in cm, length (L) in cm and weight (m) in gram of each extrudate.

ρ was then calculated as:

$$\rho = \frac{4m}{\Pi d^2 L} \tag{3.6}$$

Measurements were taken on 10 randomly selected pieces of extrudates and the results are reported as mean ± standard deviation.

3.3.12 Hardness and Crispness

Two textural characteristics of the extrudates, hardness and crispness, were determined based on a crushing method using a texture analyser model TA-XT plus (Stable Microsystems Ltd., Surrey, UK) equipped with a 30 kg load cell. An extrudate of about 40 mm in length was compressed with an aluminium cylindrical probe (Model: SMS – P/75, 75 mm diameter) at a crosshead speed of 5 mm/s to 3 mm or 90% of the diameter of the extrudate. During the test, force was recorded and the force-time curves showing several force peaks analysed for hardness and crispness using the Texture Exponent software. Hardness (N) was taken as the first peak value indicating the first rupture of snack at one point. The total number of peaks was taken as a measurement of crispness (Stojceska et al., 2008). Ten randomly selected samples were analysed and data for mean hardness and mean crispness with their standard deviation are reported as results.

3.3.13 Scanning Electron Microscopy (SEM)

Scanning electron microscopy (SEM) of the sago starch extrudates was conducted using a scanning electron microscope (JEOL 6060LV Variable Pressure SEM, Jeol (UK) Ltd., Hertfordshire, UK) to illustrate the effect of water feed, screw speed, die temperature and additives on the microstructure of extrudates. Each extrudate was prepared for SEM examination by cutting using a razor blade to obtain an intact cross-section. Samples were mounted on aluminium stubs using carbon discs, both supplied by Agar Scientific (Stansted, UK) and sputter-coated with a

thick gold palladium layer with a sputter coater (Leica EM SCD005). Images of each extrudate sample were taken at 10 kV at two different magnifications (×5 and ×14) which were indicated at the bottom of the image along with scale bars. However, images of extrudates with water feed at 20 mL/min could not be assessed due to the method of sample preparation that could not be applied to the very hard/"glassy" samples produced.

3.3.14 Water Absorption Index and Water Solubility Index

The Water Absorption Index (WAI) and Water Solubility Index (WSI) were determined according to a method developed for cereals (Anderson et al., 1969) with slight modification. Ground extrudates (2 g ± 0.01 g) were mixed with 30 mL of water in a centrifuge tube for 2 to 3 s using a vortex mixer (Heidolph REAX top, Heidolph, Schwabach, Germany). The tubes were gently stirred for 30 min at room temperature (25 °C) using roller mixer (SRT9D Stuart, Bibby Scientific Ltd., Staffordshire, UK). The samples were then centrifuged at 3,000 x*g* for 15 min (JOUAN CR3i multifunction centrifuge, Thermo Fisher Scientific, Hamphshire, UK) at 25 °C. The supernatant was decanted into an evaporating dish of known weight and dried in an oven at 105 °C (Memmert, Schwabah, Germany) overnight. The weight of sediment after removing the supernatants was measured. The WAI is the weight of the sediment obtained per gram of the dry sample. The WSI is the amount of solid recovered by evaporating the supernatant, expressed as percentages of the dry solids in the sample. The WAI and WSI were calculated as follows:

$$\text{WAI (g/g)} = \frac{\text{weight of wet sediment}}{\text{dry weight of extrudate sample}} \times 100 \quad (3.7)$$

$$\text{WSI (\%)} = \frac{\text{weight of dried supernatant}}{\text{dry weight of extrudate sample}} \times 100 \quad (3.8)$$

Determinations were made in triplicate and are reported as mean ± standard deviation.

3.3.15 Crystallinity

As starch is semi-crystalline in its native form, the type of crystallinity can be observed by X-ray diffraction and the loss of order during extrusion cooking can be monitored. Native starch and ground extrudates samples were directly placed on the X-ray plastic holders. The samples were then analysed using an X-ray diffractometer (Siemens D5005 Bruker Analytical X-ray system, Congleton, UK). The Kristalloflex 760 X-ray generator supplied CuKα radiation at 0.154 nm wavelength. Data were collected at ambient temperature (25 °C) as integrals over the angular range of 4 to 38° (2θ) at an angular interval of 0.05° following a published protocol (Fan et al., 1996). Duplicate scans made for each sample gave essentially identical diffraction patterns.

3.4 Statistical Analysis

The statistical analysis of data sets for the graphical representations was performed using Microsoft Excel 2010 (Microsoft Corporation, USA). Analysis of variance (ANOVA) including Tukey tests ($P \leq 0.05$) were performed using the SPSS programme version 21 (IBM Corporation, USA).

CHAPTER 4
Physicochemical properties of sago starch in comparison with rice and cassava starches

4.1 Introduction

As put forward in Chapters 1 and 2 sago starch is potentially a useful carbohydrate source. In Indonesia where there is a plentiful supply of sago palms and further utilisation could be sustained in an environmentally acceptable manner, sago is not widely used in manufactured foods. The starches of choice are rice and cassava. The low usage of sago starch could be due to cultural forces, but it may be due to the sago starch being difficult to use as an ingredient in high-speed manufacturing operations. To investigate this latter point, a comparison of sago, rice and cassava starches has been made.

The concept behind this work is that by understanding the different properties of the three native starches, a rational choice of starches could be made to deliver a specifically required functionality and the feasibility for the use of sago starch assessed. Values for many of the parameters measured for these starches could be found in the literature. However, due to variations within one type of starch as well as different methods used, it can make a direct comparison of samples difficult. In additional to the literature review, a series of practical work was therefore also undertaken.

The physicochemical characteristics of native starches may vary according to their botanical source. Whether physical or chemical in nature, these parameters may manifest as differences in sizes and their distributions, shape, morphology, crystalline state, the degree of branching within amylose/amylopectin chains, moisture contents as well as the levels and types of non-starch components. These assorted characteristics are directly observable using a number of techniques.

The information in this chapter is a knowledge base which may be used to identify and understand the behaviour of three types of native starches (sago, rice and cassava). Rice starch is commonly used and processed in extrusion processing as breakfast cereals which have desirable characteristics when exposed to milk (Bao and Bergman, 2004). Cassava starch was also successfully used as a feed ingredient in the production of puffed extrudates either for the whole material (Leonel et al., 2009) or as a mixture with other materials (Chang et al., 1998; Hashimoto et al., 2003). However, very limited study about utilising sago starch as a product in extrusion cooking can be found.

The properties reported in this study are based on chemical composition, particle size distribution, granule morphology, crystal form, the behaviour of starches when heated in water (swelling power, pasting and thermal properties) for sago starch and are compared to the properties of rice starch and cassava starch. The assessment of the sago starch also provides information of the exact sample of starch that will be used for the processing studies presented in Chapter 5, 6 and 7.

4.2 Literature review

In this section, some details of the three starches; sago, rice and cassava as reported in the literature are presented so that they can be compared in the latter stages of this section.

4.2.1 Sago starch

As described in section 2.1, sago starch is extracted from the trunk of sago palm (*Metroxylon*) and this plant grows throughout Southeast Asia. Sago is an important source of starch in tropical countries and it has been extensively studied by various researchers (Ahmad et al., 1999; Islam et al., 2001; Maaurf et al., 2001; Abd-Aziz, 2002; Karim et al., 2008b; Mohamed et al., 2008; Singhal et al., 2008; Tie et al., 2008). Sago starch has a multitude of uses in both food and non-food applications. In food processing, sago starch has been used as a stabiliser and thickener (Singhal et al., 2008). Unfortunately, there is only very limited information available on the utilisation of sago starch for extruded products. Information on the utilisation of sago starch can be found in section 2.1.2 and indicates that most applications are traditional and are high moisture foods.

4.2.1.1 Physicochemical properties of sago starch

The size of sago starch granules is considered to be a broad range, between 10 and 50 μm in diameter, where the average granule diameter is 32 μm (Wang et al., 1995). The granules are oval or polygonal-shaped with some truncated oval granules (Figure 4.1). Regarding the granule size distribution, sago starch tends to show a bimodal distribution when

extracted mechanically, whereas a single distribution will show from enzyme-assisted extraction (Abdullah et al., 2002).

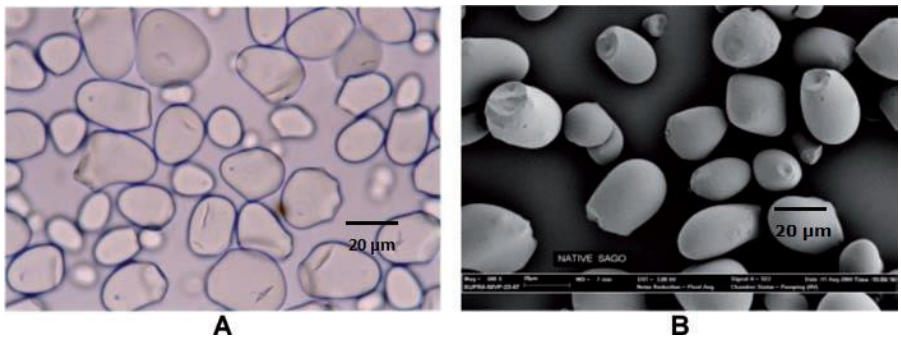

Figure 4.1. Sago starch granules observed under (A) light microscopy (400×) and (B) scanning electron microscope (600×; scale bar = 20 µm) (Karim et al., 2008b).

Ahmad et al. (1999) analysed the physicochemical properties of sago starches from 11 different manufacturers in Malaysia, Indonesia and Thailand. They reported that the proximate composition of the sago starch varied as follows; moisture content from 10.6% to 20.0%, ash from 0.06% to 0.43%, crude fat from 0.10% to 0.13%, fibre from 0.26% to 0.32%, and crude protein from 0.19% to 0.25%. The phosphorus contents in sago starch varied between 86 and 97 ppm (Takeda et al., 1989), whereas Sim et al. (1991) found 4 ppm and 104 ppm on two different batches of sago starch from *Metroxylon sagu* species. The amylose content of sago starch varied between 24% and 31% (Ahmad et al., 1999), and 23% and 29% (Tie et al., 2008). Ranges in amylose content have been reported to be most likely due to differences in the growth stage when harvesting sago (Tie et al., 2008).

Some studies (Takeda et al., 1989; Sim et al., 1991; Ahmad et al., 1999; Karim et al., 2008a; Abdorreza et al., 2012) have been carried out on the pasting properties of sago starch, either native or chemically modified.

Ahmad et al. (1999) reported two types of pasting properties for sago starches. Native sago starches showed a maximum consistency peak which then decreased sharply. Meanwhile, the pasting properties of modified sago starch featured a plateau at the maximum consistency level. Hamanishi et al. (2002) as quoted in Karim et al. (2008b) examined the physicochemical properties of native sago starch and other commercial starches and reported the peak viscosities of the pastes were in the order: potato>sago>tapioca>sweet potato>rice>corn>wheat.

Okazaki and others (2007) as quoted in Karim et al. (2008b) reported that sago starch shows a C-type diffraction pattern (a mixture of A and B crystalline types) that consists of 65% A-type and 35% B-type on average. The relative percentage varied depending on at which height of the trunk the sago starch was extracted. The accumulated starch at the top of the sago palm exhibits a C-type structure, whereas A-type dominates extraction from the bottom of the sago palm.

4.2.2 Rice starch

4.2.2.1 Introduction of rice and production of rice starch

Rice (*Oryza sativa* L.) is a staple food of more than half of the world's population, particularly in Asian countries (Juliano, 1985). It has been consumed by humans for at least 5,000 years and is cultivated on almost all continents (Bao and Bergman, 2004). The origin of rice is believed to be in China, India and Indonesia where three types of rice (Japonica, Indica, and Javanica) were first cultivated (Juliano, 1985). Starch composition plays an important role in determining the characteristics of the different types of rice.

Isolation of starch from rice mainly involves techniques to remove proteins which reportedly range from 4.5 to 15.9% (Kennedy and Burlingame, 2003), meanwhile lipids exist in rice at much lower amounts. Alkaline steeping methods are commonly used in industry and research to produce rice starches with good recovery and low residual protein contents because the majority of rice protein is alkaline soluble (Lumdubwong and Seib, 2000). The goal for the protein content of isolated rice starch is generally 0.5% or less (Bao and Bergman, 2004).

4.2.2.2 The use of rice starch

Beside consumption as after cooked in the milled form, rice is also processed into flour or starch for use in pharmaceutical, food and animal feed products. Rice starch is used in many applications as a food ingredient because of its specific characteristics. It is taste neutral in its gelatinised form, thus not affecting the final flavour of food (Bao and Bergman, 2004). Rice starches do not contain gluten and therefore it does not cause gluten specific allergic response in humans. Rice starch granules being very small in size provide a texture perception similar to that of fat particles (Champagne, 1996). Additionally, rice starches form a soft gel and therefore could be a fat replacer in foods such as flavoured milk-based beverages, ice cream, yoghurt and salad dressings. Another unique characteristic of rice starch is that it has a rapid hot-set. This is desirable in food manufacture processes such as extrusion processing of breakfast cereals as it is associated with the retention of crispness after a processed cereal is exposed to milk. Rice starch is also used to generate maltodextrins that are incorporated into foods as a filler, flavour carrier, texture modifier or sweetness reducer (Bao and Bergman, 2004).

4.2.2.3 Physicochemical properties of rice starch

The major variations in rice starch composition are the relative amounts of amylose and amylopectin (Bao and Bergman, 2004). The amylose content of the rice starch granule varies with the botanical source and is affected by climatic and soil conditions during grain development. The amylose content of rice decreases due to high temperatures, whereas cool temperatures have the reverse effect (Champagne, 1996). Amylose content of rice is specified as waxy 0-2%; very low 5-12%; low 12-20%; intermediate 20-25%; and high 25-33% (Juliano, 1984).

Rice starch granules are the smallest known to exist in cereal grains, with the size reported ranging from 3 to 10 μm. There is some variation in starch granule size between different rice genotypes (Juliano, 1984; Champagne, 1996). Sodhi and Singh (2003) reported that a group of rice varieties grown in India had starch granules from 2.4 to 5.4 μm. The average starch size from some waxy rice ranged from 4.9 to 5.7 μm (Qi et al., 2003). Rice starch granules have a smooth surface but are angular and polygonal in shape (Bao and Bergman, 2004).

As typical for cereal starches, rice starch has the A-type X-ray diffraction pattern. When starch is heated in excess water, the crystalline structure is disrupted due to the breakage of hydrogen bonds, and water molecules become linked by hydrogen bonding to the exposed hydroxyl group of amylose and amylopectin. This causes an increase in granule swelling and solubility (Bao and Bergman, 2004). Sodhi and Singh (2003) showed the sample with the lowest amylose content (7.8%) among five rice starches had the highest swelling power and lowest solubility; whereas the sample with the greatest amylose content had the lowest swelling power. Lii et al. (1995) also reported that rice starch with lower amylose content had a

higher swelling power. However, within waxy rice varieties, starch swelling power and solubility varies (Wang and Wang, 2002).

Singh et al. (2006) studied rice starch separated from 19 different Indica rice cultivars and concluded that amylose plays an important role in the pasting properties of starches. It was significantly correlated with peak viscosity, final viscosity and setback; however, the correlation was stronger with the setback.

4.2.3 Cassava starch

4.2.3.1 Introduction of cassava and production of cassava starch

Regarding botanical classification, cassava is defined as *Manihot utilisama* Pohl of the family Euphorbiaceae. *Manihot esculenta* Crantz is another name for cassava that is popularly used in publications (Grace, 1977). Cassava is known under a variety of names in different countries: *ubi ketela* (Indonesia), *manioc, rumu or yucca* (Latin America), *manioc* (Madagascar and French-speaking countries), *tapioca* (India, Malaysia), *cassava* and sometimes *cassada* (English-speaking regions, Thailand, Sri Lanka). In the tropic countries, cassava is one of the most important food crops and is the most important root crop. The roots are the main edible portion of the plant, and the starch represents a good energy carbohydrate source in the dried flour (Grace, 1977; Bradbury and Holloway, 1988).

The production method of cassava starch was reviewed by Onwueme (1978) and Corbishley and Miller (1984). Roots are peeled, washed and chopped into slices of 30-50 mm to achieve high starch yields. The roots

are then conveyed to crushing or grinding devices to produce a pulp which is subsequently suspended in water. A series of centrifugation steps are then applied to remove the fibrous material leaving the starch milk. About 0.05% sulphur dioxide should be contained in the water to prevent microbial action or fermentation at this extraction stage. The product at this stage is known as cassava starch or flour. The starch milk is passed through a degritting screen or a sand cyclone to remove foreign material and then allowed to settle. Centrifugation is applied to remove water, the remaining fine fibre and soluble. For further purification, the starch may be re-slurried and re-centrifuged. The dewatered starch cake is then dried to a moisture content of 10-14%. Finally, the dried starch is separated, ground, sifted and bagged. Production plants for the starch are located next to root growing areas to minimise transport costs and to enable the processing of roots in the shortest time. Large-scale production of cassava starch occurs in Thailand, Brazil, the Philippines and Indonesia.

4.2.3.2 The use of cassava starch

Cassava is important both for animal feed and as a raw material for starch production. The utilisation of cassava starch in native and modified form is largely used for industrial purposes, for example, production of food products and starch derivatives (dextrins, glucose, fructose, mannitol), and manufacture of sizing paper and textiles, adhesives, alcohol and in the oil drilling industries (Grace, 1977; Cock, 1985). The wide range of cassava starch utilisation is because of the properties associated with this starch compared with other sources of starch, for example it has one of the lowest gelatinisation temperatures (71 °C), a low tendency to retrograde, no residual proteinaceous material or no soil residues, non-cereal flavour, high viscosity, high water binding capacity, bland taste,

translucent paste and quite good stability (Grace, 1977; Corbishley and Miller, 1984; Cock, 1985).

4.2.3.3 Physicochemical properties of cassava starch

The chemical composition of cassava starch differs considerably depending on root variety. The results from studies on 30 varieties showed that dry-matter content of the roots varied between 25-52%, and protein content varied between 1-6% (Grace, 1977). Different environmental and processing conditions (cultivars, age, temperature and growth season, drying temperature and milling process) have marked effects on the physicochemical properties of the starch (Meuser et al., 1978; Moorthy and Ramanujam, 1986; Fernandez, 1996).

Moorthy and Ramanujam (1986) examined various physicochemical properties of cassava starch extracted from six varieties at different stages of crop growth at monthly intervals starting from 2nd- up to 18th-month stage. The granule size increased in all the six varieties up to 6th-month from the time of tuber initiation and after that remained almost constant. The amylose content did not show significant variations at different stages of growth. They also reported that the swelling volume and solubility of cassava starches vary according to variety and environmental conditions. The changes were due to a reduction in associative forces between molecules in the starch granule which may be weakened considerably in certain cultivars leading to low swelling volume and high solubility. Hence it is concluded that associative binding forces of starch molecules largely determine the stability characteristics of cassava starch under varied environment and associated physiological age of the crop.

Fernandez (1996) investigated the effects of processing and cultivar on the properties of cassava flour and starch. It has been shown that mean granule size and granule size distribution varied between cultivars. Cultivars grown in warmer climates were seen to have a higher proportion of smaller granules and a narrower granule size distribution in these starches. Regarding the processing effect, a study of the extraction of starch from tapioca chips and pellets in comparison to the extraction from tapioca roots has shown that extraction of starch from dried raw materials was more complicated than from fresh roots with more difficulty to remove impurities, which thus reduced the starch quality (Meuser et al., 1978).

Regarding the properties of cassava starch when heated in excess water, a study by Mat Hashim et al. (1992) exhibited that the addition of low levels of sodium sulphite had a dramatic effect on the structure of cassava starch pasted at 95°C. The addition of 100 ppm sulphite promoted granule disintegration resulting in a reduction in measured swelling volume to nearly 10% of its value in the absence of sulphite and enhanced the release of polysaccharide from the starch granule. This work has been continued by Paterson et al. (1994) with adding propyl gallate that completely nullified the sulphite effect on the swelling volume of cassava starches.

4.2.4 Comparison between the starches

Rice, cassava and sago are very different in the botanical origin; rice being a seed, cassava as a root and sago from the pith of the palm trunk. The composition and structuring of the granules are different plus their behaviour in water. Despite the marked differences between rice and cassava starches, both are used to make low moisture products and both

are considered useful starches for extrusion, yet sago does not seem to be as extensively studied or used commercially for extrusion cooking. To provide a direct comparison between three commercial sources of these starches, a series of experimental assessments was undertaken.

4.3 Materials and Methods

The main materials used in the research reported in this chapter were sago starch, rice starch and cassava starch. The source of the materials is given in section 3.1.1. Initially, the physicochemical properties of sago starch were analysed and compared to the properties of the two other starches. The methods for analysis are explained in section 3.3.

4.4 Results and Discussion

4.4.1 Physicochemical properties of the starches

4.4.1.1 Composition of sago starch, rice starch and cassava starch

Table 4.1 shows the composition of the sago, rice and cassava starches examined in this research. The measured moisture (wet basis) and amylose content (provided as a total of starch content on a dry basis) of the starch were obtained through the method described in section 3.3.1 and 3.3.2, respectively. Meanwhile, Table 4.2 shows the composition of sago, rice, and cassava starches from the literature.

The moisture content of the sago starch was considerably higher than that of the rice and cassava starch. This was probably due to insufficient drying in the processing of the sago starch from the small-scale local supplier of this material. The sample of sago starch retained this level of moisture throughout it use in the research which lasted over a two year period and does indicate a higher equilibrium moisture compared to the other two starches. The moisture content of sago starch from Indonesia has previously been reported to be as high as 20% (Table 4.2), which was the highest among eleven samples of sago starch from different origin (Ahmad et al., 1999). However, the values obtained in this research for all three starches are within the range expected; under average ambient temperature and humidity conditions, the moisture content of most unmodified starches is around 12% (Ahmad et al., 1999).

Table 4.1 Proximate composition of sago, rice and cassava starch. Values for moisture and amylose content are means ± SD (n = 3). Values are on a wet basis unless otherwise indicated.

Component	Starch sample		
	Sago	Rice	Cassava
Moisture (%)	14.2 ± 0.2	7.6 ± 0.3	11.4 ± 0.1
Protein (%)	< 0.1	0.23	< 0.1
Total fat (%)	< 0.5	0.6	< 0.5
Ash (%)	0.1	0.4	0.2
Phosphorus (%)	0.0082	0.0330	0.0068
Total Carbohydrate (%)	84.70	87.57	87.80
Amylose (% dwb)	33.0 ± 0.71	15.8 ± 1.07	20.9 ± 0.23

Table 4.2 Composition of sago, rice, and cassava starches from literature. Values are on a wet basis unless otherwise indicated.

Component	Type of Starch		
	Sago	Rice	Cassava
Moisture (%)	10.6-20.0[a]	10.9-12.8[e]	13 (at 65% RH and 20°C)[f], 10-13[g]
Protein (%)	0.13-0.25[a]	0.40-0.43[e]	0.1[f]
Lipids (%)	0.10-0.13[a]	0.1-0.7[e]	0.1-0.2[f,g]
Phosphorus	86-97 ppm[b]		0.01 (% dwb)[f,] 0.007-0.012[g]
Amylose* (% dwb)	23-31[a,c,d]	12-29[c,e]	17-18[c,d,f]

[a]Ahmad et al. (1999), [b]Takeda et al. (1989), [c]Oates (1997), [d]Tongdang et al. (2008) [e]Ashogbon and Akintayo (2012), [f]Swinkels (1985), [g](Moorthy, 2002).
*Amylose content determination: [a,d,e]=iodine-binding method, [c,f]=unspecified method.

Protein content refers to the peptides, amides, amino acids and enzymes, which may be present at varying levels in the sample. As explained in section 4.2 protein may be associated with the internal structure of the starch granules or may occur at the granule surface, not having been

removed during starch extraction. Sago and cassava starch both were found to have very low protein, while the protein level was at 0.23% for the rice starch. The protein content for all three starches was lower than reported in literature sources (Table 4.2); 0.13-0.25% for sago starch (Ahmad et al., 1999), 0.40-0.43% for rice starch (Ashogbon and Akintayo, 2012), and 0.1% on average for cassava starch (Swinkels, 1985). This variation is likely due to the variety or the extraction method used to produce the starch. The rice starches were obtained from Sigma-Aldrich and could have been purified to a greater degree than a typical commercial rice starch. The presence of non-carbohydrate components such as proteins and lipids influences the swelling and solubility of the starch granule on the molecular level (Leach, 1967). The significance of the presence of such components on swelling power of the three starches is discussed in section 4.4.2.1.

Total fat of all three starches was low. Cereal starches (wheat, rice and maize) naturally contain low amounts of lipids (0.6-1%) (Swinkels, 1985). However, the lipid levels of the rice starch from this study was higher than for the other samples. Lipids, particularly monoacyl lipids will induce the formation of amylose–lipid complexes during gelatinization. They will limit swelling, dispersion of the starch granules and solubilisation of amylose, hence generating opaque pastes with reduced viscosity and increased pasting temperatures (Buléon et al., 1998). Rice starch has been reported to have a greater number of intermolecular bonds such as amylose-lipid complexes (Leach, 1967). The DSC thermogram can give an indication of the existence of amylose-lipid complexes in starch, where the melting endotherm of fatty acids and monoglycerides are 90 - 110 °C. From Figure 4.6 it can be assumed that there are no lipids present in the sago

starches studied able to complex the amylose since no melting endotherm of such species can be seen in the thermograms.

The quantity of crude fat for sago samples as cited by Ahmad et al. (1999) ranged from 0.10% to 0.13% (Table 4.2). Commercial starches normally contain trace amounts of fatty acid glycerides, usually at levels less than 0.1% which can be removed by Soxhlet extraction using ether or hexane. However, hexane cannot be used for removing free fatty acid (about 0.5%–0.6%) which complex with the amylose in the starches. This requires extended extraction by using hot methanol or ethanol to give fat-free starches (Schoch, 1942).

The ash and phosphorus contents for the sago starch were very low, and the phosphorus content was comparable to that of the cassava starch. The relevance of this is that it indicates that, unlike potato tuber starch, the amylopectin in the sago is not phosphorylated. The small levels of phosphorous are probably associated with the lipids rather than being a charged group on the starch. The slight difference in the proximate composition between samples and literature (Table 4.2) could be due to different environmental conditions during growing or due to technical factors. The inorganic material normally originates from the crop from which the starch is isolated and also from the water used to process the starch.

The amylose quantification method used on samples in this thesis was the Megazyme Con A method (see section 3.3.2), and the information supplied by the supplier of this kit indicated that a standard deviation of ± 5% is normally acceptable. It was found that the sago starch sample contained higher levels of amylose (33.0%) in comparison to the cassava (20.9%)

and the rice starch (15.8%). Table 4.2 shows composition including amylose contents from the literature cited (various method of amylose content determination). The various values in the amylose content of sago starch are most likely the result of variation in cultivar, harvest at different growth stages and variation in extraction processes (Tie et al., 2008). However, the results of the amylose levels would seem to indicate that the macromolecular structures in the sago starch are different from both the rice and cassava starches. The amylose levels of sago starch would seem higher than those typically measured for cassava starch.

4.4.1.2 Granule size distribution

Particle size analysis was carried out to determine the granule size distribution of the three starches (dry samples) according to the method outlined in section 3.3.4. The results are shown in Figure 4.2 and characteristic distribution parameters are reported in Table 4.3. Sago and cassava starches showed a monomodal distribution while rice starch showed a bimodal pattern probably due to the aggregated nature of this sample. This monomodal distribution indicated that sago starch used in this research was most likely extracted based on the enzyme-assisted method since Abdullah et al. (2002) reported that sago starch extracted mechanically tends to show a bimodal distribution. In terms of distribution, it revealed that the particle size distribution (volume based) of sago starch was the narrowest. As opposed to sago starch, rice starch has the broadest particle size distribution.

The characteristic distribution parameters as shown in Table 4.3 give information about D[4,3] which is the mean diameter on a volume basis. Meanwhile, 'span' indicated the width of granules size distribution which one of the common values used for laser diffraction results (Horiba

Instruments, 2012). The definition of the span can be seen in the Equation (3.2).

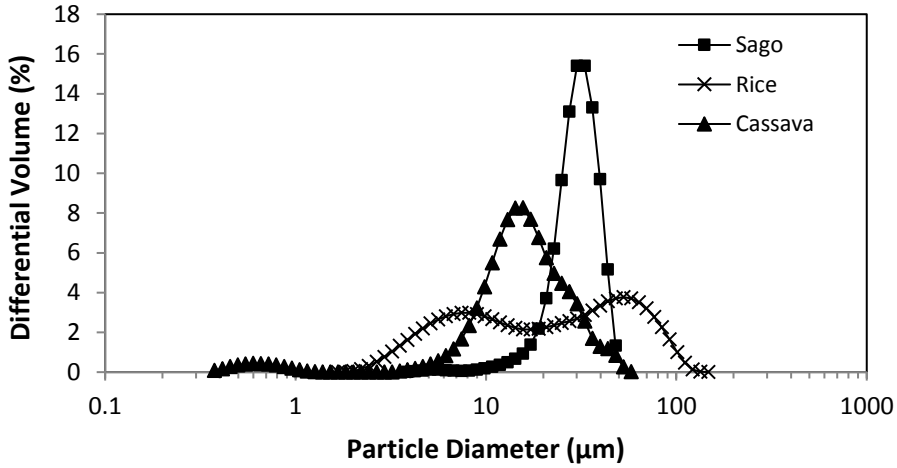

Figure 4.2 Particle size distributions of sago, rice and cassava starches determined on the dry samples utilising laser diffraction equipment.

Table 4.3 Characteristic volume based particle size parameters for distributions shown in Figure 4.2. Values are means ± SD (n = 3). Means within a column related to a particular parameter with the same superscript are not significantly different (p>0.05).

Starch sample	D[4,3] (µm)	D10 (µm)	D50 (µm)	D90 (µm)	Span
Sago	32.0^{a} ±0.05	22.4^{a} ±0.03	32.2^{a} ±0.04	42.3^{a} ±0.1	0.62^{a} ±0.00
Rice	31.5^{a} ±0.45	5.1^{b} ± 0.01	30.0^{b} ±0.15	72.9^{b} ±1.6	3.08^{b} ±0.07
Cassava	17.1^{b} ±0.17	8.1^{c} ± 0.12	15.6^{c} ±0.09	29.0^{c} ±0.25	1.34^{c} ±0.00

The mean granule size (volume-based) obtained for the sago starch is in good agreement with previous studies (Ahmad et al., 1999). Wang et al. (1995) reported that sago starch granules have a broad size range, between 10 and 50 µm in diameter with an average granule diameter of 32 µm. Sago starch granules are generally bigger than those of rice (3 to

10 μm) or cassava (5 to 25 μm) (Karim et al., 2008b). However, the mean diameter of rice starch was much higher than previously reported sizes by Swinkels (1985). This is probably due to the aggregated nature of this sample seen in Figure 4.2 where the sizes represent rice particles rather than individual starch granule. Meanwhile, the mean granule size for cassava starch was 17.1 μm which was within the expected range found in the literature (Swinkels, 1985).

4.4.1.3 Granule morphology

Figure 4.3 shows bright field and polarised light micrographs of all three starches (method given in section 3.3.5). The images are in agreement with the granule size data (as indicated in Figure 4.2 and Table 4.3). It is clearly evident that sago starch has the largest granules among the starches studied here as shown in the micrographs.

As can be seen from the micrographs, granule shape of the three starch samples also differs. Sago starch granules are oval, while rice starch granules are polygonal and angular, and cassava starch granules are oval and truncated. These observations are in good agreement with previous reports (Ahmad et al., 1999; Swinkels, 1985). When viewed under polarised light (Figure 4.3), a dark Maltese cross was evident for all three starches confirming that they were native starch samples. The 'Maltese crosses' that were observable under polarised light microscopy are an indication that there is spherical crystallinity in the starch granules (Copeland et al., 2009). It is also noteworthy that the micrographs taken on the rice starch sample with bright field light confirm considerable aggregation as suggested based on the granule size data shown in the previous section. Due to the aggregation and its small size, the Maltese

crosses of rice starch were not as clear under the polarised light as for the other samples.

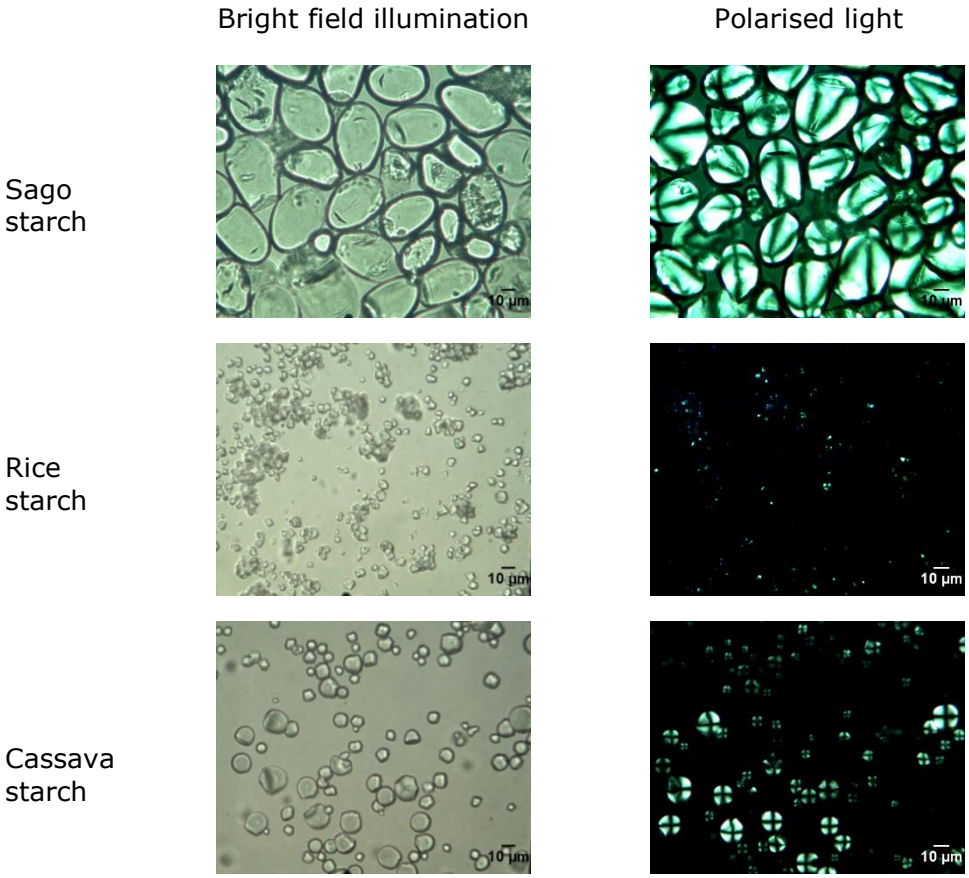

Figure 4.3 Micrographs acquired under bright field and polarised light (vertical) for different starches granules (horizontal). All scale bars correspond to 10 µm.

4.4.1.4 Crystallinity

The type of structures formed by the A chains of amylopectin to create the crystallinity can be detected by X-ray (see section 2.2.3 and Figure 2.6). Rice starch always gives pattern in the A form, but cassava starch has been reported to show mixed diffraction patterns. Sago starch seems to be highly varied in the amylopectin crystallinity (see section 4.2.1.1).

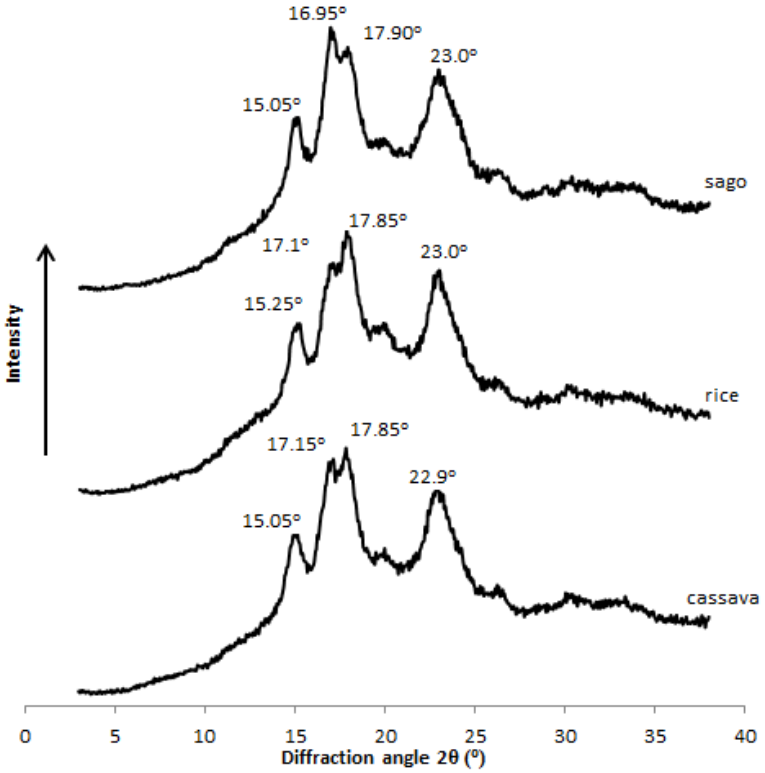

Figure 4.4 X-ray diffraction patterns for the sago, rice, and cassava starch samples.

Figure 4.4 shows X-ray diffraction patterns of the three starches, and it is immediately obvious that they are similar. They feature four strong peaks at 2θ values of about 15°, split 17°, 18° and 23° which is characteristic for A-type starches (Zobel, 1988). Although it can be difficult to see small levels of B crystallites in the overall pattern, there is no obvious peak at about 6°, 20° and the second peak in association with that at 23° (Figure 2.6). This result does not support reports in the literature that C-type crystalline structure are typical for sago (Ahmad et al., 1999; Karim et al., 2008b; Adawiyah et al., 2013) and cassava (Asaoka et al., 1991; Gorinstein and Lii, 1992). An A-type XRD pattern is reported for rice starch (Shih et al., 2007), which is the typical pattern for a cereal starch (Zobel, 1988).

The amount of crystallinity indicated by the X-ray patterns of starches typical shows that between 15 and 50% of the material in native starch granules is in the crystalline form (Swinkels, 1985). The measurement of starch crystallinity has a large source of error and, depending on a material, can grossly over or underestimate crystalline scattering (Frost et al., 2009). The relative crystallinity of the cassava starch in this study was the highest (34.1%), followed by the rice and sago starches (31.4% and 25.3%, respectively). On the other hand, in this study it can be seen from Figure 4.4 that no clear difference of the X-ray patterns between the samples exists. This means that the polymorphic type and the crystallinity did not differ despite some differences in starch structures i.e. amylose content (Table 4.1). These differences are probably not high enough to induce a change in the crystalline structure. The differences of relative crystallinity value of the three starches are probably due to the difficulty of the method because of the small crystal size and the role of hydration. The variation of relative crystallinity values of native starch depends not only on the origin and the hydration of starch but also on the technique used (Buléon et al., 1998; Zobel, 1988).

4.4.2 Behaviour of starches when heated in water

Many applications using starches involves heating them in water. The thermal transition that the starches undergo and the interactions with the water at both a granule and macromolecular level differentiate the starches and can define their potential as food ingredients.

4.4.2.1 Swelling power

The swelling power of the starch granules was measured as described in section 3.3.6. The results are presented in Table 4.4 and expressed as

grams of swollen sample per gram of sample weight (dry basis) as defined by Equation (3.3). It indicates the water holding capacity of starch and has generally been used to demonstrate differences between various types of starch (Crosbie, 1991; Sasaki and Matsuki, 1998; Li and Yeh, 2001). There was an experimental challenge faced for sago and cassava samples when separating the moisture-filled gelatinised starch granule pellet from its supernatant. This was because the supernatant and starch gels pellets were translucent, so there was a visual challenge to differentiate the two.

Table 4.4 Swelling power of sago, rice and cassava starches at 95 °C. Values are means ± SD (n = 3). Means with the same superscript are not significantly different (p>0.05).

Starch sample	Swelling power (g/g)
Sago	29.0^{a} ± 3.8
Rice	12.5^{b} ± 1.5
Cassava	34.6^{a} ± 3.0

From Table 4.4 it can be seen that the swelling power of the sago starch at 95 °C is not significantly different to the swelling power of the cassava starch, but for both starches swelling power is significantly higher than for rice starch. These results agree well with Ahmad and Williams (1998) who reported that the swelling power of eleven sago starch samples from different manufacturers was comparable to cassava. Values for swelling power of cassava (at 95 °C) as reported by Swinkels (1985) was 71 g/g, but the methods used in different laboratories can be difficult to compare. Swelling power of waxy rice starches at 95 °C have been shown to vary even when carried out at the same time (Wang and Wang, 2002).

Swelling power is thought to be affected by several factors. According to Tester and Morrison (1990), the swelling behaviour of cereal starch is primarily related to amylopectin structure. Other factors reported to influence swelling power include the ratio of amylose and amylopectin, the extent of chemical cross-bonding within the granules (Schoch, 1964), non-carbohydrate substances such as lipid or phosphate (Leach et al., 1959) and protein (Wang and Seib, 1996).

The higher swelling power of sago compared to rice starch and its comparative value to cassava is interesting. The high lipid and protein content of rice starch (Table 4.1), as expected for a cereal starch, most likely contributes to the inhibition of swelling, possibly due to an increase in the number of amylose-lipid complexes and reduction of amylose mobility due to other protein. The clarity of the gelatinised starch pastes, and hence the challenge in differentiating swollen granule from supernatant is an indication of no or low levels of amylose complexation. Leach (1967) reported that certain starches, for example, maize, rice and sorghum, show restricted swelling compared to the waxy types due to the presence of stronger and a greater number of intermolecular bonds such as amylose-lipid complexes. It would normally be expected that the much larger sago starch granules would allow for greater swelling which may have been countered by the higher amylose levels in these granules (as measured by the Megazyme assay in section 4.4.1.1).

4.4.2.2 Pasting properties

The swelling power looks at the ability of the starch granules to imbibe water when heated, but does not reflect their stability to shear. Shear is an important factor in most food processes. The pasting behaviour of the starch samples was analysed with the Rapid Visco Analyser (RVA) as

described in section 3.3.7.1. The pasting viscosity profiles of the three starches are presented in Figure 4.5, and the corresponding mean values for the characteristic pasting parameters are summarised in Table 4.5.

It can be seen from Figure 4.5 that the shape of the pasting profiles of the sago and cassava starches are comparable while for the rice starch it is distinctly different. Similarities include peak time and width of the pasting profile around the viscosity peak whereas the peak viscosity itself was higher for the cassava sample. The pasting temperature (temperature at which initial swelling of starch granules takes place when suspended in water to a level that has a major impact on viscosity) of the sago starch was higher than the cassava starch and similar to the rice. For the sago and cassava starches, the viscosities rose rapidly, but the increase was much slower for the rice starch. The rice had been shown to be a mixture of rice starch granules and particles of rice and these may have had different behaviours causing a slower viscosity rise.

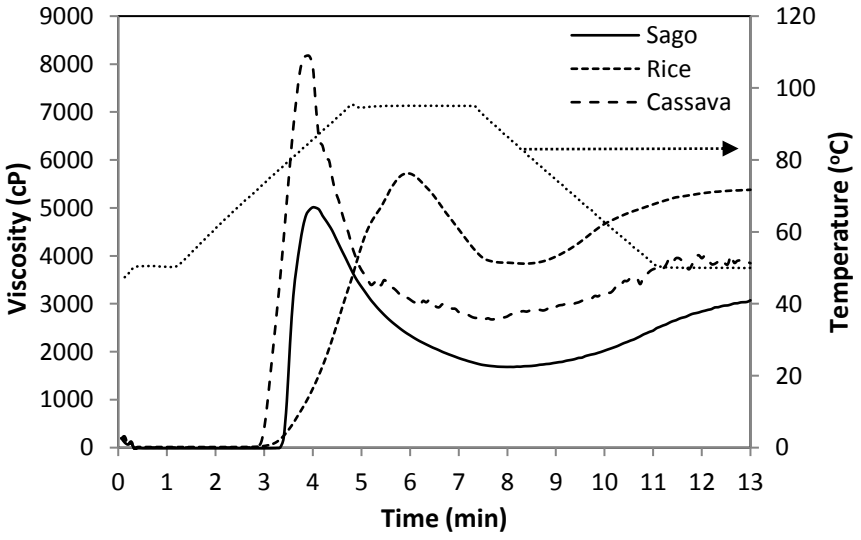

Figure 4.5 Pasting properties of sago starch, rice starch and cassava starch determined with the RVA. Temperature profile is indicated in the graph and mixing speed was at 960 rpm for the first 10 s and then at 160 rpm throughout the remainder of the test.

Table 4.5 RVA results for sago, rice and cassava starches. Values are means ± SD (n = 3). Means within a column related to a particular parameter with the same superscript are not significantly different (p>0.05).

Starch sample	Peak	Trough	Break-down	Final	Setback	Pasting temp.
	Viscosity (cP)					(°C)
Sago	5012[a] ± 16	1683[a] ±108	3329[a] ± 117	3033[a] ±23	1350[ab] ± 88	77.3[a] ± 0.5
Rice	5721[b] ± 16	3835[b] ±32	1886[b] ± 48	5382[b] ±34	1547[a] ± 26	74.8[b] ± 0.5
Cassava	8208[c] ± 11	2650[c] ±102	5558[c] ± 96	3903[c] ±70	1253[b] ± 170	71.3[c] ± 0.5

The peak viscosity, defined as the maximum viscosity recorded prior to the initiation of sample cooling (Tie et al., 2008), is associated with the maximum degree of swelling of the majority of the starch granules and these are essentially still intact, i.e., having not burst or suffered shear damage. Highest peak viscosity was recorded for the cassava sample which also had the highest swelling power (Table 4.4). Lowest peak viscosity was assumed by the sago starch sample which may be a consequence of the comparatively highest content of amylose (Table 4.1). High amylose content and hence, less amylopectin, may contribute to lower peak viscosity because swelling of starch granules and pasting is associated with the amylopectin level and structure (Jane et al., 1999). However, it could also be due to the swollen granules being very fragile and breaking as soon as they begin to swell. Data of the swelling power would predict high peak viscosity if shear was not an issue. Breakdown values, the difference between the peak values and the through, relate to the vulnerability of the granules to breakdown. Sago and cassava starches have major breakdown viscosity decrease as showing in Table 4.5.

After heating and shearing, the starch macromolecules could be expected to be in solution and the final viscosity may reflect their hydrodynamic volume and hence relate to their molecular weight. However, for these starches this is likely not to be the case and viscosities probably indicate aggregates of the starch polymers. When starch pastes are cooled, re-association between the starch molecules occurs with a contribution of amylose. The final viscosity in the RVA was measured at 50 °C with only 2 min of holding time and while the sample was sheared. It would be expected that no amylopectin retrogradation would occur. It is likely that some amylose-lipid association could occur.

4.4.2.3 Thermal properties

The RVA results showed the impact of temperature on the physical attributes of the three starches. To comprehend these thermal transitions in more detail, the samples were measured for their thermal properties using differential calorimetry. The gelatinisation and retrogradation properties of the three starch samples were quantified using DSC as described in section 3.3.8. The gelatinisation and retrogradation temperatures (onset, T_o; peak, T_p; and endset, T_e), and enthalpy (ΔH) of sago, rice, and cassava starches are presented in Table 4.6. The actual DSC thermograms of the samples are shown in Figure 4.6 and Figure 4.7.

Table 4.6 Thermal properties of sago, rice and cassava starches as measured by DSC at a heating rate of 10 °C/min. The values under "retrogradation" were acquired after seven days of storage at 4 °C.

Starch sample	Gelatinisation				Retrogradation			
	T_o	T_p	T_e	ΔH_g	T_o	T_p	T_e	ΔH_r
	(°C)			(J/g)	(°C)			(J/g)
Sago	69.7	76.0	86.6	16.4	47.9	59.9	71.1	3.9
Rice	63.1	70.8	82.8	10.6	91.6	98.3	105.2	0.9
Cassava	64.0	71.8	84.9	14.1	45.7	57.9	68.5	0.6

The highest T_o, T_p and T_e of gelatinisation were observed for the sago starch, whereas the rice starch showed the lowest values for these three characteristic temperatures. The T_p value for the sago starch was detected at 76 °C, similar to 75 - 77 °C obtained by Tie et al. (2008) for sago starches harvested at different growth stages. However, some researchers reported lower T_p; approximately 70 °C (Ahmad et al., 1999; Maaurf et al., 2001), and about 67 °C for sago starch (Adawiyah et al., 2013). The higher peak gelatinisation temperatures for the sago starch indicated that the crystallites undergoing melting were more stable than in the other samples. This may reflect more crystal perfection or perhaps longer a A chain (Buléon et al., 1998).

The amount of crystallinity is typically reflected in the total energy required to melt out the crystalline and helices order. This is reflected in the higher value for the gelatinisation enthalpy (ΔH_g) of 16.4 J/g of the sago starch. The transition temperatures of the rice starch in this study were higher but ΔH_g is lower than those obtained by Li and Yeh (2001) who used rice starch isolated from Japonica rice that acquired T_o 57.7 °C, T_p 65.1 °C and ΔH_g 11.5 J/g. This could be attributed to the different source of rice starch used going along with a different amylopectin crystalline structure (Adawiyah et al., 2013), but again the question of the purity of the rice starch powder as to whether it was granular or in clumps may be relevant. Meanwhile, the results agreed well with literature for T_o, T_p and ΔH_g of cassava starch: 64.5 °C, 71 °C and 13.0 J/g, respectively (Li and Yeh, 2001).

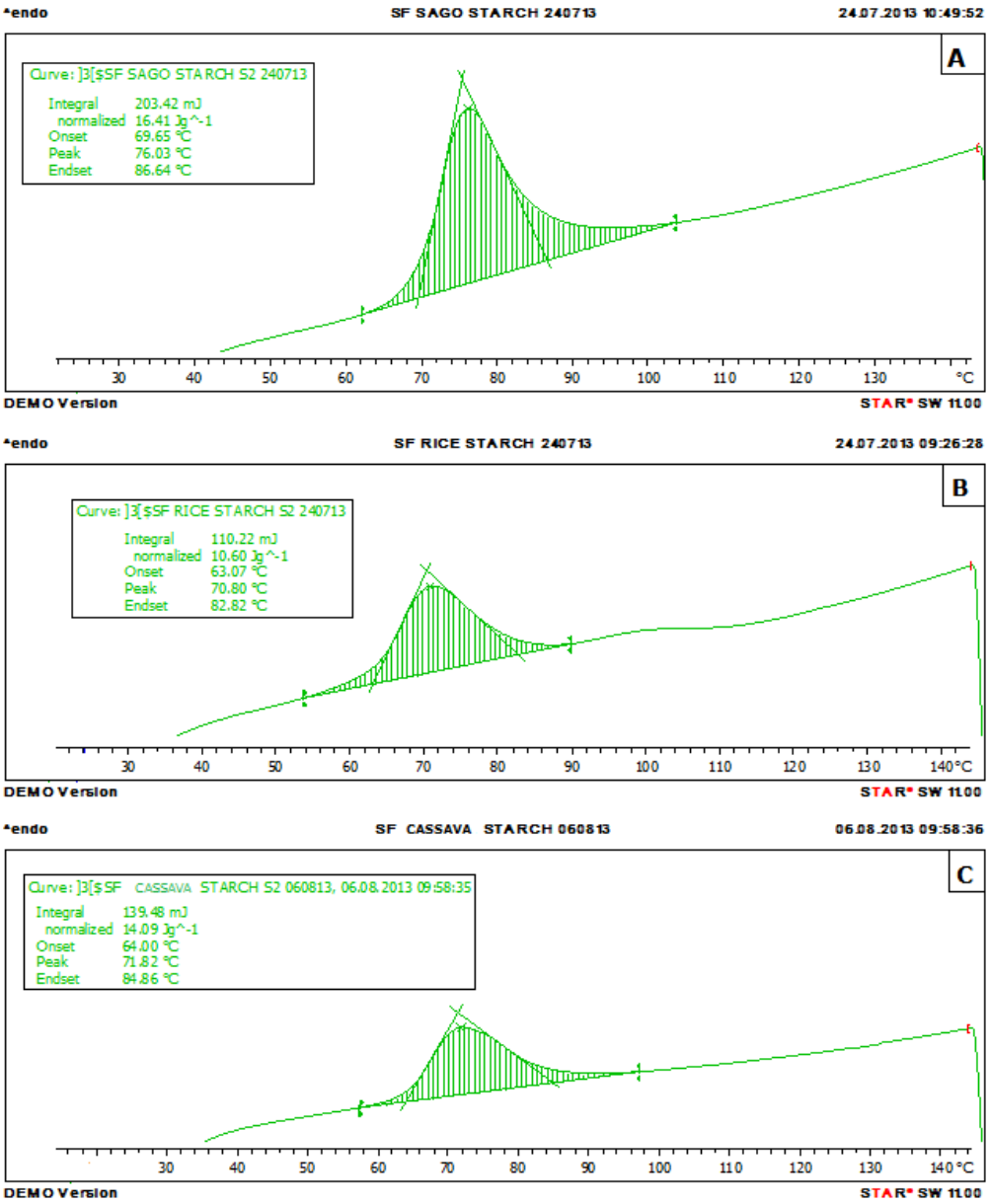

Figure 4.6 DSC thermogram of starch samples-water system with heating rate of 10 °C/min; A, sago; B, rice; and C, cassava. The legend shows gelatinisation temperature and enthalpy values.

Although the DSC endotherms obtained for starch are typically associated with the amylopectin fraction of the granule, it is known that the amylose may play a very significant role. It is possible that the sago starch is showing, all be it at modest levels, a delayed endotherm due to the amylose integrity with the ability of the amylopectin to hydrate and loose order. Furthermore, the variations in ΔH_g could represent differences in

bonding forces between the double helices that form the amylopectin crystallites, which resulted in different alignment of hydrogen bonds within starch molecules (Cooke and Gidley, 1992; McPherson and Jane, 1999). Hence, a higher ΔH_g should lead to higher granule stability and gelatinisation temperature which is obvious in this study for the sago starch.

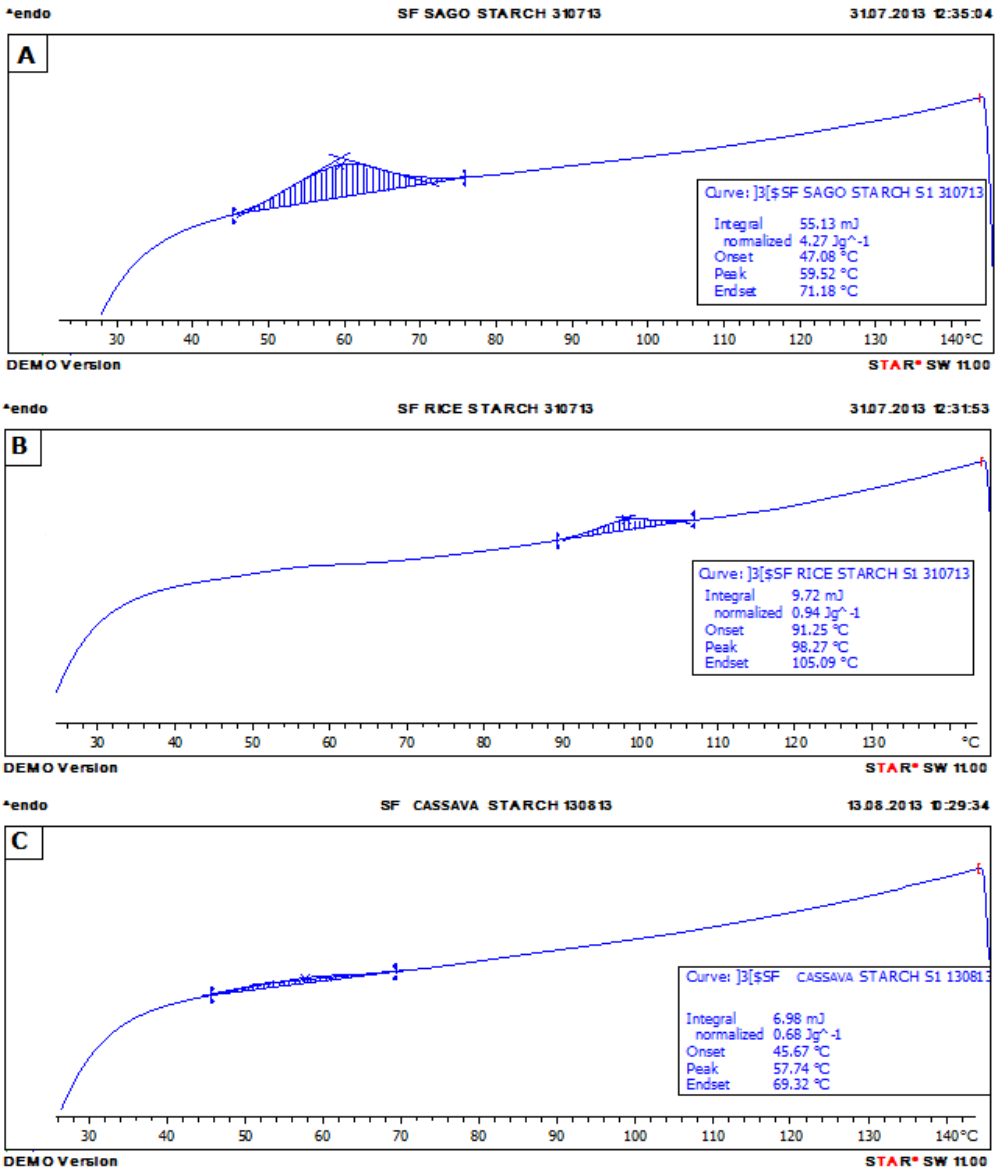

Figure 4.7 DSC thermogram of starch samples-water system with heating rate of 10 °C/min; A, sago; B, rice; and C, cassava. The legend shows retrogradation temperature and enthalpy values.

The RVA is not a good method to establish if starches will undergo significant amylopectin retrogradation. As the starches of interest had been heated in water and stored in the DSC pans, rescanning the samples would indicate if retrogradation had occurred.

The gelatinised starches were reheated after being stored at 4 °C for seven days, and the change of temperatures and enthalpies were observed (Table 4.6). The molecular interactions (mainly hydrogen bonding between starch chains) that occur after cooling of the gelatinised starch paste are known as retrogradation, involving the gelation of amylose, i.e., a formation of gel network and recrystallization of amylopectin (Miles et al., 1985; Eerlingen et al., 1994; Hoover, 2001). It can be seen from Table 4.6 that temperature and enthalpy values were lower for the retrograded starches with the exception of the temperatures of the rice starch. The lower onset temperature for the retrograded sample is normally associated with the fact that recrystallization of amylopectin branched chains occurs in a less ordered manner in the stored gels, compared to that present in the native form (Sandhu and Singh, 2007). The T_p for the retrograded sago and cassava starches was in the range of 55 to 60 °C as typical T_p of amylopectin as a starch fraction that is responsible for retrogradation (Russell, 1987). No enthalpies were seen for the rice starch in the region observed for the melting of the amylopectin in the first run. The enthalpies observed may well represent the melting of the amylose-lipid complexes. It is relevant that no enthalpy peaks were observed for the sago and cassava starches at these temperatures.

The retrograded starches in Table 4.6 showed lower enthalpy than their native counterparts. This could be due to the weaker starch crystallinity of retrograded starch (Sasaki et al., 2000). Moreover, ΔH_r for the three

starches ranged from 0.6 to 3.9 J/g where cassava had a much lower value than the sago starch. This study was not designed to maximise the retrogradation, but it is of interest to note that retrogradation enthalpies as high as 9.9 J/g have been reported in the literature (Tie et al., 2008). This is an indication that sago starch does have a strong tendency for amylopectin retrogradation.

4.5 Conclusions

The first clear difference observed for the sago starch in this study was that the moisture was high. Although this could reflect different drying of the starch post isolation, there should have been time for it to come to an equilibrium hydration on storage in the same conditions as the rice and cassava starches. Potato starch often has high moisture contents (~18%) under these conditions (Swinkels, 1985), but this is normally attributed to the phosphate groups attached to the amylopectin macromolecules.

Phosphate can be associated with lipids for example, so the presence of phosphate is no guarantee of their presence as part of the starch molecular structures. The phosphate levels measured for sago were about ten times lower than those reported for potato (Swinkels, 1985). The levels of ash were similar to those of cassava, so it can be assumed that the sago starch is not phosphorylated.

Tuber and root starches are considered low in lipid and protein, in comparison with cereal starches, and this does seem to be the case for the sago. Other supporting evidence for this conclusion is that in the DSC there are no signs of amylase lipid complexation, the sago pastes were very clear and the granule swelling seems to occur in one stage and the granules will breakdown under shear. One surprise when estimating the starches was the high levels of amylose measured for the sago starch. There are significant differences between the sago starch, rice and cassava in their assessment during the Megazyme assay procedure that was based of the amylopectin with Conconavalin A.

Despite information in the literature that sago and cassava starches may contain packing of the amylopectin in both the A and B type format, only the A pattern was observed for these samples. The crystallite form and the amount, as estimated from X-ray diffraction, showed no obvious differences between the samples.

Observation of the granules shows that the sago starch has very large granules (32 μm), even in comparison to the cassava. The rice grains are normally considered to be the smallest of the starches routinely processed. The example of rice starch used in this study seemed to have a wide range of sizes. Visualisation of the rice confirmed that much of the starch was in aggregates and that the size of the flour particles was not the size of the native granules. Granule size is often thought relevant for swelling volumes, but the cassava (granule size 17 μm) showed the highest swelling volume but was close to that of sago. Heating the starches in the excess water again showed that the cassava could hydrate and swell to a greater extent than the other starches. The pattern of pasting profile for the cassava and sago were very similar and showed high swelling and then breakdown, associated with poor stabilisation of the swollen granule, but then these starches do not have lipid in the granules and also the protein content is low. It is these factors that may differentiate them from the rice.

The DSC indicates that the peak and end temperature for the sago starch were considered as high (76 and 86.6 °C, respectively). This is in line with this starch being an A-type starch rather than B, as observed under the X-ray diffraction. The enthalpies are also high for the sago starch and this should reflect the amount of double helices in the sample. If the amylose is high in this sample, it means that the amylopectin must have a high

proportion of the A chains in an ordered form. The high enthalpies associated with potato starch are normally considered to be due to the extra-long A chains of the amylopectin. It may be that the sago also has long A chains, or it could be that high levels of the amylose, as detected by the Conconavalin A method, are associated with the amylopectin order. The longer chains and high levels of moisture are often associated with B crystallite formation, so although only the A pattern was seen for the sago, under slightly different growing conditions the C pattern may well dominate.

The rates and levels of amylopectin retrogradation are also associated with the A chain lengths and temperature and moisture levels on storage. All of the samples run on the DSC were stored at 4 °C and rerun to measure the recrystallization. The sago starch showed significant amounts of amylopectin reordering, while there was only little for the cassava. The rice only showed the presence of amylose-lipid complexes.

The sago starch is different from the other two starches measured. In many ways its granule size and indication that it may have long A chains in the amylopectin make it look more like a potato tuber starch, but it is not phosphorylated. Generally, root starches are thought to breakdown rapidly under thermal or chemical treatment, but there is no indication from the current data that this might be true for the sago. Its gelatinisation temperature is high, and despite its large granule size, it has a moderate swelling volume and peak viscosity with the only moderate breakdown of the paste viscosity on shearing. There seems no indication that there are indigenous lipids present, but if monoglycerides were added it could be predicted that they would greatly change the behaviour of sago starch.

A goal of the work presented in this thesis was to demonstrate that sago starch could be used in thermomechanical extrusion. The data from this chapter does show that the sago starch may have different properties compared with other starches typically used for this application. What the experimental work presented in this chapter did not explore was how sago starch would behave under moderate moisture contents and when the starch forms a melt. This is explored in the following chapter.

CHAPTER 5

Impact of iron fortification on the extrusion processing properties of sago starch evaluated through capillary rheometry

5.1 Introduction

Results from the previous chapter would indicate that sago starch may be very different from two starches commonly used to make extruded snack products. These differences may mean that the processing conditions for thermomechanical extrusion may need to be set outside the ranges typically used for rice or cassava with little information available to direct the choice of settings for sago. The study of this sago starch was therefore to establish: 1) whether sago starch could form a stable melt,
2) the impact of temperature on the starch conversion of sago starch,
3) the flow behaviour of sago starch melts,
and to use the information for the design of the extruder experiment.

The loss of starch granule integrity and formation of the melt are considered critical features in thermomechanical extrusion and it is these changes in state that may be trackable using the capillary rheometer (Madeka and Kokini, 1992; Sandoval and Barreiro, 2007) and by investigating the material "extruded" from this equipment.

To the best of our knowledge there are no reports in the literature on the rheological properties of sago starch melts. The impact of the presence of

iron (ferrous sulphate), which would be included as a nutritive additive, on the relevant rheological properties and starch conversion of the sago starch will be established using the capillary rheometer and will bring additional information to that of using the sago starch alone.

5.2 Literature review

Food systems are generally complex. Some food materials will turn into a melt under conditions of high temperature, pressure and shear. On the loss of order, other complex physicochemical changes may take place and degradation can occur. These changes affect the processing history of the melt and therefore influence the rheological properties, which in turn can alter the processing. One process in which the rheology of the system is of particular important is extrusion cooking (Senouci and Smith, 1988).

The rheological properties of starch can be particularly difficult to define due to the many different types of molecular assemblies that can be formed and the complex relationships with water (see section 2.2.8 about starch conversion). Mixing native starches with water creates a dough, which is an inhomogeneous mass with the starch granules taking up some water, the water acting as a plasticiser, but there will be a discontinuity in moisture level between the starch granules and the surrounding aqueous phase. Within the granules, there is also a discontinuity in moisture level due the presence of crystalline and amorphous phases. Depending on the temperature and levels of moisture or plasticiser, there can be a loss of order (molecular and crystalline) promoting equilibration of the starch moisture. Thus a homogeneous melt can be formed.

5.2.1 Rheological properties of gelatinised starch dispersions

Most of the rheological discussions on starches are based on their behaviour at relatively low solids and therefore the dominance is for the swollen starch granule behaviour. Gelatinised starch dispersions have a

non-Newtonian, time-dependent, viscoelastic behaviour and their rheological properties are highly dependent on the gelatinisation procedure (Senouci and Smith, 1988; Doublier et al., 1986). Data from studies on rheological behaviour of gelatinised starch dispersions are not easily comparable as they are reported on experimental work obtained with different measurement systems and with different gelatinisation procedures in terms of agitation, cooking temperature and heating rate (Lagarrigue and Alvarez, 2001). Dilatancy can be observed even though the behaviour of starch paste is most often shear-thinning.

Gelatinised starch dispersions are usually represented by the power law model. It has been suggested that dough or molten starch materials are pseudoplastic and shear viscosity behaviour can be adequately described by the power law model in the range 1 – 1500/s (Bhattacharya and Hanna, 1987; Senouci and Smith, 1988), see Equation (5.1).

$$\eta = K\dot{\gamma}^{n-1} \tag{5.1}$$

Where η is the apparent viscosity and $\dot{\gamma}$ is the shear rate, K and n are parameters of the power law model known as consistency (Pa s^n) and flow indexes, respectively.

Compared to measurement of low solids systems, the rheological measures of higher solid starch melts are much less studied. However, the relevance of thermomechanical extrusion to the manufacture of food products has encouraged measurements of food melts. To carry out the measurements, various methods have long been used. Typically off-line determinations use capillary rheometers (Senouci and Smith, 1988; Parker et al., 1989; Madeka and Kokini, 1992; Sandoval and Barreiro, 2007), but the use of a long die, fed directly by the extruder, can be an alternative to

acquire on-line rheological data at the extruder die (Bhattacharya and Padmanhabhan, 1992; Vergnes et al., 1993; Drozdek and Faller, 2002).

5.2.2 Capillary rheometer

The shear rheological properties of viscoelastic fluids, especially polymer melts, are extensively determined with a capillary rheometer (Figure 5.1). In this device, the polymer sample is forced by a piston or by pressure from a reservoir through the capillary, which is usually vertical. It can be detached from the viscometer so that it is possible to make measurements with other capillaries that have different entrance angles or different values of length L or diameter D. Often a capillary rheometer will consist of two barrels, one fitted with a long capillary die and the other with a die considered to have zero length (see Figure 5.1). The barrels are filled with a polymer solution or with a dough and then heat is added to the system to provide the experimental temperature (Gupta, 2000).

When the thermal equilibrium is reached, extrusion is begun, and the volumetric flow rate (Q) of the polymer or dough coming from the capillary at a given pressure drop is recorded. The apparent shear rate $\dot{\gamma}_{app}$ in the capillary is given by:

$$\dot{\gamma}_{app} = \frac{32Q}{\prod D^3} \tag{5.1}$$

Where Q is the volumetric flow rate and D is the capillary diameter.

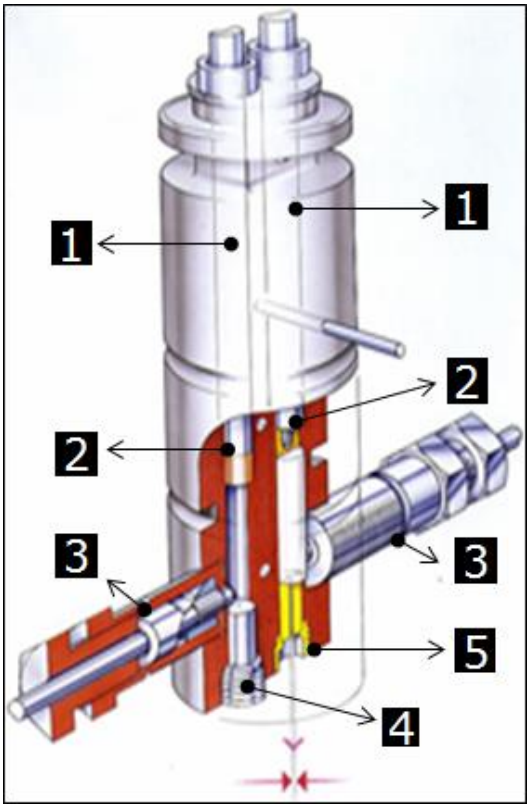

Figure 5.1 Schema of capillary rheometer used in this study. 1, barrels; 2, piston tip; 3, transducers; 4, capillary die; 5, orifice die (Malvern Instruments, 2006).

When moving the pistons down, the pressure profiles are measured at the entry to and exit from the capillary die. To obtain the true measure of the pressure loss that does not account in the simple measure of shear viscosity, a correction called the Bagley correction is normally applied. To adjust this correction, the usage of at least two different (L/D) dies is necessary, see Equation (5.2) and then the flow behaviour index can be described by Equation (5.3). The wall shear stress τ_w was determined from Bagley correction and given by:

$$\tau_w = \frac{\Delta P}{4(L/D)} \tag{5.2}$$

Where ΔP is the pressure drop over the capillary, L is the capillary length and D is the capillary diameter.

The value of n, the flow behaviour index being defined by:

$$n = \frac{d(\log \tau_w)}{d\left(\log \dot{\gamma}_{app}\right)} \tag{5.3}$$

Regarding the range of shear rate and shear stress, dies of different length to diameter (L/D) ratios can be used and various pressure drops along the dies applied. These can cover a wide range of shear rates (10^{-1}/s – 10^{6}/s) as well as a wide range of shear stresses (10^{2} – 10^{7} Pa). In the work reported in this thesis one capillary die and one zero length (orifice die) were used.

Due to the non-Newtonian behaviour of the melts, a further correction to the shear rate is needed to obtain the true wall shear rate, the Rabinowitch correction (Senouci and Smith, 1988), see Equation (5.4)

$$\dot{\gamma}_w = \frac{3n+1}{4n}\dot{\gamma}_{app} \tag{5.4}$$

Where $\dot{\gamma}_w$ is the true wall shear rate, n is the flow behaviour index. The wall shear stress τ_w and the true wall shear rate $\dot{\gamma}_w$ can then be used to determine the rheological behaviour and the materials being studied, see Equation (5.5).

The apparent viscosity of sago starch samples (η), at constant shear rate, was therefore calculated as follows:

$$\eta = \frac{\tau_w}{\dot{\gamma}_w} = K\dot{\gamma}_w^{\,n-1} \tag{5.5}$$

Where K and n are parameters of the power law model known as consistency (Pa s^n) and flow indexes, respectively.

The advantages of the capillary rheometer are not only it can operate at high shear rates, but also it is relatively easy to fill, and the test temperatures and shear rates are varied readily. Additionally, the shear rates are similar to the conditions actually found in extrusion. However, the principal disadvantage of this instrument is that the shear rate is not uniform. Other disadvantages are wall slip phenomenon and it can be difficult to clean (Gupta, 2000; Manias, 2012).

A drawback of capillary rheometry, as opposed to on-line rheometry at the extruder die, is that the moisture content of the formulation may have to be adjusted to higher levels to facilitate processing in the capillary rheometer. At moisture levels an extruder can handle, blockage of narrow capillaries has been observed (Vergnes et al., 1993 for instance; Drozdek and Faller, 2002; Li et al., 2004). For capillary rheometer analysis, it is worth noting that a pre-prepared dough is applied to the "extrusion process", whereas dry ingredients and water / liquid ingredients tend to be fed directly, through independent ports, into the barrel during conventional thermomechanical extrusion.

However, the capillary rheometer allows fundamental information to be obtained on melts at carefully controlled temperatures and shear rates. For the study of sago starch, with and without addition the iron, knowledge from the capillary rheometer could be useful to set up the thermomechanical extruder.

5.3 Materials and Methods

5.3.1 Material

The main material used for study in this chapter was sago starch, meanwhile the additive was ferrous sulphate heptahydrate ($Fe_2SO_4.7H_2O$), which were described in section 3.1. Sample and their codes are presented in Table 5.1.

Table 5.1 Samples used in capillary rheometer experiment.

Material(s)	Treatment		Code of sample
Sago starch	Native, raw		RSS
	Added 30% water (wwb) and processed in capillary rheometer at temperature (°C):	70	SS70
		80	SS80
		90	SS90
		100	SS100
Sago starch + ferrous sulphate	Native, raw		RSF
	Added 30% water (wwb) and processed in capillary rheometer at temperature (°C):	70	SF70
		80	SF80
		90	SF90
		100	SF100

5.3.2 Methods

5.3.2.1 Preparation of moistened samples (doughs)

Two types of moistened sample were made from raw sago starch. First was the sample without iron addition and second was fortified with iron. To make the moistened samples, raw sago starch was adjusted to 30% moisture (wwb) by slowly adding water while the starch was continuously mixed in a household food processor (Kenwood Limited, Havant, UK) at

medium speed to obtain a dough. Meanwhile for preparation of the iron-fortified moistened sample, the iron compound was dissolved in the water used for hydration to achieve 80 mg ferrous sulphate per 100 g sago starch. The samples were then sieved through a colander to eliminate lumps and left sealed overnight at 4 °C to reach equilibrium of moisture content. To validate the moisture content samples were dried (1 - 2 g) to constant weight in an oven at 105 °C. Rheological studies were then carried out by capillary rheometer at different processing temperatures using these moistened samples (Table 5.1).

5.3.2.2 Capillary rheometry process and analysis of rheological properties

The rheological properties of the moistened samples (at water content of 30% wwb), relevant to extrusion cooking, were assessed using capillary rheometry. A capillary rheometer (Rosand RH7 Rheometers, Malvern Instruments Ltd., UK) with a two barrel system (Figure 5.1) was used to process the samples while collecting rheology data. The equipment featured a drive unit that pushes two pistons into two barrels of 15 mm diameter and approximately 270 mm in length. Different apparent shear rates were applied by changing the piston speed. A capillary and orifice die, with the same diameter (2 mm), but of different lengths (32 and 0 mm, respectively), were fixed to the exit of the barrels. The orifice die was used in conjunction with the capillary die to be able to apply the Bagley correction (Senouci and Smith, 1988). Using the instrument's software (Flowmaster^{TM}), a set wall temperature was chosen (70, 80, 90, 100 °C) and the speed of the piston varied to give apparent shear rates ($\dot{\gamma}_{app}$) varying between from 10 to 500 s^{-1}. Approximately 76 g of sample was required to fill the two barrels with equal quantities of dough. A pre-test

sequence was used in order to compress the sample in the barrel to exclude any trapped air and to let the whole sample reach thermal equilibrium. This sequence consisted of four stages as follows: compression 1 with a speed of 50 mm/min, pre-heat 1 for 5 min, compression 2 (same as compression 1) and pre-heat 2 for 4 min. Each experiment at the same temperature was repeated three times using fresh dough. The samples emerging from the dies were collected and used for further analyses.

5.3.2.3 Processed samples

The processed samples emerging from the capillary rheometer were collected. The samples were named corresponding to their processing temperature: SS70, SS80, SS90 and SS100 for samples without iron, SF70, SF80, SF90, and SF100 for samples with iron addition (Table 5.1). They were vacuum dried (Gallenkamp vacuum oven, Fistreem International Ltd., UK) at 50 °C and 250 mbar for 15 h and then sealed into plastic bags. Moisture content of these dried samples was in the range of 7-8% (wwb). Prior to analysis of thermal, pasting and microstructure properties, these dried samples were milled with a Laboratory Mill (model 3600 Perten Instruments, Sweden) and the powder fraction that passed through a 250 μm sieve utilised.

5.3.2.4 Analysis of samples

The methods for analysis were explained in section 3.3. They included thermal properties, pasting behaviour and microstructure of the ground samples. The RSS and RSF samples were analysed together with the processed samples.

5.4 Results and Discussion

The sago dough prepared at 30% moisture (wwb) could be extruded from the capillary rheometer as a continuous rope of material. The formation of the stable extrudate occurred for all temperatures and piston speeds. None of the extrudates showed noticeable expansion as they emerged from the die.

5.4.1 Visual observation

Figure 5.2 shows an example of the non- and iron-fortified sago starch dough that had been processed using a capillary rheometer and cut into samples of about 5 cm in length. Both samples showed stable extrudates. It is noticeable that they differ in their colour, which was white for non-fortified samples and light brown for iron-fortified. One of the major challenges of iron fortification is thought to be undesirable off-colour development. When using highly bioavailable iron, for example ferrous sulphate, foods and beverages can dramatically change colour and this impacts on the recommendation of very short storage times due to undesirable colour changes that occur (Clydesdale, 1998).

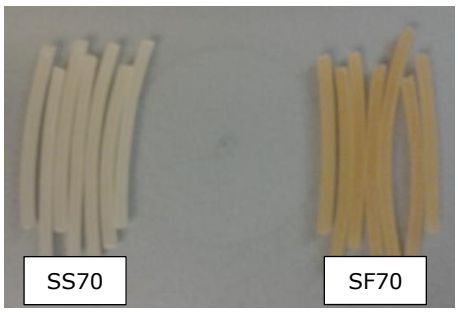

Figure 5.2 Samples from capillary rheometer processing; SS70 and SF70.

5.4.2 Rheological properties

The sago starch doughs were processed in a capillary rheometer at temperatures of 70, 80, 90 and 100 °C. The stable extrudates achieved for the sago starch allows for some consideration of the rheology of the samples as they form in the die. Treatment of the raw data can provide information on the true wall shear rate and the wall shear stress (see section 5.2.2). Figure 5.3 shows the viscosity curves as a function of true wall shear rate.

All samples show a viscosity decrease with increasing shear rate in concordance with pseudoplastic behaviour. Over the shear rate range analysed, and for all four temperatures, the viscosity decrease is linear in the double logarithmic diagram indicating that it follows power law behaviour and therefore values of the consistency (*K*) and flow behaviour indices (*n*) can be calculated (see Table 5.2). For each type of sample, the flow behaviour index shows an increasing trend with increasing temperature although it is only significantly higher at the highest analysis temperature (100 °C). The consistency values fall as the temperature increases.

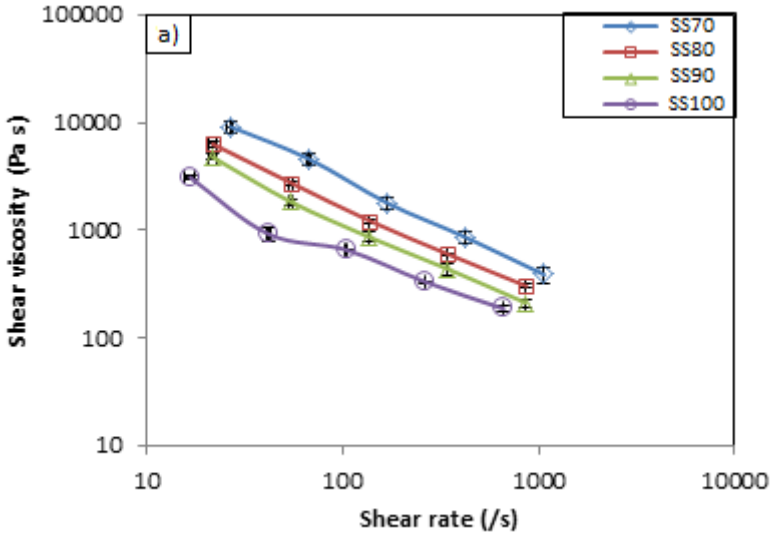

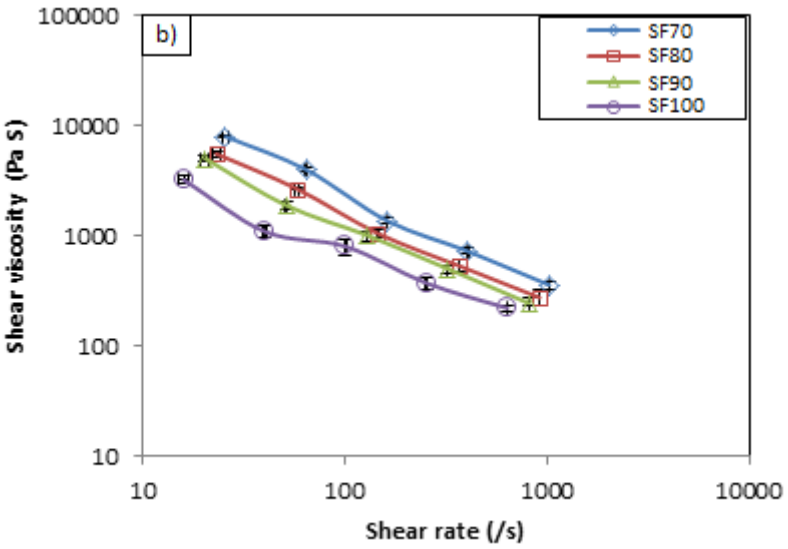

Figure 5.3 a) and b) Variation of shear viscosity with temperatures set; (a), non-iron fortified samples and (b), iron-fortified samples. The legend correspond the processing temperature at capillary rheometer.

Table 5.2 Consistency (*K*) and flow behaviour indices (*n*) of processed sago starch non- and iron-fortified samples at various temperatures. Capillary extrusion performed at 30% water content (wwb). Values are means ± SD (n = 3). Means within a column related to a particular parameter with the same superscript are not significantly different ($p>0.05$).

Sago starch sample	Barrel temperature (°C)	*K* (kPa s^n)	*n*
SS70	70	164.9^{c}±34.7	0.13^{a}±0.02
SS80	80	75.5^{b}± 1.7	0.18^{a}± 0
SS90	90	57.2^{ab}±15.2	0.18^{a}±0.02
SS100	100	19.2^{a}± 6.6	0.28^{bc}±0.05
SF70	70	128.9^{c}±18.5	0.14^{a}±0.02
SF80	80	74.8^{b}±19.0	0.17^{a}±0.04
SF90	90	50.9^{ab}± 9.7	0.20^{ab}±0.04
SF100	100	19.0^{a}± 4.7	0.30^{c}±0.04

This general trend of the viscosity behaviour with temperature and shear rate is in agreement with previous findings reported for oat, wheat flour

and wheat starch (Singh and Smith, 1999), corn starch (Sandoval and Barreiro, 2007), maize starch (Vergnes and Villemaire, 1987) and potato starch (Valle et al., 1995). It has been suggested that an increase of the flow behaviour index (*n*) is an indication of molecular degradation of starch-based materials (Bhattacharya et al., 1994) and therefore the power law index, *n*, has been taken as a measure of degradation. If the polymer degrades with increasing shear then the viscosity will decrease. Without major changes to the physical or chemical properties of the material being processed, it would be expected that viscosity would fall with increasing temperature.

The reason for the characteristic of the starches from the temperature relationship would be expected because of the changes occurring to the starch at the temperatures and moisture contents used. Previous information which was shown in Chapter 4 (see section 4.4.2.3) indicated that the melting temperature of sago starch in excess water was 76 °C. This was carried out at a solid starch:water ratio of 1:3. In the capillary rheometer, the starch:water ratio was about 2:1 and it is known that moisture contents impact on temperatures of melting. Melting temperature is an important material property to ensure that the temperatures chosen for the rheological experiments are appropriate for the material to melt and flow in the capillary rheometer (Sandoval and Barreiro, 2007). It is possible that the moisture contents and temperatures chosen did not convert the starch from its semi-crystalline state.

Although the state of the starch may not have altered, this capillary rheometer experiment indicates that the sago starch can form a stable extrudate, that will shear thin and the viscosity is lowered as the temperature increases from 70 to 100 °C. This would not be the case for

starches pasted in excess water (see section 4.4.2.2). The other finding relevant to future studies was, except for colour, the inclusion of the iron is not having an impact on the rheology properties of the sago starch.

5.4.3 Status of the sago starch

The capillary rheometer can be considered a processing device that subjects the starches to the temperatures they could experience during thermomechanical extrusion. The shear regimes may not be as great the samples created during the thermomechanical extrusion. The samples from the capillary rheometer experiments can be assessed to establish the changes in the samples' physicochemical characteristics. For the analysis, the capillary rheometer extrudates were dried and milled (methods given in section 5.3.2.3).

5.4.4 Thermal properties

The extent of starch loss of order after processing by the capillary rheometer was measured by DSC as in the method in section 3.3.8. Figure 5.4 shows the typical DSC thermogram of the samples without iron; the raw and the processed samples at the capillary rheometer. Table 5.3 shows the values of the characteristic parameters of the DSC traces and the percentage of transformation (lost) of starch (Equation 3.4).

The gelatinisation enthalpy (ΔH) of processed samples was lower than for the raw samples (RSS and RSF), and must indicate that the starch in the processed samples lost order during processing in the capillary rheometer. It can be seen from Figure 5.4 that the enthalpy of the raw sago starch was greater than the processed samples and this decreased in line with increasing processing temperatures (SS70 to SS100). The temperature

corresponding to the peak also increased as processed temperature increased. These characteristics for the DSC results were also observed on the processed samples with iron (figure not shown).

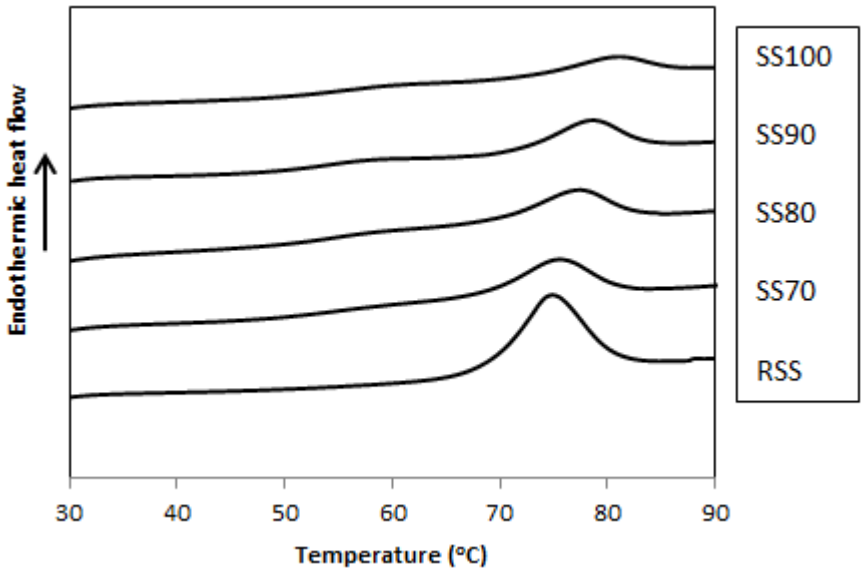

Figure 5.4 Typical DSC thermograms at a heating rate of 10 °C/min of raw (RSS) and processed non-fortified sago starch (SS) at various temperatures (shown next to the graph). DSC profiles performed with a starch/water ratio of about 1:3 (curves have been displaced on the y-axis for clarity).

A plot of enthalpy loss versus temperature of the raw sago starch as it was heated in the DSC is shown in Figure 5.5. On the same figure are the % loss of enthalpies, as compared to the starting values of 13 J/g, measured by DSC for each of the capillary rheometer processed samples. This would indicate that at a temperature of 70 °C for the raw sago starch, only about 10% of the enthalpy was lost, yet the capillary rheometer processed samples at this temperature shows 4-5 times this amount of lost order, perhaps equivalent to that expected at >75 °C. There can be several reasons for this miss match including that the temperature recorded for the capillary rheometer may not reflect the actual temperature of the

extrudate samples; the frictional forces may cause some temperature elevation or that duration of heating is relevant to amount of order loss. It is maintained that shear, in the form of specific mechanical energy, causes major differences to starches when near their melt temperature. Although shear forces between twin-screw extruders and capillary rheometer may not be comparable, the shear experienced by the starch may reflect the importance of this factor in the loss of order in the sago. Also indicated in Figure 5.5 is that there was still some order retained by samples heated in the capillary rheometer at 90 and 100 °C, while for raw sago starch, if heated to these temperatures in the DSC and in the presence of 1:3 starch water ratios, the loss of enthalpy would have been much greater. Lai and Kokini (1991) demonstrated that both temperature and moisture content have major influences on the enthalpy of transition of starches.

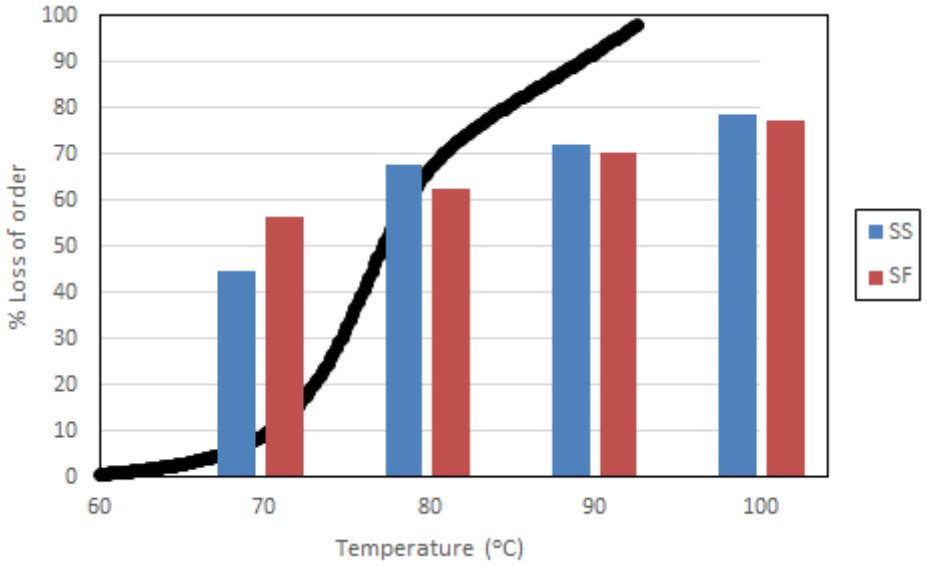

Figure 5.5 Percentage loss of order, as measured by DSC when sago samples were at a starch/water ratio of 1:3 and a heating rate of 10 °C/min was used. Black line represents the cumulative loss of order of raw (RSS) as enthalpy is lost during heating in the DSC. Bars represent loss of enthalpies (%) for the processed non-fortified (SS) and fortified (SF) sago starch, which had been heated in the capillary rheometer to the nominal temperatures indicated in the figure (70, 80, 90, 100 °C).

The processing conditions in the capillary rheometer involves a combination of shear and thermal treatment and these occur to different levels in extrusion cooking. It is thought that during the extrusion process, the starches lose their structural integrity due to increased shearing and kneading (Singh et al., 2010).

The addition of iron to the starch matrix may have had an impact on starch order loss and hence rheology and performance of sago starch extrudates. However, ferrous sulphate inclusion shows very little difference in the percentage of the starch transformation. The iron present in ferrous sulphate may have interacted with starch and resulted in iron-starch complexing (Hood and O'SHEA, 1977). The concept is that cations get adsorbed to the starch granule, but do not penetrate into the granule caused such complexing and this could then slightly reduce the starch loss of order (Hussain et al., 2013).

Table 5.3 Gelatinisation enthalpy and % loss of enthalpies evaluated by DSC measurements at a heating rate of 10 °C/min for raw sago starch (RSS and RSF) and processed samples (SS and SF) at various temperatures (no replication undertaken).

Sago starch sample	Barrel temperature (°C)	DSC	
		ΔH (J/g)	x (%)
RSS	n/a	ΔH_0 (J/g): 13.19	0
RSF	n/a	ΔH_0 (J/g): 13.03	0
SS	70	7.77	44.7
	80	4.60	68.0
	90	3.91	72.3
	100	2.98	78.9
SF	70	5.88	56.5
	80	5.08	62.5
	90	3.92	70.7
	100	2.93	77.6

Table 5.3 shows that the amount of loss of order of processed sago starch, with and without iron, increased as the temperature was increased. Results showed that for temperatures up to 100 °C, molten and non-fully molten material coexisted in the extrudates, but always a stable extrudate occurred. At higher temperatures, a complete melt may be formed as predicted by the previous studies by Núñez et al. (2010) for ready-to-eat starchy formulation with oat and rice flour as major components.

5.4.5 Pasting behaviour

An additional way of assessing the conversion of processed starchy material is to examine its behaviour in excess water with increasing temperature. The pre-dried and powdered capillary rheometer extrudates were therefore examined by using the RVA (method given in section 3.3.7.1). The RVA pasting profiles of raw and processed samples from the capillary rheometer at a moisture content of 30% are shown in Figure 5.6. The first thing to note is that no cold water peak is seen for any of the samples. A decrease in the peak viscosities was obtained for samples that were processed. The decrease followed the increasing temperature of processing for the SF samples that contained ferrous sulphate.

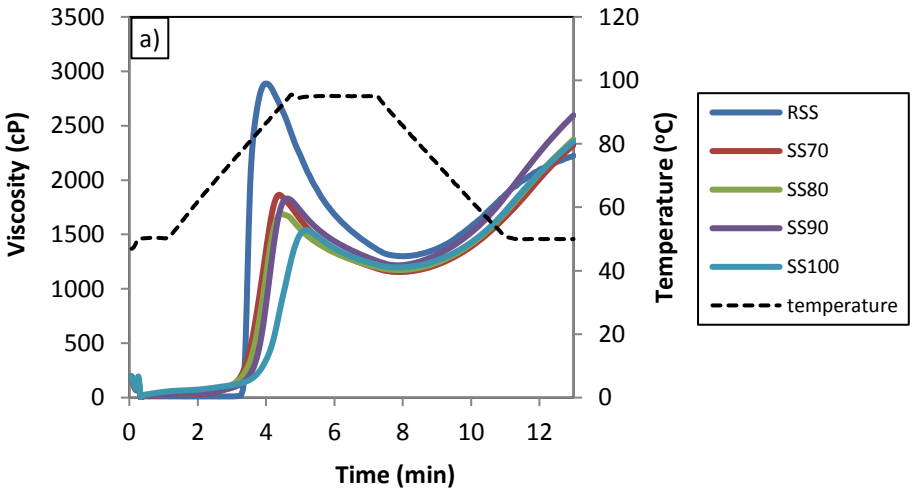

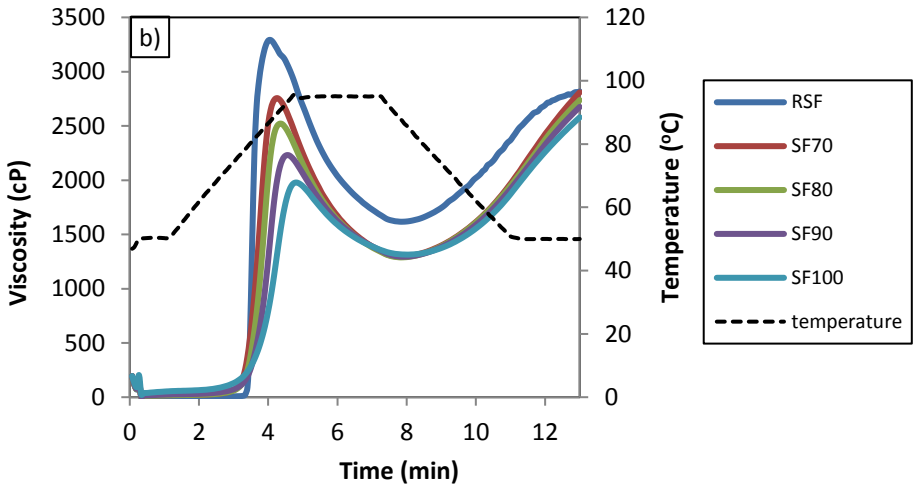

Figure 5.6 a) and b) RVA profiles of raw and processed samples at various temperatures: (a), without iron; and (b) with iron. The legend shows samples code (Table 5.1). Graph is based on averaged data (n=3).

Figure 5.6 and Table 5.4 show that the peak and hot paste viscosities obtained for processed samples in the capillary rheometer were significantly lower than that of the raw sago starch. The lower peak viscosities of processed samples compared to raw samples (RSS and RSF) may indicate that there was the loss of starch crystallinity during the processing. According to Bucher (1998), intense cooking processes will drive high levels of gelatinisation and molecular fragmentation that reduce viscosities in the pasting profiles. The addition of an iron fortification (ferrous sulphate) significantly (p<0.05) affected the peak viscosity of processed sago starch created at the different temperatures. All the iron-fortified processed samples showed considerably higher peak viscosity values compared with the non-fortified samples, if compared at the same processing temperatures. This may indicate that a greater amount of change had occurred in non-fortified sago starch. This result agreed well with Hussain et al. (2013) who studied viscous and thermal behaviour of vitamin A and iron-fortified reconstituted rice which found that sample

with the addition of iron fortificant (micronized ferric pyrophosphate) showed relatively higher peak viscosity values than that of without iron.

Table 5.4 Pasting properties by RVA measurements for raw and processed sago starch, non- and iron-fortified at various temperatures. Values are means ± SD (n = 3). Means within a column related to a particular parameter with the same superscript are not significantly different (p>0.05).

Sample	Barrel tempe-rature (°C)	Peak viscosity (cP)	Hot viscosity (cP)	End viscosity (cP)
RSS	n/a	2890^{f} ± 13.9	1300^{cd} ± 8.2	2226^{a} ± 41.8
RSF	n/a	3294^{g} ± 35.9	1617^{e} ± 33.3	2821^{e} ± 52.0
SS	70	1864^{bc} ± 20.3	1155^{a} ± 18.2	2340^{ab} ± 8.5
	80	1689^{a} ± 36.7	1173^{a} ± 22.9	2392^{ab} ± 32.9
	90	1830^{b} ± 56.7	1216^{abc} ± 48.6	2616^{cd} ± 95.3
	100	1585^{a} ± 78.0	1207^{ab} ± 32.6	2431^{bc}± 134.7
SF	70	2756^{f} ± 23.1	1294^{cd} ± 14.4	2832^{e} ± 33.5
	80	2520^{e} ± 38.9	1289^{bcd} ± 16.4	2758^{de} ± 54.8
	90	2230^{d} ± 51.2	1294^{cd} ± 14.5	2695^{de} ± 32.0
	100	1978^{c} ± 73.5	1314^{d} ± 48.3	2598^{cd} ± 90.1

The addition of chemicals, including salts, to starches is known to cause changes to their pasting behaviour (Paterson et al., 1996). Iron-starch complexing, as a result from an interaction between the starch and iron as present in an oxidised form of ferrous sulphate, possibly could explain the higher peak value and less gelatinisation in iron-fortified processed sago starch. However, very low levels of iron are thought to be bound by starch (Chabot and Hood, 1976). Hood and O'SHEA (1977) reported that the interaction of metallic cations with carbohydrate was demonstrated for both ionic and non-ionic carbohydrates; the formed complex is referred as

an adduct and can occur among alkali metals (Li, Na, K), alkali earth metals (Be, Mg, K), transitional elements (Fe, Ni, Zn, Cu) and multi-donor liquid molecules, which contain properly oriented hydroxyl group. Although the interactions between metals and sugar polysaccharides have been studied extensively (Gyurcsik and Nagy, 2000), the question about how metals, especially iron, interact with polysaccharides is still unanswered.

5.4.6 Microstructure

The previous two assessments indicate some, but not total loss of order occurred during processing with the capillary rheometer. A direct way to access starch granule changes is by microscopic observation. Figure 5.7 shows sago starch doughs and powdered extrudates from the capillary rheometer, which were viewed with a microscope using polarised light. When sago doughs were processed with the capillary rheometer at temperatures of 70, 80, 90 and 100 °C, much birefringence was lost indicating that the crystallinity of these granules was altered. However, due to grouping of starch granules after processing, it is quite hard to observe the birefringence. Micrographs shown in Figure 5.7 demonstrate that the increasing of temperature enhanced this loss of crystallinity. Interestingly there remained significant order, reminiscent of granule structures observable in the processed samples. Even though some crystallinity was lost, the processed extrudates do not resemble homogenous amorphous masses.

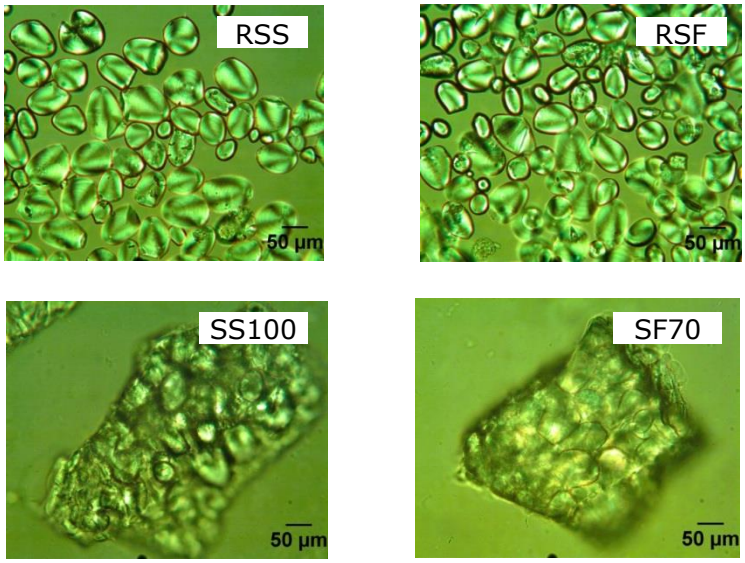

Figure 5.7 Microscopic observations using polarised light of raw sago starch (RSS and RSF), and the processed samples at temperature 100 °C (SS100) and 70 °C (SF70).

5.4.7 Starch conversion during rheological experiment

Examination of the capillary rheometer extrudates shows that crystalline order was lost and perhaps there was a greater loss than could have been predicted from just short term temperature effects (as occurs when heating in the DSC). At 70 °C and at the low moisture of the doughs, it could have been anticipated that the granules structures would not have altered. However, significant loss of order was measured in the samples from the capillary rheometer. Despite lost in birefringence and loss of order (as seen through DSC) samples needed extended heating before swelling was detected. This could be due to the particulates still retaining structures, perhaps the remaining of molten granules were stabilised through amylose interactions.

The homogenous melts without structural order, normally thought to be necessary to achieve directly expanded snacks do not seem to have been achieved in the capillary rheometer. The addition of iron, at concentrations consummate with fortification, did not have a major impact. If anything the inclusion of 80 mg ferrous sulphate heptahydrate in 100 gram of starch decreased the levels of converted starch as assessed by the methods used.

5.5 Conclusions

The capillary rheometer was used to establish the performance of sago starch at the temperatures and moisture contents used in extrusion. At temperatures of 70 to 100 °C, a stable extrudate was formed. The temperature did not affect the visual appearance of the extrudate, but the inclusion of ferrous sulphate did make the extrudate brown in colour. None of the extrudates expanded on leaving the die and by visual assessment their consistencies were similar. None of the samples resembled a clear, translucent, plastic melt, but rather the samples were white and turbid.

Capillary data demonstrated the shear thinning behaviour of non- and iron-fortified sago starch dough and the rheological data could be fitted to the power law. These results were in agreement with previous reports from previous authors for starchy products (Vergnes and Villemaire, 1987; Valle et al., 1995; Singh and Smith, 1999; Sandoval and Barreiro, 2007). The consistency coefficient decreased and the flow behaviour index increased of the samples at increasing temperatures. Meanwhile, the addition of iron sulphate heptahydrate at 80 mg/100 g of sago starch did not show a significant effect on the flow behaviour or the apparent viscosity of the processed sago starch.

The % loss of enthalpies of extruded SS and SF increased as the temperature increased. DSC and RVA measurements evidenced that a moderate shearing treatment at temperatures between 70 and 100 °C, as studied here, were able to decrease the order within the sago starch, but there were significant structures remaining in the processed products. These retained structures may have stopped the processed samples

hydrating in cold water. The rheological behaviour of iron-fortified sago starch on this lab-scale suggests that it may be possible to use sago for a directly expanded snack and the data measured can inform the set-up of the manufacturing equipment. For a directly expanded snack product made from sago starch, the temperatures and shear will need to be greater than used for the capillary rheometer studies. Since extrusion processing of sago starch is apparently not affected by the presence of iron at the conditions used in the capillary rheometer, there is no reason not to try this compound in the thermomechanical extrusion trials.

CHAPTER 6
Extrusion processing of sago starch

6.1 Introduction

Sago starch can be supplied in great quantity in Indonesia and could therefore be used as a food commodity thereby contributing to the food security program in this land. In previous chapters investigations on this key raw ingredient sago starch, were reported and how the properties of this material changed with temperature and shear (Chapter 4 and 5) were described. Although the sago starch may behave differently in some ways than the more traditional starches used in snack manufacture, the variations did not seem to be of such significance that the possibility of processing the sago starch would be ruled out.

Extrusion cooking is used worldwide for the production of many types of foods, including snacks. The technology is popular for the manufacture of snack foods owing to the technological advantages over traditional food processing techniques. Extruded snacks consist mainly of cereal or starch blends that are extruded with a certain amount of water. One of the materials that may be possible to use for the production of expanded snacks is sago starch; manufacture of such a product near where it can be easily grown would have many advantages (Abd-Aziz, 2002). Sago starch is a well establish food ingredient, especially in South East Asia where it is processed both traditionally and industrially. With thermomechanical extrusion, which is one of the fastest growing and most

important food-processing technologies of recent years, sago starch may be processed into various products, such as extruded snacks, which in turn will add to the economic value of this raw ingredient.

The twin-screw extrusion cooker is a food processing machine that can be used to produce a broad range of microstructural transformations in starchy food materials. There are some advantages for using the twin-screw extruder rather than the single screw type, for example, its mixing efficiency, self-cleaning opportunity, high productivity and flexible feed material handling (Moscicki and van Zuilichem, 2011).

For extruded products, their structure, both micro and macro, is influenced by the changes that occur in the physicochemical properties of the materials during processing. The changes are important factors in determining the eating quality and nutritional attributes of the extrudates and affect properties such as viscosity, water solubility and gelling behaviour (Moscicki and van Zuilichem, 2011). Typically the raw ingredients undergo hydration, high shear, high temperature, high pressure and rapid dehydration in directly expanded extruded snack formation (Harper, 1981). Under these harsh regimes, materials such as starch will lose much of their natural order, for example, crystallinity, melting of the helices and may be even depolymerisation of the amylopectin. The changes in the starch structure will impact on the ability of the melt material to expand, driven by water being flashed off as steam, as the melt exits the extruder (Moraru and Kokini, 2003). After leaving the extruder, if the materials are still in a rubbery state, as the material cools there will be potential for re-crystallisation of amylose and amylopectin.

The aim of the work reported in this chapter was to investigate if thermomechanical extrusion of sago starch could be achieved so that an expanded product could be made. Of particular interest were the effects of screw speed, water feed and die temperature on the physicochemical material properties of the extrudates. A twin-screw extruder was used which allowed die pressure and torque for the screws to be logged. The extrudates were assessed for moisture content, expansion, density, colour and texture. The extrudates were further ground to evaluate their viscosity behaviour, water absorption and solubility, microstructure and crystallinity.

This research was accomplished in two sets of extrusion trials. In the first set of trials, screw speed and water feed were varied while in the second set of trials the impact of die temperature at constant screw speed was explored. A brief literature review on extrusion processing of starchy materials is given before reporting the experimental work and conclusions.

6.2 Literature review of extrusion processing of starchy materials

Extruded foods consist mainly of cereals, starches, and vegetable proteins. These ingredients have a significant role in providing structure, texture, mouth feel, bulk, and other characteristics desired for specific finished products (Launay and Lisch, 1983). Starchy food materials, like corn, rice and semolina are ideal candidates for extrusion processing (Chinnaswamy and Hanna, 1988b). One important contribution of starch as a functional ingredient in extruded products is the expansion. The expansion gives the product crispness and is therefore important for the acceptability of expanded snack products, for example, a fish cracker (Noorakmar et al., 2012).

The gelatinisation mechanism of starch granules in excess water which includes swelling and loss of amylose from the granules, does not occur during extrusion. There is not enough moisture present during extrusion to allow for gelatinisation and the residence time inside the extruder tends not to be long enough for the temperature alone to melt the crystalline domains of starches (Harper, 1981; Lai and Kokini, 1991). Therefore mechanical shear forces are the primary contributor to starch disruption during extrusion cooking. This energy breaks the granular structure, provides fast humidification of the starch material resulting in starch melting.

While the content of starch does not change during extrusion processing, there is dependency of extrusion operating conditions on the degree of starch fragmentation and molecular degradation as well as on the final

structure of the extruded material. These extrusion operating conditions include feed material composition; size and moisture content; thermal and mechanical energy input during processing; extrusion geometry and die profile; material residence time affected by feed rate, screw speed, water addition and barrel length (Anderson et al., 1970; Doublier et al., 1986; Lai and Kokini, 1991). In terms of starch digestibility, high temperature and shear intensity in a typical extrusion cooking process cause almost total starch gelatinisation or melting or dextrinisation leading to increased starch digestibility (Singh et al., 2010).

An extensive body of literature on the effect of the aforementioned extrusion processing variables on product quality of starchy materials can be found. Quality parameter in general assessed include expansion, density, porosity, water absorption/solubility index, colour, crispness and sensory evaluation. The general consensus is that the moisture content of the feed material is a critical processing variable for product quality, where an increasing feed moisture content negatively correlates to expansion and positively correlates to bulk density of the extrudates (Alvarez-Martinez et al., 1988; Chinnaswamy and Hanna, 1988b; Badrie and Mellowes, 1991; Iwe and Ngoddy, 1998; Őzer et al., 2004; Thymi et al., 2005; Singh et al., 2007; Nurtama and Lin, 2009; Leonel et al., 2009).

Other extrusion processing variables that have been studied extensively with the feed moisture are screw speed and temperature. Altan et al. (2008) studied the effect of die temperature, screw speed and tomato pomace level on system parameters and product responses of 20 different combinations barley flour and tomato pomace extrudates. The system parameters and product responses were most affected by changes in temperature, pomace level and to a lesser extent by screw speed.

Structural properties of extruded corn grits were measured by Thymi et al. (2005) with varied feed rate, screw speed, product temperature (the temperature in the barrel screw and die) and feed moisture content on an extruder. They found that extruded product apparent density, porosity and expansion ratio were dependent on feed moisture content, residence time and temperature while there was no effect of screw speed. Porosity and expansion ratio of extruded products decreased significantly with feed moisture content and residence time, while temperature rises resulted in products of higher porosity and expansion ratio.

Owusu-Ansah et al. (1984) reported that all the extrusion variables studied (temperature, screw speed and feed moisture) were significantly related to the expansion of corn starch extrudates. The most significant variables for expansion was feed moisture, and for breaking strength were screw speed and feed moisture. The same extrusion variables were also studied by Chakraborty et al. (2011) on different millet–legume blend ratio extrudates. The moisture content had a predominant effect upon expansion, WAI and crispness, while density was most susceptible to the variations in screw speed.

Furthermore, Chinnaswamy and Hanna (1988a; 1988b) studied extrusion of starches with different amylose contents using various chemicals and found that the degree of gelatinisation of starch could be altered by temperature applied and the addition of chemical substances as well. Knowing the relationship between the extrusion variables, raw material qualities, molecular degradation with and without chemicals, and expansion volume will allow us to use starch more efficiently to produce extruded snacks.

6.3 Materials and Methods

6.3.1 Materials

The main material used in the research reported in this chapter was sago starch supplied by PT Riau Sago Lestari, Indonesia and it was used as received.

6.3.2 Methods

There were two set of extrusion trials performed in this Chapter. Trial one was at variable screw speed and water feed rate, while trial two is at variable die temperature. The general extrusion processing and extrudate analysis were the same for both trials.

6.3.2.1 Extrusion processing

A schematic of the extrusion processing equipment is shown in Figure 6.1. The extruder was a Prism TSE 24 MC (Thermo Fisher, UK) fitted with two screws that will convey, mix, shear and meter the material to a round 3 mm diameter die. The length to diameter ratio of the screws was 40:1, with the screws being 24 mm across the flights. In this study, the screws consisted of two general types: conveying and mixing elements. All of the mixing elements were F60° (60° forwarding). Specifically they were: 30 x conveying elements (each 24 mm long); 6 x mixing elements F60° (each with a width of 6 mm); 3 x conveying flights; 7 x mixing elements; 2.25 x conveying flights; and 1 x extension end flight (36 mm long). Figure 6.2 shows the screw configuration and the function.

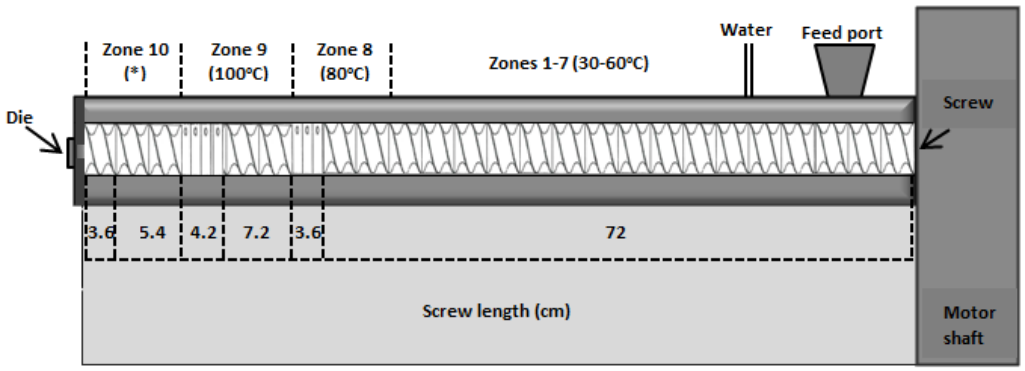

Figure 6.1 Schematic of the extruder; 1-7 are mixing or conveying zones, 8 and 9 are a mixing and kneading zone, respectively, 10 is a metering zone where the temperature vary based on the trials (based on Abson et al. (2014)).

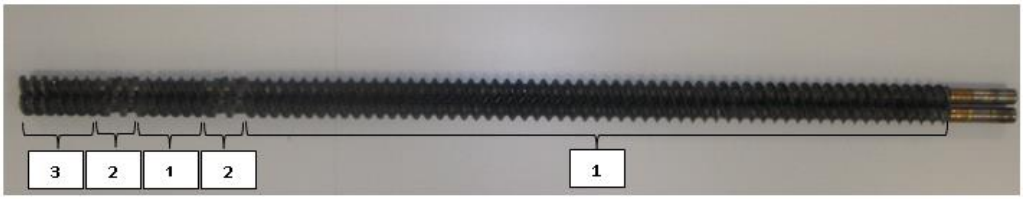

Figure 6.2 Screw configuration used in this study; (1) mixing and conveying, (2) kneading, (3) metering.

Sago, as provided, was used as the dry feed for the extrusion. The feed rate was always 8 kg/h and this was regulated using a calibrated gravimetric screw feeder (model DDW-DS(R)28N Brabender Technologie GMBH & Co. KG, Duisburg, Germany). The dry powder was conveyed along the screw where a water feed was introduced. The amount of liquid was regulated via a peristaltic pump (model 520S, Watson-Marlow Ltd., Cornwall, UK) and was adjusted to provide a range of moisture additions; 4, 7, 10, 15 and 20 mL/min for trial one while it was adjusted to 4 and 7 mL/min for trial two.

The solid feed and moisture additions were mixed by the screws and the blend heated. The extruder barrel had ten heating zones and the temperature of each of the zones is indicated in Figure 6.1. The

temperature of the final heating zone corresponds to the die temperature and this was constant 140 °C for trial one, while it was set at 120, 140 and 160 °C for trial two. The screw speeds were set to 200, 300 or 400 rpm for trial one and constant at 300 rpm for trial two. As samples emerged from the die, they were collected and manually cut to suitable lengths using a scissor. The moisture content of these fresh extrudates was measured. Some samples were dried at 45 °C for 18 h and these were used for the further analysis as described in section 6.3.2.2.

The exact temperatures along the barrel, the back pressure and torque were measured and these data collected to ascertain the processing regimes during the extrusion runs. The specific mechanical energy (SME) input was calculated using the formula given in Equation (6.1).

$$\text{SME} = \frac{\textit{Screw torque}\ (\text{Nm}) \times \textit{screw speed}\ (\text{rad/s}) \times \textit{number of screws}}{\textit{feed rate}\ (\text{kg/s})} \qquad (6.1)$$

The units of SME are J/kg or Wh/kg.

6.3.2.2 Extrudate analysis

Utilising methods introduced in Chapter 3 (Materials and Methods) the sago starch based extrudates were analysed for a number of starch material properties as well as those associated with the expanded end products such as appearance, cellular microstructure (Scanning Electron Microscopy method given in section 3.3.13), colour (method given in section 3.3.9), expansion ratio (method given in section 3.3.10), bulk density (method given in section 3.3.11) and texture (method given in section 3.3.12).

Furthermore, the extrudates were then ground and the powders used for a series of assessments that would indicate the physicochemical behaviour and how it changed on processing. The assessments were water absorption index and water solubility index (method given in section 3.3.14), paste viscosity (method given in section 3.3.7.2), birefringence (method given in section 3.3.5) and crystallinity (method given in section 3.3.15).

Prior to analysis for water absorption index, water solubility index, viscosity, birefringence and crystallinity, the extrudates were milled using a hammer mill (laboratory mill 3600, Perten, UK) and coffee grinder (KG49, De'Longhi, Hampshire, UK) and passed through a laboratory sieve with a spacing of 250 μm. Material which did not pass through the sieve after grinding was reground and sieved again particularly for extrudates produced at water feed rate of 20 mL/min.

6.4 Extrusion processing of sago starch at variable screw speed and water feed rate

Initial extrusion trials were carried out to ascertain if thermomechanical extrusion would be a suitable method to process sago starch to create an expanded product. Major factors that influence the behaviour of starchy products are related to the mechanical and thermal energies to which the extrudates melt within the extruder is subject. Various authors (Anderson et al., 1970; Doublier et al., 1986; Alvarez-Martinez et al., 1988; Chinnaswamy and Hanna, 1988b; Badrie and Mellowes, 1991; Lai and Kokini, 1991; Iwe and Ngoddy, 1998; Őzer et al., 2004; Singh et al., 2007; Leonel et al., 2009; Nurtama and Lin, 2009) suggested that screw speed and viscosity of the melt which can be controlled by moisture content, can influence the extrudates properties. To investigate the properties of sago starch extrudates, two processing variable were therefore looked at in detail. One variable was screw speed which was 200, 300 and 400 rpm. The other variable was to change the water addition level that consisted of 4, 7, 10, 15 or 20 mL/min and this corresponded to 16.5, 18.3, 20, 22.7 and 25.2% water in the melt as the moisture content of the sago starch. Die temperature was kept constant at 140 °C and the feed rate of sago starch was constant at 8 kg/h throughout.

6.4.1 Torque and specific mechanical energy input

By changing the screw speed and the moisture content it could be expected that the sago is subjected to different shear regimes, see Equation (6.1). Within the barrel, the sago particles could be expected to hydrate, lose molecular order/starch crystallinity, melt and form a

homogenous matrix and if the shear is sufficient, then molecules will be depolymerised as the high viscosity melt flows between the screw tip and the barrel wall. It is also possible that chemical reactions will occur that change the physicochemical nature of the polymer melt.

Figure 6.3 shows the variation of the torque with specific mechanical energy (SME) input and screw speed. For the range of screw speeds and water feed rates applied at the otherwise constant processing conditions, the torque increased nearly linear with SME when the water feed rate was decreased. There is no discontinuity and this result agrees well with Ollett et al. (1990) who investigated the effect of screw configuration and its interaction with extrusion moisture and barrel temperature in controlling the microstructure of extruded maize grits.

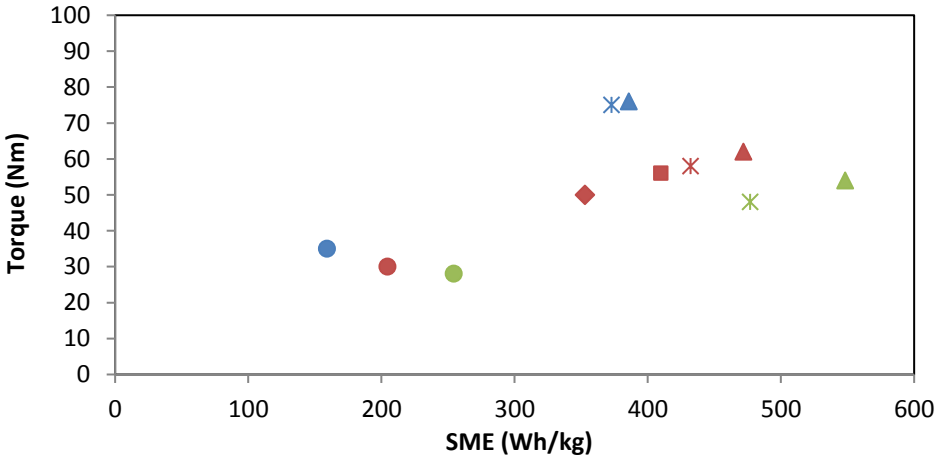

Figure 6.3 Variation of torque with screw speed and specific mechanical energy (SME) input. Screw speed (rpm): blue, 200; red, 300; green, 400. Water feed (mL/min): ▲, 4; ✳, 7; ■, 10; ◆, 15; ●, 20.

From Figure 6.3, it can be seen that a major change in the average molecular weight of the starch polymers seems unlikely due to the continuity in the data points which is approaching a linear relationship

between torque and SME as explained by the definition of SME, see Equation (6.1). Reducing water feed rate, as the level of plasticiser, could be expected to increase the resistance to the flow of the material. It is possible that this plasticiser effect is negated if the molecular weight of the polymer is very much reduced due to depolymerisation occurring in the high shear regimes. Furthermore, the torque decreased as the screw speed was raised and this may indicate that there is some molecular change, or that the polymer shear thins, or that the screw is no longer fully conveying the material at the higher speeds.

6.4.2 Moisture content of the extrudates as they exit the extruder

The temperature at the die of the extruder was set at 140 °C and therefore it could be expected that water within the product would flash off as steam as the product leaves the extruder. The amount of water loss would be dependent on the total water in the product and the structures being formed as the product expands due to the steam generation. Figure 6.4 reports the moisture content of the extruded samples produced at different screw speed and water feed and also shows the calculated moisture content of the melt for the different feed rates. It should be noted that only one run per processing parameter was carried out and the moisture data is based on the analyses of three extrudates per run. Extruder runs on different days may give rise to variation in the moisture of the extrudates gathered at the end of the equipment. However, it is clear that all samples have lost moisture as they exited the extruder.

With regards to screw speed, extrudates produced at the highest water feed of 20 mL/min had the highest moisture content indicative of a loss of

about 10% moisture. Meanwhile, there was no significant difference (p>0.05) in moisture content for extrudates, collected at the die, produced at water feed of 4, 7, 10 and 15 mL/min at screw speed of 300 rpm, despite the melts having different moisture levels. The results indicate that at these four water feed rates the extrudates quickly came to constant moisture on exiting the die. At the highest feed moisture, equivalent to a melt moisture content of 25.2%, there is a step change in the moisture content of the extrudates. This could be due to either the temperature being insufficient to evaporate the excess water or that the structures formed do not allow for moisture diffusion through the matrix in these high moisture samples.

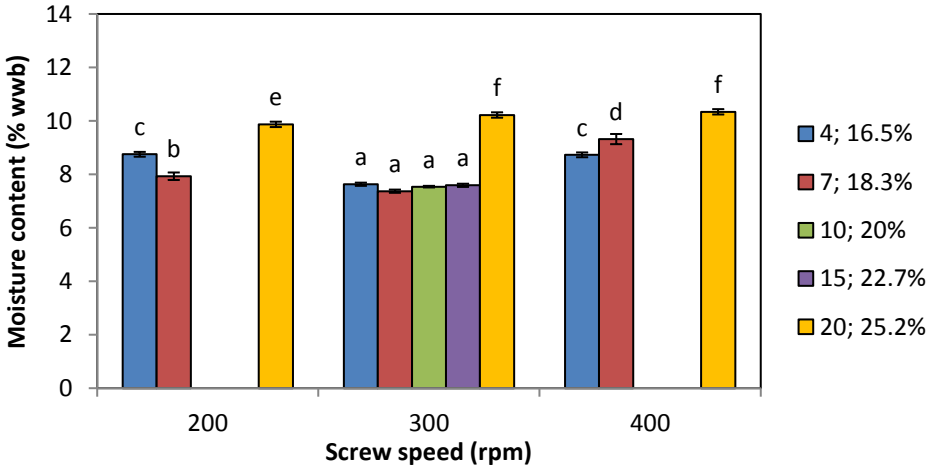

Figure 6.4 The moisture content of extrudates produced at different screw speeds and different water feeds. The legend shows water feed in mL/min; % moisture content of the melt (wwb). Bars represent mean ± SD of 3 replicates. Bars denoted by the same letter are not significantly different (p>0.05).

6.4.3 Physical material properties of the extrudates

The samples from the extrusion processing runs were dried at 45 °C for 18 h and then these materials were subjected to a series of observations and

measurements. In the following results are presented first followed by discussion due to interrelationships between the parameters.

6.4.3.1 Appearance

All of the extrudates collected from the runs at 300 rpm and variable water feed rate are shown in Figure 6.5. The diameter of all of the samples is in excess of 3 mm corresponding to the die diameter manifesting that all samples show expansion. The pictures indicate that there are bubbles within the matrix, but there are also other structural features. The sample created at the lowest feed rate (a) shows the greatest expansion and a fairly uniform bubble pattern. At slightly increased feed rate of 10 and 15 mL/min (c and d), the extrudates show a folded layering structure. There is a tendency for a decrease in diameter as the moisture increases, but the sample extruded at the highest feed rate (e) shows some areas of high expansion, followed by an area of few bubbles where the diameter is low and the sample looks shiny and "glassy". The bulk densities of the extrudates will be discussed later.

Figure 6.5 Photographs of extrudates produced at constant screw speed 300 rpm and at different water feeds: a, 4; b, 7; c, 10; d, 15 and e, 20 mL/min.

In Figure 6.6, pictures of the extrudates are arranged so that the impact of screw speed and the water feed rate on appearance can be easily compared. The impact of screw speed at constant water feed is complex

and there could well be an interaction between screw speed and the moisture content of the melt. There appears to be a minimal impact of screw speed at the lowest water feed of 4 mL/min. The extrudate diameter decreased slightly with increasing screw speed. The extrudate appears to be showing a folded layering structure at their surface for the 400 rpm sample at 4 mL/min feed rate. When the water feed was 7 mL/min the extrudates were similar to those created at 4 mL/min. Again, the gross structure at the highest screw speed is more irregular, this time featuring blobs at the surface rather than the folds seen previously.

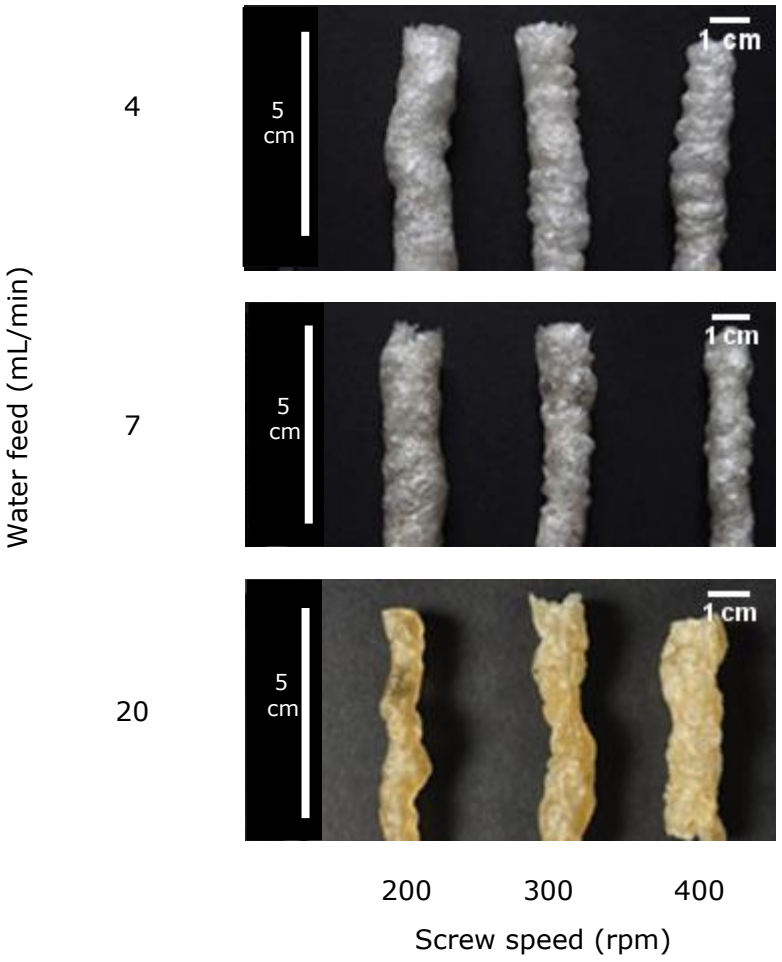

Figure 6.6 Photographs of extrudates produced at different screw speeds (vertical) and at different water feeds (horizontal).

An increase in screw speed from 200 to 400 rpm resulted in an increase in the expansion of the extrudates at water feed of 20 mL/min (Figure 6.6). Moreover, extrudates produced at this water feed rate appeared to be very hard and "glassy" making their appearance very different from the other extruded samples in this experiment. The extrudates show some major variations, but the change in surface characteristics could well be based on bubble stability and the size of the air pockets. To investigate this in some detail, the extrudates were subjected to Scanning Electron Microscopy (SEM) to visualise the cellular microstructure.

6.4.3.2 Cellular microstructure

The cellular microstructure of the extrudates is shown in Figure 6.7 by means of scanning electron micrographs (method given in section 3.3.13). Unfortunately, no images are available for 20 mL/min as explained in the description of the method. By comparison regarding water feed rate, the smallest air cells and most homogeneous size of air cells were found in extrudates produced at 15 mL/min water feed rate. This is followed by the extrudates produced at 10 mL/min and 7 mL/min where the size of air cells increased with decreasing water feed. Extrudates processed at 4 mL/min water feed rate have the largest sized and intense number of air cells in a structure of many layers. On the other hand, extrudates processed at different screw speed but the same water feed rate (4 or 7 mL/min) showed the same characteristics of the air cells.

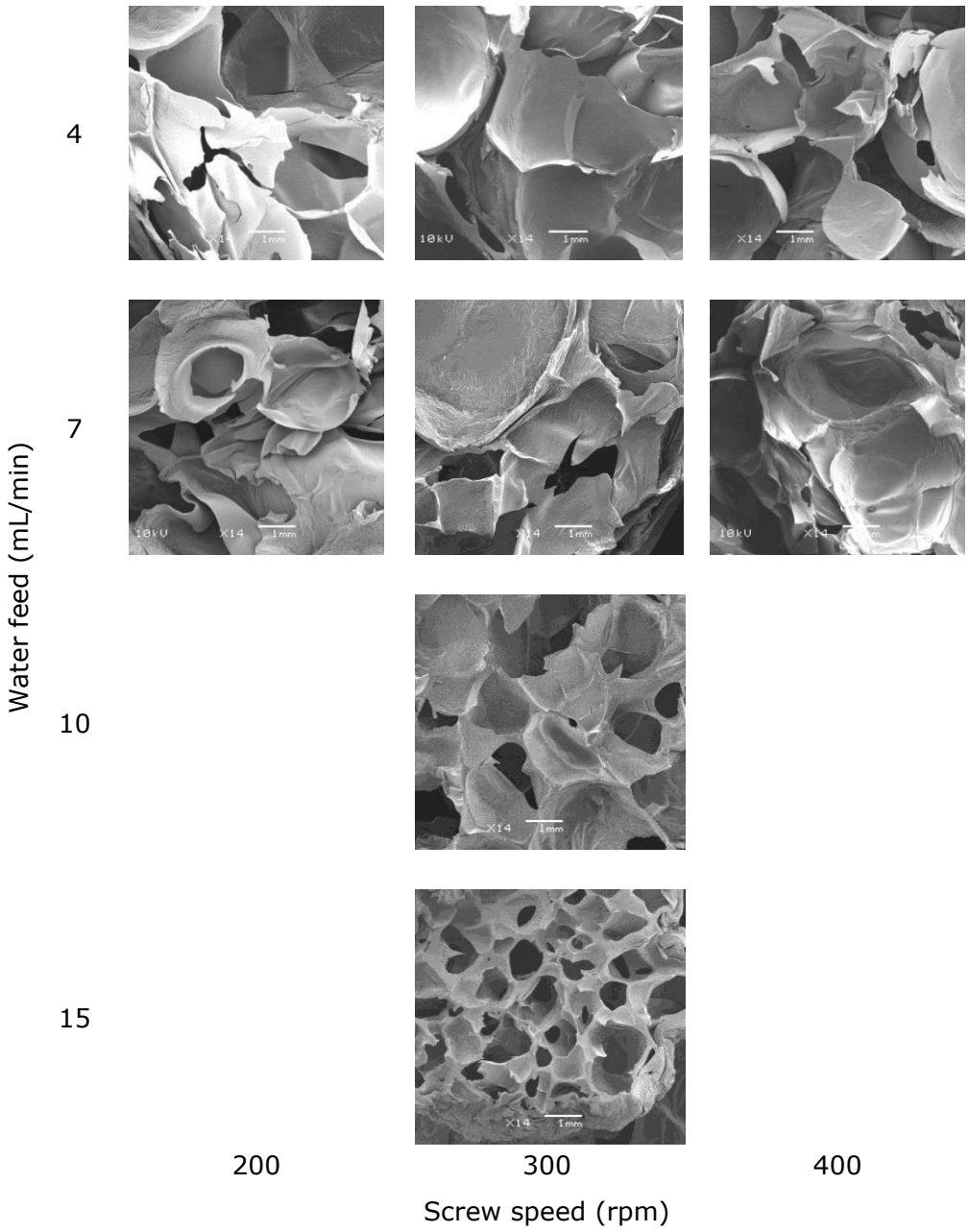

Figure 6.7 Scanning Electron Microscopy (SEM) pictures of extrudates produced at different screw speeds (vertical) and at different water feeds (horizontal).

6.4.3.3 Colour

The same feed materials, sago starch and water, were used to create the expanded extrudates, the only difference being in the water feed rate. However, visually the samples appeared to be different in colour. To try

and measure these differences, the extrudates were used directly for the measurement of colour using the Hunter colorimeter (see the method in section 3.3.9). Values for *L**, *a**, *b** were acquired for ten extrudates taken from the single processing runs and the data are shown in Table 6.1. Analysis of variance indicated that the effect of screw speed and water feed rate on extrudate colour was significant *(p*>0.05). It shows *L** values from the experiments varied widely between 29.3 and 60.5. The lightness value (*L**) increased with increasing in water feed until 15 mL/min. In fact, extrudates made at 20 mL/min water feed rate showed major differences for *L** and *a** values when compared with the other products. Screw speed appeared to have no significant impact for all of the colour parameters when compared to equivalent levels of water feed except *a** values of samples produced at 4 mL/min water feed.

Table 6.1 Colour properties of extrudates produced at different screw speeds and different water feeds. Values are means ± SD (n = 10). Means within a column with the same superscript are not significantly different (*p*>0.05).

Screw speed (rpm); water feed (mL/min)	*L** (lightness; zero for black to 100 for perfect white)	*a** (negative values for greenness to positive values for redness)	*b** (negative values for blueness to positive values for yellowness)
200;4	52.5^{de}±0.05	-0.11^{a}±0.04	3.83^{a}±0.72
200;7	51.2^{c}±0.61	0.02^{bcd}±0.02	4.33^{bc}±0.42
200;20	29.8^{a}±0.26	0.77^{h}±0.08	5.92^{e}±0.04
300;4	48.9^{b}±1.20	-0.03^{b}±0.08	3.90^{ab}±0.37
300;7	52.8^{d}±1.66	0.05^{cd}±0.04	4.39^{c}±0.05
300;10	58.3^{e}±0.04	-0.02^{bc}±0.01	5.17^{d}±0.16
300;15	60.5^{f}±0.17	0.38^{f}±0.02	7.17^{f}±0.06
300;20	29.3^{a}±1.24	0.63^{g}±0.04	5.89^{e}±0.32
400;4	48.3^{b}±1.06	0.19^{e}±0.02	4.80^{cd}±0.07
400;7	52.9^{d}±0.77	0.05^{d}±0.02	4.72^{cd}±0.40
400;20	29.5^{a}±0.55	0.58^{g}±0.05	5.06^{d}±0.11

The redness (*a** value) of the products varied significantly. Increasing water feed rate up to 20 mL/min resulted in extrudates with a higher redness value, while no significant increase in redness with increased screw speed was detected in samples produced at 7 mL/min water feed. There tended to be an increase in the yellowness (*b** value) of the products as levels of water feed increased at all levels of screw speed. The exceptions are that for extrudates produced at 20 mL/min and 300 rpm, the yellow value did not increase in comparison with the slightly lower moisture samples. For samples produced at the highest screw speeds, there is no trend in the colour associated with the water feed.

6.4.3.4 Expansion ratio

The effects of extrusion conditions on the expansion ratio of the extrudates (defined in section 3.3.10) are shown in Figure 6.8. The expansion ratio of the extrudates ranged from 1.68 to 3.81. The effect of screw speed on the expansion ratio varied in all extrudates.

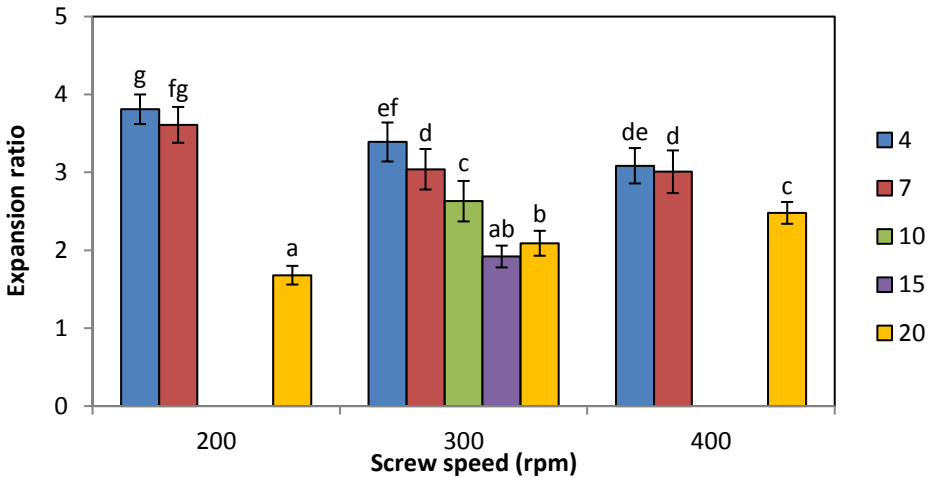

Figure 6.8 Expansion ratio of extrudates produced at different screw speeds and different water feeds. The legend shows water feed in mL/min. Bars represent mean ± SD of 10 replicates. Bars denoted by the same letter are not significantly different (p>0.05).

As can be seen in Figure 6.8, increasing screw speed from 200 to 300 rpm significantly decreased the expansion ratio of extrudates processed at water feed rates of 4 and 7 mL/min and became not significant from 300 to 400 rpm. On the other hand, extrudates manufactured at a water feed rate of 20 mL/min exhibited a significant increase in the expansion when increasing screw speed. Figure 6.8 also shows that increased water feed rate from 4 to 15 mL/min particularly at 300 rpm screw speed significantly decreased extrudate expansion.

6.4.3.5 Bulk density

The effect of process variables on the bulk density of extrudates are presented in Figure 6.9 and across all samples, the values vary between 0.17 and 1.34 g/cm^3. The bulk density of samples processed at 4, 7 and 10 mL/min water feed showed no significant difference for all of the screw speeds applied. Increasing water feed to 15 and 20 mL/min increased the bulk density of the samples. The highest value was obtained for samples processed at the highest water feed and the lowest screw speed (20 mL/min at 200 rpm).

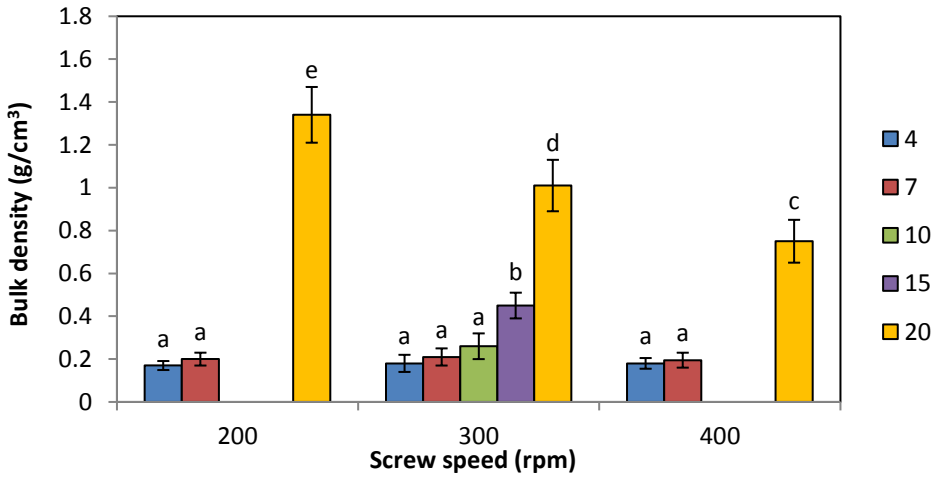

Figure 6.9 Bulk density of extrudates produced at different screw speed and different water feed. The legend shows water feed in mL/min. Bars represent mean ± SD of 10 replicates. Bars denoted by the same letter are not significantly different (p>0.05).

6.4.3.6 *Texture properties*

The texture of the extrudates was examined based on the two parameters of hardness and crispness. These were measured with a texture analyser utilising the methods described in section 3.3.12. Figure 6.10 shows examples of the force texture profile for two extrudates. Hardness was taken as the first peak value indicating the first rupture of the snack while the total number of peaks was taken as a measurement of crispness (Stojceska et al., 2008). From the results of the two samples shown in Figure 6.10, it is clear that water feed rate has an impact on the texture profile and thus hardness and crispness. No values could be obtained for the sample manufactured at the highest water feed rate (20 mL/min) due to a very hard and "glassy" texture and no breaking at the chosen measurement parameters.

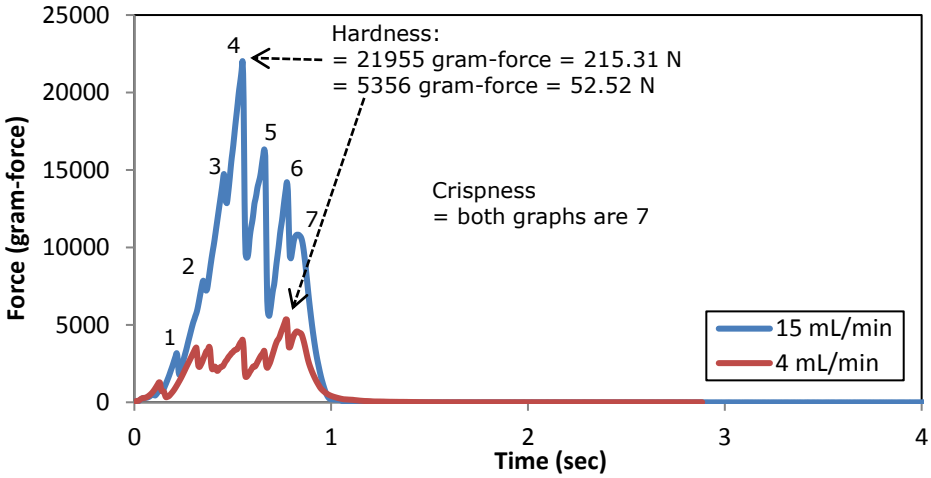

Figure 6.10 Force texture profile for two extrudates obtained by the crushing method.

The results for hardness are shown in Figure 6.11. From the figure, it can be concluded that increasing water feed above 7 mL/min led to extrudates of significantly increased hardness. Figure 6.12 shows results for the

crispness of the extrudates. Water feed was found to have a significant effect on extrudates crispness. Increasing water feed from 4 to 7 mL/min significantly decreased the crispness of the sago extrudates at the screw speed of 200 and 400 rpm, where at 300 rpm the crispness decreased at water feed of 20 mL/min. Concerning the screw speed effect, there are no significant differences of hardness and crispness for 4 mL/min extrudates at all screw speed applied.

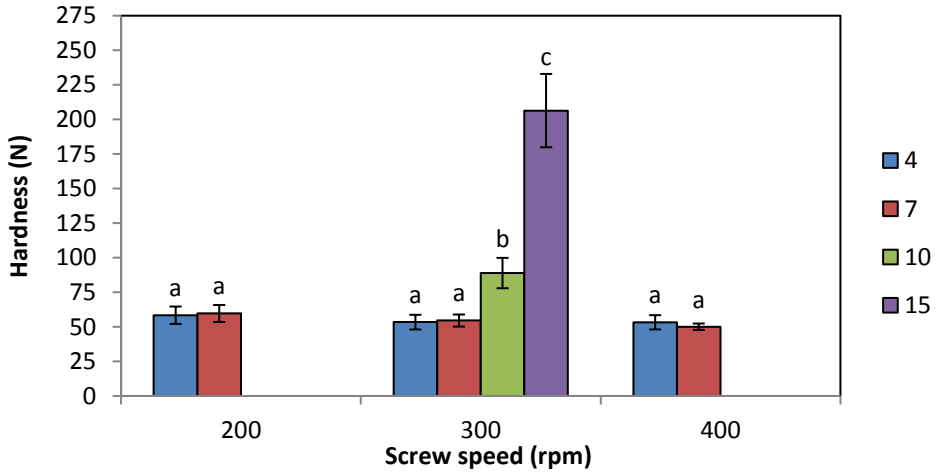

Figure 6.11 Hardness of extrudates produced at different screw speed and different water feed. The legend shows water feed in mL/min. Bars represent mean ± SD of 10 replicates. Bars denoted by the same letter are not significantly different (p>0.05).

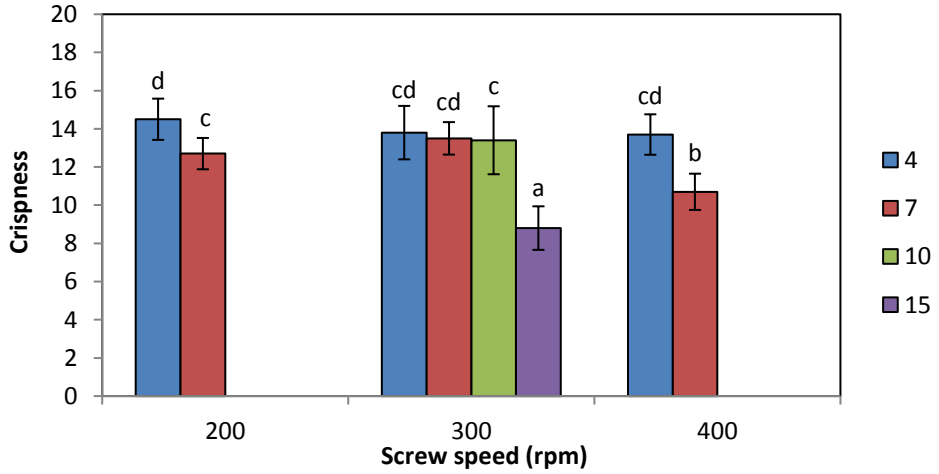

Figure 6.12 Crispness of extrudates produced at different screw speed and different water feed. The legend shows water feed in mL/min. Bars represent mean ± SD of 10 replicates. Bars denoted by the same letter are not significantly different (p>0.05).

6.4.3.7 Discussion of physical material properties of the extrudates

Observations and measured data show that screw speed and water feed rate both have a substantial impact on the properties of the sago starch extrudates. Although the screw speed plays a role in changing the specific mechanical energy, it is the water feed rate and hence the moisture content of the melt that seems to dominate the changes in properties of the extrudates. At the lower melt moisture contents of between 16.5% and 22.7% wwb, moisture is flashed off at the die to produce extrudates of about 8-9% moisture. This means that much more water is blown off at the higher moisture content, and this must be relevant as it is the flash off of the water as steam that expands the product. At the highest melt moisture of 25.2% (wwb) less water flashed off, so expansion was not related directly to the amount of steam flash off.

As visualised and measured through cellular microstructure, expansion, bulk density and texture, nucleation and bubble growth and the differences in the size of air cells of the extrudates provided information about its physicochemical material properties.

Cellular microstructure showed that at the lowest water feed rate the extrudates contained large prominent air cells with thin walls. However, the product extruded at the highest moisture level had irregularly shaped air cells, which were incompletely developed and not uniform in size. At the higher water levels, extrudates had been less porous, less expanded and harder. Similar observations have been reported in published literature, for example, Owusu-Ansah et al. (1984) stated that structural

examination revealed that reduced feed moisture was essential for the development of a porous structure.

The bubble growth, which is driven by the pressure difference between the interior of the growing bubble and atmospheric pressure resisted primarily by the viscosity of the bubble wall, dominates the expansion at high moisture content and high temperature (Padmanabhan and Bhattacharya, 1989). Hence, water feed has been found to be the main factor affecting extrudate density and expansion. Water feed rate that is melt moisture affects the viscoelastic properties of the melt and these, in turn, affect expansion. In the following, the elastic effects are considered first followed by the viscous effect.

The high dependence of bulk density and expansion on water feed would reflect its influence on the elasticity characteristics of the starch-based material. Increased water feed during extrusion would change the amylopectin molecular structure of the material, reducing the melt elasticity thus decreasing the expansion but increasing the density of extrudate (Ding et al., 2005). This phenomenon correlates with the observation that extrudates resulting from melts with higher moisture contents appeared harder after cooling than those with lower moistures (characterised by porous structure and expanded). This is probably because vapour pressure is lower during extrusion (probably due to a reduced barrel temperature) resulting in a lower flashing off of moisture and finally in a reduced expansion ratio (Hagenimana et al., 2006). Furthermore, in twin-screw extrusion, screw speed is regarded as having little effect on extrudate expansion (Martín-Cabrejas et al., 1999) and this would seem to be the case when extruding the sago starch.

The water acts as a plasticiser to the starch-based material and the mechanical energy dissipation in the extruder and thus bubble growth is compressed. The compressed bubble growth would result in a dense product and reduced crispness of the extrudates (Ding et al., 2005). Chakraborty et al. (2011) also concluded that moisture content played a more overwhelming effect on the hardness of the extrudates than other processing variables in the extrusion of millet–legume. During the extrusion process, the elastic swell effect and bubble growth effect both contribute to the structure change of starch (Padmanabhan and Bhattacharya, 1989).

The other role of water will be lubrication in the barrel and the viscosity of the melt, and this is relevant to the viscosity of the bubble wall. This leads to consider about properties of the physicochemical of the extrudates.

6.4.4 Physicochemical material properties of the extrudates

After measuring and observing the physical properties of the extrudates, the extrudates were ground and their behaviour in association with excess water was investigated to highlight how the starches have changed through the extrusion process. It should be noted that all samples extruded at 20 mL/min water feed rate were difficult to mill to achieve an appropriate size (<250 μm). To obtain the samples, they were repeatedly milled, rather than a single pass as used for the other feed rate extrudates. It is noted that the density of the particles and the particle shape could alter the physicochemical estimates as used in this work, in addition to characteristics of the starch (Mitchell et al., 1997). As with the previous section, data are presented first followed by discussion.

6.4.4.1 Water absorption index

The sago starch starts as a semi-crystalline material. Its physicochemical properties are detailed in Chapter 4. The native starch shows little solubility or swelling. Extrudates, ground to particles to a size in line with that of the sago starch, show very different properties.

Figure 6.13 shows the water absorption index (WAI) of the extrudates as a function of screw speed, see Equation (3.7) for the WAI calculation. The measured WAI of sago starch extrudates ranged between 3.92 and 8.99 g/g. The graph shows that the highest values of WAI were obtained for extrudates produced at a water feed of 20 mL/min at the screw speed of 300 rpm. Increasing water feed from 4 to 7 mL/min did not affect WAI of the extrudates at all screw speeds applied, while an increase from 10 to 20 mL/min significantly affected the WAI. Figure 6.13 also shows that increasing screw speed during extrusion may decrease the WAI values at water feed of 4 mL/min.

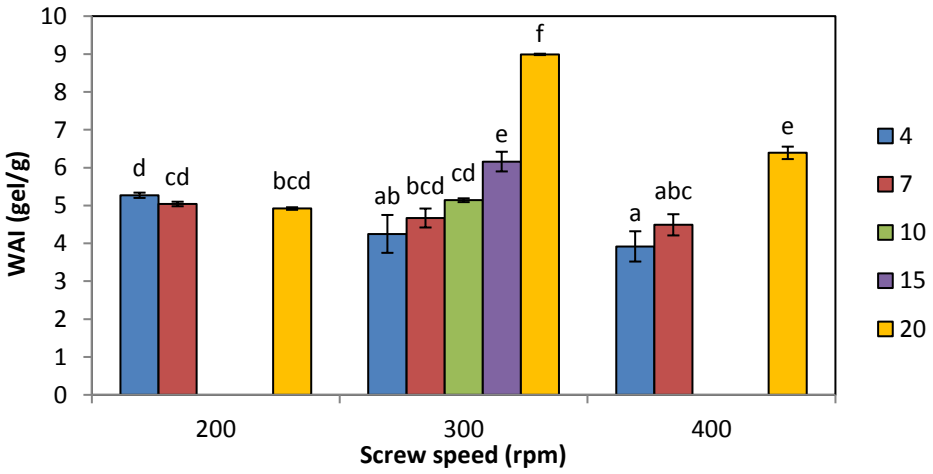

Figure 6.13 WAI of extrudates produced at different screw speed and different water feed. The legend shows water feed in mL/min. Bars represent mean ± SD of 3 replicates. Bars denoted by the same letter are not significantly different (p>0.05).

6.4.4.2 *Water solubility index*

The effect of extrusion conditions on WSI of extrudates as defined by Equation (3.8) is shown in Figure 6.14. Water feed and screw speed were found to have a significant effect on the WSI of the extrudates. WSI decreased as water feed increased above 10 mL/min during extrusion cooking. Increasing screw speed did not significantly affect the WSI of the extrudates produced at a water feed of 7 mL/min, but showed a significant inconsistent trend for that of 4 and 20 mL/min.

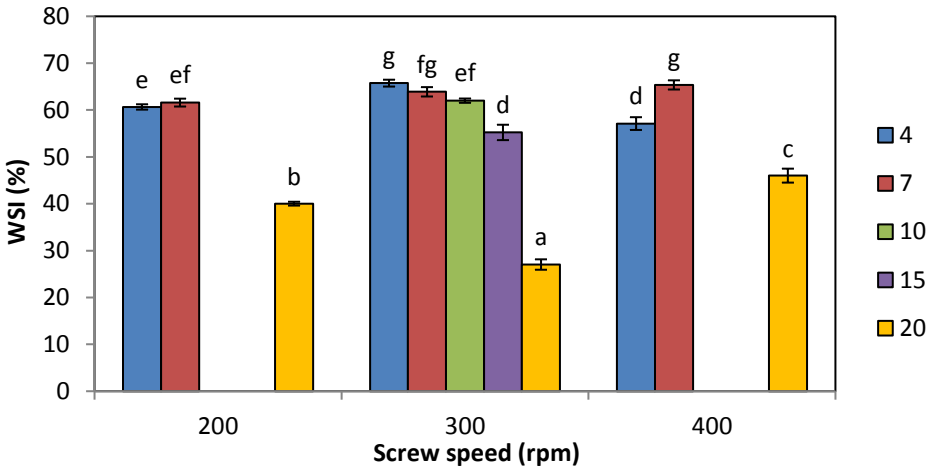

Figure 6.14 WSI of extrudates produced at different screw speed and different water feed. The legend shows water feed in mL/min. Bars represent mean ± SD of 3 replicates. Bars denoted by the same letter are not significantly different (p>0.05).

6.4.4.3 *Paste viscosity*

The pasting profiles acquired with the Rapid Visco Analyser (RVA) give information of cold and hot paste viscosity as the powdered samples are heated and stirred in a controlled way (method given in section 3.3.7.2). Figure 6.15 shows the RVA viscosity profiles of extrudates produced at different screw speeds and water feeds. The characteristic values of the RVA profiles are reported in Table 6.2.

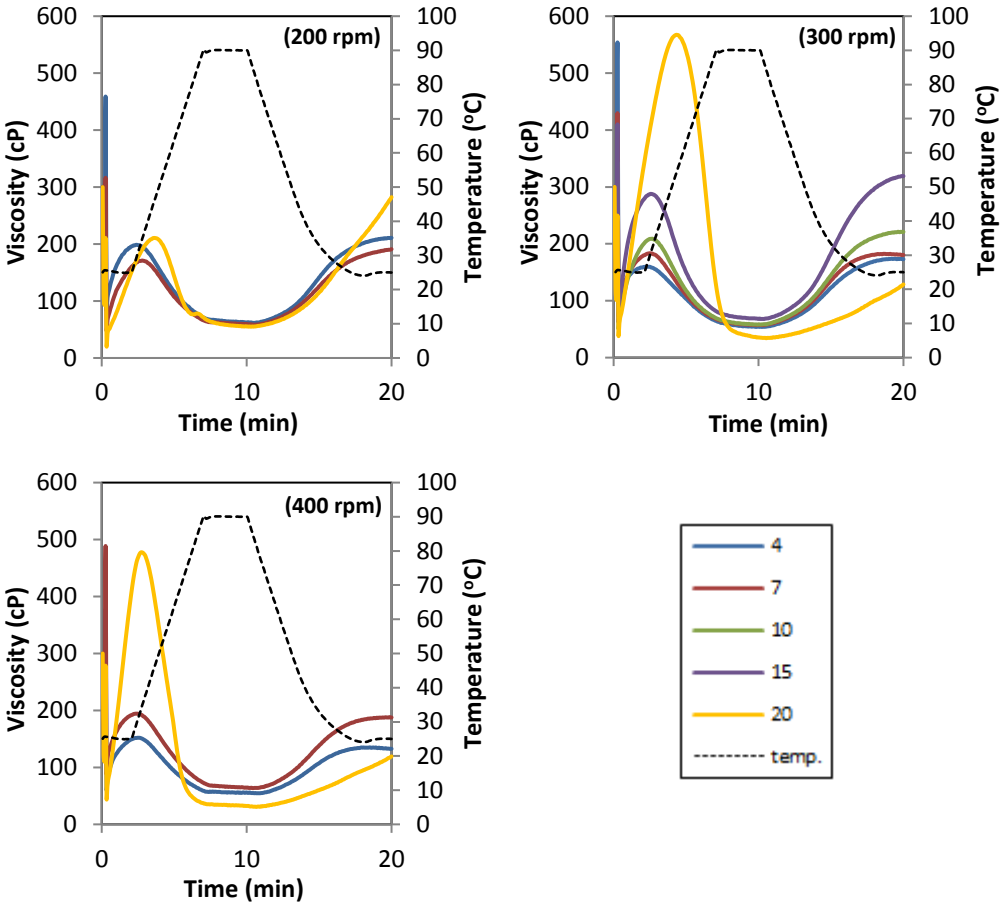

Figure 6.15 Viscosity of extrudates produced at different screw speed and different water feed. The legend shows water feed in mL/min.

Clearly, Table 6.2 shows, at screw speeds of 300 and 400 rpm, water feed has a significant effect on cold peak viscosities (the highest peak of the graph) between the lower feed rates (4, 7, 10, 15 mL/min) and the highest (20 mL/min). The values varied widely from 149 to 410 cP where the highest water feed led to the highest cold peak viscosity. The breakdown viscosity showed a similar trend where water feed above 15 mL/min led to a paste with significantly higher values. On the other hand, the final viscosity of the paste produced from the extrudates was not significantly different regarding water feed rate during extrusion processing (values were between 120 and 319 cP). Table 6.2 also shows

that screw speed did not have a significant effect on paste viscosity when the sago starch was extruded at constant water feed (4 or 7 mL/min).

Table 6.2 RVA results for extrudates produced at different screw speed and different water feed. Values are means ± SD (n = 3). Means within a column related to a particular parameter with the same superscript are not significantly different (p>0.05).

Screw speed (rpm); water feed (mL/min)	Cold Peak	Hold	Break-down	Final	Setback	Peak Time (min)
	Viscosity (cP)					
200;4	196^{cd} ± 16	62^{bc} ± 4.5	137^{cde} ± 12	211^{cd} ± 20	149^{bc} ± 16	2.2^{ab} ± 0.1
200;7	160^{abc} ± 4.2	58^{b} ± 1.0	113^{abc} ± 2.9	191^{bcd} ± 8.3	133^{abc} ± 9.3	2.6^{cd} ± 0.14
200;20	152^{a} ± 8.6	55^{b} ±1.5	156^{e} ± 6.1	285^{ef} ± 45	230^{d} ± 45	3.6^{e} ± 0.2
300;4	159^{ab} ± 2.1	54^{b} ± 2.0	106^{abc} ± 2.0	173^{abcd} ± 30	119^{abc} ± 28	2.1^{a} ± 0.1
300;7	180^{abcd} ± 3.1	57^{b} ± 4.4	126^{abcde} ± 0.6	180^{abcd} ± 2.0	123^{abc} ± 3.0	2.3^{ab} ± 0.1
300;10	200^{d} ± 5.0	58^{b} ± 1.7	151de ± 2.0	221de ± 5.5	163^{c} ± 4.2	2.5^{bcd} ± 0.1
300;15	278^{e} ± 9.1	68^{c} ± 1.7	220^{f} ± 5.6	319^{f} ± 15	251^{d} ± 14	2.5^{bcd} ± 0.03
300;20	335^{f} ± 9.5	34^{a} ± 1.7	533^{h} ± 10	130^{ab} ± 12	96^{ab} ± 11	4.3^{f} ± 0.04
400;4	149^{a} ± 3.1	55^{b} ± 0.6	97^{a} ± 2.5	132^{ab} ± 3.5	78^{a} ± 3.5	2.3^{ab} ± 0.07
400;7	192^{bcd} ± 35	64^{bc} ± 9.1	131^{bcde} ± 26	188^{bcd} ± 52	124^{abc} ± 43	2.3^{ab} ± 0.04
400;20	410^{g} ± 12	30^{a} ± 1.5	447^{g} ± 21	120^{a} ± 13	90^{ab} ± 12	2.7^{d} ± 0.04

The cold water swelling indicated by cold peak viscosity from the RVA measurement as well as water absorption index is indicative of the native granular starch disruption. Often cold peak viscosity and water absorption index show a bell-shaped relationship with the SME values as the integrity

of the native starch granule are lost and the macromolecular structures are broken down (Mitchell et al., 1997). It can be seen in Figure 6.16, the graph shows a bell-shaped relationship between the two parameters concerning with cold water swelling when plotted against the SME values. The lower SME values (<300 Wh/kg) of the graphs represent the high water feed rates.

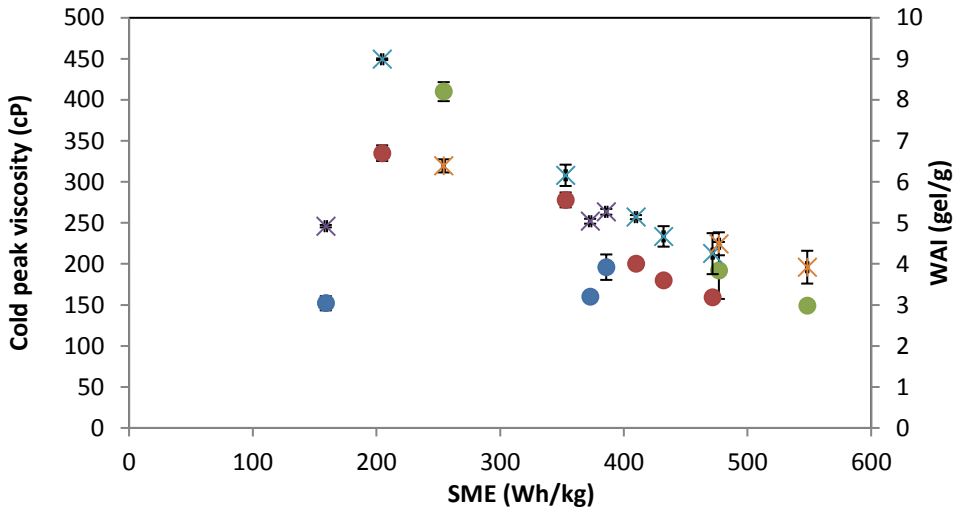

Figure 6.16 Variation of cold peak viscosity and water absorption index with specific mechanical energy (SME) input. Marker: ●, cold peak viscosity; ×, water absorption index. Screw speed (rpm): blue and purple, 200; red and light blue, 300; green and orange, 400.

6.4.4.4 Birefringence

The birefringence observation of the starches is shown in Figure 6.17. The pictures were acquired using microscopy on dry ground extrudates onto which there was an addition of one drop of deionised water and glycerol (method given in section 3.3.5). The pictures indicate that extrudate particles had very little observable birefringent structure under polarised light. Only a few Malteses crosses are observed and these may be due to contamination from unprocessed starch.

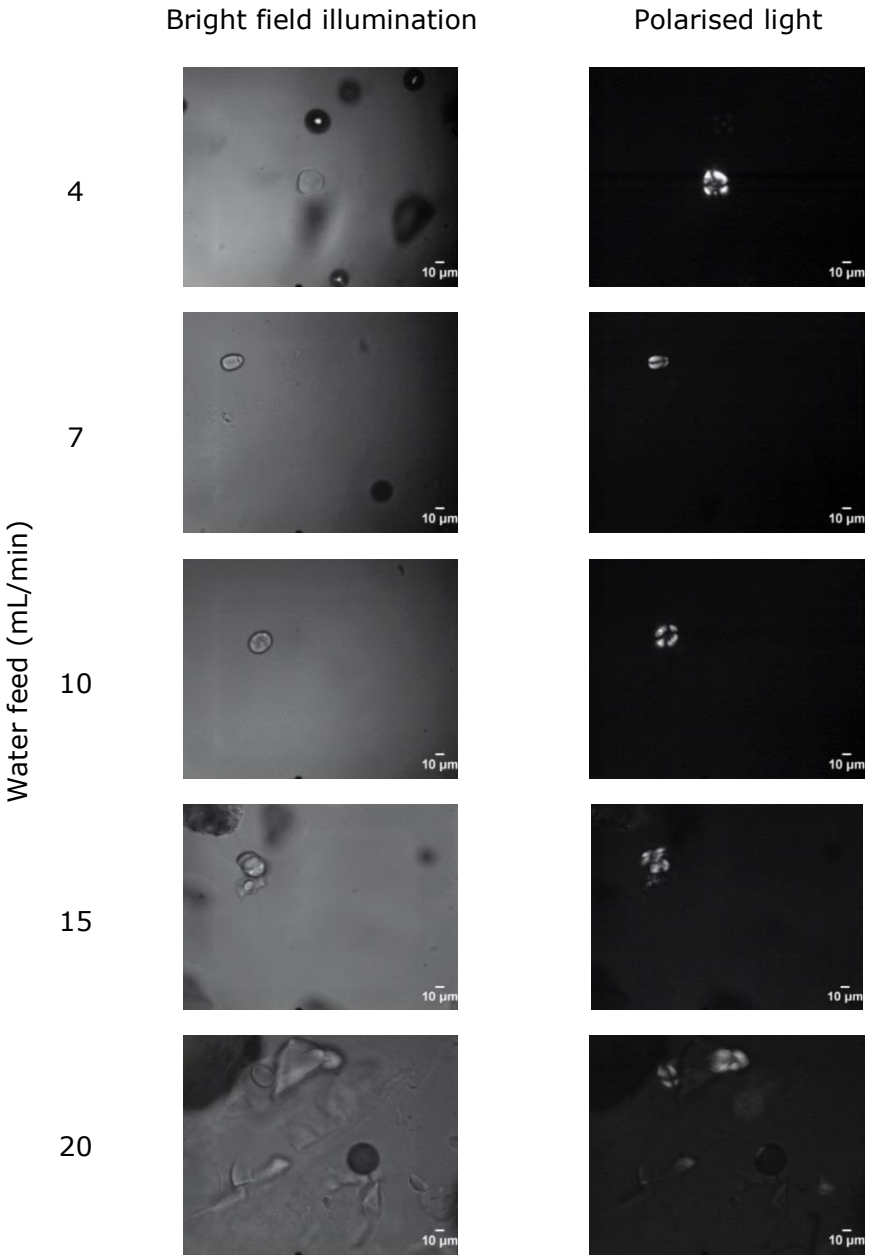

Figure 6.17 Images of the ground extrudates under bright field illumination and polarised light; produced at screw speed 300 rpm and different water feeds, as indicated in the first column.

6.4.4.5 Crystallinity

Using the X-ray diffraction technique, the data presented in Figure 6.18 suggests that the extruded sago starch has different features within the XRD pattern from that of native starch. Native sago starch shows four

strong peaks at 2θ values of about 15°, 17°, 18° and 23° which is characteristic for A-type starches (Figure 4.4). It appears that the native sago starch granule order is completely lost as assessed by X-ray when extrusion is carried out. The screw speed and water feed did not affect the X-ray pattern observed for these extruded samples.

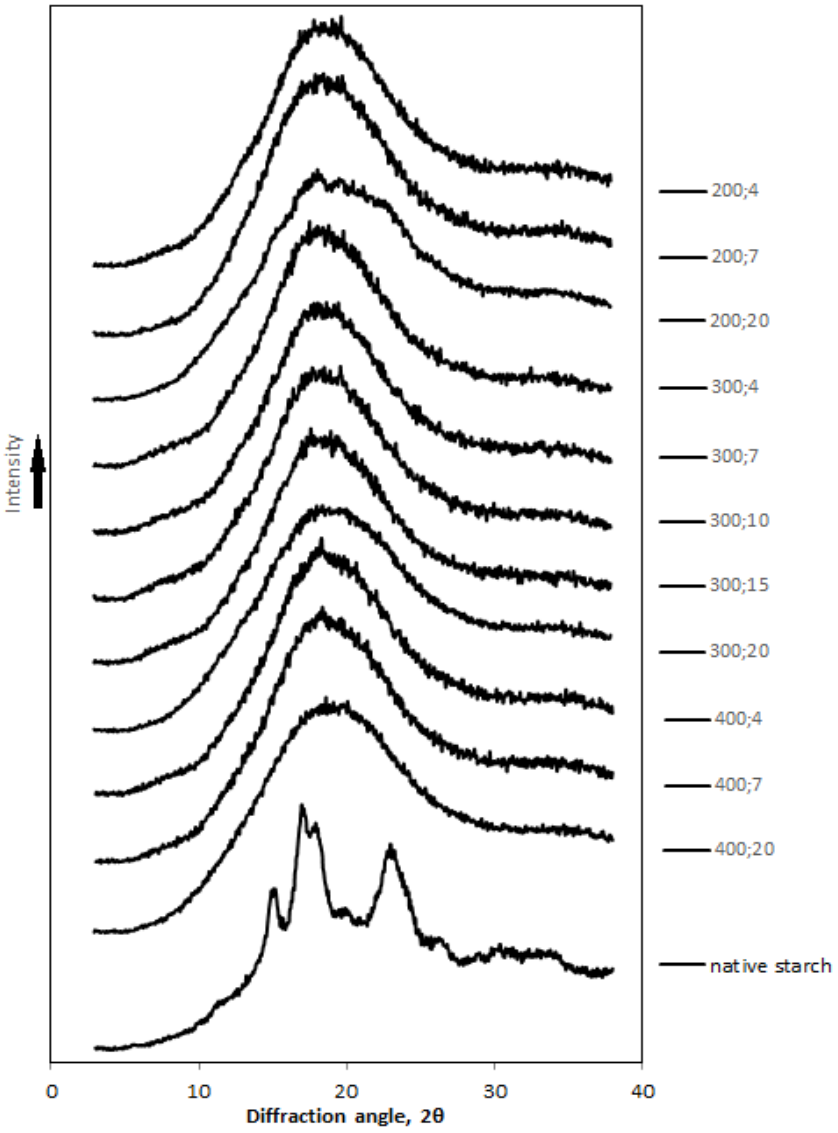

Figure 6.18 Effect of different screw speed and different water feed on X-ray diffractogram. The legend shows screw speed (rpm); water feed (mL/min) and the native sago starch.

6.4.4.6 Discussion of physicochemical material properties of the extrudates

Examination of the microstructures and hydration properties of the extrudates were carried out on milled samples. These ground samples all had particle sizes <250 μm, but it was noted that the extrudates produced at high moisture (20 mL/min) needed to be milled multiple times to achieve these dimension. These dense structures indicate little or no expansion of the samples at high water feed rates.

The data of particle hydration, swelling and solubility showed that major alterations in the starch-water interactions have occurred as a result of extrusion processing. There were two measurements of the powdered extrudates swelling in cold water. These were water absorption index (WAI) and cold water paste viscosity. The water absorption index is generally attributed to the ability of the starch to swell and hydrate in excess water. From the WAI results in Figure 6.13, the ground extrudates produced at water feed of above 10 mL/min show high swelling in cold water where that of 20 mL/min showed the highest ability to swell. This phenomenon can also be observed from the RVA curves in Figure 6.15, where the samples extruded at 20 mL/min water feed had the highest cold peak viscosity. Starches that contain order, due to the presence of helices and crystals, have very limited ability to swell in cold water. Once the granules have lost order, they are able to swell in cold water, and high volumes are achieved for the starches (Lai and Kokini, 1991). Meanwhile, the screw speed did not show a consistent result regarding the swelling of ground extrudates in the cold water.

Regarding water solubility index (Figure 6.14), the results are in accordance with the water absorption index where the ground extrudates produced at water feed of above 10 mL/min show low solubility in cold water where that of 20 mL/min showed the lowest solubility. Altan et al. (2009) observed an increase in the water solubility index of barley extrudates with increasing screw speed that may be related to increasing specific mechanical energy with screw speed. The high mechanical shear caused breakdown of macromolecules to small molecules with higher solubility. A similar effect was not observed for the sago starch extrudates in this study.

Sago starch extrudates gave a final viscosity between 120 and 319 cP. Final viscosity of the RVA represents the viscosity of the macromolecules when all the starch granules are disrupted as the particles have been heated and stirred in excess water. Hagenimana et al. (2006) stated that final viscosity indicates the extent of starch retrogradation that occurs during the cooling process. The final viscosity of the extrudates generally decreases with increased screw speed, where the effect of water feed more appears on the SME rather than final viscosity. Some reports on cooking extrusion of food materials have shown that final viscosity is significantly affected by moisture content, screw speed and temperature (Colonna and Mercier, 1984; Mason and Hoseney, 1985; Hagenimana et al., 2006). However, in this study, the final viscosity was not clearly affected by those factors (Table 6.2). The plot of the two material properties based on swelling in excess water (cold peak viscosity and water absorption index) against SME (Figure 6.16) clearly shows the bell-shape curve and it indicates that SME inputs above 300 Wh/kg reduce the polymer's potential to have high hydrodynamic volumes. As the mechanical energy increases, it could be expected that more molecular

breakage would occur and there was a decrease in water absorption index as hydrodynamic volume would be observed. This curve also could be interpreted as showing the relationship of the water feed rate on the viscosity of the melt in the extruder. Water addition into the melt at a limited amount below 25% (Figure 6.4) causes a viscous melt, which undergoes high levels of shear in the barrel. Increasing the moisture content is reported to result in a lower starch conversion for different products during the extrusion process (Madeka and Kokini, 1992).

Images of the extrudates particles under polarised light shows that sago starches have lost their structures during extrusion cooking. Figure 6.17 displays the typical micrograph for the sago extrudates and the lack of birefringent structure. X-ray diffraction (Figure 6.18) also shows that all of the extruded samples were amorphous. This contrasts with native sago starch as the starting material.

6.4.5 Conclusions

The results showed that the properties of the extrudates were more pronounced on water feed rate rather than screw speed. Of particular interest are extrudates produced at lower water feed of 4 and 7 mL/min that had noticeable results on expansion, crispness and swelling on the extrudates. These water feed rates will be applied for the next trials in addition to the range of die temperatures that will also be another relevant extrusion variable. The screw speed was kept at 300 rpm as changing the screw speed from the first trial do not have a major impact on the physical and physicochemical material properties of sago starch extrudates.

6.5 Extrusion processing of sago starch at variable die temperature and water feed rate

The experiment to ascertain if thermomechanical extrusion would be a suitable method to process sago starch to create an expanded snack was continued with a second trial. Previously, the initial extrusion trials were carried out with screw speed and water feed rate as the processing variables. The second processing trials looked at varying the die temperatures at a chosen water feed and screw speed.

Some authors have studied the major effect of die temperature in extrusion processing. Altan et al. (2008) reported that change in the die temperature (140 to 160 °C) and pomace level had the most effect on the properties of 20 different combinations of barley flour and tomato pomace extrudates while screw speed had a lesser effect. Another study by Thymi et al. (2005) showed that product temperature (the temperature in the barrel screw and die; 100 – 260 °C) together with feed moisture content and residence time significantly affected some of the structural properties of extruded corn grits.

In this subchapter the results of extrusion trials conducted at die temperatures of 120, 140, 160 °C and water feed rates adjusted to 4 and 7 mL/min are reported and discussed. Water feed of 4 and 7 mL/min and the constant screw speed of 300 rpm were chosen for the second trials from the results of the first trials. The feed rate of sago starch was also constant at 8 kg/h throughout.

6.5.1 Torque and specific mechanical energy input

The results of torque and specific mechanical energy are shown in Figure 6.19. As could be expected with only a change in the die temperature the SME and torque were not much affected compared to the impact of the water feed rate change from 4 to 7 mL/min. The purpose of this trial was to establish the relevance of the temperature of the extruding materials as it exits the die into normal ambient temperatures or pressures. It must, however, be recognised that the change in die temperature will impact on the other zones of the extruder. Temperature control within this ThermoFisher Prism extruder may not be significantly robust to hold the precise set temperatures when zones differ by more than 20 °C. However, Figure 6.19 shows that change in the die temperature and therefore flow of material in the barrel were not enough to have a major change on the mechanical inputs. The main impact of changing the die temperature was therefore expected to be on the expansion properties of the extrudates.

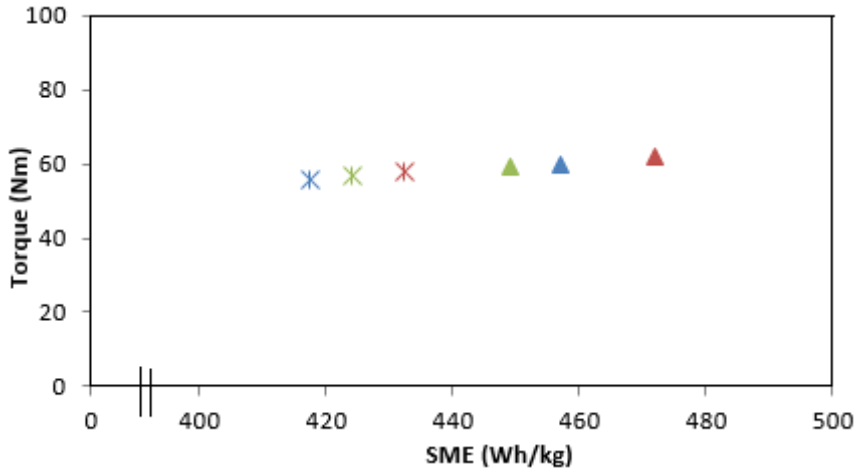

Figure 6.19 Variation of torque with screw speed and specific mechanical energy (SME) input. Die temperature (°C): blue, 120; red, 140; green, 160. Water feed (mL/min): ▲, 4 and ∗, 7.

6.5.2 Moisture content of the extrudates as they exit the extruder

Figure 6.20 shows the moisture content of the extruded samples produced at different die temperature and water feed and also reports the calculated moisture content of the melt for the different water feed rates. As stated before, there was only one run per processing parameter carried out and the moisture data is based on the analyses of three extrudates per run. It is clear that all of the samples have lost moisture as they exit the extruder, but were all reasonably close between 7.37 and 7.94% (wwb). Extrudates produced at the lowest die temperature of 120 °C had the highest moisture content compared to that of 140 and 160 °C. The results indicate that at this lower die temperature, the temperature of the extruding material may be insufficient to allow as much evaporation of the water as occurred when the extrudates exited the die at the higher temperatures. However, at all temperatures and water feed rates major volumes of water were flashed off.

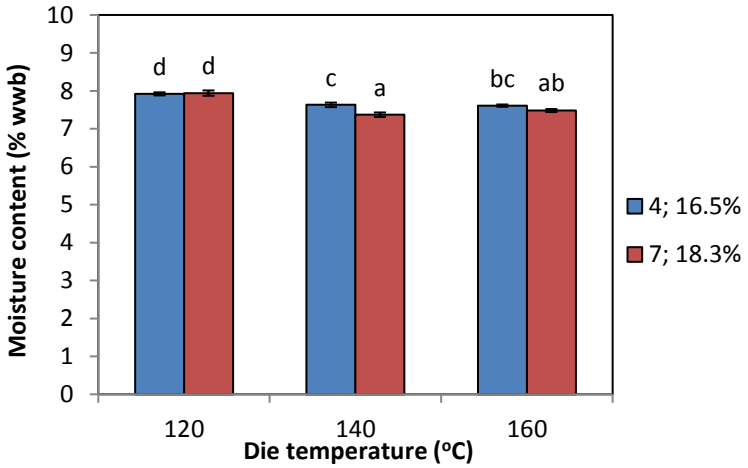

Figure 6.20 Moisture content of extrudates produced at different die temperature and different water feed. The legend shows water feed in mL/min and % moisture content of the melt (wwb). Bars represent mean ± SD of 3 replicates. Bars denoted by the same letter are not significantly different (p>0.05).

6.5.3 Physical material properties of the extrudates

In the following results are presented first followed by discussion due to interrelationships between the parameters.

6.5.3.1 Appearance

The extrudates that were collected from the extrusion runs at different die temperatures at water feed of 4 and 7 mL/min are depicted in Figure 6.21. All samples show expansion bubbles within the matrix with no major differences. The bubble pattern looks fairly uniform, although the sample produced at a die temperature of 120 °C shows slightly more bubbles were produced. There was no observable tendency for a difference in diameter and colour of extrudates as the die temperature increased. The measured expansion, bulk density and colour of the extrudates are discussed in a later section. Despite the extrudates not showing major variations, they were subjected to scanning electron microscopy (SEM) to examine the cellular microstructure of the bubbles and cell walls in more detail.

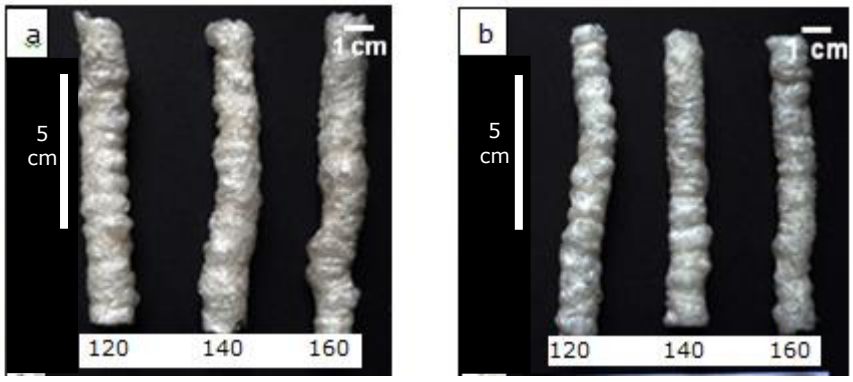

Figure 6.21 Photographs of extrudates produced at different die temperature as indicated underneath the extrudates and at water feed: a, 4 and b, 7 mL/min.

6.5.3.2 Cellular microstructure

Figure 6.22 shows the cellular microstructures of the extrudates by means of scanning electron micrographs. For extrudates produced at a water feed of 4 mL/min the thickest cell walls were found in extrudates produced with a die temperature of 120 °C. This was also observed in extrudates produced at a water feed of 7 mL/min. The rest of the extrudates produced at the same water feed and higher die temperature appeared to have thinner cell walls.

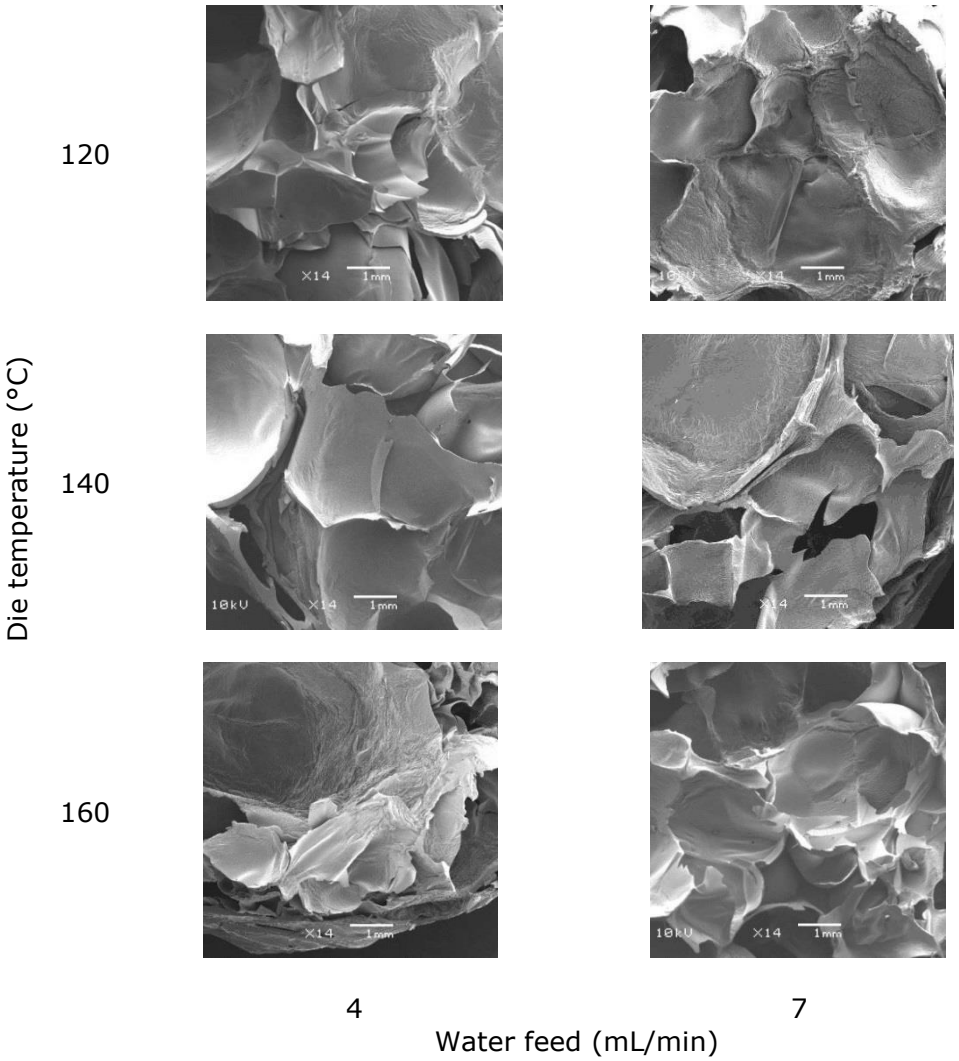

Figure 6.22 Scanning Electron Microscopy (SEM) pictures of extrudates produced at different die temperature (horizontal) and different water feed (vertical).

6.5.3.3 Colour

The whole pieces of the sago starch extrudates produced with the different extruder die temperatures did not appear to be different in colour as judged by visual inspection. A Hunter colorimeter was used to validate this observation. Values for *L**, *a**, *b** were measured on ten extrudates taken from the single processing runs and the data is shown in Table 6.3. The *L** values quantifying lightness of the extrudates increased with the increasing die temperature when processed at a water feed of 7 mL/min. The *L** value of extrudates produced at water feed of 4 mL/min, as well as *a** and *b** values of the extrudates, on the other hand, showed inconsistent trends.

Table 6.3 Colour properties of extrudates produced at different die temperature and different water feed. Values are means ± SD (n = 10). Means within a column related to a particular parameter with the same superscript are not significantly different ($p>0.05$).

Die temperature (°C); water feed (mL/min)	*L** (lightness; zero for black to 100 for perfect white)	*a** (negative values for greenness to positive values for redness)	*b** (negative values for blueness to positive values for yellowness)
120;4	43.72^{ab}±3.84	0.05^{ab}±0.10	4.83^{bc}±0.05
120;7	42.58^{a}±0.03	0.26^{c}±0.01	5.01^{c}±0.37
140;4	48.9^{c}±1.2	-0.03^{a}±0.08	3.90^{a}±0.37
140;7	52.83^{d}±1.66	0.05^{ab}±0.04	4.39^{b}±0.05
160;4	45.34^{b}±1.60	0.12^{b}±0.05	4.47^{b}±0.58
160;7	55.99^{e}±0.63	0.02^{a}±0.04	4.83^{bc}±0.35

6.5.3.4 *Expansion ratio*

Figure 6.23 shows the effects of extrusion conditions on the expansion ratio of the extrudates. It is clear that changing die temperature between 120 and 160 °C did not significantly affect the expansion ratio of the extrudates. On the other hand, processing at increased moisture content (4 to 7 mL/min) at all die temperatures lead to extrudates with a significantly decreased expansion ratio (p>0.05).

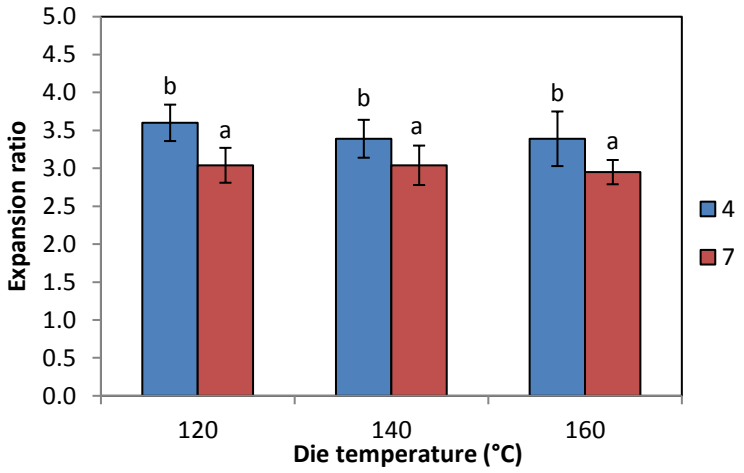

Figure 6.23 Expansion ratio of extrudates produced at different die temperature and different water feed. The legend shows water feed in mL/min. Bars represent mean ± SD of 10 replicates. Bars denoted by the same letter are not significantly different (p>0.05).

6.5.3.5 *Bulk density*

The effect of process variables on the bulk density of the extrudates is presented in Figure 6.24. The bulk density of extrudates produced at different die temperature show little difference, neither did the change in water feed rates (4 or 7 mL/min) have much impact. The highest bulk density was found for the extrudate produced at 7 mL/min water feed and 120 °C die temperature, which differed significantly from the value

measured for the extrudate produced at the same die temperature but at lower water feed (4 mL/min).

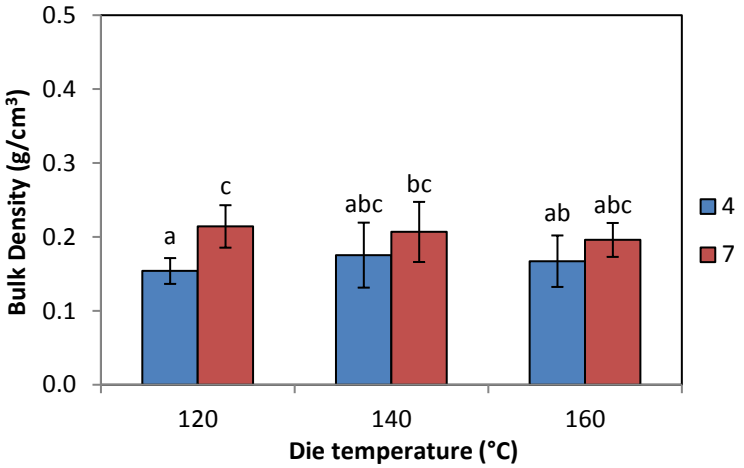

Figure 6.24 Bulk density of extrudates produced at different die temperature and different water feed. The legend shows water feed in mL/min. Bars represent mean ± SD of 10 replicates. Bars denoted by the same letter are not significantly different (p>0.05).

6.5.3.6 Texture properties

The texture of the extrudates was examined based on the two parameters of hardness and crispness. Figure 6.25 shows the results for hardness. It can be seen that the hardness of the samples produced at water feed of 4 mL/min was not significantly different (p>0.05) when different die temperatures were chosen. On the other hand, this was not applicable for samples processed at 7 mL/min water feed, although the trend with die temperature was not consistent. Comparing by water feed rate, an increase from 4 to 7 mL/min produced significantly harder extrudates except at 140 °C die temperature.

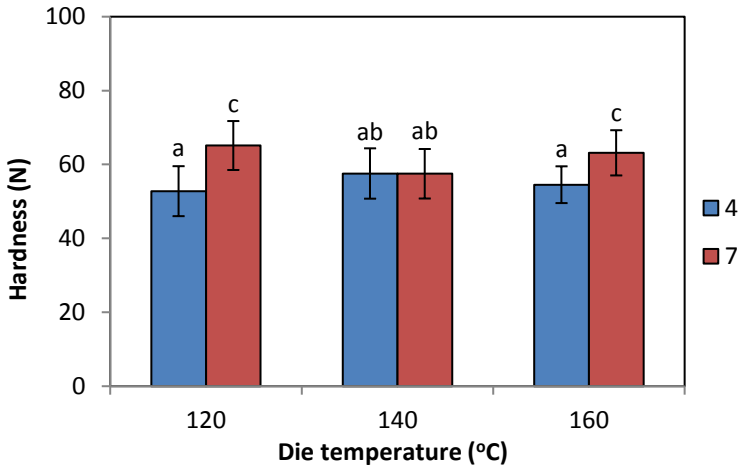

Figure 6.25 Hardness of extrudates produced at different die temperature and different water feed. The legend shows water feed in mL/min. Bars represent mean ± SD of 10 replicates. Bars denoted by the same letter are not significantly different (p>0.05).

Figure 6.26 gives information about the crispness of the extrudates. There were no significant differences (p>0.05) of crispness across the values for the whole sample produced in this second set of extrusion trials.

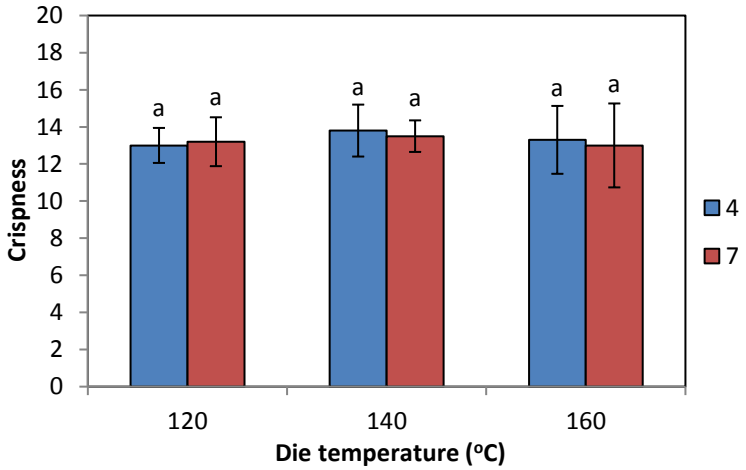

Figure 6.26 Crispness of extrudates produced at different die temperature and different water feed. The legend shows water feed in mL/min. Bars represent mean ± SD of 10 replicates. Bars denoted by the same letter are not significantly different (p>0.05).

6.5.3.7 Discussion of physical material properties of the extrudates

From the results it is clear that changing die temperature at 120, 140 and 160 °C did not affect majorly of the physical properties of the extrudates. The exception is for extrudates produced at a water feed of 7 mL/min, where changing die temperature from 120 to 140 °C increased lightness and decreased hardness. Meanwhile, it is clear that the samples extruded at the lower temperature lost slightly less moisture and may have had thicker cell walls, but the differences were minor at both water feed rates.

The flashing off of moisture from the extrudate as it emerges from the die represents the mechanism for the expansion of the bubbles, but is also relevant for the plasticisation of the bubble wall (Kokini et al., 1992). The moisture and the fragmented starch would lower the viscosity of the wall and can allow greater expansion (Mercier and Feillet, 1975). If the moisture loss is insufficient during expansion then the bubble wall materials does not go through the glass transition and remains flexible and rubbery. Hence when the driving force of the water changing to steam of greater volume no longer occurs then the bubbles can shrink back to a smaller size.

6.5.4 Physicochemical material properties of the extrudates

The extrudates were ground after visual inspection and measurement of their physical properties undertaken. Their behaviour in association with excess water was investigated to highlight how the sago starch had changed through the extrusion process. As with the previous section, results from the observations are presented first and followed by discussion.

6.5.4.1 Water absorption index

Figure 6.27 shows the water absorption index (WAI) of the extrudates as a function of die temperature. The extrudates exhibited WAI values in the range of 4.00 – 4.77 g/g, but there were no significant differences (p>0.05) across the whole sample set.

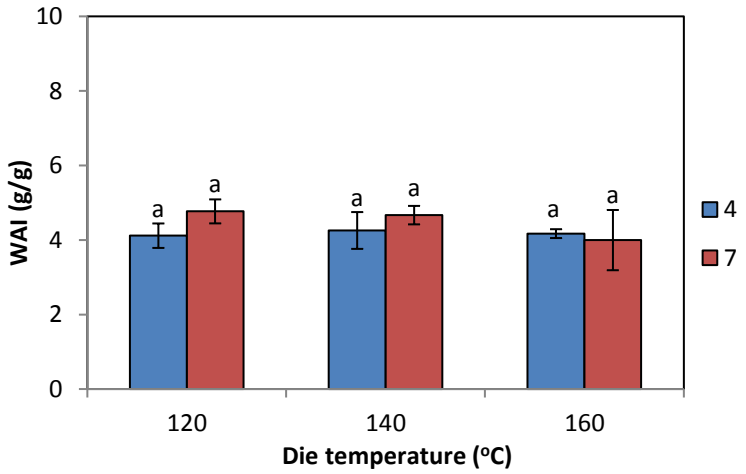

Figure 6.27 WAI of extrudates produced at different die temperature and different water feed. The legend shows water feed in mL/min. Bars represent mean ± SD of 3 replicates. Bars denoted by the same letter are not significantly different (p>0.05).

6.5.4.2 *Water solubility index*

The effect of different die temperature on the WSI of the extrudates is shown in Figure 6.28. The values ranged from 63.89 to 66.91% and there were no significant differences (p>0.05) across the whole sample set.

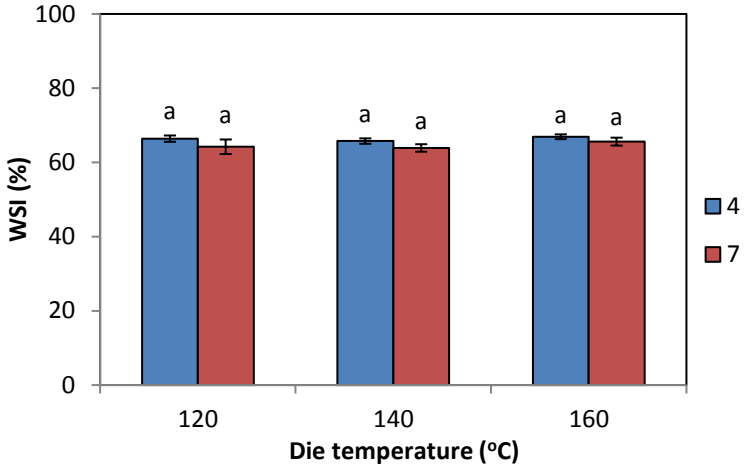

Figure 6.28 WSI of extrudates produced at different die temperature and different water feed. The legend shows water feed in mL/min. Bars represent mean ± SD of 3 replicates. Bars denoted by the same letter are not significantly different (p>0.05).

6.5.4.3 *Paste viscosity*

The pasting properties for extrudates produced at a water feed rate of 4 and 7 mL/min and die temperatures of 120, 140 and 160 °C are presented in Figure 6.29 and Table 6.4. The cold peak viscosity of extrudates produced at 4 mL/min water feed at all die temperatures did not differ significantly from one another (p>0.05). This also showed by that of 7 mL/min. However, the cold peak viscosity of 4 mL/min extrudates (159 – 167 cP) was significantly lower than that of 7 mL/min.

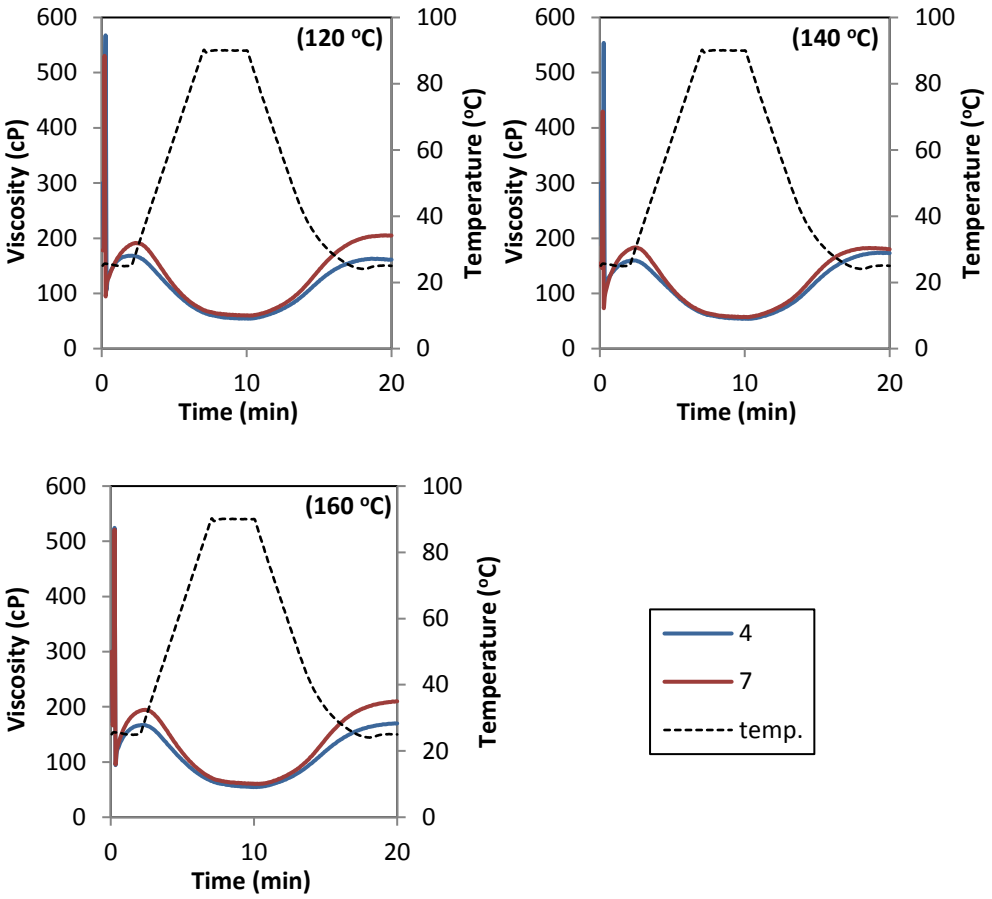

Figure 6.29 Viscosity of extrudates produced at different die temperatures and different water feeds. The legend shows water feed in mL/min.

The breakdown viscosity of extrudates produced at a water feed rate of 4 mL/min at all die temperatures was also lower than that of extrudates at the higher water feed of 7 mL/min. The values show an inconsistent trend when die temperature was increased from 120 to 160 °C. Extrudates with higher cold peak viscosity had a higher breakdown viscosity (Table 6.4). On the other hand, final viscosity did not vary significantly (p>0.05) among the extrudates with different die temperatures either for 4 or 7 mL/min of water feed rates.

Table 6.4 RVA results for extrudates produced at different screw speed and different water feed. Values are means ± SD (n = 3). Means within a column related to a particular parameter with the same superscript are not significantly different (p>0.05).

Die tempe-rature (°C); water feed (mL/min)	Cold Peak	Hold	Break-down	Final	Setback	Peak Time (min)
	Viscosity (cP)					
120;4	168^{a} ± 2.5	54^{a} ± 0.6	114^{b} ± 2.0	161^{a} ± 4.4	107^{a} ± 3.8	1.89^{a} ± 0.1
120;7	188^{bc} ± 2.7	60^{a} ± 1.0	132^{cd} ± 1.2	205^{b} ± 19	145^{ab} ± 18	2.33^{d} ± 0.01
140;4	159^{a} ± 2.1	54^{a} ± 2.0	106^{a} ± 2.0	173^{ab} ± 30	119^{ab} ± 28	2.12^{bc} ± 0.1
140;7	180^{b} ± 3.1	57^{a} ± 4.4	126^{c} ± 0.6	180^{ab} ± 2.0	123^{ab} ± 3.0	2.31^{cd} ± 0.1
160;4	167^{a} ± 1.5	55^{a} ± 2.5	112^{ab} ± 1.2	170^{ab} ± 6.7	116^{ab} ± 7.0	2.01^{ab} ± 0.1
160;7	193^{c} ± 7.2	60^{a} ± 1.5	135^{d} ± 5.5	210^{b} ± 12	150^{b} ± 12	2.29^{cd} ± 0.1

Figure 6.30 reflects the water absorption and cold water viscosity of the powdered extrudates in relation with the SME values. There was some decline in cold water swelling with increasing SME.

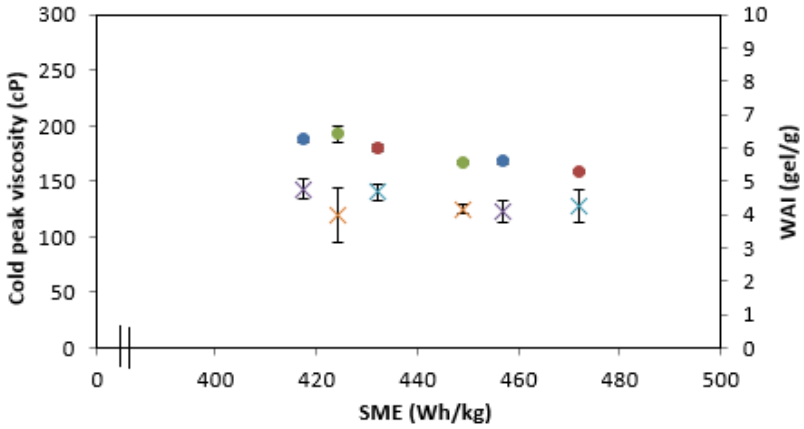

Figure 6.30 Variation of cold peak viscosity and water absorption index with specific mechanical energy (SME) input. Marker: ●, cold peak viscosity; ×, water absorption index. Screw speed (rpm): blue and purple, 200; red and light blue, 300; green and orange, 400.

6.5.4.4 Birefringence

The birefringence observation of the extrudates was revealed through microscopy (Figure 6.31). The micrographs were similar to those obtained with extrudates produced at different screw speeds and water feed rates (Figure 6.17) and showed a very little observable birefringent structure of extrudate particles under polarised light. The few granules showing Malteses crosses were still thought to be contamination of unprocessed starch.

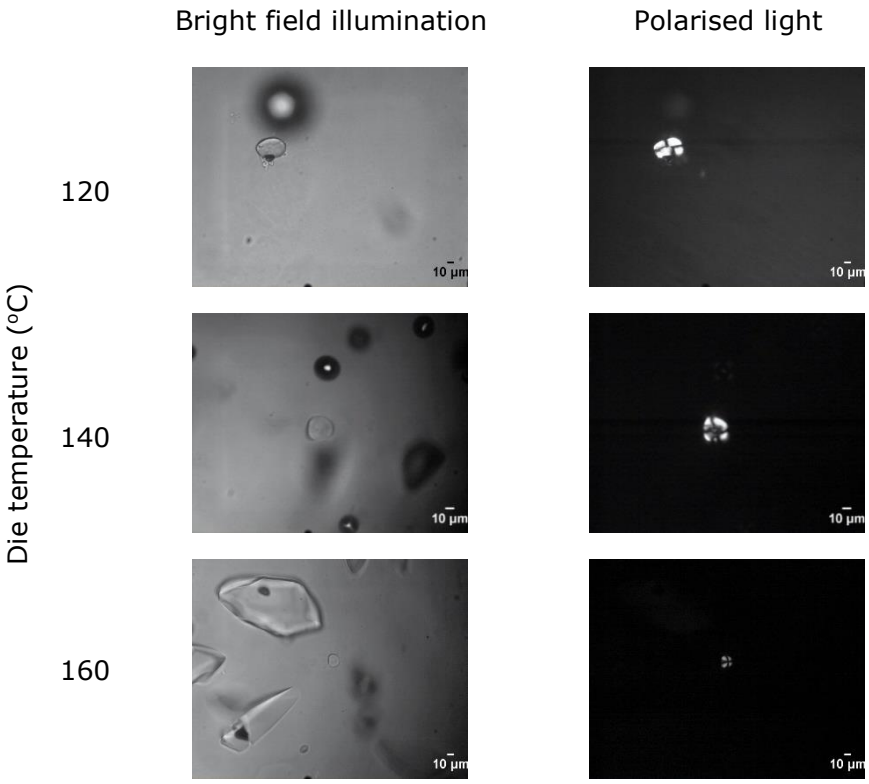

Figure 6.31 Images of ground extrudates under bright field illumination and polarised light; produced at water feed 4 mL/min and at different die temperature.

6.5.4.5 Crystallinity

The X-ray patterns to detect crystallinity of the extrudates are presented in Figure 6.32. These show that all of the samples are amorphous in

contrast with the starting material. The range of die temperatures and water feeds used in this set of experiments do not seem to affect the X-ray pattern of the resultant extrudates.

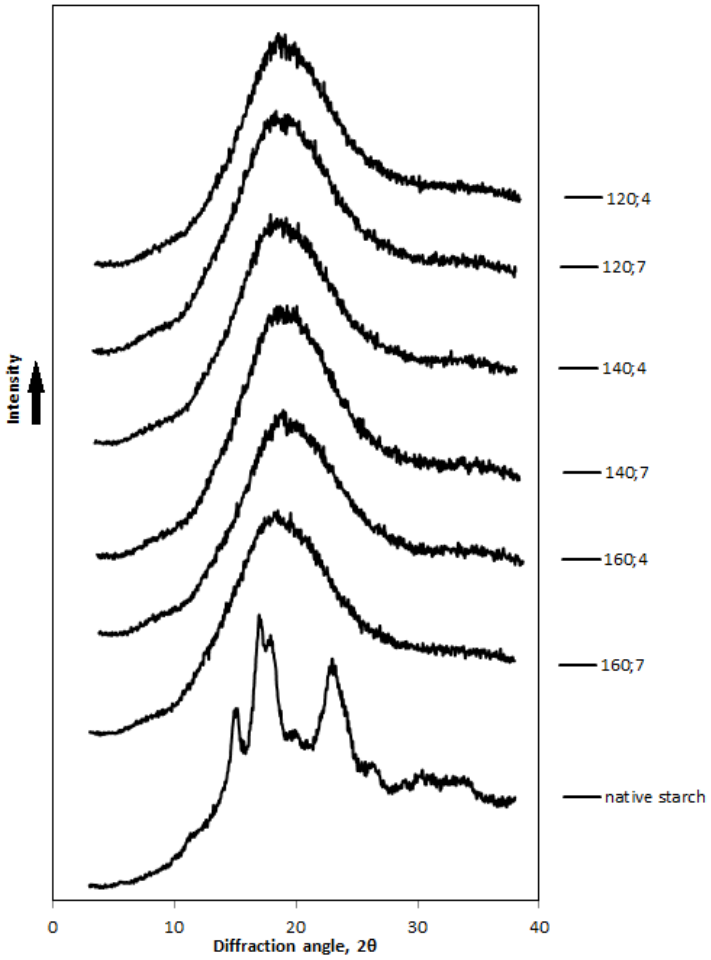

Figure 6.32 Effect of different die temperature and different water feed rates on X-ray diffractogram. The legend shows die temperature (°C); water feed (mL/min) and the native sago starch.

6.5.4.6 Discussion of physicochemical material properties of the extrudates

If the methodology used to investigate powdered extrudates behaviours in excess water reflects the starch conversion from the granular form to breakup of the molecular structure, then the change in die temperatures

used in this work had very little impact on the starch conversion. Even the change from 4 to 7 mL/min water feed rate (16.5 to 18.3% moisture in the barrel) did not have a great impact on the conversion. The range of SMEs was not so different (variation of 50 Wh/kg) and so this could have been expected (El-Dash et al., 1983). The starch conversion occurs in the barrel as the sago starch is subjected to heat and shear where the molten starch mass is conveyed along the barrel and the die temperature did not have much impact on the conditions within the barrel.

The small impact of changing die temperature rather than water feed rate from this study agrees well with the published literature. Chakraborty et al. (2011) reported that die heat temperature did not significantly affect the density of millet-legume blended extrudates. Other processing variables, for example, screw speed, moisture content and barrel temperature, on the other hand, resulted in a significant effect. Yu et al. (2012) reported that physical properties of the extruded material were affected by the barrel temperature, screw speed and moisture feed. Ilo et al. (1996) found that the apparent viscosity and the mechanical energy consumption in the extruder were most dependent on the feed moisture content.

6.5.5 Conclusions

Observation and the experimental results from this trial show that the extrudates formed by changing the die temperatures (120, 140 and 160 °C) did not result in any major effect on sago starch when extruded. The differences in the water feed rates within the extruder are still relevant at all of the temperatures, particularly on colour, hardness, and cold peak viscosity aspects.

6.6 Conclusions

Based on the results of this chapter, it can be concluded that expanded extrudates can be produced from sago starch without any other additives than water. Variation in the water feed rates within the range applied in this research have a major impact on all of the physical and microstructural properties of sago starch extrudates that were examined in this study. The extrudate that appeared to be very different from all of the other samples was that processed at a water feed rate of 20 mL/min. This appeared to be a hard "glassy" sample which was unsuitable for direct eating and retained significantly more moisture than the other samples on exiting the die. On the other hand, the range of screw speed applied here (200, 300 and 400 rpm) had very little impact on the properties of the extrudates. Furthermore, the water feed rates also still dominate the effect of extrudates properties rather than die temperature applied (120, 140 and 160 °C). The water feed rates are linked to the viscosity of the material within the barrel and therefore the amounts of specific mechanical energy to which the starch melt is subjected.

From the current work it is concluded that sago could be used to form a directly expanded product using the following processing parameters, feed rate 8 kg/h sago starch, screw speed of 300 rpm, die temperature at 140°C, moisture 16.5-18.3% wwb and these should be the processing parameters for the next step of this study which was to nutritionally fortify the extrudates.

CHAPTER 7
Extrusion processing of iron-fortified sago starch product

7.1 Introduction

The emphasis of this project was to use sago starch as a carrier for added nutrient in an easy to eat format. The study in Chapter 6 shows that sago starch forms a directly expanded product using the processing parameters which were followed in this chapter to fortify the extrudates nutritionally.

Food fortification is able to provide micronutrients to a population without requiring significant changes in the individual diet choices and consumption patterns. One of micronutrient deficiencies that is still a problem in many countries is iron (WHO, 2002). In developed countries, nutritional iron deficiency is the main etiologic factor responsible for anaemia, meanwhile, in the developing countries of Africa and Asia, this contributes to about 50% of anaemia incidents (WHO, 2006).

However, iron fortification may cause an unacceptable flavour as a result of the oxidation-mediated rancidity of fats and metallic aftertaste. Iron inclusion may also cause undesirable colour changes resulting from oxidation and interactions with anthocyanins, flavonoids and tannins. In addition, the type of food and beverage that contains the iron, as well the iron source, has an influence on the iron's bioavailability. There are components that are contained in many staple foods (e.g., rice and beans)

and daily consumed beverages (e.g., coffee, tea and milk) such as phytic acid, phenol and soy protein that could interfere with iron absorption (Hurrell, 1997; Mellican et al., 2003; Mehansho, 2006).

The challenge for iron fortification is that the iron compounds are apt to negatively influencing the sensory qualities of foods and those that have been identified as causing fewer sensory changes then tend to be poorly bioavailable and may provoke precipitation (Douglas et al., 1981). Water-soluble compounds such as ferrous sulphate are more bioavailable, but are also highly reactive with the food matrix, often producing oxidation and unacceptable colour changes. Despite this ferrous sulphate, as it is the least expensive compound, is widely used to fortify infant formulae, pasta and cereal flour that are stored for only short periods. It is also suitable for refined wheat flour with low levels of iron inhibitors, for example, phytates (Hurrell, 2002; Uauy et al., 2002).

The presence of ascorbic acid in foods that contain iron is known to lessen the discolouration of the products during processing (Nojeim and Clydesdale, 1981). Regarding iron absorption, ascorbic acid is known to improve the bioavailability of both soluble and insoluble iron sources (Theuer, 2008). Cook and Monsen (1977) demonstrated that 500 mg ascorbic acid taken with a meal increased absorption of iron about six-fold, whereas the same quantity had little effect when taken 4 or 8 h before the meal. However, methods of food preparation, especially cooking at high temperatures (Disler et al., 1975), may lead to oxidation of the ascorbic acid and the loss of its beneficial properties. It should be noted that in this current study the bioavailability of the iron and ascorbic acid was not assessed.

The addition of ascorbic acid to the extrusion cooking may well affect the starch. Work on cassava starch by Sriburi et al. (1999) indicated that the starches may also be altered in some circumstances by the presence of ascorbic acid. Furthermore, studies by Sriburi and Hill (2000) showed that the inclusion of ascorbic acid or a reduction in pH during extrusion alters cassava starch. In presence of ascorbic acid higher levels of starch conversion were observed as measured by solubility, water absorption and changes in viscosity. However, there was no alteration of the expansion of the acid containing extruded products even though the viscosity of the materials had been affected by the acid environment.

The aim of the work reported in this chapter was to investigate the extrusion processing behaviour of iron-fortified sago starch. The particular interest was the effects of additives, which were iron and ascorbic acid singularly and in combination, on the physical and physicochemical material properties of the extrudates.

7.2 Literature review

7.2.1 Fortifying foods with iron

Iron fortification of appropriate food items combined with iron supplements in specific population groups has proven to be efficient to tackle Iron deficiency anaemia (IDA) (Hurrell, 1997) which is still one of the nutritional problems particularly in developing countries (WHO, 2002). The food vehicle and the iron fortificant compound must be safe and acceptable to and widely consumed by the target population (Milman, 2011). Currently, there are a number of iron sources available as food fortificants (Hurrell, 1997). Based on bioavailability, these iron fortificants are classified into highly bioavailable and poorly bioavailable. Highly bioavailable iron sources, for example, include ferrous sulphate and ferrous fumarate, which are soluble in neutral or acidic aqueous environments but may cause organoleptic changes through fat oxidation and are therefore often only applicable to products with short stored product shelf life. Ferrous sulphate is a very common and cheap iron fortificant. Those with poor bioavailability, for example, include ferric pyrophosphate and elemental powders, which are insoluble in water and poorly soluble in dilute acid but are more compatible with the foods used. Other types of iron fortificants applied in foods are the protected iron compounds such as sodium ferric EDTA (NaFeEDTA) and microencapsulated forms which are not expected to bring about any negative effects to foods as well and have high solubility as an iron chelate (Hurrell, 1997).

In rice fortification, several techniques have been reported, such as polymer coating of micronutrients (including iron) (Peil et al., 1982). Due

to lack of appropriate technologies and technical problems, none of the techniques have been used extensively for iron fortification in developing countries (Moretti et al., 2005). A promising extrusion technology for iron-fortified rice grains has been reported by Kapanidis and Lee (1996). With ferrous sulphate, they produced acceptable coloured iron-fortified rice grains through acidification of the rice flour to a pH of 0.5. However, the cooked product presented a metallic aftertaste and was less acceptable than Jasmine rice. Removing the acidification step this method was applied by Moretti et al. (2005) to produce extruded fortified rice grains containing 0.5 g and 1 g Fe/100 g based on different iron fortification compounds. Fortified rice and unfortified rice were compared in both raw and cooked forms. The data showed that ferric pyrophosphate in the extrusion premix successfully delivered iron-fortified rice closely resembled natural unfortified rice. The other iron fortification compounds (elemental iron, NaFeEDTA, ferrous sulphate and encapsulated form) were unsuitable because of colour changes.

As mentioned before, one of the major challenges of iron fortification is undesirable off-colour development. Colour has a strong influence on the sensory perception of the food taste and can indicate the quality of the product. When using highly bioavailable iron, foods and beverages can clearly change colour and therefore these iron sources can realistically only be applied to products of short shelf life (Clydesdale, 1998). Other studies have shown that adding iron to milk (Coccodrilli and Shah, 1985), soy infant formula (Theuer, 2008), baby cereals (Hurrell et al., 1989) and chocolate milk (Douglas et al., 1981) causes undesirable colour changes to occur. A study by Kiskini et al. (2012) showed that iron compounds that were either water insoluble or protected for example in polymer coating

seem to cause undesirable effects on the final characteristics of gluten-free bread.

7.2.2 Role of Ascorbic acid

Ascorbic acid is found in nature with the main sources of ascorbic acid being fruits and vegetables (especially citrus fruit and peppers). It is also produced by the kidney of some animals. Ascorbic acid is often added to foods because humans are not able to produce it. Beside as nutrient, ascorbic acid is added to foods as an antioxidant and to prevent the browning of fresh and canned fruits and vegetables. Ascorbic acid supports the absorption of iron and the formation of collagen (Kirby et al., 1991). It enhances iron solubility, which is crucial to absorption, by reducing the iron (Camire et al., 1990).

Ascorbic acid has sufficient stability during cured-meat processing to inhibit the pigment-light induced degradation and it is applied in brewed products such as beer to avoid the formation of haze. Ascorbic acid or in the generic term known as vitamin C is often added as a fortificant to produce nutritious product onto fruit juices, fruit-flavoured drinks, juice added soda waters, dry cocktails or beverages, cereal-based products, and milk (Borenstein, 1987). In bread making ascorbic acid is an acceptable additive as an effective improver (Fitchett and Frazier, 1986).

Furthermore, ascorbic acid is an antioxidant. In water it is oxidised to dehydroascorbic acid, then to diketogulonic, oxalic and threonic acids. The first reaction is reversible, but the subsequent ones are not. This is the reason why its content in food can decrease during food preparation and

storage. It is also recognised to be one of the most heat-sensitive nutrients in foods (Esteve et al., 1999).

When foods containing ascorbic acid are heated a range of chemical interactions could take place. Work by Vallès-Pàmies et al. (1997) and Paterson et al. (1996) showed that the addition of chemicals, particularly sulphite and ascorbic acid, to starches caused changes to their pre- and post-pasting behaviour.

It is well recognised that iron fortification of foods is problematic in terms of product taste, colour, stability and bioavailability. Mehansho (2006) has studied new approaches in iron fortification technology. One of the approaches is electrochemical chemistry (redox modulation). Ferrous compounds in general are known to be oxidised to the ferric form when added to foods and beverages. Hence, redox (reduction-oxidation) modulation was applied to prevent the oxidation of ferrous (Fe^{2+}) to ferric (Fe^{3+}) which with time precipitates as rust. The environment was made reducing rather than oxidising by lowering the pH (adding organic acids and reducing agents, respectively). Lowering pH with citric acid and redox potential with ascorbic acid in this study proved that it could prevent the oxidation of ferrous iron to ferric (Mehansho, 2006).

7.3 Materials and Methods

7.3.1 Materials

The main material used in the research reported in this chapter was sago starch from the same batch as used for the work reported in Chapter 4, 5 and 6. It was supplied by PT Riau Sago Lestari, Indonesia, and used as received. As additives ferrous sulphate heptahydrate ($Fe_2SO_4.7H_2O$) and ascorbic acid were used. They were purchased from Fischer Scientific, UK and Sigma Aldrich, UK, respectively, and used without further purification.

7.3.2 Methods

7.3.2.1 Extrusion processing

The extrusion processing as reported in this chapter was similar to the process described in section 6.3.2.1. Additionally, for the samples produced and reported in this chapter, there was chemical fortification. The chemical components as additives were dissolved in the water feed to give concentrations of 80 mg of ferrous sulphate in 100 g of the sago starch as solid feed. When ascorbic acid was added, it was also dissolved in the water along with the ferrous sulphate and the acid addition was adjusted to give a concentration of 1:6 ferrous sulphate to ascorbic acid, based on recommendation ratio (WHO, 2006). There were three types of samples and the codes for the additives in this trial were: Fe (iron), AA (ascorbic acid) and ALL (iron and ascorbic acid). For comparison relevant results from trials not involving additives as reported in Chapter 6 are included in the results presentation in this Chapter and these are labelled NIL.

7.3.2.2 Extrudate analysis

For the methods used to analyse the samples the reader is referred to section 3.3 and the particular section is mentioned at each experimental section below.

7.4 Results and Discussion

In this chapter, the results of the extrusion trials to produce fortified sago products are reported and discussed. Based on the results reported in Chapter 6 all trials were conducted at constant screw speed of 300 rpm and water feed rate was varied between 4, 7 and 20 mL/min. Die temperature was kept at 140 °C and the feed rate of sago starch was 8 kg/hr throughout. Iron and/or ascorbic acid were added at the concentration mentioned before (80 mg of ferrous sulphate in 100 g of solid sago starch feed; 1:6 ferrous sulphate:ascorbic acid in water feed where both additives were used).

7.4.1 Torque and specific mechanical energy input

Sago starch was the main material in this trial and was subjected to the same screw speed and die temperature, but water feed levels varied. The results shown in Figure 7.1 reveal that for the range of water feed rates applied, at the otherwise constant processing conditions, the torque increased with an increase of SME when the water feed rate was decreased mainly when changes in water feed at 20 mL/min. Some symbols in Figure 7.1 overlap and cannot be found due to the adjacent data. The effect of water feed rate as plasticiser has been discussed in section 6.4.1 where the resistance to flow of the material could increase with reducing water feed rate as the level of plasticiser. The addition of iron and ascorbic acid could be expected not to affect the SME and torque as the concentrations were low.

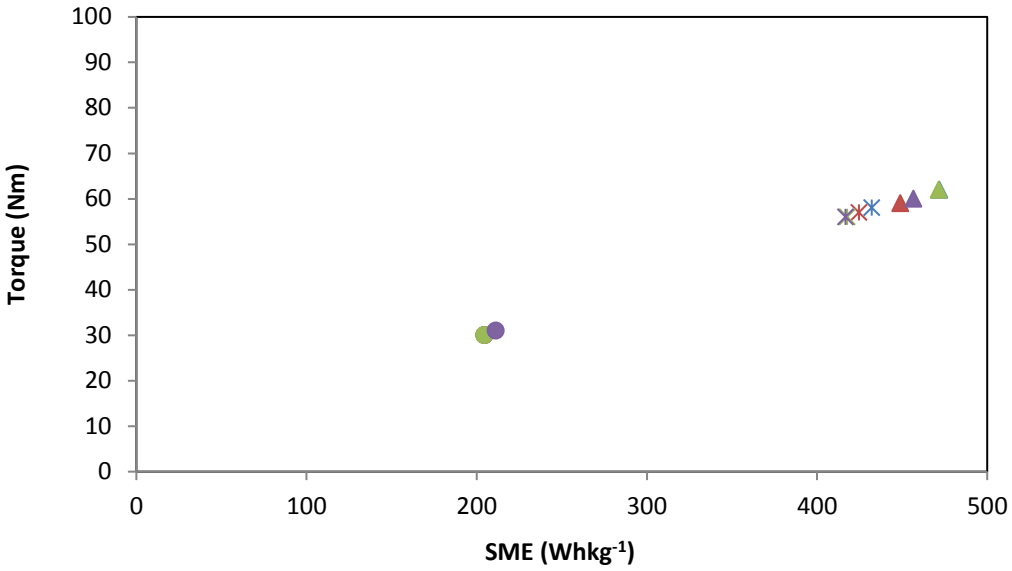

Figure 7.1 Variation of torque and specific mechanical energy (SME) input. Additives: blue, NIL; red, Fe; green, AA; purple, ALL. Water feed (mL/min):▲, 4; ✳, 7; ●, 20.

7.4.2 Moisture content of the extrudates as they exit the extruder

The die temperature of the extruder was set at 140 °C and therefore as expected when the extrudates exited the extruder, water was lost in the form of vapour. As seen for the samples discussed in Chapter 6, the highest moisture content was found on the samples produced at the highest water feed rate (20 mL/min). This sample formed the melt containing 25% wwb moisture in the beginning then lost moisture to form extrudates of ~10% moisture. This value was higher than that of the other two feed rates. Figure 7.2 indicates that at water feed rates of 4 and 7 mL/min presence of additives resulted in a significant increase in the moisture content of the extrudates compared to the samples without additives.

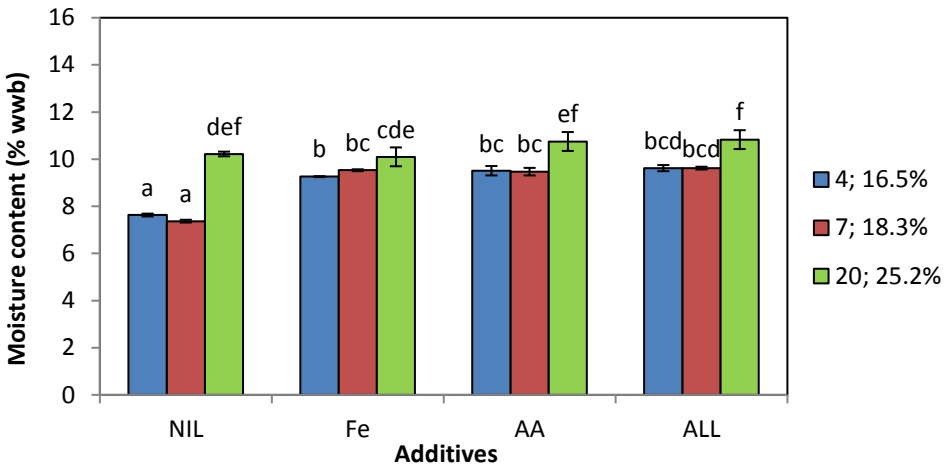

Figure 7.2 The moisture content of extrudates produced with different additives and at different water feed. The legend shows water feed in mL/min and % moisture content of the melt (wwb). Bars represent mean ± SD of 3 replicates. Bars denoted by the same letter are not significantly different (p>0.05).

7.4.3 Physical material properties of the extrudates

Some samples from the extruder trials were dried at 45 °C for 18 h and then these materials were subjected to a series of observations and measurements. In the following results are presented first followed by discussion due to interrelationships between the parameters.

7.4.3.1 Visual observation

Photographs of all of the extrudates collected from trials with changing additives and water feed rates (4, 7 and 20 mL/min) are shown in Figure 7.3. All of the samples show expansion, but the extrudates created at the water feed of 20 mL/min looked hard and "glassy", making them appear very different from the other extruded samples in this experiment. The pictures reveal the fairly uniform bubbles for the extrudates that were produced at the water feed of 4 and 7 mL/min. There was an observable tendency for a difference in diameter and colour of the extrudates with the addition of iron and/or ascorbic acid. The sample produced without

additives (NIL) shows the lowest expansion and it was most yellowish in colour. The impact of iron and ascorbic acid seemed complex and there could well be an interaction between the chemical(s) and the moisture content of the melt. However, when the water feed was 7 mL/min, the physical appearances of the extrudates were similar to those produced at 4 mL/min.

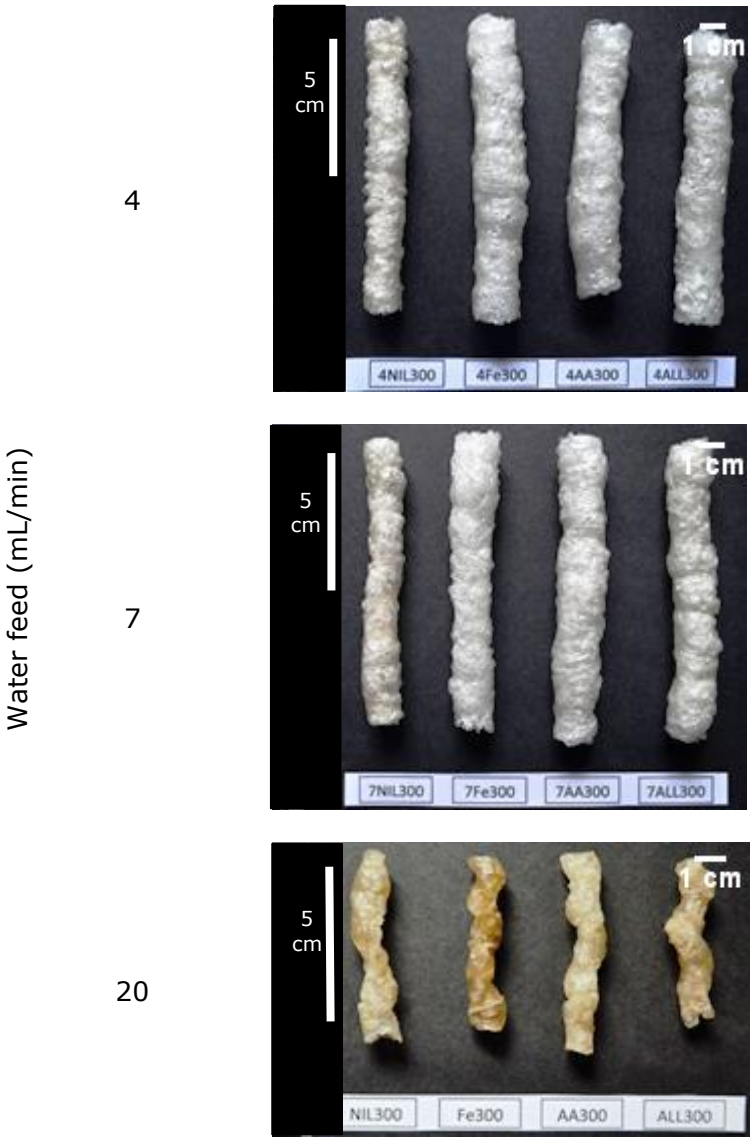

Figure 7.3 Photographs of extrudates produced at constant screw speed 300 rpm and with different additives (horizontal) and at different water feed (vertical).

7.4.3.2 Cellular microstructure

The cellular microstructure of the expanded samples was revealed by scanning electron microscopy. Figure 7.4 shows the micrographs acquired on samples produced at 4 and 7 mL/min water feed; samples produced at 20 mL/min water feed were not imaged as explained in section 3.3.13. All of the micrographs show that the shape of air cells is roughly circular independent of additive and water feed.

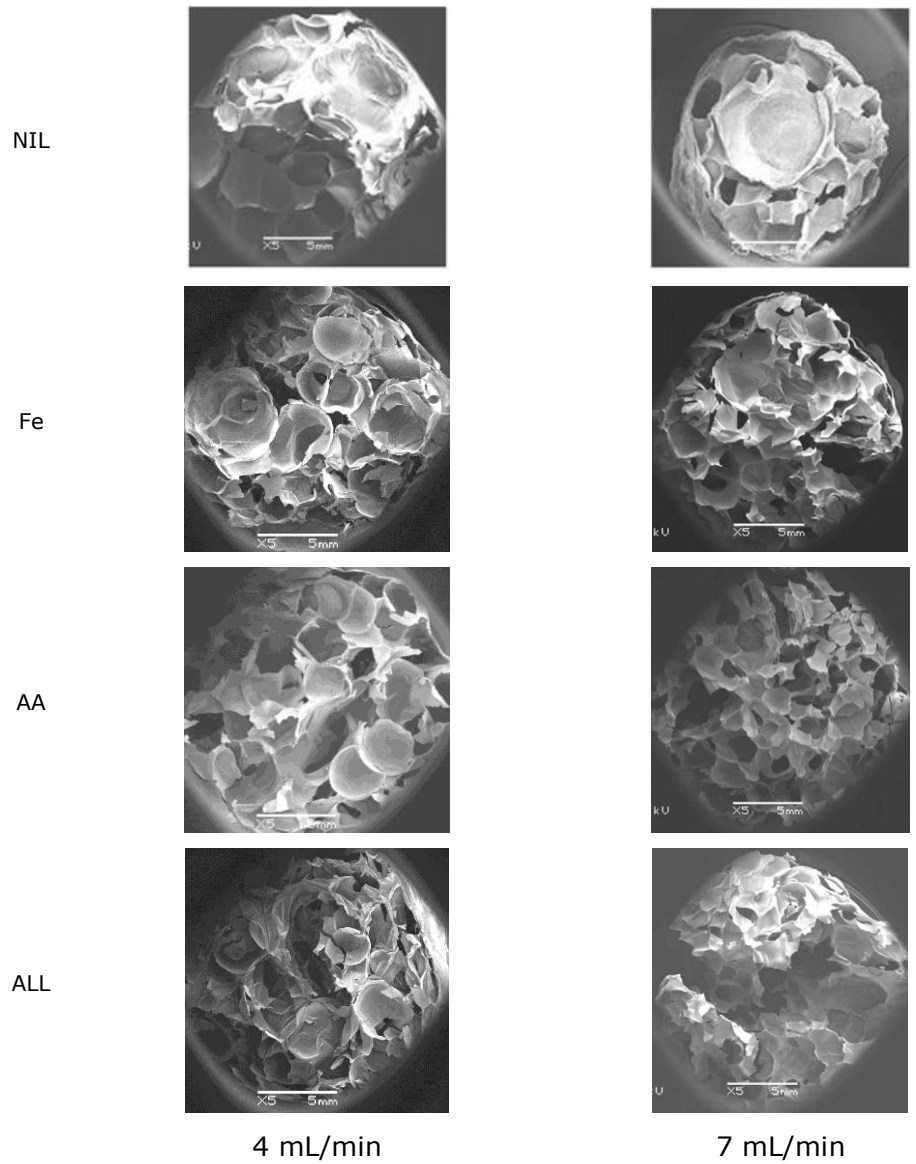

Figure 7.4 Scanning Electron Microscopy (SEM) pictures of extrudates produced with different additives (horizontal) and at different water feed (vertical). All scale bars correspond to 5 mm.

Extrudates without additives (NIL) showed differences in the characteristics of the spherical air cells compared to the samples with additives. The air cells were of greater size and therefore lower in number. The air cells found in the extrudates produced with the addition of both iron and ascorbic acid (ALL) were smallest and most numerous and these appeared to be present throughout the structure. On the other hand, extrudates produced at different water feed rate (4 or 7 mL/min) showed the same characteristics for the air cells. The number and air cell structure of the samples produced at 20 mL/min would be expected to be very different due to their increased hardness and "glassy" appearance.

7.4.3.3 Colour

Colour characteristics of the whole extrudates are shown in Table 7.1 (see the method in section 3.3.9). The *L**, *a**, *b** values of extrudates processed without and with different additives varied significantly which is in agreement with the visual observations reported in section 7.4.3.1. Extrudates produced at water feed of 20 mL/min showed the lowest *L** values. Higher *L** values correspond to greater whiteness, whereas the low *L** values for extrudates produced at water feed of 20 mL/min resembled its dark yellow colour. Extrudates without additives produced at water feed rates of 4 and 7 mL/min were significantly different from samples with additives regarding *L** values. For the sample produced at water feed of 4 mL/min, the addition of iron (Fe) showed an increased *L** value, followed by that of ascorbic acid (AA) and both of iron and ascorbic acid (ALL). Meanwhile, for the samples produced at water feed of 7 mL/min, the highest *L** value was the extrudates with the addition of iron alone. In terms of water feed rate, increasing the water feed from 4 to 20 mL/min in the extruder decreased the *L** values for the extrudates with addition of ascorbic acid (AA) and for iron plus ascorbic acid (ALL), whereas for

extrudates without addition (NIL) and with iron (Fe), the *L** values increased from 4 to 7 mL/min and decreased for the 20 mL/min samples.

Table 7.1 Colour properties of extrudates produced with different additives and at different water feeds. Values are means ± SD (n = 10). Means within a column related to a particular parameter with the same superscript are not significantly different (p>0.05).

Additives; water feed (mL/min)	*L** (lightness; zero for black to 100 for perfect white)	*a** (negative values for greenness to positive values for redness)	*b** (negative values for blueness to positive values for yellowness)
NIL;4	48.9^{d}±1.2	-0.03^{e}±0.08	3.90^{d}±0.37
NIL;7	52.8^{g}±1.66	0.05^{f}±0.04	4.39^{e}±0.05
NIL;20	29.3^{ab}±1.24	0.63^{g}±0.04	5.89^{g}±0.32
Fe;4	51.6^{fg}±0.41	-0.33^{bc}±0.02	1.7^{ab}±0.17
Fe;7	58.8^{i}±0.25	-0.42^{a}±0.03	1.47^{a}±0.06
Fe;20	28.5^{a}±0.15	0.78^{h}±0.03	5.38^{f}±0.46
AA;4	55.4^{h}±0.51	-0.33^{bc}±0.02	1.74^{ab}±0.07
AA;7	49.9^{de}±0.91	-0.27^{c}±0.02	1.98^{b}±0.12
AA;20	42.1^{c}±0.4	-0.12^{d}±0.03	7.66^{h}±0.08
ALL;4	57.4^{i}±0.37	-0.37^{ab}±0.03	1.83^{b}±0.19
ALL;7	50.7^{ef}±0.32	-0.17^{d}±0.02	2.72^{c}±0.07
ALL;20	30.3^{b}±1.6	0.6^{g}±0.07	5.86^{g}±0.4

Negative *a** values were recorded for most of the extrudates except that of extrudates produced at water feed of 20 mL/min, whereas the opposite was observed for *b** values. The negative *a** value (which represents greenness) was highest for extrudates produced at water feed of 7 mL/min with iron addition and that of 4 mL/min with iron plus ascorbic acid addition (ALL). Application of additives to the extrudates lowered *a** and *b** values significantly, except for extrudates produced at water feed of 20 mL/min. The effect was different between 4 and 7 mL/min water feed rates where there was an increase of the *a** values for extrudates produced at 7 mL/min of water feed with addition of iron, ascorbic acid

and both of them and no significant difference for that of 4 mL/min for all application of additives (p>0.05). Moreover, by comparing water feed rates, increasing the water feed from 4 to 20 mL/min in the extruder increased the a^* values of extrudates without addition (NIL), with addition of ascorbic acid (AA) and for iron plus ascorbic acid (ALL), whereas for extrudates with iron (Fe) the L^* values decreased from 4 to 7 mL/min and increased to 20 mL/min of water feed.

Table 7.1 shows all extrudates had positive b^* values (yellowness) where extrudates produced at water feed of 20 mL/min showed the highest values. The addition of additives for extrudates produced at water feed of 4 and 7 mL/min considerably lowered the b^* values compared to that of samples without additives (NIL). The different additives did not affect the b^* values of extrudates produced at water feed of 4 mL/min. Meanwhile the b^* values of the extrudates produced at 7 mL/min increased significantly between the additive samples in the order: addition of iron, ascorbic acid, and both of them. Regarding feed rates, increasing the water feed from 4 to 20 mL/min in the extruder significantly increased the b^* values of all extrudates (p>0.05).

7.4.3.4 Expansion ratio

Figure 7.5 exhibits the impact of added iron and ascorbic acid on the expansion ratio of the sago starch extrudates (method given in section 3.3.10). As expected, increasing water feed from 4 to 20 mL/min resulted in a significant decrease in the extrudates expansion. Expansion of extrudates produced at water feed of 4 mL/min increased significantly with the addition of all type of the additives.

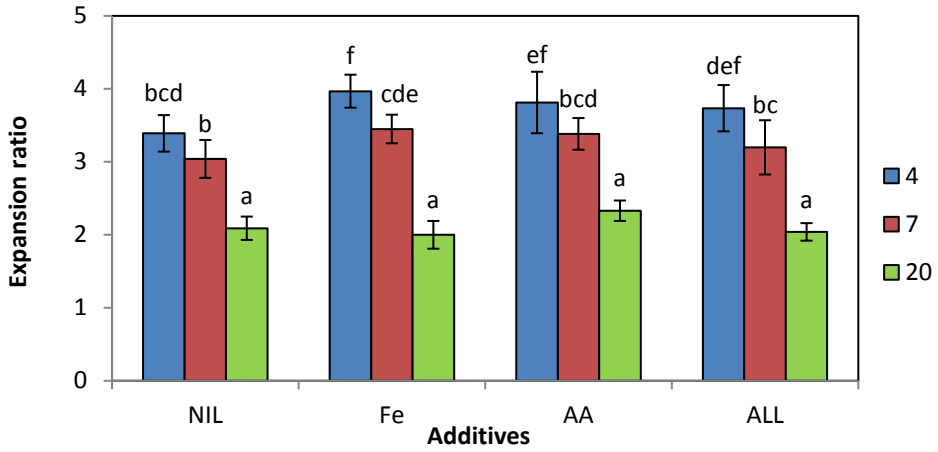

Figure 7.5 Expansion ratio of extrudates produced with different additives and at different water feed. The legend shows water feed in mL/min. Bars represent mean ± SD of 10 replicates. Bars denoted by the same letter are not significantly different (p>0.05).

7.4.3.5 Bulk density

The extrudates showed bulk densities (method given in section 3.3.11) in the range of 0.08 and 1.14 g/cm^3 (Figure 7.6) and the highest density was obtained for extrudates produced at water feed of 20 mL/min. For extrudates produced at the same water feed, the application of all types of the additives did not show any significant difference (p>0.05). On the other hand, an increase in water feed from 7 to 20 mL/min increased the extrudates density significantly.

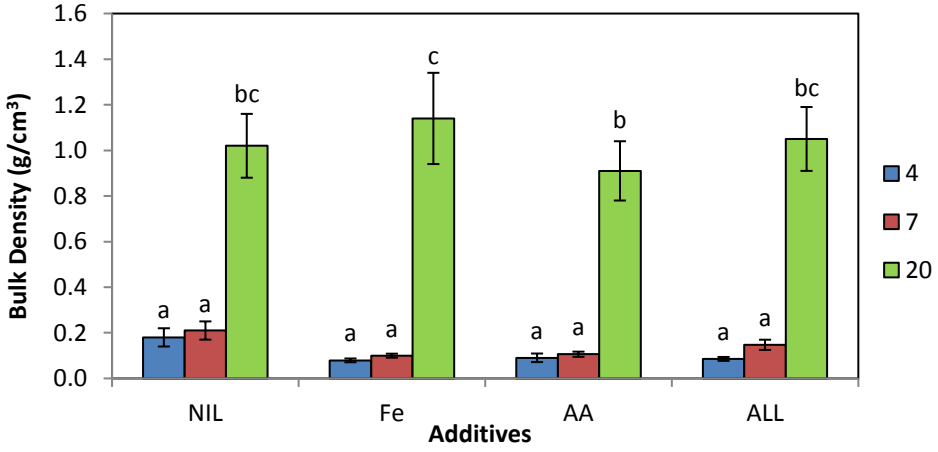

Figure 7.6 Bulk density of extrudates produced with different additives and at different water feed. The legend shows water feed in mL/min. Bars represent mean ± SD of 10 replicates. Bars denoted by the same letter are not significantly different (p>0.05).

7.4.3.6 Texture properties

The texture of the extrudates was examined based on the two parameters of hardness and crispness (see methods in section 3.3.12). Unfortunately, no values could be obtained for the highest moisture samples (produced at water feed of 20 mL/min) due to their very hard and "glassy" texture. It can be observed from Figure 7.7 that the hardness of the extrudates produced at 4 mL/min water feed decreased significantly with the addition of iron and ascorbic acid (Fe, AA and ALL), whereas in the case of 7 mL/min water feed the hardness decreased significantly only with the addition of both additives (ALL). Moreover, regarding water feed rate, increasing water feed from 4 to 7 mL/min resulted in significantly increased the hardness of extrudates with all type of addition (Fe, AA and ALL).

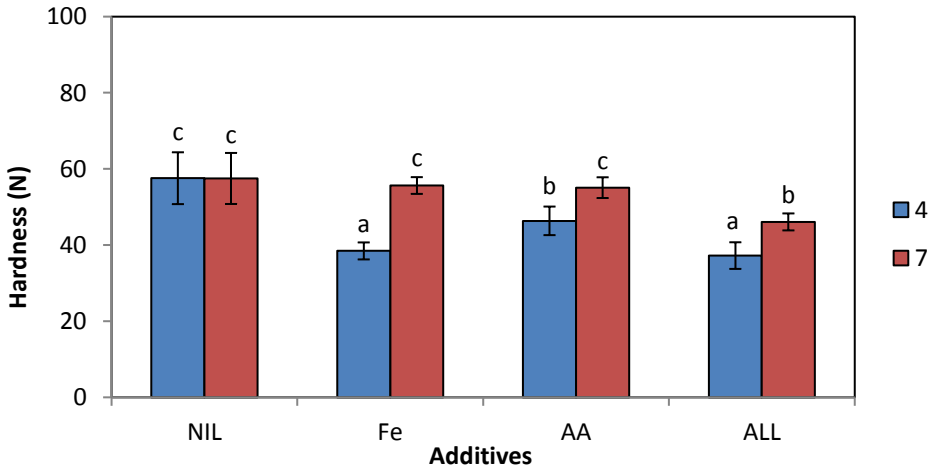

Figure 7.7 Hardness of extrudates produced with different additives and at different water feed. The legend shows water feed in mL/min. Bars represent mean ± SD of 10 replicates. Bars denoted by the same letter are not significantly different (p>0.05).

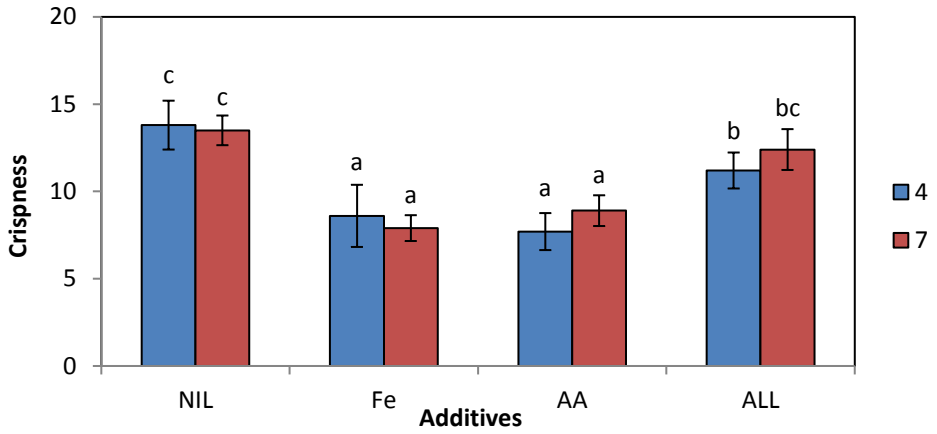

Figure 7.8 Crispness of extrudates produced with different additives and at different water feed. The legend shows water feed in mL/min. Bars represent mean ± SD of 10 replicates. Bars denoted by the same letter are not significantly different (p>0.05).

The results for crispness are shown in Figure 7.8. From the figure, it can be observed that crispness of the extrudates produced at water feed of 4 and 7 mL/min decreased significantly compared to the crispness of extrudates without additives with the addition of all types of additives (Fe, AA and ALL). The crispness of extrudates produced with the addition of each iron (Fe) and ascorbic acid only (AA) was lower than when both of them (ALL) were present. Meanwhile, extrudates produced at different water feed rate (4 and 7 mL/min) did not show significant differences of crispness when the same type of additives was present.

7.4.3.7 Discussion of physical material properties of the extrudates

Ferrous sulphate heptahydrate is used in the fortification of several foods (bread, flours, pasta, infant formulas, etc.) as inexpensive source of highly bioavailable iron (Cook and Reusser, 1983). However, the utilisation of this highly reactive form of iron is limited due to oxidation that causes quality deterioration of iron-fortified products. The oxidation of ferrous iron

to the ferric state, followed by formation of insoluble yellow-brown ferric hydroxide polymers, can be retarded in acidic conditions and ascorbic acid in model systems and in foods (Nojeim and Clydesdale, 1981). Hence, the addition of ascorbic acid to the iron-fortified extrudates in this study was intended to enhance their colour properties.

From the visual observation, it was shown that additives play a key role in the colour of the extrudates. Extrudates with additives became lighter and whiter in comparison with extrudates without additives. This visual observation was confirmed with colour measurements using the HunterLab, where *L** value of extrudates produced at water feed of 4 mL/min without additives (NIL) were lower compared to that of with additives. However, findings for the Fe sample did not agree with the study by Kapanidis and Lee (1996) that showed addition of iron, without acidification, resulted in brown colour formation that was documented by the substantially decreased lightness, *L** value, and increased red colour of the extrudate (*a** value) compared to the control (sample consisted of rice starch and water). Furthermore, the presence of ascorbic acid (either for ascorbic acid only or iron plus ascorbic acid samples) caused lighter coloured extrudates compared to those that contained iron (Fe) except for extrudates produced at water feed of 7 mL/min. This could be due to the formation of purple iron ascorbate complexes resulting in extrudates with lighter colour (Gorman and Clydesdale, 1983). It was notable that samples produced at water feed of 4 and 7 mL/min were very different in their whole appearance compared with samples created at a water feed of 20 mL/min. One parameter that could show the differences was the *L** value, where the higher the water feed the lower the *L** value particularly extrudates with addition of ascorbic acid (AA) and iron plus ascorbic acid (ALL).

Visual observation also showed that extrudates with additives (Fe, AA and ALL) were more expanded compared to the non-additives samples (NIL). This observation is in line with data for the expansion ratio measurements for extrudates produced at water feed of 4 mL/min, when Fe, AA and ALL were present compared to the NIL samples. Extrudates produced at the water feed of 7 mL/min only showed the enhanced expansion for the sample with iron, and the expansion for iron was not different from the other additive samples. However, the additives did not affect the bulk density of extrudates, except at the water feed of 20 mL/min. These observations are clearly related to the extrudate microstructure which in turn impacts on texture properties and these are discussed at the end of the following paragraph.

Scanning electron microscopy demonstrated an increase in number and decrease in size of the air cells throughout the additive samples. The number of air cells, despite their decrease in size could be the reason for the greater expansion of extrudates with all types of additives produced at 4 mL/min water feed. The differences in the cellular microstructure had an impact on the texture of the extrudates. Additives were associated with decreasing hardness and crispness of the extrudates produced at 4 mL/min water feed. At the higher water feed rate (7 mL/min) the changes in hardness and crispness were less pronounced. On the other hand, no obvious differences observed in cellular structure of extrudates produced at 4 and 7 mL/min water feed.

The hardness values reflect the maximum force required to compress the sample, the hardest element, while the crispness looks at failure events. The lower crispness values for the additive samples became indicative of multiple failures of the thin cell walls noted in the SEM micrographs.

Differences in structural and textural characteristics among the extrudates may be attributed to variation in the way in which the starchy materials and air create the microstructure. The nucleation of the water vapour cells that expand and cause the bubble structure is relevant to the number of cells present in the extrudate. The viscosity and elasticity of the bubble wall will often determine the size of the bubbles. The pressures for expansion will relate to the temperature and amount of steam. At temperature below 100 °C, the expansion would predominantly result from the elastic effect. If the extrudate temperature is much higher, puffing occurs due to the tendency of the water vapour to escape from the extrudates (Padmanabhan and Bhattacharya, 1989).

It is well established that the extruder conditions will alter the viscosity of the starch as it depolymerises in the high shear extrusion environment. What is not known is if the iron and ascorbic acid, added separately or both of them together, in the extrusion cooking could be important to the starch conversion levels and therefore the viscosity of the starch melt in the extruder. This leads to consideration about the starchy component and what happens to the native starch in extrusion cooking. The next stage in the experimental work was, therefore, to grind up the extrudates and analyse the factors reflecting the starch changes during extrusion.

7.4.4 Physicochemical material properties of the extrudates

As with the Chapter 6, after measuring and observing the physical properties of the extrudates, they were ground and their behaviour in association with excess water was investigated to focus on how the

starches have changed through the extrusion process. All of the results are presented followed by their combined discussion in the last section.

7.4.4.1 Water absorption index

Water absorption indices (measurement given in section 3.3.14) are presented in Figure 7.9. The measured WAI of the extrudates ranged between 3.43 and 10.30 g/g dry sample. The addition of the all types of additives decreased the WAI of extrudates produced at 4 mL/min water feed significantly. A significant effect was also observed for the addition of ascorbic acid (AA) on WAI of extrudates produced at water feeds of 7 mL/min where the WAI increased. On the other hand, the addition of both iron and ascorbic acid (ALL) did not affect significantly (p>0.05) the WAI of the extrudates produced at water feed rates of 7 and 20 mL/min. Figure 7.9 also gives information that increasing water feed in the extruder from 4 to 20 mL/min increased WAI of the extrudates significantly except for extrudates produced at water feed rates of 4 and 7 mL/min without additives (NIL).

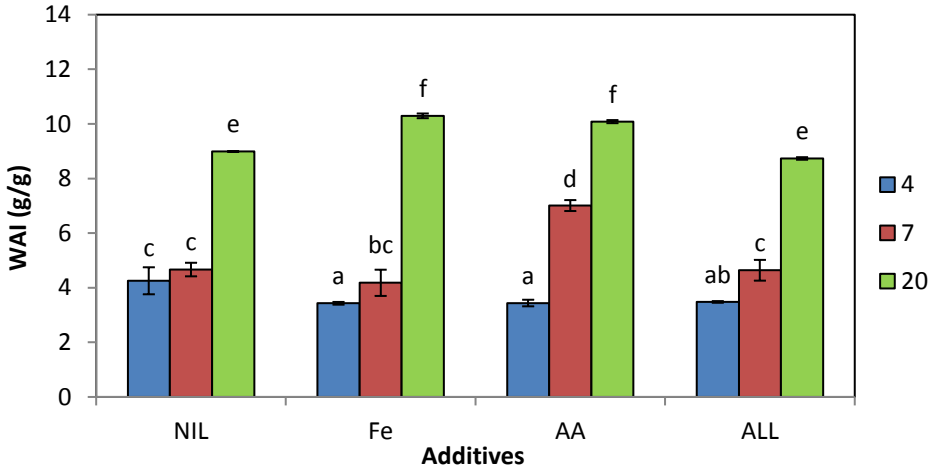

Figure 7.9 WAI of extrudates produced with different additives and at different water feed. The legend shows water feed in mL/min. Bars represent mean ± SD of 3 replicates. Bars denoted by the same letter are not significantly different (p>0.05).

7.4.4.2 Water solubility index

Effects of fortification on WSI of sago starch extrudates are shown in Figure 7.10 (method given in section 3.3.14). The values of WSI varied from 18.8% to 68.3% for the extrudates. Use of all types of the additives did not cause a significant change (p>0.05) in the WSI of extrudates created at 4 mL/min water feed. Meanwhile, WSI of the extrudates produced at 7 mL/min water feed decreased significantly with the addition of iron (Fe) and ascorbic acid (AA) and this was the same effect occurred for extrudates produced at 20 mL/min water feed with the addition of Fe, AA and ALL. By comparing the water feed rates, increasing water feed rate from 4 to 20 mL/min decreased the WSI significantly particularly at 20 mL/min.

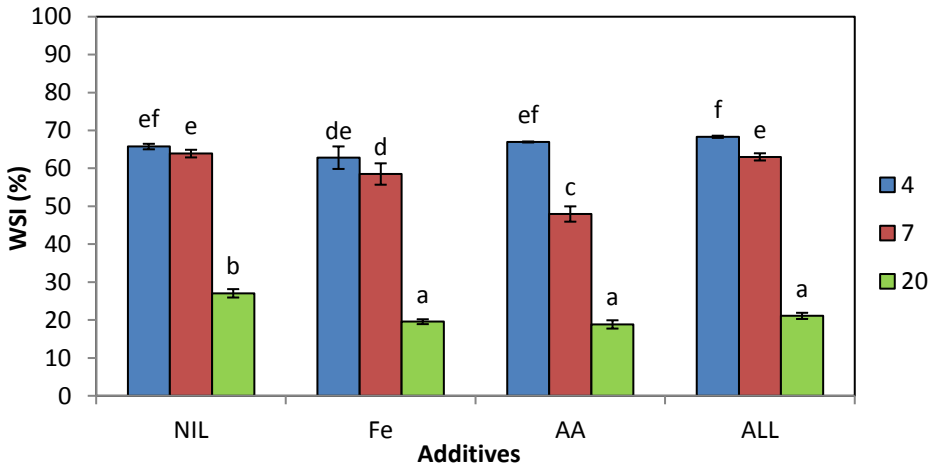

Figure 7.10 WSI of extrudates produced with different additives and at different water feed. The legend shows water feed in mL/min. Bars represent mean ± SD of 3 replicates. Bars denoted by the same letter are not significantly different (p>0.05).

7.4.4.3 Paste viscosity

The pasting properties of the various extrudates prepared from the sago starch with and without additives are presented in Figure 7.11 and Table

7.2 (method given in section 3.3.7.2). The extrudates displayed significant variation in their pasting behaviour, and both the water feed rate and the additives seemed to have an impact. Extrudates at water feed of 7 mL/min with ascorbic acid (AA) showed the highest cold peak viscosity (1358 cP), whereas the extrudates without additives (NIL) at water feed 4 and 7 mL/min had the lowest values.

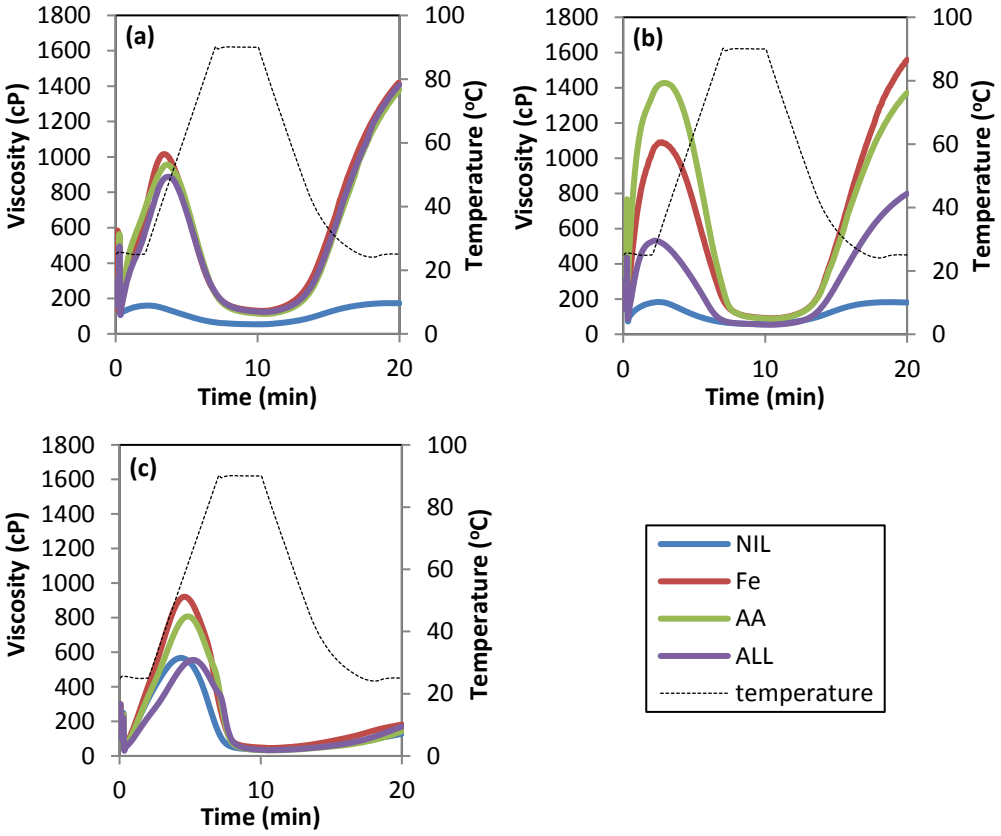

Figure 7.11 (a, b, c) Paste viscosity of extrudates produced with different additives (legends) and at different water feed (mL/min): (a), 4; (b), 7 and (c), 20.

When the extrudates were made at the lowest water feed rate (4 mL/min, Figure 7.11a), the sample with no additives showed very low viscosity throughout the pasting, but all of the samples with additives showed very similar viscosity and pasting properties, i.e. the cold water swelling and high final viscosity. Meanwhile, for extrudates produced at 7 mL/min water feed (Figure 7.11b), in presence of and depending on the type of additive

these showed a higher cold peak viscosity. Additionally, a final viscosity which in height also depended on the type of additive occurred. No additive or the combination of both iron and ascorbic acid resulted in lower cold peak viscosity and lower final viscosity in contrast to the presence of the ascorbic acid or iron alone. As can be seen in Figure 7.11 (c) for extrudates produced at a 20 mL/min water feed, these samples took some time to hydrate but showed swelling in reasonably cool conditions with the peak in swelling occurring at 50 °C.

Table 7.2 RVA results for extrudate produced with different additives and at different water feeds. Values are means ± SD (n = 3). Means within a column related to a particular parameter with the same superscript are not significantly different (p>0.05).

Additives; water feed (mL/min)	Cold peak	Hold	Break-down	Final	Setback	Peak Time (min)
	Viscosity (cP)					
NIL;4	159^{a} ±2.1	54^{bc} ±2.0	106^{a} ±2.0	173^{a} ±30	119^{a} ±28	2.1^{a} ±0.1
NIL;7	180^{ab} ±3.1	57^{c} ±4.4	126^{a} ±0.6	180^{a} ±2.0	123^{a} ±3.0	2.3^{a} ±0.1
NIL;20	335^{c} ±9.5	34^{a} ±1.7	533^{b} ±10	130^{a} ±12	96^{a} ±11	4.3^{e} ±0.04
Fe;4	631^{f} ±29	130^{f} ±7.2	887^{e} ±44	1419^{cd} ±130	1290^{c} ±128	3.5^{d} ±0.04
Fe;7	1037^{h} ±4.7	91^{d} ±2.3	1001^{f} ±6.4	1566^{d} ±9.5	1476^{d} ±12	2.5^{b} ±0.1
Fe;20	413^{d} ±41	46^{b} ±3.1	876^{e} ±11	183^{a} ±23	138^{a} ±24	4.5^{f} ±0.08
AA;4	708^{g} ±7.6	112^{e} ±1.5	844^{de} ±8.9	1387^{c} ±65	1275^{c} ±67	3.5^{d} ±0.04
AA;7	1358^{i} ±33	88^{d} ±0.01	1340^{g} ±37	1377^{c} ±99	1289^{c} ±99	2.8^{c} ±0.08
AA;20	352^{cd} ±6.6	32^{a} ±2.3	775^{cd} ±15	145^{a} ±23	113^{a} ±21	4.8^{g} ±0.04
ALL;4	576^{ef} ±36	124^{f} ±4.0	766^{c} ±45	1414^{cd} ±45	1290^{c} ±43	3.7^{d} ±0.1
ALL;7	528^{e} ±6.1	54^{bc} ±1.2	478^{b} ±4.8	801^{b} ±30	748^{b} ±30	2.1^{a} ±0.01
ALL;20	230^{b} ±9.6	34^{a} ±2.5	522^{b} ±28	171^{a} ±33	138^{a} ±30	5.1^{h} ±0.04

Following the peak the viscosity decrease and further the viscosity development on cooling is the same for all four samples processed at 20 mL/min then the viscosity at the end of the pasting cycle of these samples were all very low.

To understand the impact of the extrusion processing conditions on the pasting properties of the sago starch extrudates and the role additives play further, Figure 7.12 shows cold peak viscosity and water absorption index against SME value. It can be observed that the cold peak viscosity (Figure 7.12a) varies greatly between the samples clustered in two groups of similar SME. Therefore the additives may be playing a greater role than just reflecting the energy input via extrusion. For the water absorption index in relation with the SME (Figure 7.12b), the data indicate a relationship of decreasing water absorbance with increased energy and decreased water feed rate, without the additive being implicated in the changes.

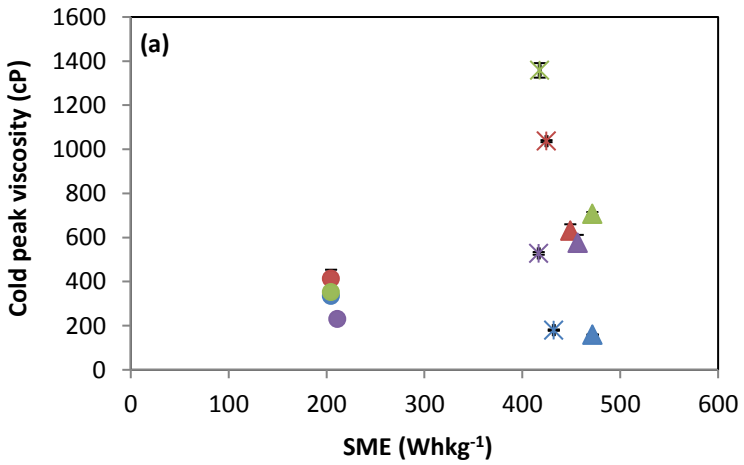

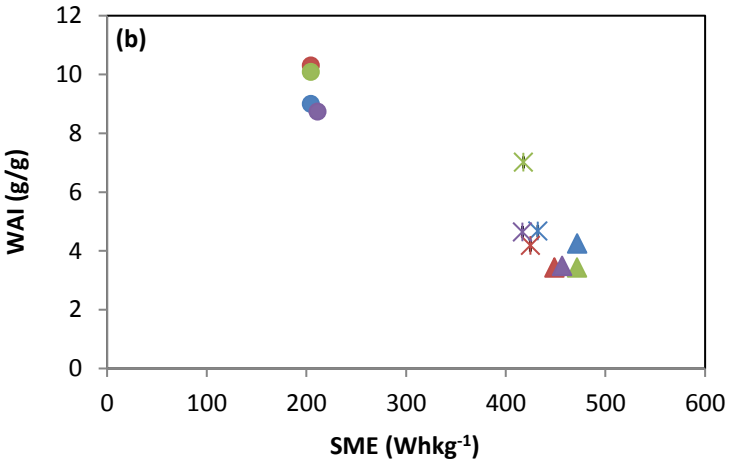

Figure 7.12 Variation of cold peak viscosity (a) and water absorption index (b) with specific mechanical energy (SME) input. Additives: blue, NIL; red, Fe; green, AA; purple, ALL. Water feed (mL/min.): ▲, 4; ✳, 7; ●, 20.

7.4.4.4 Birefringence

The birefringence to state of starch gelatinisation of extrudates with and without additives was revealed through microscopy (Figure 7.13) using brightfield illumination and polarised light (see method in section 3.3.5). There are only results for extrudates produced at 4 mL/min water feed presented to illustrate the point and for the other water feed rates it was the same. The polarised light pictures show the almost complete absence of intact starch granules as indicated by very small amounts of Maltese crosses.

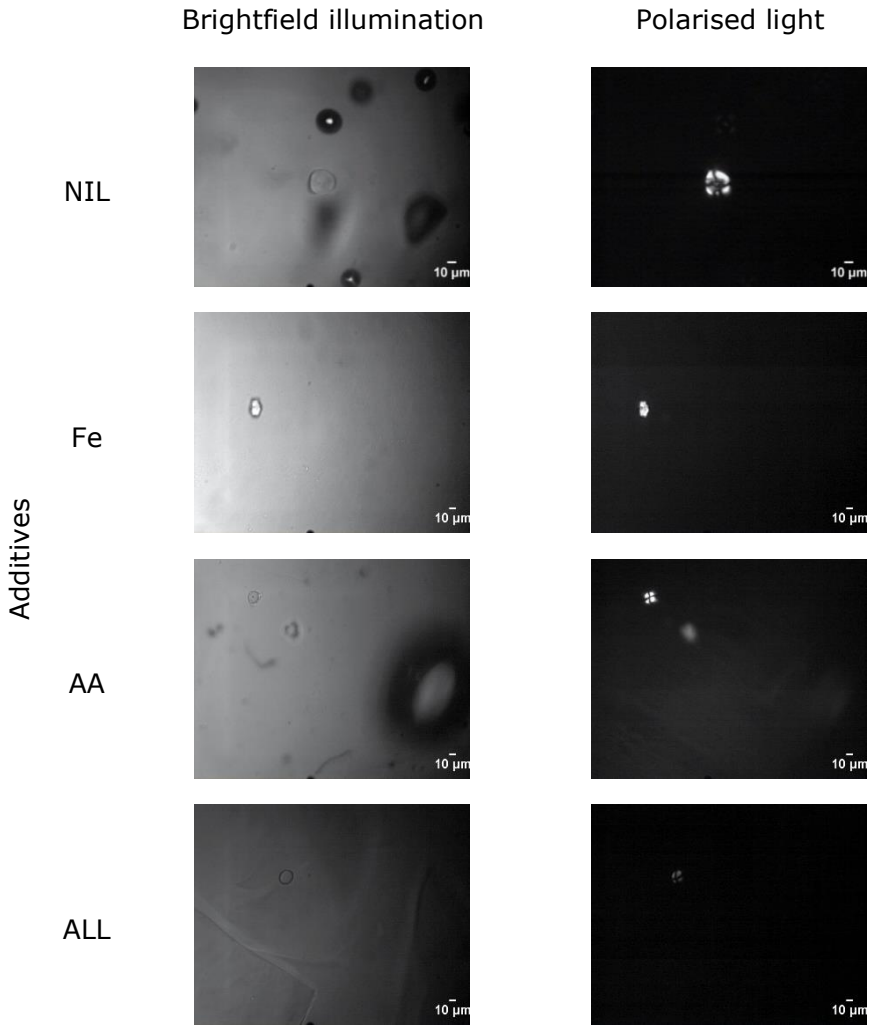

Figure 7.13 Images of sago starch ground extrudates using brightfield illumination and polarised light; produced at 4 mL/min water feed and with different additives (horizontal).

7.4.4.5 Crystallinity

Figure 7.14 shows the crystallinity of the extrudates as assessed by X-ray diffraction (method given in section 3.3.15). The peaks indicative of the native sago starch X-ray diffraction are not apparent in the diffraction patterns acquired on the extrudate samples. The order of the native sago granule order appears to be completely lost when extrusion is carried out in both the absence and presence of additives. The type of additives (iron,

ascorbic acid and both of them) and water feed rate did not affect the X-ray pattern of these extrudates.

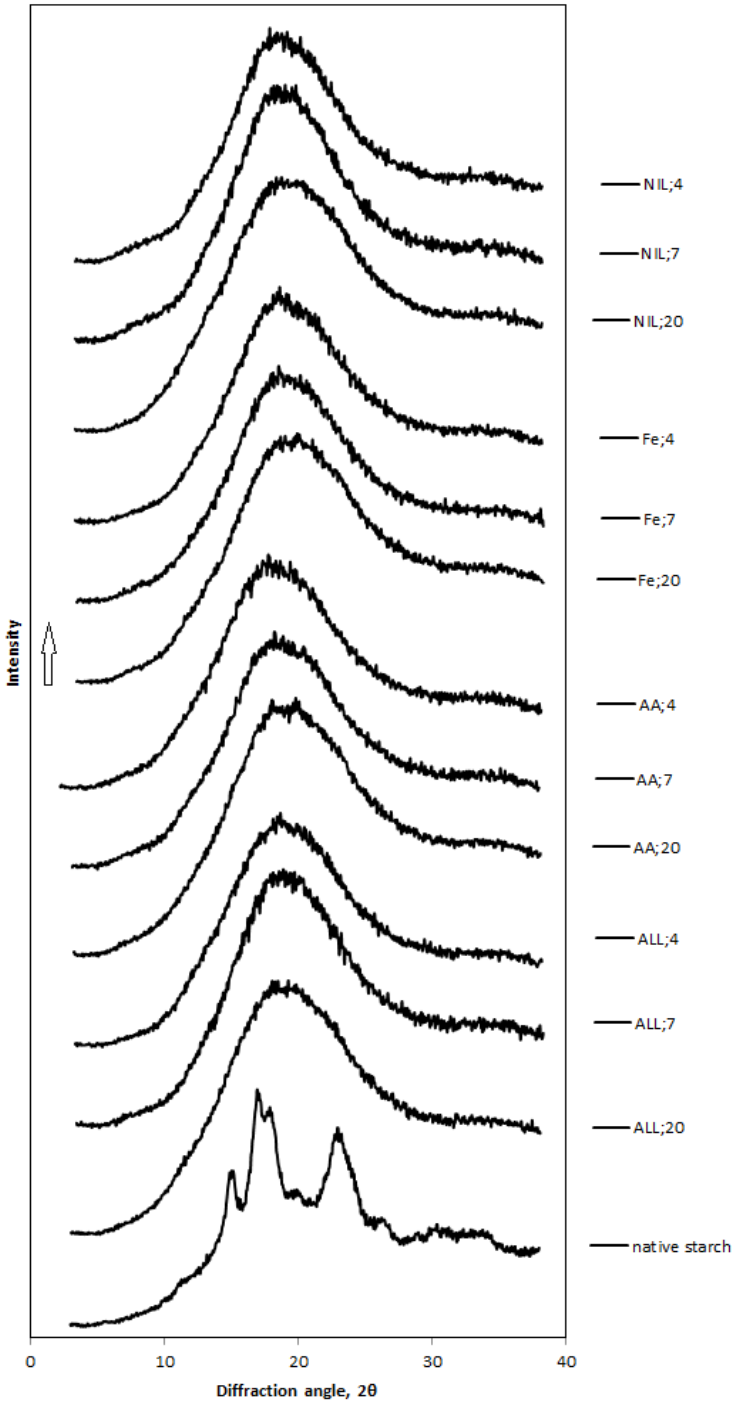

Figure 7.14. Effect of additives and water feed on X-ray diffractogram. Legend shows additives; water feed (mL/min).

7.4.4.6 Discussion of physicochemical material properties of the extrudates

In this research, the addition of iron and ascorbic acid to the extruder feed showed some impacts on the physicochemical properties of the extrudates as indicated by the examination of the ground fortified sago starch extrudates in excess water.

A low WAI and a high WSI may indicate that the starch has undergone extensive conversion. The results obtained for these two parameters after the addition of the additives are illustrated in Figure 7.9 and Figure 7.10. WAI results show significant changes (decrease) due to the addition of all types of additives (Fe, AA and ALL) for extrudates at 4 mL/min water feed. Concerning the addition of iron (Fe) only, the interaction of the iron when in its oxidised form, ferric state, with the starch could result in some iron-starch complexing, which possibly could explain the WAI and WSI values found for the iron-fortified extrudates. This is supported by the work of Mehansho (2006) on the two iron forms that are commonly used in food fortification. These are ferrous (Fe^{2+}) and ferric (Fe^{3+}) and they readily form complexes with electron-rich components. However, the WAI and WSI results for the extrudates with iron (Fe) only particularly that processed 7 and 20 mL/min water feed do not seem to play a major role on impacting on starch conversion.

With regard to ascorbic acid addition, decreased WAI for extrudates at 4 mL/min water feed could be because ascorbic acid encourages the loss of order and the molecular breakdown of the starch (Sriburi and Hill, 2000). However, the results for the extrudates produced at 7 and 20 mL/min water feed disagree with the previous statement for ascorbic acid (AA)

addition since at these two water feed rates the WAI increased and WSI decreased therefore probably indicated the low loss of order thus molecular breakdown. Meanwhile, the addition of both iron and ascorbic acid (ALL) seemed to generally not affect WAI and WSI with the exception of WAI decreasing for the extrudate processed at 4 mL/min and WSI decreasing for the extrudate processed at 20 mL/min.

Pasting properties are used to estimate the functional properties of starch-based products, as they affect their texture and digestibility (Maziya-Dixon et al., 2007; Ajanaku et al., 2012). From Figure 7.11 and Table 7.2 a marked change in the pasting properties of extrudates without additives over the addition of iron and ascorbic acid is observed. Clearly, the addition of all types of additives significantly affected the cold peak viscosity and final viscosity of the pasting properties of the extrudates. For extrudates produced at water feed rates of 4 and 7 mL/min, the extrudates with additives showed significant higher cold peak and final viscosity values than the extrudates without additives.

A higher cold peak viscosity is an indication of an enhanced level of gelatinisation in the extruded products (Singh et al., 2009). As stated before, iron-starch complexing is possibly the reason behind this and could explain the higher cold peak value and higher degree of gelatinisation in iron-fortified extrudates. Meanwhile, regarding the ascorbic acid addition, these results could be explained by the concept that during the extrusion, ascorbic acid has affected the starch polymer so that depolymerization of the starch macromolecules has occurred (Sriburi and Hill, 2000). However, the addition of additives to extrudates produced at 20 mL/min water feed did not affect either cold peak or final viscosity probably due to a higher

rate of water feed in the extruder giving no expansion and no change in functional properties as observed for the other extrudates.

Observation of starch granules of ground extrudates using microscopy (birefringence) and X-ray diffraction showed that extrusion cooking alters the starch from the native structure. The addition of iron (Fe), ascorbic acid (AA) and both of them did not show significant differences of the starch granules.

7.5 Conclusions

Iron-fortified extrudates from sago starch have been produced with and without ascorbic acid addition. The concept of acidification as a process capable of reducing discolorations due to iron fortification could design products with improved iron nutritional value. Physical properties of the extrudates showed that the presence of additives when extruding at low water feed rate (4 mL/min in this study) created lighter colour, greater expansion, and lower hardness of the extrudates compared to that of higher water feed rates. The physicochemical properties of the ground extrudates were mainly affected by the water feed rate where the lower the water feed the higher the starch conversion. Additionally, the incorporation of ascorbic acid affected the properties of the extrudates at the lower water feed rates.

Of great interest was the appearance of the extrudates with both iron and ascorbic acid inclusion. The products not only appeared lighter in colour in the presence of the ascorbic acid but also showed greater expansion. This feature could be of major importance in the formation of iron-fortified sago starch. Moreover, it is anticipated that optimisation of the preparation methods and extrusion conditions will further improve the quality of the extrudates and should be studied in the future since such fortified products can be helpful in fighting anaemia, especially in Indonesia.

CHAPTER 8
General Conclusions and Further Work

This PhD research aimed to generate the fundamental understanding of extrusion processing of sago starch with a goal to produce an iron-fortified snack as a healthy snack for young children. Utilisation of sago starch is in line to address issues of food security in Indonesia, where the government wishes to implement a food diversification policy. The campaign for "*One day without rice*" is one example of the drive for decreasing the dependency on rice. This initiative provides an opportunity to boost the use of sago starch as a more widely used food material, which could be encouraged with the production of a processed nutritious food, for example, a snack product. Snacks are consumed extensively by all groups of people around the world and can be used as a means of administering nutritious components of foods to the consumers. Additionally, a snack is a portion of food that is often smaller than a regular meal and is liked by children, a demographic group at a high-risk group of iron deficiency anaemia (IDA). Fortification of sago starch or sago starch based products with iron could be a promising strategy to combat (Iron Deficiency Anaemia) IDA and encourage consumption of a home grown crop, but it will be a challenge because of the lack of widespread consumption of sago starch and it tends to be underutilised in processed foods. Therefore, it is clear that there is an opportunity for developing a beneficial snack from sago starch that could be extruded and puffed and is fortified with iron.

Rice starch and cassava starch are chosen over sago starch as a food ingredient even in countries plentiful in the palm starch and where its utilisation would decrease imports of the cereals and root starch. Cassava starch and rice starch are known to be very different from each other and there are many reasons presented in the literature why these starches could be advantageously used in food manufacture processes that benefit from their differing properties. Sago starch is much less well represented regarding identifying its composition and physicochemical characteristics. While there are many cereals, seed and root or tuber starches, there are few that are commercially available from the pith of palm trees.

Compared to rice and cassava starches, there are fewer number of references on processing sago starch by extrusion cooking. A continuity research in this area had been established (Govindasamy et al., 1995; Govindasamy et al., 1996; Govindasamy et al., 1997a; Govindasamy et al., 1997b; Govindasamy et al., 1997c; Govindasamy et al., 1997d). Furthermore, a study by Ansharullah (1997) focused on the characterisation of sago starch and investigated its modification through extrusion, as well as its possible uses in a food application. The results of the study showed that the modification products obtained from extrusion cooking might be used directly in a food system, and might be suitable to be used as a pre-gelatinised starch. Another study by Alias and Karim (2006) was on extruded corn grits using a single screw extruder with a substitution of 20% rice and 20% sago. Extrudates that contained sago starch showed a better quality extruded snack in terms of expansion ratio, bulk density, cutting-force and colour as compared to 100% corn extruded snack, but was not as good as extruded snack made by 80% corn + 20% rice. From personal communication with people in the sago starch factory in Riau, Indonesia, there is information that they had been trying to

extrude sago starch, but were not successful due to the stickiness of the material.

Based on the study of literature and information gained, there is a real driver to understand the sago starch and to use this understanding to optimise the extruding conditions to allow the material to function as a fortified snack product.

8.1 Sago starch

As stated there is less information about sago starch as compared with many other starch sources therefore to look at the sago starch in more detail was an important step. The sago starch used throughout the work reported in this thesis is a commercial starch coming from the factory in Riau, Indonesia, the third biggest sago palm area in Indonesia (Flach, 1997). This means that the starch used is indicative of the commercial samples that would be available in Indonesia for full production of a commercial product. However, this sample of sago may not be representative of other sago starches from other locations or extraction methods.

The sago starch in this study was compared with two other starches that are typically used for application in thermomechanical extrusion. Regarding the chemical properties, sago starch has a low level of protein, lipid, ash, and phosphorous. Rice, like any cereal starch, has lipid associated with the starch granule and this impacts on the starch behaviour particularly because of interactions between the amylose and

lipid to form complexes (Leach, 1967). Cassava starch contains much smaller quantities of lipids so that the effect is not so pronounced and therefore does not form amylose lipid complexes unless lipid is added to the starch (Moorthy, 2002). The sago does appear to be more like cassava than rice in this aspect. Figure 4.6 shows the DSC of the sago starch and no lipid amylose complexation is seen. This may well be relevant in the extrusion process as there was rhetorical evidence that extruded samples were "sticky" and this is often rectified by the addition of monoglycerides to the product to bind the "sticky" amylose into amylose-lipid complexes (Hoover and Hadziyev, 1981). As the sago does not contain naturally occurring lipids, addition of monoglycerides may be a way of rectifying the problems.

The levels of phosphorous within the starch could also be relevant to the performance of the sago. The amylopectin of potato starches are phosphorylated and this gives them specific swelling properties in different ionic environments (Leach, 1967). Cassava starch a root tuber, rather than the stem tuber of potato and the phosphorous content is much less than that of potato starch (Moorthy, 2002). There was no evidence that sago starch was composed of a charged polymer. This is relevant for the impact of adding the iron fortification to the starches.

Another aspect of the composition of the sago starch worthy of consideration if it is to be used as a raw material in a manufactured extrusion product is the amylose levels. The straight chained macromolecules are thought to align in the extruder and give rise to a denser packed melt. The amylopectin is more likely to depolymerise in the extruder and thus increase the levels of small molecular weight substances that may act as plasticisers for the melt (Lai and Kokini, 1991). So a

product with higher levels of amylose and lower amylopectin may be relevant to the performance of the starch. There is always a question on the correct procedures for the measurement of amylose amylopectin ratios. In this work, the method of measurement was based on the precipitation of the amylopectin with Concanavalin A (Megazyme kit). The method requires solubilisation of the starch, and it is known that this can be difficult. However, the other two starches were assessed by the same procedure and the sago had the highest amylose levels at 33% (dwb).

The packing order for the amylopectin within the native granule may be relevant for the melting characteristics and also the way in which the granules swell on heating. The literature suggests that sago starches may show C-type crystallinity, a mixture of the A and B forms (Ahmad et al., 1999; Karim et al., 2008b; Adawiyah et al., 2013). This has been reported for cassava starches in the past (Gorinstein and Lii, 1992), although it is generally recognised that today commercial cassava starches are A-types, with no B crystals detectable (Defloor et al., 1998). Using the screening methods applied in this work the sago starch appeared to be A-type, the monoclinic form of crystal packing that had lower water molecules associated with the crystal than the B-type crystals. Further studies could have been carried out to see if any B-type crystals could be detected, for example better X-ray data or using solid-state NMR (Buléon et al., 1998).

The peak temperature (T_p) for the melting of sago starch was 76 °C (starch and water ratio 1:3), higher than for the other two comparative starches used, although the range of temperature between T_o and T_e was no higher than the other starches (Table 4.6). The polarised light pictures for the sago starch is shown in Figure 8.1a and clearly shows the Maltese cross pattern throughout the granule and this is rather different than when

looking at a legume starch for example pea starch (Figure 8.1b), where the packing of the crystals and therefore the birefringence reflects the mixed crystals (Wang et al., 1998). The conclusion for the commercial sago starch used in this work does seem to represent a crystalline packing order dominated by A-type.

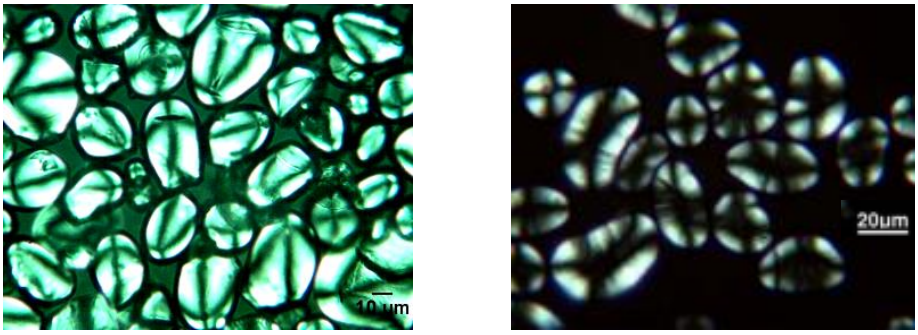

(a) (b)

Figure 8.1 Micrographs acquired under polarised light; (a) native sago starch (from this study); and (b) native pea starch (Chung et al., 2009). Scale bars indicated in the each micrograph.

The granule sizes of the commercial sago starch are large (32 µm) and showed a monomodal distribution. If the starches had different forms of amylopectin packing then it could be expected that the granule swelling may be different as one crystal format may melt before the other. Even though sago starch had a bigger size of granules than cassava starch, its swelling power was slightly lower. This lower extent for swelling and hydrating when heating in excess water compared to cassava may be a factor relating to the amylose level. Sago and cassava starch were similar in their pasting profiles (excess water + sheared). The viscosity values for the sago starch were less than those measured for the cassava starch, demonstrating the lower swelling values. The end viscosity for the sago starch was also low and this, along with the DSC high T_p value for sago may well indicate that sago starch is a robust starch, despite the lack of

lipids to reinforce the granules. The high enthalpies recorded in the DSC measures for sago starch are commonly associated with material like potato starch and this is thought to be due to the extra-long A chains of the amylopectin (Buléon et al., 1998). No work on comparative chain length of the amylopectin was carried out in this work. Sago starch does have different properties compared with rice and cassava starches, in many ways it looks more like a potato tuber starch, but it is not phosphorylated.

The sago starch chosen for the work did not conform in all aspects to previously reported information for this starch source. It is different from the two starch sources commonly used in Indonesia for the manufacture of snack foods, but there is nothing in its behaviour, as assessed from chemical composition and behaviour in excess water systems that would seem to exclude it from use in a thermomechanically manufactured snack product.

8.2 Processing

Figure 8.2 shows a generic graph that represents the state diagram for starches in water. The terms *gelatinisation* on this graph is used to denote the start of the melting endotherm (T_o) in DSC heating and the term *melting* marks at the end (T_e). The measured T_p of the sago starch was 76 °C when measured at three times as much water as starch. The T_o and T_e values were 70 and 87 °C and these should correspond to a Y_w value in Figure 8.2 of 0.75. It is worth noting that sago starch had higher requirements for temperature to melt than many starches and therefore

would be at the upper edge of such a generic prediction of behaviour as shown in Figure 8.2.

Extrusion of breakfast cereals and snacks is usually conducted at moisture contents ranging from 12% to 16% wet basis (Lai and Kokini, 1991). In the extruder the high water levels would reduce viscosity, make the product at the end of die not expand and would require major drying facilities to turn the extrudate into a stable product. Therefore water contents typically used are <20% and as a consequence of the low water levels it would be predicted that there would be a concomitant increase in the melting temperatures of the crystalline regions of the starches.

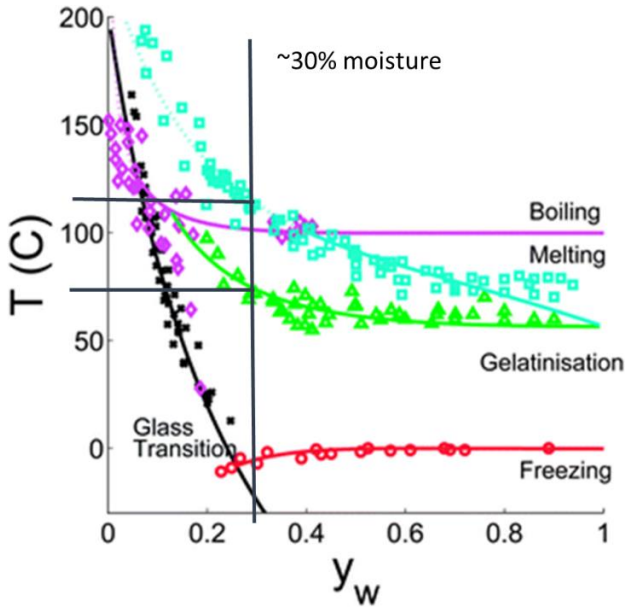

Figure 8.2 State diagram of starch, with some experimental data, where y_w is mass fraction of water (Van der Sman and Meinders, 2011). Black lines added to denote behaviour at 30% moisture have been added to indicate start of order loss occurring at ~70 °C and final loss of crystallinity occurring in excess 100 °C.

Doughs of approximately 67% sago starch and 33% water (i.e. y_w of 0.33) were investigated by a capillary rheometer. At this water content it could

be predicted that temperatures of 70 °C would plasticise the starch, but the amount of melting of the crystalline region would be very low. Even at the higher water content of 75% the amount of order loss at 70 °C was predicted to be <10% (Figure 5.5). Yet samples processed at this temperature showed order loss in the region of 45-57%, about 4-5 times much higher than predicted from the DSC endotherms or the theoretical state diagrams. When the temperatures of processing in the capillary were higher (100 °C) for these low moisture samples the loss of order was less than predicted from high moisture samples in the DSC, but the state diagram implies that full melting at these lower moisture contents should not have occurred because the elevated melting temperatures.

All the sago starch samples formed a stable extrudate from the capillary rheometer, but the string of material formed from the capillary die was opaque, rather than the glassy material that may have been expected if all the starch had lost its ordered matrix. This may imply that the some starch order was lost, but not all. This was backed up by the DSC data. The non- and iron-fortified samples showed a shear thinning behaviour in the capillary rheometer which could be fitted to the power law as the other starchy products starch (Vergnes and Villemaire, 1987; Valle et al., 1995; Singh and Smith, 1999; Sandoval and Barreiro, 2007). The consistency coefficient decreased and the flow behaviour index increased for the shear viscosity of the samples at increasing temperatures. The higher than expected loss of order when processing may be due to the vulnerability of the plasticised granules to shear forces, rather than the temperatures being applied. This may be relevant for the extrusion processes where the shear forces will be much greater than those experienced within the capillary rheometer.

Data derived from the samples in the capillary rheometer certainly implies that greater temperature and forces should be applied to the sago starch if all order is to be lost from the system and for the extrudates to expand when leaving the die. As a consequence of the capillary data, the twin-screw extruder was set up to have a major impact on the starch.

Figure 8.3 shows an enlarged picture of one of the pair of screws used to manufacture the sago extrudate. This image is of the last quarter of the length of the screws and the main shear is created only in this portion, the rest of the screw just conveys the materials.

Figure 8.3 Portion of the screw before the die of the extruder used for the study of sago starch; (1) mixing and conveying, (2) kneading, (3) metering.

The thermomechanical extruder used in the current work (see Figure 2.12) was an experimental machine with a long barrel compared to its diameter; the length to diameter ratio was 40:1. This is not typical of commercial extruders and therefore the screw configuration was adjusted so that the key shearing elements were just in front of the die and therefore the extruder conditions could be replicated in a shorter barrelled machine which would be typically used to manufacture a directly expanded snack product. The die fitted to the extruder was a simple pin hole design,

although more sophisticated designs could be used if other shaped products were required. Using this set up the sago starch could be extruded to make an expanded product.

Throughout the work, the feed rate of the sago was maintained at 8 kg/h, which is towards the upper end of the rates used for this equipment. High processing rates are one of the factors required for commercial operations of the extruder and therefore this higher rate is beneficial, although it should be noted that maize grits will run at even higher volumes, up to 10 kg/h (Singh et al., 1998). The screw speed was varied between 200 and 400 rpm. The temperatures were set along the barrel at 30 to 120 °C and the die temperature altered between 120 and 160 °C. However, the factor that caused the greatest impact on the extrudates was the amount of added moisture to the barrel of the extruder. The water was feed into the barrel using a peristaltic pump set at different rates. Moisture was also presents as part of the sago starch, which had a moisture content of 14% (wwb). The total amount of moisture in the barrel of the extruder to form the melt therefore varied between 16.5 and 25% (wwb). This corresponds to y_w values on the state diagram Figure 8.2 of 0.16 and 0.24. At these moisture contents and duration of heating little starch conversion should have occurred, but analyses of the extrudates showed that little crystallinity remained in any of the processed samples. The starches were more converted than those processed within the capillary rheometer, despite the processing times being much shorter.

Within the extruder the shear energy is calculated as the specific mechanical energy (SME) (see Equation (6.1), section 6.3.2.1). The impact of the SME on the starch conversion measures of starches is well documented, for example Figure 8.4 shows, using solubility as a marker

for starch breakdown, that increased temperature and SME cause more breakdown.

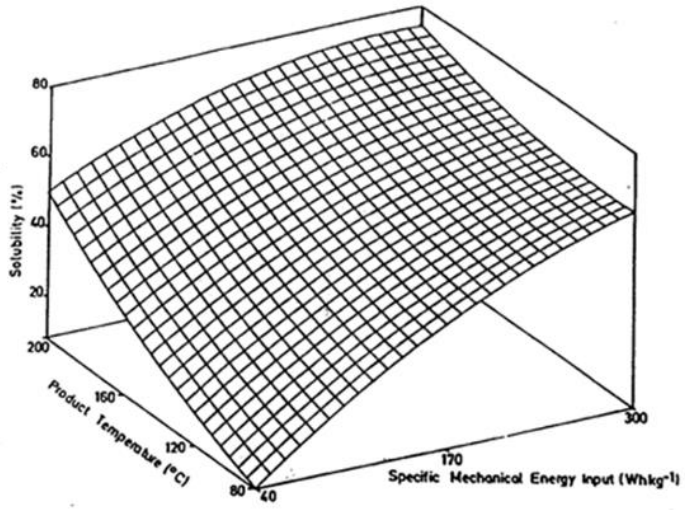

Figure 8.4 Relationship between SME, solubility and product temperature for extruded wheat starch (Meuser et al., 1987).

To create a suitable snack, the sago starch would need to form a puffed product. At the lower water contents, the products were puffing to achieve bulk densities in the region of between 0.15 and 0.2 g/cm^3. This is in the region were the product had the expected bite and crispness associated with a directly expanded snack product. What was not anticipated was the high SME values required to achieve this level of expansion. The calculated values for the energy inputs were 400-500 Wh/kg. The measure for starch conversion, as in the solubility, cold water uptake measures and RVA profiles do not indicate that there has been major depolymerisation of the starch. Too great a loss of molecular weight in the starch can result in high levels of small sugars and these will act as plasticisers therefore although the starch matrix may expand well as it emerges from the die it can shrink again. This is because the loss of water occurring is not sufficient to bring the starch matrix from its rubbery state to the glass where it can retain its

bubble structure once the internal pressures inside the bubble (the water vapour) is lost.

It had been reported that stickiness was a problem in sago starch extrusion, the samples made during the current work would not be described as being too sticky. Once expanded the loss of moisture was significant and the products had a light texture. The extrudates had a moisture content of ~8% after they had flashed off their moisture on emerging from the extruder. This should be reduced if the products are to retain a suitable shelf life. From the studies on changing the processing parameters recommendations for the successful extrusion of sago starch to create a puffed snack could be made.

8.3 Fortification

A major goal for the work was to establish if fortification of the sago starch was possible. About 40% of the world's population (i.e. more than 2 billion individuals) are thought to suffer from anaemia, i.e. low blood haemoglobin. Fortified foods often fail to reach the poorest segments of the general population due to their low purchasing power and an underdeveloped distribution channel. The use the indigenous sago starch to form a simple expanded snack product could address some of the issues of low iron intake in children and women in Indonesia. Poor absorption of iron can occur if the carrier material used in the manufacture of fortified foods is not carefully chosen, for example, if phytates are present and these occur in other potential base materials for extruded products, such as legumes or cereals. Raw materials with a high level of

phenolic compounds (for example present in sorghum and millet) also reduce iron uptake (Hurrell, 2002). Sago starch, as extracted from the sago palm, is low in these materials and therefore should make a useful carrier for the micronutrients.

Due to the low levels of protein and lipid in the sago starch it was thought possible that this starch may be particularly vulnerable to redox depolymerisation, as demonstrated for cassava starch (Sriburi and Hill, 2000). The colouration due to the iron could also be a problem. In the capillary rheometer samples the extrudates containing iron were dark in colour.

Inclusion of iron at a level of 800 ppm did not seem to have a major effect on the extrusion. The samples with the higher expansion levels were still light in colour and expanded to give the same bulk densities as the non-fortified samples. Fortification of iron, as ferrous sulphate, at the concentration of 80 mg in 100 g sago starch and ascorbic acid (ratio 1:6) appeared to even enhance the physical properties in terms of colour and expansion.

From this study it can therefore be concluded that expanded snacks could be made from sago starch by a twin-screw extruder using the following processing parameters; feed rate of 8 kg sago starch/h, screw speed of 300 rpm, die temperature at 140 °C, and water feed rates at 4 mL/min (equivalent to 16.5% moisture, wwb). This product can be fortified with iron and ascorbic acid. These processing conditions produces an expanded product with a crisp texture.

8.4 Achievement of project targets

Figure 8.5 suggests the barriers that may need to be overcome when proposing a fortified food. As this research shows some of these technical barriers have been evaluated and can be overcome. The need for iron fortification for much of the population of Indonesia has been established and the need has been recognised at a local and national level. This is evidenced by the scholarship, which was awarded to study sago starch and iron fortification that allowed the work programme described in this thesis to be carried out.

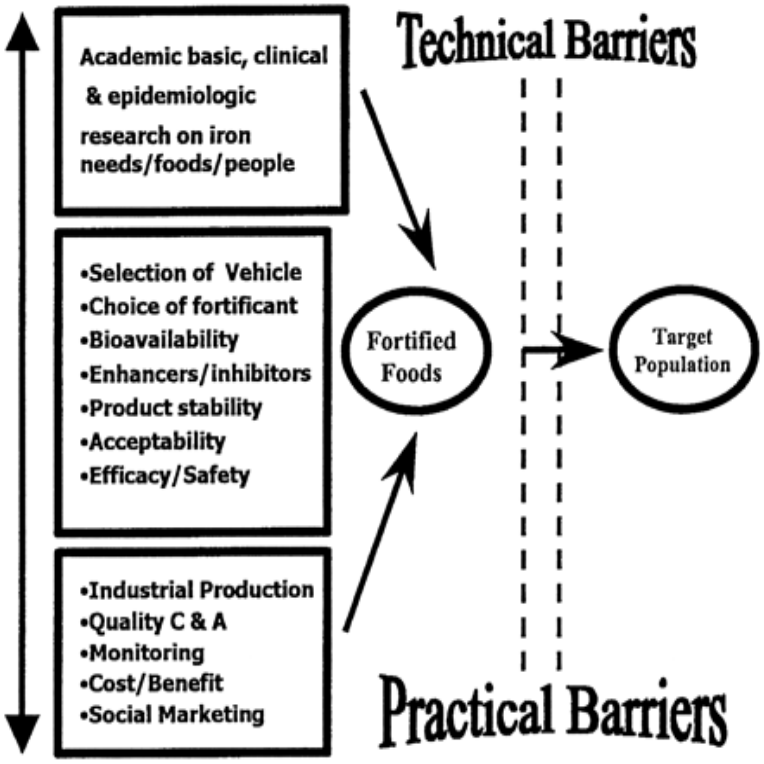

Figure 8.5 Technical barriers are impediments that need to be considered in the design, formulation, production and evaluation of fortified foods (Uauy et al., 2002).

The vehicle to act as a carrier for the fortification was the chief area of study in this research, to fit in with the needs of target population and for commercial and national support, sago was chosen as the material to be fortified. The work demonstrates that this could be an excellent choice. The ability of the material to form a directly expanded product allows efficient manufacture and an easy eat for the population. The fortification materials used are those recommended for iron deficiency and the use of ascorbic acid is also from the recommendation for micronutrients associated with iron fortification of foods.

8.5 Further Work: Product efficacy, stability and consumer acceptance

An area not covered in this project was the bioavailability of the iron and the iron and ascorbates status as active components. Post-extrusion the sago starch rapidly picked up cold water and had a high water solubility index it would, therefore, be expected that it would be easily digested. The low levels of non-starch carbohydrates would suggest that little binding of the iron would occur to reduce the availability of iron. This is an area that would need testing in further work if the project was taken forward as a fortified commercial product.

Except from general observation no stability testing of the products has been carried out. The low/no oil levels should mean that lipid oxidation would not be a problem in the product. Control of moisture contents are likely to be important so that the extrudates retain their crispy texture.

Another major area not addressed in the current project was the acceptability and liking of the product. This would need to be evaluated with the target population. Often extruded snacks are flavour enhanced and this may encourage more uptake. The calculations of the energy intakes and levels of fortification may also need some thought.

The other key area noted by Uauy et al. (2002) was the importance industrial production and the cost of the products. Of relevance for the work carried out and reported in this thesis is that the sago starch was supplied by a commercial company who have an interest in promoting the starch and has processing facilities to make the expanded snack. Data on the processing, especially the SME values are directly transferable to their processing procedures and they are already keen to try and manufacture the expanded product. If the commercial company can produce the expanded products then the local drivers of use of sago starch and the inclusion of iron will help with the marketing of the product and produce support for its widespread use in targeted locations and populations. Quality parameters used to evaluate the raw sago starches and the extrudates developed and then reported in this thesis can be used for quality control and assurance. In addition tests for the levels of fortification need to be used.

Another area that does require further work is directly related to the sago starch source as an additional screening of sago from different locations is required. The polymorphism and stability of the sago starch were not expected from the published literature. Whether this was due to the precise sago starch used or whether all Indonesian sago starch conforms to this pattern needs to be established if this resource is going to be made more widely available for use in food production using high shear regimes.

REFERENCES

ABD-AZIZ, S. 2002. Sago starch and its utilisation. *Journal of Bioscience and Bioengineering,* 94**,** 526-529.

ABDORREZA, M. N., ROBAL, M., CHENG, L. H., TAJUL, A. Y. & KARIM, A. A. 2012. Physicochemical, thermal, and rheological properties of acid-hydrolyzed sago (Metroxylon sagu) starch. *LWT - Food Science and Technology,* 46**,** 135-141.

ABDULLAH, M. Z., EAN, Y. P., SHARIZA, A. R., MANAN, D. M. A., MUTALIB, M. J., KARIM, A. A. & MOHD AZEMI, B. M. N. 2002. Quality improvement of sago (Metroxylon sagu) starch processing. *In:* KAINUMA, K., OKAZAKI, M., TOYODA, Y. & CECIL, J. E. (eds.) *Proceedings of the International Symposium on Sago (Sago 2001).* Tokyo, Japan: Universal Academy Press Inc.

ABSON, R., GADDIPATI, S. R., HORT, J., MITCHELL, J. R., WOLF, B. & HILL, S. E. 2014. A comparison of the sensory and rheological properties of molecular and particulate forms of xanthan gum. *Food Hydrocolloids,* 35**,** 85-90.

ADAWIYAH, D. R., SASAKI, T. & KOHYAMA, K. 2013. Characterization of arenga starch in comparison with sago starch. *Carbohydrate Polymers,* 92**,** 2306-2313.

AHMAD, F. B. & WILLIAMS, P. A. 1998. Rheological properties of sago starch. *Journal of agricultural and food chemistry,* 46**,** 4060-4065.

AHMAD, F. B., WILLIAMS, P. A., DOUBLIER, J.-L., DURAND, S. & BULEON, A. 1999. Physico-chemical characterisation of sago starch. *Carbohydrate Polymers,* 38**,** 361-370.

AJANAKU, K., AJANAKU, C., EDOBOR-OSOH, A. & NWINYI, O. C. 2012. Nutritive Value of Sorghum Ogi Fortified with Groundnut Seed (Arachis) hypogaea. *Nutritive Value of Sorghum Ogi Fortified with Groundnut Seed (Arachis) hypogaea,* 7**,** 82-88.

AKDOGAN, H. 1999. High moisture food extrusion. *International Journal of Food Science & Technology,* 34**,** 195-207.

ALIAS, P. & KARIM, M. D. A. 2006. Perkembangan Hasilan Makanan Melalui Teknologi Ekstrusi. Penang, Malaysia: Universiti Sains Malaysia.

ALTAN, A., MCCARTHY, K. L. & MASKAN, M. 2008. Evaluation of snack foods from barley–tomato pomace blends by extrusion processing. *Journal of Food Engineering,* 84**,** 231-242.

ALTAN, A., MCCARTHY, K. L. & MASKAN, M. 2009. Effect of Extrusion Cooking on Functional Properties and in vitro Starch Digestibility of Barley-Based Extrudates from Fruit and Vegetable By-Products. *Journal of Food Science,* 74**,** E77-E86.

ALVAREZ-MARTINEZ, L., KONDURY, K. P. & HARPER, J. M. 1988. A General Model for Expansion of Extruded Products. *Journal of Food Science,* 53**,** 609-615.

ANDERSON, R., CONWAY, H. & PEPLINSKI, A. 1970. Gelatinization of corn grits by roll cooking, extrusion cooking and steaming. *Starch-Stärke,* 22**,** 130-135.

ANDERSON, R., CONWAY, H., PFEIFER, V. & GRIFFIN, E. 1969. Gelatinization of corn grits by roll-and extrusion-cooking. *Cereal Science Today,* 14**,** 4-12.

ANSHARULLAH 1997. *Characterisation and Extrusion of Metroxylon Sago Starch: Thesis Submitted for the Degree of Doctor of Philosophy in the School of Food Sciences, University of Western Sydney, Hawkesbury, Richmond NSW, Australia*, School of Food Sciences, University of Western Sydney, Hawkesbury.

ANTON, A. A., FULCHER, R. G. & ARNTFIELD, S. D. 2009. Physical and nutritional impact of fortification of corn starch-based extruded snacks with common bean (Phaseolus vulgaris L.) flour: Effects of bean addition and extrusion cooking. *Food Chemistry,* 113**,** 989-996.

ASAOKA, M., BLANSHARD, J. & RICKARD, J. 1991. Seasonal effects on the physico-chemical properties of starch from four cultivars of cassava. *Starch-Stärke,* 43**,** 455-459.

ASHOGBON, A. & AKINTAYO, E. 2012. Morphological, functional and pasting properties of starches separated from rice cultivars grown in Nigeria. *International Food Research Journal,* 19**,** 665-671.
AYOUB, A., LIU, Y., MILLER, D. D. & RIZVI, S. S. 2013. The effect of low shear on the development of fortified extruded rice products. *Starch-Stärke,* 65**,** 517-526.
BADRIE, N. & MELLOWES, W. A. 1991. Effect of Extrusion Variables on Cassava Extrudates. *Journal of Food Science,* 56**,** 1334-1337.
BAO, J. & BERGMAN, C. J. 2004. The functionality of rice starch. *In:* ELIASSON, A.-C. (ed.) *Starch in food: Structure, function and applications.* Boca Raton, Fl: Woodhead Publishing Ltd. and CRC Press LLC.
BHATTACHARYA, M., AND & PADMANHABHAN, M. 1992. On-line rheologicalmeasurements of food dough during extrusion cooking. *In:* KOKINI, J. L., HO, C.-T. & KARWE, M. V. (eds.) *Food Extrusion Science and Technology.* New York, N.Y: Marcel Dekker Inc.
BHATTACHARYA, M. & HANNA, M. A. 1987. Kinetics of Starch Gelatinization During Extrusion Cooking. *Journal of Food Science,* 52**,** 764-766.
BHATTACHARYA, M., SEETHAMRAJU, K. & PADMANABHAN, M. 1994. Entrance pressure drop studies of corn meal dough during extrusion cooking. *Polymer Engineering & Science,* 34**,** 1187-1195.
BORENSTEIN, B. 1987. The role of ascorbic acid in foods. *Food Technology,* 41**,** 98-99.
BRADBURY, J. H. & HOLLOWAY, W. D. 1988. *Chemistry of tropical root crops: significance for nutrition and agriculture in the Pacific,* Canberra, Australian Centre for International Agricultural Research.
BRADLEY, R. L. 2003. Moisture and Total Solids Analysis. *In:* NIELSEN, S. S. (ed.) *Food Analysis.* Third edition ed. New York: Kluwer Academic/Plenum Publishers.
BRENNAN, C., BRENNAN, M., DERBYSHIRE, E. & TIWARI, B. K. 2011. Effects of extrusion on the polyphenols, vitamins and antioxidant activity of foods. *Trends in Food Science & Technology,* 22**,** 570-575.
BRENNAN, M. A., DERBYSHIRE, E., TIWARI, B. K. & BRENNAN, C. S. 2013. Ready-to-eat snack products: the role of extrusion technology in developing consumer acceptable and nutritious snacks. *International Journal of Food Science & Technology,* 48**,** 893-902.
BUCHER, S. 1998. Chemical and physicochemical characterization of commercial breakfast cereals. *Cereal foods world,* 43.
BULÉON, A., COLONNA, P., PLANCHOT, V. & BALL, S. 1998. Starch granules: structure and biosynthesis. *International journal of biological macromolecules,* 23**,** 85-112.
CAMIRE, M. E., CAMIRE, A. & KRUMHAR, K. 1990. Chemical and nutritional changes in foods during extrusion. *Critical Reviews in Food Science & Nutrition,* 29**,** 35-57.
CHABOT, J. F. & HOOD, L. F. 1976. Interaction of Iron Compounds and Starch Granules. *Starch - Stärke,* 28**,** 264-267.
CHAKRABORTY, S. K., SINGH, D. S., KUMBHAR, B. K. & CHAKRABORTY, S. 2011. Millet–legume blended extrudates characteristics and process optimization using RSM. *Food and Bioproducts Processing,* 89**,** 492-499.
CHAMPAGNE, E. T. 1996. Rice starch composition and characteristics. *Cereal Foods World,* 41 833-838.
CHEN, Z. 2003. *Physicochemical properties of sweet potato starches and their application in noodle products*, Wageningen Universiteit.
CHINNASWAMY, R. & HANNA, M. 1988a. Expansion, Color and Shear Strength Properties of Com Starches Extrusion-Cooked with Urea and Salts. *Starch-Stärke,* 40**,** 186-190.
CHINNASWAMY, R. & HANNA, M. 1988b. Relationship between amylose content and extrusion-expansion properties of com starches. *Cereal Chem,* 65**,** 138-147.
CHIU, H.-W., PENG, J.-C., TSAI, S.-J., TSAY, J.-R. & LUI, W.-B. 2013. Process optimization by response surface methodology and characteristics investigation of corn extrudate fortified with yam (Dioscorea alata L.). *Food and Bioprocess Technology,* 6**,** 1494-1504.

CHUNG, H.-J., LIU, Q. & HOOVER, R. 2009. Impact of annealing and heat-moisture treatment on rapidly digestible, slowly digestible and resistant starch levels in native and gelatinized corn, pea and lentil starches. *Carbohydrate Polymers,* 75**,** 436-447.

CLYDESDALE, F. 1998. Color: origin, stability, measurement and quality. *In:* TAUB, I. A. & SINGH, R. P. (eds.) *Food Storage Stability.* Boca Raton: CRC Press LLC.

COCCODRILLI, G. & SHAH, N. 1985. Beverages. *In:* CLYDESDALE, F. M. & WIEMER, K. L. (eds.) *Iron Fortification of Foods.* Orlando, FL: Academic Press, Inc.

COCK, J. H. 1985. *Cassava, New potential for a neglected crop,* Colorado, Westview Press.

COLONNA, P. & MERCIER, C. 1984. Macromolecular structure of wrinkled- and smooth-pea starch components. *Carbohydrate Research,* 126**,** 233-247.

COLONNA, P., TAYEB, J. & MERCIER, C. 1989. Extrusion cooking of starch and starchy products. *In:* C. MERCIER, P. LINKO & HARPER, J. M. (eds.) *Extrusion Cooking.* St Paul, MN, USA: American Association of Cereal Chemists, Inc.

COOK, J. D. & MONSEN, E. R. 1977. Vitamin C, the common cold, and iron absorption. *The American journal of clinical nutrition,* 30**,** 235-241.

COOK, J. D. & REUSSER, M. E. 1983. Iron fortification: an update. *The American journal of clinical nutrition,* 38**,** 648-659.

COOKE, D. & GIDLEY, M. J. 1992. Loss of crystalline and molecular order during starch gelatinisation: origin of the enthalpic transition. *Carbohydrate Research,* 227**,** 103-112.

COPELAND, L., BLAZEK, J., SALMAN, H. & TANG, M. C. 2009. Form and functionality of starch. *Food Hydrocolloids,* 23**,** 1527-1534.

CORBISHLEY, D. A. & MILLER, W. 1984. Tapioca, Arrowroot, and Sago starches: Production. *In:* WHISTLER, R. L., BEMILLER, J. N. & PASCHALL, E. F. (eds.) *Starch, Chemistry and Technology.* 2nd ed. New York: Academic Press. Inc

CROSBIE, G. B. 1991. The relationship between starch swelling properties, paste viscosity and boiled noodle quality in wheat flours. *Journal of Cereal Science,* 13**,** 145-150.

CUI, S. W. 2005. *Food carbohydrates: chemistry, physical properties, and applications*, Taylor & Francis Boca Raton, FL.

DEFLOOR, I., DEHING, I. & DELCOUR, J. 1998. Physico-Chemical Properties of Cassava Starch. *Starch-Stärke,* 50**,** 58-64.

DING, Q.-B., AINSWORTH, P., TUCKER, G. & MARSON, H. 2005. The effect of extrusion conditions on the physicochemical properties and sensory characteristics of rice-based expanded snacks. *Journal of Food Engineering,* 66**,** 283-289.

DIOSADY, L., PATON, D., ROSEN, N., RUBIN, L. & ATHANASSOULIAS, C. 1985. Degradation of wheat starch in a single-screw extruder: mechano-kinetic breakdown of cooked starch. *Journal of Food Science,* 50**,** 1697-1699.

DISLER, P., LYNCH, S., CHARLTON, R., BOTHWELL, T., WALKER, R. & MAYET, F. 1975. Studies on the fortification of cane sugar with iron and ascorbic acid. *British Journal of Nutrition,* 34**,** 141-152.

DJAZULI, M. & BRADBURY, J. H. 1999. Cyanogen content of cassava roots and flour in Indonesia. *Food Chemistry,* 65**,** 523-525.

DONOVAN, J. W. 1979. Phase transitions of the starch–water system. *Biopolymers,* 18**,** 263-275.

DOUBLIER, J., COLONNA, P. & MERCIER, C. 1986. Extrusion cooking and drum drying of wheat starch. II. Rheological characterization of starch pastes. *Cereal Chem,* 63**,** 240-246.

DOUGLAS, F. W., RAINEY, N., WONG, N., EDMONDSON, L. & LACROIX, D. 1981. Color, flavor, and iron bioavailability in iron-fortified chocolate milk. *Journal of Dairy Science,* 64**,** 1785-1793.

DROZDEK, K. D. & FALLER, J. F. 2002. Use of a dual orifice die for on-line extruder measurement of flow behavior index in starchy foods. *Journal of Food Engineering,* 55**,** 79-88.

EERLINGEN, R., JACOBS, H. & DELCOUR, J. 1994. Enzyme-resistant starch. 5. Effect of retrogradation of waxy maize starch on enzyme susceptibility. *Cereal Chemistry,* 71**,** 351-355.

EL-DASH, A. A., GONZALES, R. & CIOL, M. 1983. Response surface methodology in the control of thermoplastic extrusion of starch. *Journal of Food Engineering,* 2**,** 129-152.
ELIASSON, A.-C. & GUDMUNDSSON, M. 2006. *Starch: Physicochemical and Functional Aspects,* Boca Raton, FL, CRC Press.
ESTEVE, M. J., FRÍGOLA, A., MARTORELL, L. & RODRIGO, C. 1999. Kinetics of green asparagus ascorbic acid heated in a high-temperature thermoresistometer. *Zeitschrift für Lebensmitteluntersuchung und-Forschung A,* 208**,** 144-147.
EVANS, I. D. & HAISMAN, D. R. 1982. The Effect of Solutes on the Gelatinization Temperature Range of Potato Starch. *Starch - Stärke,* 34**,** 224-231.
FAN, J., MITCHELL, J. R. & BLANSHARD, J. M. V. 1996. The effect of sugars on the extrusion of maize grits: II. Starch conversion. *International Journal of Food Science & Technology,* 31**,** 67-76.
FAUBION, J., HOSENEY, R. & SEIB, P. 1982. Functionality of grain components in extrusion. *Cereal foods world,* 27**,** 212-&.
FERNANDEZ, A. Q. 1996. *Effects of processing procedures and cultivar on the properties of cassava flour and starch.* PhD, University of Nottingham.
FITCHETT, C. S., AND & FRAZIER, P. J. 1986. Action of oxidants and other improvers. *In:* J. M. V. BLANSHARD, P. J. FRAZIER, A. & GAILLARD, T. (eds.) *Chemistry and physics of baking: Materials,*
processes, and products. London: The Royal Society of Chemistry.
FLACH, M. 1997. *Sago palm: Metroxylon sagu Rottb. Promoting the conservation and use of underutilized and neglected crops. 13,* Italy, International Plant Genetic Resources Institute.
FROST, K., KAMINSKI, D., KIRWAN, G., LASCARIS, E. & SHANKS, R. 2009. Crystallinity and structure of starch using wide angle X-ray scattering. *Carbohydrate Polymers,* 78**,** 543-548.
GABBOTT, P. 2008. A practical introduction to differential scanning calorimetry. *In:* GABBOTT, P. (ed.) *Principles and applications of thermal analysis.* Oxford: Blackwell Publishing Ltd.
GALLIARD, T. & BOWLER, P. 1987. *Morphology and composition of starch,* Chichester, John Wiley & Sons Inc.
GIBSON, T. S., SOLAH, V. A. & MCCLEARY, B. V. 1997. A Procedure to Measure Amylose in Cereal Starches and Flours with Concanavalin A. *Journal of Cereal Science,* 25**,** 111-119.
GILES, H. F., JR., WAGNER, J. R., JR. & MOUNT, E. M., III 2005. Twin Screw Extruder Equipment. *Extrusion: The Definitive Processing Guide and Handbook.* Norwich, NY: William Andrew Publishing/Plastics Design Library.
GORINSTEIN, S. & LII, C. Y. 1992. The effects of enzyme hydrolysis on the properties of potato, cassava and amaranth starches. *Starch-Stärke,* 44**,** 461-466.
GORMAN, J. E. & CLYDESDALE, F. M. 1983. The Behavior and Stability of Iron-Ascorbate Complexes in Solution. *Journal of Food Science,* 48**,** 1217-1220.
GOVINDASAMY, S., CAMPANELLA, O. & OATES, C. 1995. Influence of extrusion variables on subsequent saccharification behaviour of sago starch. *Food Chemistry,* 54**,** 289-296.
GOVINDASAMY, S., CAMPANELLA, O. & OATES, C. 1996. High moisture twin-screw extrusion of sago starch: 1. Influence on granule morphology and structure. *Carbohydrate Polymers,* 30**,** 275-286.
GOVINDASAMY, S., CAMPANELLA, O. & OATES, C. 1997a. Enzymatic hydrolysis and saccharification optimisation of sago starch in a twin-screw extruder. *Journal of Food Engineering,* 32**,** 427-446.
GOVINDASAMY, S., CAMPANELLA, O. & OATES, C. 1997b. Enzymatic hydrolysis of sago starch in a twin-screw extruder. *Journal of Food Engineering,* 32**,** 403-426.
GOVINDASAMY, S., CAMPANELLA, O. & OATES, C. 1997c. High moisture twin screw extrusion of sago starch. II. Saccharification as influenced by thermomechanical history. *Carbohydrate Polymers,* 32**,** 267-274.
GOVINDASAMY, S., CAMPANELLA, O. & OATES, C. 1997d. The single screw extruder as a bioreactor for sago starch hydrolysis. *Food Chemistry,* 60**,** 1-11.

GRACE, M. R. 1977. Cassava Processing. Food and Agriculture Organization of the United Nations.
GRISP 2013. Rice Almanac. 4th ed. Los Baños (Philippines): International Rice Research Institute.
GUJSKA, E. & KHAN, K. 1990. Effect of temperature on properties of extrudates from high starch fractions of navy, pinto and garbanzo beans. *Journal of Food Science,* 55**,** 466-469.
GUPTA, R. K. 2000. *Polymer and Composite Rheology,* New York, Marcel Dekker Inc.
GUY, R. C. E. 1986. Extrusion cooking versus conventional baking. *In:* BLANSHARD, J. M. V., FRAZIER, P. J. & GAILLARD, T. (eds.) *Chemistry and Physics of Baking.* Nottingham: Royal Society of Chemistry.
GYURCSIK, B. & NAGY, L. 2000. Carbohydrates as ligands: coordination equilibria and structure of the metal complexes. *Coordination Chemistry Reviews,* 203**,** 81-149.
HAGENIMANA, A., DING, X. & FANG, T. 2006. Evaluation of rice flour modified by extrusion cooking. *Journal of Cereal Science,* 43**,** 38-46.
HARPER, J. M. 1981. *Extrusion of Foods,* Boca Raton, Florida, CRC-Press.
HARPER, J. M. 1989. Food extruders and their applications. *In:* C.MERCIER, P LINKO & HARPER., J. (eds.) *Extrusion cooking.* St Paul, MN, USA: American Association of Cereal Chemists, Inc.
HOOD, L. & O'SHEA, G. 1977. CALCIUM BINDING BY HYDROXYPROPYL DISTARCH PHOSPHATE AND UNMODIFIED STARCI-IES1.
HOOVER, R. 2001. Composition, molecular structure, and physicochemical properties of tuber and root starches: a review. *Carbohydrate Polymers,* 45**,** 253-267.
HOOVER, R. & HADZIYEV, D. 1981. Characterization of potato starch and its monoglyceride complexes. *Starch-Stärke,* 33**,** 290-300.
HORIBA INSTRUMENTS, I. 2012. A guidebook to particle size analysis. Irvine, CA: Horiba Instruments, Inc.
HUNNELL, J. W., YASUMATSU, K. & MORITAKA, S. 1985. Iron Enrichment of Rice. *In:* CLYDESDALE, F. M. & WIEMER, K. L. (eds.) *Iron Fortification of Foods.* Orlando, FL: Academic Press, Inc.
HURRELL, R. 2002. How to ensure adequate iron absorption from iron-fortified food. *Nutrition reviews,* 60**,** S7.
HURRELL, R. F. 1997. Preventing iron deficiency through food fortification. *Nutrition reviews,* 55**,** 210-222.
HURRELL, R. F., FURNISS, D. E., BURRI, J., WHITTAKER, P., LYNCH, S. R. & COOK, J. D. 1989. Iron fortification of infant cereals: a proposal for the use of ferrous fumarate or ferrous succinate. *The American journal of clinical nutrition,* 49**,** 1274-1282.
HUSSAIN, S. Z., SINGH, B. & NAIK, H. R. 2013. Viscous and thermal behaviour of vitamin A and iron-fortified reconstituted rice. *International Journal of Food Science & Technology*.
ILO, S. & BERGHOFER, E. 1999. Kinetics of colour changes during extrusion cooking of maize grits. *Journal of Food Engineering,* 39**,** 73-80.
ILO, S., TOMSCHIK, U., BERGHOFER, E. & MUNDIGLER, N. 1996. The effect of extrusion operating conditions on the apparent viscosity and the properties of extrudates in twin-screw extrusion cooking of maize grits. *LWT-Food Science and Technology,* 29**,** 593-598.
IPB. 2010. *Welcoming Food Day with Sago* [Online]. Bogor, Indonesia: IPB Bogor. [Accessed 24 September 2015.
ISLAM, M., MOHD, D., MANAN, A., NOOR, B. M. & AZEMI, M. 2001. Effect of temperature and starch concentration on the intrinsic viscosity and critical concentration of sago starch (Metroxylon sagu). *Starch-Stärke,* 53**,** 90-94.
IWE, M. & NGODDY, P. 1998. Proximate composition and some functional properties of extrusion cooked soybean and sweet potato blends. *Plant Foods for Human Nutrition,* 53**,** 121-132.
JANE, J., CHEN, Y., LEE, L., MCPHERSON, A., WONG, K., RADOSAVLJEVIC, M. & KASEMSUWAN, T. 1999. Effects of amylopectin branch chain length and amylose content on the gelatinization and pasting properties of starch 1. *Cereal Chemistry,* 76**,** 629-637.

JULIANO, B. O. 1984. Rice starch: Production, properties and uses. *In:* WHISTLER, R. L., BEMILLER, J. N. & PASCHALL, E. F. (eds.) *Starch, Chemistry and Technology.* 2nd ed. New York: Academic Press. Inc

JULIANO, B. O. 1985. Criteria and tests for rice grain qualities. *In:* JULIANO, B. O. (ed.) *Rice chemistry and technology.* St. Paul, MN: American Association of Cereal Chemists.

KAMAL, S. M. M., MAHMUD, S. N., HUSSAIN, S. A. & AHMADUN, F. R. 2007. Improvement on sago flour processing. *International Journal of Engineering and Technology,* 4**,** 8-14.

KAPANIDIS, A. N. & LEE, T.-C. 1996. Novel method for the production of color-compatible ferrous sulfate-fortified simulated rice through extrusion. *Journal of agricultural and food chemistry,* 44**,** 522-525.

KARIM, A. A., NADIHA, M. Z., CHEN, F. K., PHUAH, Y. P., CHUI, Y. M. & FAZILAH, A. 2008a. Pasting and retrogradation properties of alkali-treated sago (Metroxylon sagu) starch. *Food Hydrocolloids,* 22**,** 1044-1053.

KARIM, A. A., TIE, A. P.-L., MANAN, D. M. A. & ZAIDUL, I. S. M. 2008b. Starch from the Sago (Metroxylon sagu) Palm Tree—Properties, Prospects, and Challenges as a New Industrial Source for Food and Other Uses. *Comprehensive Reviews in Food Science and Food Safety,* 7**,** 215-228.

KENNEDY, G. & BURLINGAME, B. 2003. Analysis of food composition data on rice from a plant genetic resources perspective. *Food Chemistry,* 80**,** 589-596.

KIRBY, C., WHITTLE, C., RIGBY, N., COXON, D. & LAW, B. 1991. Stabilization of ascorbic acid by microencapsulation in liposomes. *International Journal of Food Science & Technology,* 26**,** 437-449.

KISKINI, A., KAPSOKEFALOU, M., YANNIOTIS, S. & MANDALA, I. 2012. Effect of iron fortification on physical and sensory quality of gluten-free bread. *Food and Bioprocess Technology,* 5**,** 385-390.

KOKINI, J. L., CHANG, C. N. & LAI, L. S. 1992. The role of rheological properties on extrudate expansion. *In:* KOKINI, J. L., HO, C.-T. & KARWE, M. V. (eds.) *Food Extrusion Science and Technology.* New York, N.Y: Marcel Dekker Inc.

LAGARRIGUE, S. & ALVAREZ, G. 2001. The rheology of starch dispersions at high temperatures and high shear rates: a review. *Journal of Food Engineering,* 50**,** 189-202.

LAI, L. & KOKINI, J. 1991. Physicochemical changes and rheological properties of starch during extrusion.(a review). *Biotechnology Progress,* 7**,** 251-266.

LAUNAY, B. & LISCH, J. 1983. Twin-screw extrusion cooking of starches: flow behaviour of starch pastes, expansion and mechanical properties of extrudates. *Journal of Food Engineering,* 2**,** 259-280.

LEACH, H. W. 1967. Gelatinization of starch. *In:* WHISTLER, R. L. & PASCHALL, E. F. (eds.) *Starch: Chemistry and Technology.* New York: Academic Press.

LEACH, H. W., MCCOWEN, L. & SCHOCH, T. J. 1959. Structure of the starch granule. I. Swelling and solubility patterns of various starches. *Cereal Chem,* 36**,** 534-544.

LEONEL, M., FREITAS, T. S. D. & MISCHAN, M. M. 2009. Physical characteristics of extruded cassava starch. *Scientia Agricola,* 66**,** 486-493.

LI, J.-Y. & YEH, A.-I. 2001. Relationships between thermal, rheological characteristics and swelling power for various starches. *Journal of Food Engineering,* 50**,** 141-148.

LI, P., CAMPANELLA, O. & HARDACRE, A. 2004. Using an in-line slit-die viscometer to study the effects of extrusion parameters on corn melt rheology. *Cereal Chemistry,* 81**,** 70-76.

LII, C.-Y., SHAO, Y.-Y. & TSENG, K.-H. 1995. Gelation mechanism and rheological properties of rice starch. *Cereal Chemistry,* 72**,** 393-400.

LII, C. Y., TSAI, M. L. & TSENG, K. H. 1996. Effect of amylose content on the rheological property of rice starch. *Cereal Chemistry,* 73**,** 415-420.

LIU, Q. 2005. Understanding starches and their role in foods. *In:* CUI, S. W. (ed.) *Food carbohydrates: Chemistry, physical properties and applications.* Boca Raton, FL: CRC Press.

LUMDUBWONG, N. & SEIB, P. 2000. Rice starch isolation by alkaline protease digestion of wet-milled rice flour. *Journal of Cereal Science,* 31**,** 63-74.

MAAURF, A. G., CHE MAN, Y. B., ASBI, B. A., JUNAINAH, A. H. & KENNEDY, J. F. 2001. Gelatinisation of sago starch in the presence of sucrose and sodium

chloride as assessed by differential scanning calorimetry. *Carbohydrate Polymers,* 45**,** 335-345.
MADEKA, H. & KOKINI, J. 1992. Effect of addition of zein and gliadin on the rheological properties of amylopectin starch with low-to-intermediate moisture. *Cereal Chemistry,* 69**,** 489-494.
MALVERN INSTRUMENTS, L. 2006. *Rosand RH7/RH10 User Manual,* England, Malvern Instruments Ltd.
MALVIYA, R., SRIVASTAVA, P., PANDURANGAN, A., BANSAL, M. & SHARMA, P. K. 2010. A Brief Review on Thermo-rheological Properties of Starch Obtained from "Metroxylon sagu". *World Applied Sciences Journal,* 9**,** 553-560.
MANIAS, E. 2012. Rheometry_2. Pennsylvania State University.
MARTÍN-CABREJAS, M. A., JAIME, L., KARANJA, C., DOWNIE, A. J., PARKER, M. L., LOPEZ-ANDREU, F. J., MAINA, G., ESTEBAN, R. M., SMITH, A. C. & WALDRON, K. W. 1999. Modifications to physicochemical and nutritional properties of hard-to-cook beans (Phaseolus vulgaris L.) by extrusion cooking. *Journal of agricultural and food chemistry,* 47**,** 1174-1182.
MASON, W. R. & HOSENEY, R. 1985. *Factors affecting the viscosity of extrusion cooked wheat starch.* Kansas State University.
MAT HASHIM, D., MOORTHY, S., MITCHELL, J., HILL, S., LINFOOT, K. & BLANSHARD, J. 1992. The effect of low levels of antioxidants on the swelling and solubility of cassava starch. *Starch-Stärke,* 44**,** 471-475.
MAZIYA-DIXON, B., DIXON, A. G. & ADEBOWALE, A. R. A. 2007. Targeting different end uses of cassava: genotypic variations for cyanogenic potentials and pasting properties. *International Journal of Food Science & Technology,* 42**,** 969-976.
MCPHERSON, A. & JANE, J. 1999. Comparison of waxy potato with other root and tuber starches. *Carbohydrate polymers,* 40**,** 57-70.
MEHANSHO, H. 2006. Iron fortification technology development: new approaches. *The Journal of nutrition,* 136**,** 1059-1063.
MELLICAN, R. I., LI, J., MEHANSHO, H. & NIELSEN, S. S. 2003. The role of iron and the factors affecting off-color development of polyphenols. *Journal of agricultural and food chemistry,* 51**,** 2304-2316.
MERCIER, C. & FEILLET, P. 1975. Modification of carbohydrate components by extrusion-cooking of cereal products [Wheat, rice, corn]. *Cereal Chemistry*.
MEUSER, F., PFALLER, W. & LENGERICH, B. V. 1987. Technological aspects regarding specific changes to the characteristic properties of extrudates by HTST-extrusion cooking. *In:* O'CONNOR, C. (ed.) *Extrusion Technology for the Food Industry.* New York: Elsevier Applied Science.
MEUSER, F., SMOLNIK, H.-D., RAJANI, C. & GIESEMANN, H. G. 1978. Comparison of starch extraction from tapioca chips, pellets and roots. *Starch-Stärke,* 30**,** 299-306.
MILES, M. J., MORRIS, V. J., ORFORD, P. D. & RING, S. G. 1985. The roles of amylose and amylopectin in the gelation and retrogradation of starch. *Carbohydrate Research,* 135**,** 271-281.
MILMAN, N. 2011. Anemia—still a major health problem in many parts of the world! *Annals of hematology,* 90**,** 369-377.
MITCHELL, J. R., HILL, S. E., PATERSON, L. A., VALLÈS-PÀMIES, B., BARCLAY, F. A. & BLANSHARD, J. M. V. 1997. The role of molecular weight in the conversion of starch. *In:* P.J. FRAZIER, P. RICHMOND, A. & DONALD, A. M. (eds.) *Starch-structure and functionality.* London: Royal Society of Chemistry.
MOHAMED, A., JAMILAH, B., ABBAS, K. A., ABDUL RAHMAN, R. & ROSELINA, K. 2008. A Review on Physicochemical and Thermorheological Properties of Sago Starch. *American Journal of Agricultural and Biological Sciences,* 3**,** 639-646.
MOORTHY, S. & RAMANUJAM, T. 1986. Variation in properties of starch in cassava varieties in relation to age of the crop. *Starch-Stärke,* 38**,** 58-61.
MOORTHY, S. N. 2002. Physicochemical and functional properties of tropical tuber starches: a review. *Starch-Stärke,* 54**,** 559-592.
MORARU, C. & KOKINI, J. 2003. Nucleation and expansion during extrusion and microwave heating of cereal foods. *Comprehensive Reviews in Food Science and Food Safety,* 2**,** 147-165.

MORETTI, D., LEE, T. C., ZIMMERMANN, M. B., NUESSLI, J. & HURRELL, R. F. 2005. Development and Evaluation of Iron-fortified Extruded Rice Grains. *Journal of Food Science,* 70**,** S330-S336.
MOSCICKI, L. & VAN ZUILICHEM, D. J. 2011. Extrusion-cooking and related technique. *Extrusion-cooking techniques: applications, theory and sustainability. Wiley, Weinheim***,** 1-24.
NASHED, G., RUTGERS, R. P. & SOPADE, P. A. 2003. The plasticisation effect of glycerol and water on the gelatinisation of wheat starch. *Starch-Stärke,* 55**,** 131-137.
NEMŢANU, M. R. & BRAŞOVEANU, M. 2010. Functional Properties of Some Non-conventional Treated Starches. *In:* ELNASHAR, M. (ed.) *Biopolymers.* Sciyo.
NOJEIM, S. & CLYDESDALE, F. 1981. Effect of pH and ascorbic acid on iron valence in model systems and in foods. *Journal of Food Science,* 46**,** 606-611.
NOORAKMAR, A. W., CHEOW, C. S., NORIZZAH, A. R., MOHD ZAHID, A. & RUZAINA, I. 2012. Effect of orange sweet potato (Ipomoea batatas) flour on the physical properties of fried extruded fish crackers. *International Food Research Journal,* 19**,** 657-664.
NÚÑEZ, M., DELLA VALLE, G. & SANDOVAL, A. J. 2010. Shear and elongational viscosities of a complex starchy formulation for extrusion cooking. *Food Research International,* 43**,** 2093-2100.
NURTAMA, B. & LIN, J. 2009. Effects of process variables on the physical properties of taro extrudate. *World Journal of Dairy and Food Sciences,* 4**,** 154-159.
OATES, C. G. 1997. Towards an understanding of starch granule structure and hydrolysis. *Trends in Food Science & Technology,* 8**,** 375-382.
OLLETT, A. L., PARKER, R., SMITH, A. C., MILES, M. J. & MORRIS, V. J. 1990. Microstructural changes during the twin-screw extrusion cooking of maize grits. *Carbohydrate Polymers,* 13**,** 69-84.
ONWUEME, I. C. 1978. *The tropical tuber crops: yams, cassava, sweet potato, and cocoyams,* Chichester, John Wiley & Sons.
OWUSU-ANSAH, J., VAN DE VOORT, F. & STANLEY, D. 1984. Textural and microstructural changes in corn starch as a function of extrusion variables. *Canadian Institute of Food Science and Technology Journal,* 17**,** 65-70.
ŐZER, E. A., İBANOĞLU, Ş., AINSWORTH, P. & YAĞMUR, C. 2004. Expansion characteristics of a nutritious extruded snack food using response surface methodology. *European Food Research and Technology,* 218**,** 474-479.
PADMANABHAN, M. & BHATTACHARYA, M. 1989. Extrudate expansion during extrusion cooking of foods. *Cereal foods world (USA)*.
PARADA, J., AGUILERA, J. M. & BRENNAN, C. 2011. Effect of guar gum content on some physical and nutritional properties of extruded products. *Journal of Food Engineering,* 103**,** 324-332.
PARKER, R., LAI-FOOK, R., OLLET, A., & & SMITH, A. 1989. The rheology of food "melts" and its application to extrusion processing. *In:* CARTER, R. E. (ed.) *Rheology of Food, Pharmaceutical and Biological Materials with General Rheology.* London: Elsevier Applied Science.
PATERSON, L., MITCHELL, J. R., HILL, S. E. & BLANSHARD, J. 1996. Evidence for sulfite induced oxidative reductive depolymerisation of starch polysaccharides. *Carbohydrate Research,* 292**,** 143-151.
PATERSON, L. A., HASHIM, D. B., HILL, S. E., MITCHELL, J. R. & BLANSHARD, J. 1994. The effect of low levels of sulphite on the swelling and solubility of starches. *Starch-Stärke,* 46**,** 288-291.
PEIL, A., BARRETT, F., RHA, C. & LANGER, R. 1982. Retention of Micronutrients by Polymer Coatings Used to Fortify Rice. *Journal of Food Science,* 47**,** 260-262.
PETITOT, M., ABECASSIS, J. & MICARD, V. 2009. Structuring of pasta components during processing: impact on starch and protein digestibility and allergenicity. *Trends in Food Science & Technology,* 20**,** 521-532.
POMERANZ, Y. 1991. *Functional properties of food components*, Academic Press.
PURWANI, E., WIDANINGRUM, THAHIR, R. & MUSLICH 2006. Effect of heat moisture treatment of sago starch on its noodle quality. *Indonesian Journal of Agricultural Science,* 7**,** 8-14.

QI, X., TESTER, R., SNAPE, C. & ANSELL, R. 2003. Molecular basis of the gelatinisation and swelling characteristics of waxy rice starches grown in the same location during the same season. *Journal of Cereal Science,* 37**,** 363-376.

RIAZ, M. N. 2001. Selecting the right extruder. *In:* GUY, R. (ed.) *Extrusion Cooking, Technology and Application.* Cambridge, England: Woodhead Publishing Limited.

RIAZ, M. N. & ROKEY, G. J. 2012. Selecting the right type of extruder: single screw and twin screw extruders for food and feed production. *Extrusion problems solved: Food, pet food and feed.* Cambridge: Woodhead Publishing Limited.

RUSSELL, P. L. 1987. The ageing of gels from starches of different amylose/amylopectin content studied by differential scanning calorimetry. *Journal of Cereal Science,* 6**,** 147-158.

RYU, G., NEUMANN, P. & WALKER, C. 1993. Effects of Some Baking Ingredients on Physical and Structural Properties. *Cereal Chem,* 70**,** 29l-297.

SANDHU, K. S. & SINGH, N. 2007. Some properties of corn starches II: Physicochemical, gelatinization, retrogradation, pasting and gel textural properties. *Food Chemistry,* 101**,** 1499-1507.

SANDOVAL, A. & BARREIRO, J. 2007. Off-line capillary rheometry of corn starch: Effects of temperature, moisture content and shear rate. *LWT-Food Science and Technology,* 40**,** 43-48.

SASAKI, T. & MATSUKI, J. 1998. Effect of wheat starch structure on swelling power. *Cereal Chemistry,* 75**,** 525-529.

SASAKI, T., YASUI, T. & MATSUKI, J. 2000. Effect of amylose content on gelatinization, retrogradation, and pasting properties of starches from waxy and nonwaxy wheat and their F1 seeds. *Cereal Chemistry,* 77**,** 58-63.

SAUNDERS, J., IZYDORCZYK, M. & LEVIN, D. B. 2011. *Limitations and Challenges for Wheat-Based Bioethanol Production*.

SCHOCH, T. 1964. Swelling power and solubility of granular starches. *Methods in carbohydrate chemistry,* 4**,** 106-108.

SCHOCH, T. J. 1942. Fractionation of starch by selective precipitation with butanol. *Journal of the American Chemical Society,* 64**,** 2957-2961.

SENOUCI, A. & SMITH, A. 1988. An experimental study of food melt rheology. *Rheologica Acta,* 27**,** 546-554.

SHIH, F., KING, J., DAIGLE, K., AN, H.-J. & ALI, R. 2007. Physicochemical properties of rice starch modified by hydrothermal treatments. *Cereal chemistry,* 84**,** 527-531.

SIAW, C. L., IDRUS, A. Z. & YU, S. Y. 1985. Intermediate technology for fish cracker ('keropok') production. *International Journal of Food Science & Technology,* 20**,** 17-21.

SIM, J. Sago industry in the state of Sarawak, Malaysia. Sago-'85: Proceedings of the Third International Sago Symposium. Ibaraki, Japan: The Sago Palm Research Fund. p, 1986. 39-49.

SIM, S. L., OATES, C. G. & WONG, H. A. 1991. Studies on Sago Starch. Part I: Characterization and Comparison of Sago Starches Obtained from Metroxylon sagu Processed at Different Times. *Starch - Stärke,* 43**,** 459-466.

SINGH, B., SEKHON, K. S. & SINGH, N. 2007. Effects of moisture, temperature and level of pea grits on extrusion behaviour and product characteristics of rice. *Food Chemistry,* 100**,** 198-202.

SINGH, J., DARTOIS, A. & KAUR, L. 2010. Starch digestibility in food matrix: a review. *Trends in Food Science & Technology,* 21**,** 168-180.

SINGH, J., KAUR, L., MCCARTHY, O. J., MOUGHAN, P. J. & SINGH, H. 2009. Development and characterization of extruded snacks from New Zealand Taewa (Maori potato) flours. *Food Research International,* 42**,** 666-673.

SINGH, N., KAUR, L., SANDHU, K. S., KAUR, J. & NISHINARI, K. 2006. Relationships between physicochemical, morphological, thermal, rheological properties of rice starches. *Food Hydrocolloids,* 20**,** 532-542.

SINGH, N., SINGH, J., KAUR, L., SINGH SODHI, N. & SINGH GILL, B. 2003. Morphological, thermal and rheological properties of starches from different botanical sources. *Food Chemistry,* 81**,** 219-231.

SINGH, N., SMITH, A. & FRAME, N. 1998. Effect of process variables and monoglycerides on extrusion of maize grits using two sizes of extruder. *Journal of Food Engineering,* 35**,** 91-109.
SINGH, N. & SMITH, A. C. 1999. Rheological behaviour of different cereals using capillary rheometry. *Journal of Food Engineering,* 39**,** 203-209.
SINGHAL, R. S., KENNEDY, J. F., GOPALAKRISHNAN, S. M., KACZMAREK, A., KNILL, C. J. & AKMAR, P. F. 2008. Industrial production, processing, and utilization of sago palm-derived products. *Carbohydrate Polymers,* 72**,** 1-20.
SINJAL, D. 2008. *Pak Harto dan Pertanian Padi* [Online]. Jakarta, Indonesia: PT Permata Wacana Lestari. [Accessed 10 May 2016.
SODHI, N. S. & SINGH, N. 2003. Morphological, thermal and rheological properties of starches separated from rice cultivars grown in India. *Food Chemistry,* 80**,** 99-108.
SRIBURI, P. & HILL, S. E. 2000. Extrusion of cassava starch with either variations in ascorbic acid concentration or pH. *International Journal of Food Science & Technology,* 35**,** 141-154.
SRIBURI, P., HILL, S. E. & MITCHELL, J. R. 1999. Effects of L-ascorbic acid on the conversion of cassava starch. *Food Hydrocolloids,* 13**,** 177-183.
STOJCESKA, V., AINSWORTH, P., PLUNKETT, A., İBANOĞLU, E. & İBANOĞLU, Ş. 2008. Cauliflower by-products as a new source of dietary fibre, antioxidants and proteins in cereal based ready-to-eat expanded snacks. *Journal of Food Engineering,* 87**,** 554-563.
SUDARGO, T., NISA, F. Z., HELMIYATI, S., KUSUMA, R. J., ARJUNA, T. & SEPTIANA, R. D. 2013. Tempeh with Iron Fortification to Overcome Iron Deficiency Anemia. *Pakistan Journal of Nutrition,* 12**,** 815.
SVEGMARK, K., HELMERSSON, K., NILSSON, G., NILSSON, P.-O., ANDERSSON, R. & SVENSSON, E. 2002. Comparison of potato amylopectin starches and potato starches—influence of year and variety. *Carbohydrate Polymers,* 47**,** 331-340.
SWINKELS, J. 1985. Composition and properties of commercial native starches. *Starch-Stärke,* 37**,** 1-5.
TAKEDA, Y., TAKEDA, C., SUZUKI, A. & HIZUKURI, S. 1989. Structures and Properties of Sago Starches with Low and High Viscosities on Amylography. *Journal of Food Science,* 54**,** 177-182.
TESTER, R. F. & KARKALAS, J. 1996. Swelling and gelatinization of oat starches. *Cereal Chemistry,* 73**,** 271-277.
TESTER, R. F. & MORRISON, W. R. 1990. Swelling and gelatinization of cereal starches. I. Effects of amylopectin, amylose, and lipids. *Cereal Chem,* 67**,** 551-557.
THEUER, R. C. 2008. Iron-fortified infant cereals. *Food Reviews International,* 24**,** 277-310.
THOMAS, D. & ATWELL, W. 1997. Gelatinization, Pasting, and Retrogradation. *Starches.* AACC Int Press.
THYMI, S., KROKIDA, M. K., PAPPA, A. & MAROULIS, Z. B. 2005. Structural properties of extruded corn starch. *Journal of Food Engineering,* 68**,** 519-526.
TIE, A. P. L., KARIM, A. A. & MANAN, D. M. A. 2008. Physicochemical properties of starch in sago palms (Metroxylon sagu) at different growth stages. *Starch-Stärke,* 60**,** 408-416.
TONGDANG, T., MEENUN, M. & CHAINUI, J. 2008. Effect of sago starch addition and steaming time on making cassava cracker (Keropok). *Starch-Stärke,* 60**,** 568-576.
UAUY, R., HERTRAMPF, E. & REDDY, M. 2002. Iron fortification of foods: overcoming technical and practical barriers. *The Journal of nutrition,* 132**,** 849S-852S.
VALLE, G. D., BOCHÉ, Y., COLONNA, P. & VERGNES, B. 1995. The extrusion behaviour of potato starch. *Carbohydrate Polymers,* 28**,** 255-264.
VALLÈS-PÀMIES, B., BARCLAY, F., HILL, S. E., MITCHELL, J. R., PATERSON, L. & BLANSHARD, J. 1997. The effects of low molecular weight additives on the viscosities of cassava starch. *Carbohydrate Polymers,* 34**,** 31-38.

VAN DER SMAN, R. & MEINDERS, M. 2011. Prediction of the state diagram of starch water mixtures using the Flory–Huggins free volume theory. *Soft Matter,* 7**,** 429-442.
VERGNES, B., DELLA VALLE, G. & TAYEB, J. 1993. A specific slit die rheometer for extruded starchy products. Design, validation and application to maize starch. *Rheologica Acta,* 32**,** 465-476.
VERGNES, B. & VILLEMAIRE, J. 1987. Rheological behaviour of low moisture molten maize starch. *Rheologica Acta,* 26**,** 570-576.
VISSER, R. G., SUURS, L. C., BRUINENBERG, P. M., BLEEKER, I. & JACOBSEN, E. 1997. Comparison Between Amylose-free and Amylose Containing Potato Starches. *Starch-Stärke,* 49**,** 438-443.
WANG, L. & SEIB, P. A. 1996. Australian salt-noodle flours and their starches compared to US wheat flours and their starches. *Cereal Chemistry,* 73**,** 167-175.
WANG, S. & COPELAND, L. 2013. Molecular disassembly of starch granules during gelatinization and its effect on starch digestibility: a review. *Food & Function,* 4**,** 1564-1580.
WANG, S., ZHANG, X., WANG, S. & COPELAND, L. 2016. Changes of multi-scale structure during mimicked DSC heating reveal the nature of starch gelatinization. *Scientific Reports,* 6.
WANG, T. L., BOGRACHEVA, T. Y. & HEDLEY, C. L. 1998. Starch: as simple as A, B, C? *Journal of Experimental Botany,* 49**,** 481-502.
WANG, W. J., POWELL, A. D. & OATES, C. G. 1995. Pattern of enzyme hydrolysis in raw sago starch: effects of processing history. *Carbohydrate Polymers,* 26**,** 91-97.
WANG, Y.-J. & WANG, L. 2002. Structures of four waxy rice starches in relation to thermal, pasting, and textural properties. *Cereal Chemistry,* 79**,** 252-256.
WHO 2002. *World Health Report, 2002 : Reducing Risks, Promoting Healthy Life,* Albany, NY, USA, World Health Organization (WHO).
WHO 2006. *Guidelines on food fortification with micronutrients,* Geneva, WHO.
YU, L., RAMASWAMY, H. S. & BOYE, J. 2012. Twin-screw extrusion of corn flour and soy protein isolate (SPI) blends: a response surface analysis. *Food and Bioprocess Technology,* 5**,** 485-497.
ZOBEL, H., YOUNG, S. & ROCCA, L. 1988. Starch gelatinization: An X-ray diffraction study. *Cereal Chem,* 65**,** 443-446.
ZOBEL, H. F. 1988. Molecules to Granules: A Comprehensive Starch Review. *Starch - Stärke,* 40**,** 44-50.